The effect of axial body loading – via the "SkinSuit" – on human movement.

Attias, Julia

Awarding institution:
King's College London

The effect of axial body loading – via the "SkinSuit" – on human movement.

Julia Attias (MSc, BSc)

ID: 1139534

Centre for Human and Applied Physiological Sciences,

King's College London

Submitted for the degree of Doctor of Philosophy (PhD)

Abstract

Bodyweight (BW) loading has been shown to increase metabolic cost and neuromuscular activity during locomotion. The Mk VI 'SkinSuit' – initially developed as a spaceflight countermeasure – provides axial body loading (ABL) intended to be equivalent to 20% 'BW' via vertical elastic-material in a manner analogous to Earth's gravity (1Gz). Thus, the aims of this thesis were to determine the influence of additional 0.2Gz ABL on physiological and biomechanical responses during exercise in ≤1Gz. Two main protocol paradigms were adopted, which evaluated the effect of additional 0.2Gz ABL during: 1) incremental exercise to voluntary exhaustion in normal gravity (thus ~1.2Gz) vs. without ABL (1Gz) and 2) simulated 0.8Gz and 0.16Gz vs. a matched equivalent during submaximal exercise.

Cardiorespiratory variables and maximal aerobic capacity ($\dot{V}O_2Max$) were unchanged between 1.2Gz vs. 1Gz during cycling and running, though time to exhaustion was reduced with both (by 13% and 10%, respectively; $p<0.05$). A steeper breathing rate (BR)/minute ventilation ($\dot{V}_{E)}$ slope evidenced during running at 1.2Gz ($p=0.044$), indicative of a more rapid, shallow breathing pattern, may have contributed to this. Performing both exercises in 1.2Gz did not induce differences in electromyographic (EMG) root mean square (RMS) amplitude or median frequency (MDF) in any lower-limb muscle, though lengthened Gastrocnemius Lateralis (GL; cycling) and Soleus (SOL; running) duration ($p<0.05$). Both the removal (BW suspension) and addition (ABL) of 0.2Gz to 1Gz elicited reductions in ventilatory variables vs. 1Gz during submaximal running ($p<0.01$) whereas EMG RMS amplitude was unchanged. Although EMG RMS amplitude was reduced in all muscles in 0.16Gz compared to 1Gz, these were not reinstated to levels equivalent to those elicited during a matched trial (MATCHED) when running with 0.2Gz ABL (016SS). GM duration was significantly greater during 016SS vs. 0.16Gz and equivalent to MATCHED.

Provision of 0.2Gz ABL in addition to ≤1Gz does not induce cardiorespiratory responses or muscle activity levels equivalent to 20% BW loading, presumably due to the absence of centre of mass displacement. However, the significant effect of additional ABL on muscle activity patterns during both cycling and running in ≤1Gz, particularly in the plantarflexors, suggests strategic modulation of locomotor control governed by the central nervous system. Unloading of 0.2Gz during high or low portions of the gravity spectrum was not potent enough to reduce the activation requirement of lower-limb muscles, making "reloading" opportunities inconceivable; thus, the optimal dose of ABL is yet to be determined.

Table of contents

List of figures and tables

Figures

Tables

List of abbreviations

ABL	Axial body loading
BDC	Bottom dead centre
BR	Breathing rate
BF	Biceps Femoris muscle
BW	Bodyweight
COM	Centre of mass
CP	Cerebral Palsy
CPG	Central pattern generators
CWS	Chest-wall strapping
ECG	Electrocardiography
EMG	Electromyography/ic
GAS	Gastrocnemius muscle (in the absence of specification as to which one)
GCT	Ground contact time
GL	Gastrocnemius Lateralis muscle
GLCS	Gravity-Loading Countermeasure SkinSuit
GM	Gastrocnemius Medialis muscle
GMAX	Gluteus Maximus muscle
GRF	Ground reaction force
Gz	Force of gravity acting in the head-to-toe direction
HR	Heart rate
HS	Heel strike
ISS	International Space Station
MDF	Median Frequency
PTS	Preferred walk to run transition speed
QUAD	Quadriceps muscle (in the absence of specification as to which one)
RER	Respiratory exchange ratio
RF	Rectus Femoris muscle
RMS	Root mean square
RPE	Rating of perceived exertion
ROM	Range of motion
SCI	Spinal cord injury
SEM	Standard error mean
SOL	Soleus muscle
TA	Tibialis Anterior muscle

TDC	Top dead centre
$\dot{V}_E$	Minute ventilation
VL	Vastus Lateralis muscle
VM	Vastus Medialis muscle
$\dot{V}O_2$	Oxygen consumption
$\dot{V}CO_2$	Carbon Dioxide production
$\dot{V}_T$	Tidal volume

Acknowledgements

Completing this PhD has not only challenged my scientific capabilities but offered me an overwhelming personal endeavour; I guess that's why they call it a doctorate of "philosophy".

My first thank you goes to King's College London and the Engineering and Physical Sciences Research Council (EPSRC) for believing I was good enough to invest in to undertake this journey. A huge thank you also goes to all of the trusty, reliable and patient participants that allowed me to put them through their paces, literally; without you there would be no thesis.

One of my most important thanks goes to my counsellor, Lyn Emberson. You have facilitated in equipping me with the resources necessary to battle my idiosyncrasies and ultimately, life. I really couldn't have done this without you and I am truly thankful.

Thank you to my supervisors, Dr David Green, Professor Thais Russomano and Dr Katya Mileva. Your expertise in your respective fields is inspirational and you have all taught me how to be a better scientist. Some extra special gratitude must go to Katya; your openness to take on and teach an amateur about neuromuscular physiology will be forever appreciated.

Dr James Waldie and Professor Dava Newman, without your creation of the SkinSuit and without the Space Medicine Office at the European Astronaut Centre supporting SkinSuit projects, I wouldn't have a research field. I thank you all sincerely. I also thank each of my collaborators from London South Bank University, the German Aerospace Centre (DLR), the European Astronaut Centre, the German Sports University and Trium as well as the technical staff from all institutions (Bill [LSBU], Wolle [DLR], Lindsay, Tony and Amy [KCL]).

To all of my CHAPS colleagues (and now friends): from keeping me company in the tea room while I dine "out of hours" to giving a listening ear, you have all been there for me and not

only do I thank you truly, I will miss you a lot. One person does deserve a mention: Phil Carvil. From when we met on the first day of our Masters, to us both having completed our PhD's; we've been through it all together and I'll always consider you a life-long friend.

I have never taken for granted my wonderful family and friends and I thank you all deeply for your continued support through my endeavours. Mum, you are there with me every step of the way, whatever I choose to do, always. I can't thank you enough for your love, care and support. Zack, my husband-to-be, what a special year this is for us; I firstly become a Dr and then shortly after, your wife. This journey of mine hasn't been easy on you from any perspective and I am so grateful to you for making my life that little bit easier through tough times. It only reinforces that we can get through all of life's challenges together, hand in hand.

Chapter 1: Introduction and review of the literature

1.1 Basic concepts relating to gravity and human movement

On Earth, gravity pulls any object of mass towards the centre of the Earth with an acceleration (g) of 9.81m.s^{-2}. As a vector quantity, acceleration possesses both direction and magnitude, where the latter is expressed as "G"; that is, the ratio between the applied acceleration and the gravitational constant (Glaister, 1978). Gravity on Earth is therefore referred to as "1G" and on other celestial bodies, is referred to as a proportion of such, i.e. gravity on the Moon is 0.16G. Direction can be given to G by reference to three axes based upon the long axis of the body (Gell, 1961), with the suffixes X, Y and Z indicating anteroposterior, mediolateral and longitudinal axes, respectively (Fig.1.1). By use of these axes, and with the body in the standard anatomical position, movements in three planes can be ascribed; X- and Z-axes form the sagittal plane, Y- and Z-axes the frontal or coronal plane and X- and Y-axes the transverse or horizontal plane (Knudson et al, 2007; Fig.1.1).

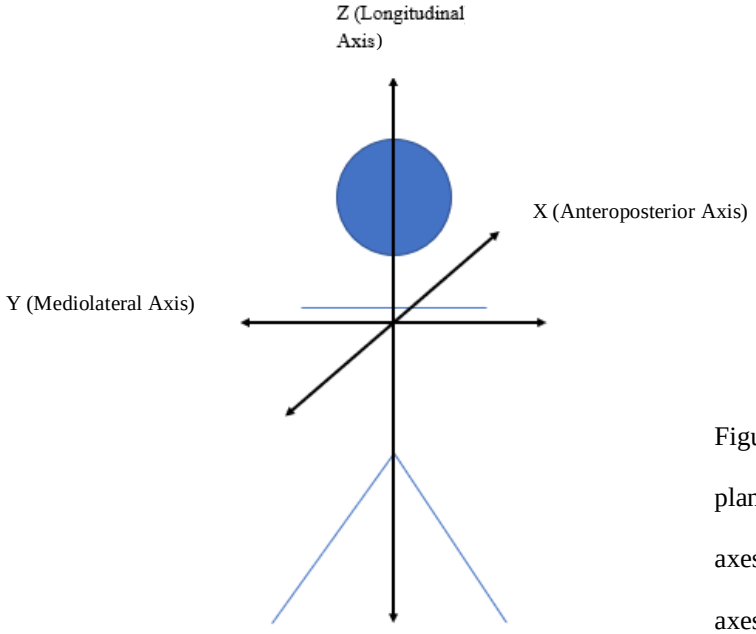

Figure 1.1: Depiction of the three human movement planes. The sagittal plane is defined by the X- and Z-axes; the frontal plane is defined by the Y- and Z-axes; and the transverse plane is defined by the X- and Y-axes.

Gravity produces a type of mechanical loading that plays an essential role in regulating the function of numerous physiological systems (Whalen, 1993). The most fundamental skeletal loading condition in 1G is caused by the static weight of the body. This static loading varies most prominently along the z-axis, as the load at any point is equal to the bodyweight (BW) above it; thus, gravity on Earth is referred to as 1Gz. The load carried at the shoulders is therefore equal to the weight of the head and neck, and gradually increases to full BW at the soles of the feet (Churchill et al, 1978; Table 1.1).

Table 1.1: Body segment data from males, depicting the proportion of body weight carried at each major body segment (Taken and adapted from Churchill et al, 1978).

Male segment volume as percent of total body volume								
Subjects	Cadaver			Living				
Studies	Clauser et al (1969)	Chandler et al (1975)	Average	Dempster (1955)	Cleaveland (1955)	Drillis et al (1966)	Katch & Waltman (1975)	Average
Head		5.4%						
Head & neck	7%				7%		7.4%	7.2%
Torso					48.1%		46.2%	47.2%
Neck & Torso	51.9%	56.9%	54.4%					
Upper arm	2.6%	2.7%	2.7%	3.5%	3.1%	3.5%		3.4%
Forearm	1.5%	1.5%	1.5%	1.5%	1.6%	1.7%		1.6%
Upper & forearm	4.1%	4.2%	4.2%	5%	4.7%	5.2%	5.6%	5.1%
Hand	0.6%	0.5%	0.6%	0.6%	0.5%	0.6%	0.7%	0.6%
Total arm	4.7%	4.7%	4.7%	5.6%	5.2%	5.8%	6.3%	5.7%
Thigh	10.3%	9.4%	9.9%	14.2%	11.2%	9.2%		12%
Shank	4.2%	3.9%	3.9%	4.9%	4.4%	4.1%		4.5%
Thigh & Shank	14.5%	13%	13.8%	19.1%	15.6%	13.3%	15.2%	15.8%
Foot	1.4%	1.1%	1.3%	1.4%	1.3%	1.3%	1.7%	1.4%
Total leg	15.9%	14.1%	15%	20.5%	16.9%	14.6%	16.9%	17.2%
Total Body	100.1%	99.9%	100%		99.3%		100%	
N	13%	6%		39%	12%	11%	24%	
Stature*	172.7%	172.1%	172.4%	174.5%	175.8%	176%	176.9%	175.8%
Weight*	65.6%	65.2%	65.4%	75.6%	71.5%	73.4%	76.2%	73.9%
Age	49.3%	54.3%	51.9%	20.6%	27.2%	20.8%	21.2%	22.5%
Total body Volume*	63%	69.6%	66.3%	71.32%**	66.7%	69.3%**	71.9%**	69.8%

* Stature is reported in centimetres, weight in kilograms and total body volume in litres

** Total body volume computed as weight : 1.06

Measurements of living subjects under 1Gz conditions have established that the centre of mass (COM) of the whole body is always in close proximity to the pelvis and appears to remain, regardless of body configuration, approximately at the level of the anterior superior iliac spine (Churchill et al, 1978). Normal daily activities, such as standing, walking, and running impose two external forces on the body: BW (constant), and the ground reaction force (GRF) composed

of BW and the inertial force accelerating and decelerating the COM during activity (Whalen, 1993). High GRFs produce large internal muscle and bone forces, which are approximately scaled by the magnitude of the GRF during steady state activities (Biewener, 1991).

1.2 The evolution of bipedal locomotion

The rationale underpinning the adoption of bipedality in hominoids has been the topic of debate for centuries (Darwin, 1871; Hewes, 1961; Rodman and McHenry, 1980; Watson et al, 2008). Aside from the prominent argument that bipedal locomotion is less energetically costly compared to quadrupedalism (Rodman and McHenry, 1980), a general concurrence amongst hypotheses is for the advantage of the hands being free (Watson et al, 2008). Benefits of such would include tool-using (Darwin, 1871), weapon-handling and throwing (Kirschmann, 1999), food-gathering (Hewes, 1961), reaching (Jolly, 1970), and infant-carrying (Etkin, 1954).

It has been recognized that apes and other nonhuman primates differ from humans by habitually adopting a more compliant form of bipedalism (Kimura, 1991) encompassing greater hip, knee and ankle flexion during the stance phase of walking; such a compliant gait would be too energetically expensive and less efficient for humans (Crompton et al., 1998). Thus, when modern humans walk, they vault over relatively stiff lower limbs in such a way that the COM is at its lowest point as the heel strikes the ground and rises to its highest point during the time the foot is in contact with the ground (Lee and Farley, 1998). This “inverted pendulum”-like gait allows for an effective exchange of gravitational potential and kinetic energy (Cavagna et al, 1976). Walking upright in this manner entails advantages but also raises new challenges including load distribution on two legs only and stabilization of the upright posture (Maus et al, 2010).

1.3 Mechanisms responsible for the maintenance and regulation of bipedal (upright) locomotion

1.3.1 Hemodynamic/cardiovascular mechanisms

The act of standing is a challenge taken for granted in humans. Due to gravity, 500-700ml of blood translocate from the upper body to venous capacitance vessels of the lower limbs and splanchnic circulation within a few seconds of standing (Mathias, 2002). This results in a decrease of venous return, right ventricle filling pressure, and ultimately cardiac output by ~20%, with a resultant drop in blood pressure. Humans developed evolutionary adaptive mechanisms to overcome this gravitational stress and became the only animals capable of maintaining the erect posture for prolonged periods of time, by means, primarily, of the autonomic nervous system (Victor, 2015). First, the shift in blood volume towards the lower part of the body is counteracted by muscle contractions which not only increase venous return by compressing capacitance vessels and preventing lower-body blood-pooling, but also increase vascular resistance (Joseph et al, 2017). Modifications in blood pressure are detected immediately by baroreceptors, located in the carotid sinus. These sense small reductions in arterial pressure or central blood volume, through deformations of the vessel wall, which trigger compensatory adjustments in the heart and vessels through the parasympathetic and sympathetic nervous systems (Sanders et al, 1988) including: arterial and venous constriction leading to elevated peripheral arterial resistance and venous return; increased cardiac muscle contractility leading to improved cardiac output and increased renal sympathetic activity resulting in renal vasoconstriction, renin synthesis, decreased glomerular filtration rate and greater sodium reabsorption (Joseph et al, 2017).

1.3.2 Neuronal mechanisms

During any particular movement task, the central nervous system is directed to hold the body's COM over its base of support (Dietz et al, 1992). Regulation of bipedal locomotion thus requires specific neuronal mechanisms and activity in the lower limb extensor muscles – often referred to as the anti-gravity muscles (Masani et al, 2013) – to maintain the body in an upright position. Information on the amount of leg loading is provided by sensory receptors, such as Ib afferents from Golgi Tendon organs located in ankle plantar flexor muscles (Gordon et al, 2009), cutaneous mechanoreceptors in the foot soles and spindles from stretched muscles (Dietz and Duysens, 2000). These sensory signals interact with and generate spinal and supra-spinal reflexes from central pattern generators (CPGs); neural circuits that produce the patterns of neural activity that underlie rhythmic motor behaviours, such as walking (Delcomyn, 1980).

A great deal of knowledge regarding the control of locomotion has been gathered using the decerebrate cat which involves the elimination of cerebral brain function by removing the cerebrum, cutting across the brain stem, or severing certain arteries in the brain stem. Such a model has proved useful because, with appropriate stimulation, fully coordinated stepping can be evoked from all four limbs (Whelan, 1996). The first significant insight with respect to extensor load receptor input on the CPG was derived from experiments on pre-mammillary cats (reviewed in Dietz and Duysens, 2000). These animals are prepared by making a transection immediately rostral to the superior colliculus and continuing rostroventrally to the rostral tip of the mammillary bodies (Whelan, 1996). Classical experiments by Brown (1911, 1912) showed that cats with a transected spinal cord and with cut dorsal roots still showed rhythmic alternating contractions in ankle flexors and extensors. This was the basis of the concept of a spinal locomotor center which Brown termed the `half-center' model. One half of this center induced activity in flexors, the other in extensors.

Duysens and Pearson (1980) conducted a study where the hind-limb of 28 premamillary cats was held in a fixed position while treadmill walking. Of these 28, 25 of the cats had additional denervation of the hind-limb by cutting the obturator, femoral, distal tibial, superficial peroneal and sural nerves as well as the posterior and medial articular nerves at the knee. The fixation gave the opportunity to induce changes of both the force and length of the ankle extensors independent of changes in hip position (hip afferents play a known role in regulating phase transitions), while these muscles were rhythmically activated in alternation with the muscles in the contralateral 'free' hind-limb. In the fixed limb, a gradually increasing stretch was applied to the Achilles tendon, resulting in an increase in both amplitude and duration of the rhythmic electromyographic (EMG) bursts of the extensors, whereas the flexor EMG bursts (Tibialis Anterior [TA]) reduced and eventually dropped out. These results provided evidence that proprioceptors in the Triceps Surae can inhibit the generation of rhythmic bursts of EMG activity in ipsilateral flexors such as the TA, due to triceps surae afferents acting on a premotoneuronal centre, or the central stepping generator itself. More recent studies have evidenced that such pathways are also active in humans (Dietz and Duysens, 2000).

1.4 The interactions between gravity and human movement and the exploitations of such

In light of the aforementioned theoretical constructs regarding Earth's gravity (1Gz) and bipedal locomotion, it is unsurprising that the interactions between the two are both accidentally and deliberately exploited by adding external load to the body. For some individuals, moving whilst being additionally-loaded is inevitable in line with the demands of their vocation, i.e. military personnel carrying armour and equipment (Knapik et al, 1996). However, other paradigms exist such as using weights attached to body segments to potentiate training stimuli in both performance-improving and rehabilitation scenarios (Cross et al, 2014).

Furthermore, whilst many studies investigating physiological responses to load carriage are used in an acute setting, longer-term trials where the loading is used for training-intervention purposes in clinical populations have also been conducted (Salem et al, 1996; Scholtes et al, 2012).

There are characteristic physiological i.e. cardiorespiratory and biomechanical – principally neuromuscular and kinematic – adaptations when moving with increased load, which are well documented and will be discussed in detail in the upcoming section. Increases in leg extensor muscle activity such as the gastrocnemius (site unspecified [GAS]; Ghori and Luckwill, 1985: Simpson et al, 2011a) and the vastus lateralis (VL; Ghori and Luckwill, 1985; Stastny et al, 2014), are intuitive considering the role of leg extensors in maintaining upright posture in the face of gravity (Masani et al, 2013). Moreover, coordination between multiple muscles is required to achieve the vast majority of motor tasks (Hug and Tucker, 2016) and thus modulation to the activity patterns of these muscles are also evident with additionally-loaded movement (Ghori and Luckwill, 1985; Simpson et al, 2012). Relatedly, kinematic changes pertaining to posture are disrupted, such as decreased step length (Martin and Nelson, 1986; Birrell and Haslam, 2009; Krupenevich et al, 2015), increased ground contact time (GCT) and step frequency (Simpson et al, 2012; Cross et al, 2014; Simperingham and Cronin, 2014) and changes to lower-extremity joint angle range of motion (ROM; Attwells et al, 2006; Simpson et al, 2012; Seay et al, 2014). These biomechanical modifications are thought to reflect the greater effort required to overcome the inertia associated with increasing load (Attwells et al., 2006). Moreover, the cardiorespiratory system undergoes transient adaptations when carrying load, predominantly linked to increases in heart rate (HR) and oxygen consumption ($\dot{V}O2$), pertaining to the additional "cost" of the task (Quesada et al, 2000; Simpson et al, 2011b) with consequential reductions in maximal exercise capacity ($\dot{V}O_2Max$; Phillips et al, 2016).

1.4.1 Loading paradigms in 1Gz

1.4.1.1 Backpacks

Backpacks are routinely worn in numerous populations, including but not limited to the military, recreational hikers, travellers and students. Most of the literature within the backpack-carrying domain focuses on walking and marching, the reasons for which are likely twofold; the prevalence of such endeavours and the impact that prolonged carriage may impart onto their physiological wellbeing.

Early work by Han et al (1992) studied 15 participants walking at 4.7km·h^{-1} with backpack loads of 6kg, 20kg, 33kg and 47kg and observed increased activation of the leg extensor muscles, namely VL and GAS. A more recent study observing female hikers walking for 8km at a self-selected pace carrying backpack loads equating to 20%, 30% and 40% additional BW showed generally linear increases in GAS activity (22%, 27% and 33% respectively), compared to BW alone (Simpson et al, 2012). The addition of backpack load equivalent to 20-50% BW has also been shown to induce a longer muscle burst duration of the VL when walking between 3.5-4.75km·h^{-1} (Ghori & Luckwill, 1995) as well as a later onset of VL activation when walking with similar load magnitudes compared to BW alone (Simpson et al, 2012; Stastny et al, 2014).

It is accepted that hip flexion increases with increasing backpack load (Seay et al, 2014), but the results are less conclusive with regards to the ankle and knee. Some studies have observed greater knee and ankle flexion with increased load, whereas others have found little or no change (Kinoshita, 1985; Tilbury-Davis et al, 1999). These discrepancies are likely linked to

the degree of knee musculature applying larger resistances to counteract the increasing load in order to optimise a certain amount of knee stiffness, which minimises the vertical excursion of the COM thus saving on the cost of extra motion (Holt et al, 2003).

When participants walked at 5km·h^{-1} carrying backpack loads ranging from 10-30kgs (~13-40% BW), each kilogram accounted for an average increase in $\dot{V}O_2$ and HR of 33.5 ml.min^{-1} and 1.1 beats per minute (bpm), respectively (Borghols et al, 1978). Furthermore, Quesada (2000) investigated individuals marching whilst carrying a backpack equivalent to 15% and 30% BW, which was shown to increase metabolic cost by 6% and 11%, respectively. Additionally, small but significant reductions in $\dot{V}O_2$peak and test duration have been reported when carrying a 25kg backpack during a walking test to exhaustion. These manifestations may likely be secondary to decreases in minute ventilation ($\dot{V}_E$; Phillips et al, 2016) as a consequence of backpack-imposed chest-wall restriction (Dominelli et al, 2012). In comparison, Simpson et al (2011b) observed increases in HR of 6.9-7.7% whilst walking for 8km at self-selected pace across three loads (20%, 30%, 40% BW). Furthermore, HR elevations of 8-10bpm have been found when walking for only 90m at 5.6km·h^{-1} (Bobet and Norman, 1984) with a 20kg backpack compared to without. However, absolute HR values could not be identified in this study, and so it is not possible to determine the percent change from rest. It is likely to be at least equivalent to, or higher than that of Simpson et al (2011b), if we assume that the group mean resting HR was 60-100bpm; normal values for healthy individuals (Laskowski, 2015), as tested in their study.

1.4.1.2 Weighted vests, belts & other clothing ensemble

Aside from backpacks, loaded interventions have also been in the form of clothing parts, such as vests and belts in both healthy and clinical populations. In contrast to backpacks, these

interventions usually place a portion of the load at the front of the body as well as the back in an attempt to minimise the backward-displaced COM.

Electromyographic activity in the soleus (SOL) and VL was found to increase by 14% and 78% when walking at ~3.5km·h^{-1} for 70 strides with 30% BW load – attached on a belt around the participants' waist – compared to without (Stephens and Yang, 1999). When walking 5 metres, 5 times, at a preferred speed with vests ranging from 9-27kg, peak activity of the gastrocnemius medialis (GM) and rectus femoris (RF) increased with the 27kg trials compared to the 9kg and 18kg trials and the no load trials, respectively (Park et al, 2014). When walking at a slightly faster speed of 4.7km·h^{-1} for 3min whilst wearing a weighted belt of either 25% BW or 50% BW, participants increased GAS (21% and 35% respectively) and SOL activity (21% and 52%, respectively; McGowan et al, 2008).

Puthoff et al (2006) studied the effect of a weighted vest that had equally front and back-distributed additional weights of 0%, 10%, 15% and 20% BW during 4min walking stages at five different speeds ranging from 3-6.4km·h^{-1}. At all speeds, oxygen consumption ($\dot{V}O_2$) increased with ≥10% BW by 6-17% compared to the 0% added BW trial. As speed was increased, the delta $\dot{V}O_2$ was magnified. This study concluded that by walking at slower speeds with the addition of these modest loads, individuals can reach metabolic cost levels similar to those at a faster speed without additional load, which has practical application for improving fitness in those with ailments that may prevent them from acquiring faster speeds.

Increased GCT and decreased flight time has been observed in studies investigating the effect of an 18kg weighted vest on sprint performance compared to a no-load condition (Cross et al, 2014). Similarly, Cronin et al (2008) observed decreased step frequency and increased stance phase duration (i.e. GCT) during sprinting whilst wearing a vest equating to an additional 15-

20% BW. Furthermore, the addition of either upper or lower-body loading of 5% BW – by virtue of a wearable exoskeleton (Lila Exogen Suit™) – promoted alterations in kinematic variables similar to those observed in the Cronin et al (2008) and Cross et al (2014) studies (Simperingham and Cronin, 2014; upper body loading: increased GCT and decreased flight time; lower body loading: increased GCT and decreased step frequency).

Weighted vests have been shown to improve leg muscle-strength in populations where either muscle weakness ensues (i.e. cerebral palsy [CP]; Scholtes et al, 2012), or preventative muscle weakness is desirable (i.e. geriatrics; Salem et al, 1996). In a study by Salem et al (1996), 7 participants with a mean age of 72yr walked with a weighted vest equivalent to 4% BW for 2-3 hours a day, 4 days a week, for 4 weeks, after which the same routine was repeated albeit with a 5% weighted vest. After the total 8-week programme, peak knee extensor force, as measured by maximal voluntary contractions on an isokinetic dynamometer was improved by 20% and 8% in the right and left legs, respectively. Scholtes et al (2012) conducted a randomised controlled trial in children with CP and assigned 25 participants to a functional group and 25 to a usual-care group. The functional group participated in a 12-week functional training program involving a 60min session three times a week. The session included four functional exercises in total, three of which provided resistance of 0.5-3kg via a weighted vest. Generally, the group assigned the training program gained isometric strength improvements, as quantified by an increase in leg press resistance to complete their six-repetition maximum (Scholtes et al, 2012). Although these studies did not incorporate neuromuscular activity level assessment, it is reasonable to assume that muscle fibre recruitment, and thus EMG amplitudes would have been greater (Sandbrink, 2012). Furthermore, it is difficult to decipher the precise contribution of the weighted-vest exercise in aiding these improvements as the training

program also included a leg-press exercise, which likely had a greater contribution to the improved leg strength in the training group considering the specificity of the exercise.

1.4.1.3 Limb loading

Loading the limbs, particularly at the distal ends (i.e. the ankle), takes advantage of an increased moment of inertia and subsequently increases metabolic cost and activity of the surrounding musculature (Hay, 1985). Therefore, most studies using limb loading have involved the requirement to potentiate further exercise stimuli in both healthy (Soule and Goldman, 1969; Martin et al, 1985) and clinical populations (Gordon, 2009).

It has been observed that $\dot{V}O_2$ increases in response to thigh load (1.7% and 3.5% for 0.25kg and 0.5kg, respectively), though the magnitude of increase was greater when similar loads were placed on the feet (3.3% and 7.2%, respectively; Martin et al, 1985). Congruent findings were reported by Jones et al (1984) and Frederick et al (1984) who observed increases in $\dot{V}O_2$ by 4.5% and 6%, respectively, for 1kg of load added to the feet when running at similar speeds. In the study by Martin et al (1985), HR also increased with the addition of 1kg load on the feet but were not significant when added to the thighs. In a study by Soule and Goldman (1969), participants walked at speeds of $4km \cdot h^{-1}$, $4.8km \cdot h^{-1}$ and $5.6km \cdot h^{-1}$ with a combination of loads ranging from 4-14kg on the hands, head or feet; increases in $\dot{V}O_2$ of ~41-50% across speeds were shown when walking with a foot load of 6kg, which was greater than any other weight in any other location.

Distal limb loading has also been shown to result in kinematic alterations related mainly to step length and frequency (Martin, 1985; Claremont and Hall, 1988; James et al, 2015), though results between studies are conflicting. This is likely related to differences in the magnitude of

load, load placement and/or the locomotive task. For example, during running, Martin (1985) found increases in stride length (1.2%) with 0.7% BW loading at the foot, whereas Claremont and Hall (1988) found 5.2% decrease in stride length with 0.45kg at the ankle.

Lower limb loading has also been applied as an intervention in those with spinal cord injury (SCI; Gordon et al, 2009; Gordon et al, 2010). Spinal cord injury (SCI) results in loss of muscle function, sensation and autonomic function in the areas served below the level of the lesion (McDonald and Sadowsky, 2002). It has been suggested that individuals with SCI have the capacity to produce locomotor patterns when they receive appropriate afferent feedback, such as proprioceptive information related to repetitive, lower limb loading and flexion/extension movements consistent with walking (Harkema, 2008). Enhancement in extensor muscle activity (SOL and GAS) has been observed when individuals with SCI "air-stepped" whilst wearing a powered orthosis around the ankle-foot to mechanically stimulate load receptors (Gordon et al, 2009; Gordon et al, 2010).

1.4.1.4 Issues associated with these loading approaches

Although the physiological benefits of load-carrying during a range of movements in multiple populations have been established, these activities are not without risk (Seay et al, 2014). Such risks are strongly associated with body COM, where the greater the deviation of the COM, the greater the instability (Schiffman, 2006), and thus the likelihood of musculoskeletal injuries, which are also related to load-exposure duration. Blacker et al (2013) had participants walk for 2 hours at 6.5km·h^{-1} with a 25kg backpack. Following the task, they observed neuromuscular impairment through a decrease in voluntary activation (i.e. central drive) or damage to the peripheral muscle, including impairment of the excitation contraction coupling process. They proposed that the decrement in muscle function may increase the risk of musculoskeletal injury

and is likely to detriment performance during physical and skilled tasks following load carriage.

Forward trunk lean is a common feature associated with load-carriage, subject primarily to loads borne on or around the back (Birrell and Haslam, 2009; Simpson et al, 2011a), where an attempt to maintain body COM over the base of support is necessary. Such a posture can increase lordosis of the spine, which can result in compression of the lumbar vertebral bodies and facet joints and increase interdiscal pressure, leading to chronic lumbar pain disorders (Smith et al. 2006). Even in studies where loads were added to the hands, postural adjustments i.e. increased knee flexion were necessary to stay balanced (Ghori and Luckwill, 1985). Furthermore, the increases in both vertical and anteroposterior GRFs with additional loading are acknowledged to contribute to overuse or repetitive strain injuries in the lower limb (Polcyn et al, 2002; Birrell and Haslam, 2010).

The way in which species interact with Earth's gravity is in a graduated, incremental fashion, where a particular body segment carries the weight of superior segments (Churchill et al, 1978). Therefore, carrying additional mass loading at one distinct body part (i.e. on the back), is instinctively not an ecologically valid approach to moving efficiently or effectively with additional load. Moreover, the use of such methods that are suitable in 1Gz become redundant in <1Gz (i.e. weightlessness) and require the need to recreate z-axis loading with an anchor at the feet.

1.4.2 Loading paradigms in <1Gz environments

1.4.2.1 Physiological issues associated with <1Gz environments

In the absence of gravity in the z-axis, numerous physiological adaptations transpire, including, but not limited to, deconditioning of the cardiorespiratory and neuromuscular systems. The most obvious environment pertaining to such is weightlessness i.e. spaceflight, which gravitationally unloads the body. The adaptation to un-weighting of each muscle group displays a consequential hierarchy in relation to their importance for weight-bearing (Berg et al, 2007). Thus, the greatest musculoskeletal deteriorations are in the plantarflexors, which is intuitive considering the work they do to continually resist the majority of BW and maintain the upright posture (Masani et al, 2013). Astronauts participating in Skylab missions ranging from 28-84 days experienced a 5-26% decline in knee extensor and flexor muscle strength (Thornton and Rummel, 1977). Furthermore, studies of cosmonauts after a 6-month spaceflight (Mir) show declines in the volume of the calf plantar flexors ranging from 6-20%, GAS and SOL of 19% and Quadriceps (QUAD) of 10% (LeBlanc et al, 2000). More recently, Trappe et al (2009) published data regarding muscle size and function from 10 astronauts after a 6 month stay on the International Space Station (ISS). The results demonstrated 10% and 15% atrophy in the GAS and SOL, respectively, quantified four days after return. Furthermore, all crew members experienced a loss in muscle function as determined by reduced maximal voluntary contraction (by 9-33%) 13 days after return, and peak power declines of 32%.

With insertion into microgravity, fluid is displaced from the lower body, to the upper body, resulting in “bird-like legs, and puffy faces” (Charles et al, 1994), causing a lower level of body fluid regulation, in part due to increased water excretion via the kidneys (Di Prampero et al, 2009). Plasma volume is reduced (hypovolemia) by approximately 8-10% (300ml) within the first 24-48 hours of microgravity (Convertino, 1995), which can contribute to reduced

ventricular filling, stroke volume and thus cardiac output (Pavy-Le Traon, 2007), left ventricle mass (Perhonen et al, 2001) and erythropoietin production (Blomqvist and Stone, 1991) leading to decreased red blood cell mass. Moreover, this combination of factors results in greater levels of orthostatic intolerance and $\dot{V}O_2$Max decrements on return to 1Gz (Convertino, 2002; Convertino, 2011). Sustained dampened and slowed muscular $\dot{V}O_2$ kinetics has been noted early post mission (6 days after return), which was not recovered 3 weeks after the mission (Hoffman et al, 2016). These findings have been linked to reduced aerobic capacities of exercising muscles and may be caused by a loss of aerobic enzyme concentration, a non-sufficient Oxygen delivery to the muscles or both (Poole et al, 2007). Collective data on astronauts participating in the first 10 years of ISS flights showed elevated HR responses during flight and shortly after return (5 days); these findings are likely due to effects of hypovolemia on compromised stroke volume, decreased end diastolic filling and possible cardiac atrophy (Moore et al, 2015).

For astronauts on the ISS, exercise is performed for ~2.5 hours per day (including set-up and stowage) in an attempt to protect bone and muscle strength and maintain physical fitness levels (Hackney et al, 2015). Nonetheless, integration with external loading, such as subject load devices, to tether crew to the base of the treadmill are essential to increase GRFs similar to those experienced in 1Gz to prevent potential diseases related to sustained microgravity exposure (e. g. osteoporosis; Cavanagh et al, 2007). Bed-rest is a commonly used surrogate to simulate the axial unloading which occurs during spaceflight (Morey-Holton, 2000). Owing to the removal of the Gz stimulus in both situations, physiological adaptation have been shown to be similar; the extent of which will differ depending on the aetiology of the bed-ridden state (Pavy Le Traon, 2007). Furthermore, studies from actual spaceflight are inevitably limited with regards to their sample size, as only a handful of crew were and still are assigned to such

missions. Studies have therefore been conducted that deliberately recruit healthy individuals to resign themselves to long-term (days, weeks or months) bed-rest (Stenger et al, 2012; Linnarsson et al, 2014) to better understand the influence of microgravity/unloading on physiological adaptation. As such, the literature in the following sections will be related to data collected actual (i.e parabolic flight) and simulated (i.e. bed rest) unloading.

1.4.2.2 Human centrifugation

The most obvious solution to tackle physiological adaptations resulting from microgravity environments is to recreate the element that is lost. As such, artificial gravity has been proposed in the form of human centrifugation for ~20 years (Kreitenberg et al, 1998). Centrifugal forces are "created" by drawing a rotating body away from a centre of rotation, caused by the inertia of the body resulting in, what appears to be, gravity (Clément and Bukley, 2007). These devices can be either motor- (Fig. 1.2a) or human-powered (Fig. 1.2b) and have been used in both simulated microgravity to reload the body to a 1Gz stimulus (Stenger et al, 2012; Linnarson et al, 2014; Rittweger et al, 2015) and in 1Gz to increase the exposure above and beyond 1Gz (Yang et al, 2007a). Whereas long arm centrifuges may have been the most familiar to the scientific community owing to their vital use in training military jet pilots, there has been a recent emergence in the use of short arm human centrifuges (SAHC; Zander et al, 2013). The latter devices operate with a shorter radius and thus faster relative velocity, necessary to generate adequate Gz loads for experiments and training. Moreover, SAHCs are particularly attractive with regards to being contained in standard space vessels, the diameter of which is sufficient to contain such a device.

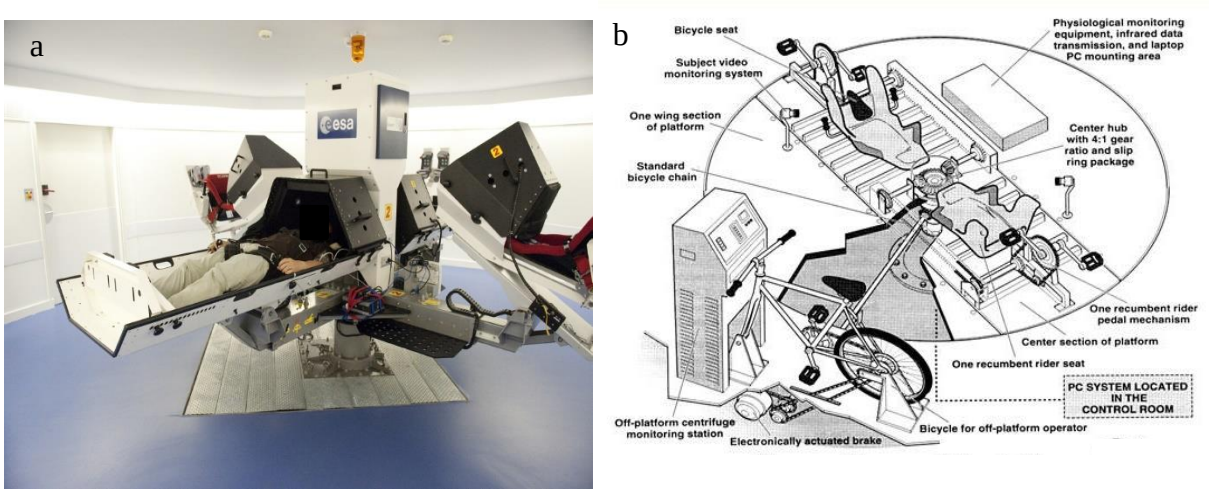

Figures 1.2 a and b: a) European Space Agency's short-arm human centrifuge at MEDES in Toulouse. This image is made available online at: http://www.medes.fr/en/the-space-clinic/the-equipments/short-arm-centrifuge.html (copyright CNES/Rachel BARRANCO, 2010); b) A cycle-based human-powered centrifuge used in artificial gravity training (Greenleaf et al, 2001). This image is made available online at https://ntrs.nasa.gov/archive/nasa/casi.ntrs.nasa.gov/20060050756.pdf (copyright NASA).

Linnarsson et al (2014) studied eleven participants who were assigned to 3 repeated 6-degree head-down bed-rest segments for 5 days each. Each trial was assigned either to no countermeasures (control), artificial gravity via centrifugation at 1Gz of one 30min bout daily (AG1) or centrifugation at 1Gz of six periods of 5min daily (AG2). Orthostatic tolerance in all participants was significantly greater when exposed to both artificial gravity treatments (AG1: 64% and AG2: 78% compared to 36% in the control condition). A strand of this study conducted by a separate research group also observed maintenance in the isometric strength of the knee extensors and flexors by both AG1 and AG2 (Rittweger et al, 2015). Stenger et al (2012) studied 15 men before and after a slightly longer duration of head-down bed rest (21 days with eight in the treatment group, comprising of a 1h exposure to 1Gz daily via centrifugation, and 7 in the control group with no treatment. They observed over a 50% attenuation in the peak aerobic power decline in the treatment group vs. the control group (-

0.39±0.11 vs. 0.17±0.06 L/min respectively). Studies involving participants performing squats on a human-powered centrifuge whilst still being exposed to the z-axis have shown that they were capable of performing squats at 3Gz that produced peak foot forces equivalent to three times greater than their own BW (Yang et al, 2007a) and those elicited during 10 repetition maximum squats with load under 1Gz conditions (Yang et al, 2007b).

There are, however, a number of concerns and impracticalities of using artificial gravity to recreate a loading stimulus, which are not only subject to those in microgravity. Potential negative physiological side effects include motion sickness, dizziness, the Coriolis effect, illusory motion, and nausea that result from head movement in a rotating environment (Lackner and DiZio, 1998). A particularly notable side-effect of the higher rotation velocity associated with SAHCs is the generation of a significant gravitation gradient along the head-to-toe axis of the subject, which can have an impact on the cardiovascular system i.e. orthostatic intolerance (Rittweger et al, 2015). In fact, a recent study by Laing et al (2016) showed that tolerance on the SAHC can be dictated based on the position of the rotational axis. Despite experiencing the same Gz level at the feet, participants were more tolerable when the rotational axis position was at the level of the heart compared to the head, or above the head. Moreover, these devices are a huge engineering feat, extremely costly, take up large amounts of space, and thus rendered impractical for many scenarios. Loading methods for spaceflight-induced physiological deconditioning that require minimal power, volume and mass, therefore, have greater desirability. Elasticated loading suits offer a viable solution in meeting these criteria.

1.4.2.3 Elasticated loading suits

The Russian “Penguin” Suit was, until recently, one of the current countermeasures utilized on the ISS by cosmonauts (Fig. 1.3). It was designed as a muscle and bone loading suit that induces

weight bearing stresses on the skeleton and resistive exercise to the musculature (Severin, 1991; Kozlovskaya et al, 1995). Upper and lower body loading along the vertical axis (z-axis) are imposed by bungee cords above and below a leather belt: from the shoulders to the belt (upper body), and from the belt to the feet (lower body; Severin, 1991). The suit, therefore, creates axial loading along the z-axis for skeletal maintenance, and resistance to the normal postural position for weight-bearing muscle stimulation and was used in conjunction with other countermeasures.

Yamashita-Goyo et al (2001) studied the effect of wearing the Penguin Suit for 10h/day as an intervention to prevent decrements in muscle size and function during a 2month bed rest, compared to a control group. The intervention group were sub split, where one group received full body loading from the suit which specifically loaded the distal tarsals of the foot by 60-70N (Penguin-1), whereas the other group wore the full ensemble but the elastic elements at the foot were disconnected (Penguin-2). The findings from the Penguin-2 group were no different to the control group. However, both fibre diameter and muscle force per cross-sectional area in the SOL were found to have been preserved in Penguin-1 compared to control; these results were attributed to the passive stretch induced by the foot loading, which may have induced a level of constant tonic SOL activity.

Nonetheless, anecdotal reports from cosmonauts express that they found the suit to be thermally intolerable and have hence cut the bungee cords as the 1-or 2-stage loading is highly uncomfortable (Waldie, 2005). Furthermore, this 2-stage loading regime does not accurately recreate the nature in which gravity is experienced in 1Gz (Churchill et al, 1978) and thus remains subject to the aforementioned pitfalls of loading paradigms in 1Gz (section 1.4.1.4).

Figures 1.3 a-d: The Russian Penguin Suit: a) the front of the suit (left); b) the back (middle), c) donning with its full assembly and ankle attachments (right) and d) The Adeli Suit. The images of the Penguin Suit are made

available online at http://www.maxuta.com/maxuta/collections/034_space_zvezda/034033_penguin.htm and the image of the Adeli Suit is taken and adapted from Ko et al, 2015.

The Penguin Suit has also been explored as a therapeutic agent in children with CP, though is termed the Adeli Suit the "Adeli" Suit (Bar-Haim et al, 2008; Bailes et al, 2011). The suit is comprised of a vest, shorts, knee pads and shoes, all connected with elastic cords which are adjusted by therapists to imitate normal flexor and extensor patterns of major muscle groups in an attempt to reposition limbs to correct abnormal muscle alignment (Ko et al, 2015; Fig. 1.3d&e). Semenova (1997) argued that this method would reduce pathological synergies, restore normal muscular synergies, and apply loads to antigravity musculature that would normalize the afferent vestibulo-proprioceptive input. Two recent studies investigated functional measures via the Gross Motor Function Measure (GMFM) after 3 (Bailes et al, 2011) or 4 weeks (Bar-Haim et al, 2006) of "suit" treatment, in children with CP. The GMFM is a criterion-referenced observational measure that was developed and validated to assess children with cerebral palsy (Russell et al, 2000). The 88 items of the GMFM are measured by observation of the child and scored on a 4-point ordinal scale (0=does not initiate, 1=initiates <10% of activity, 2=partially completes 10% to <100% of activity, 3=completes activity). The items are weighted equally and grouped into 5 dimensions: (1) lying and rolling (17 items), (2) sitting (20 items), (3) crawling and kneeling (14 items), (4) standing (13 items), and (5) walking, running, jumping (24 items); children without motor delays can generally accomplish all of the items. The studies by Bailes et al (2011) and Bar-Haim (2006) failed to observe significant improvements in gross motor function, though were arguably limited by the functional measures they employed. Understanding changes in muscle activation levels, patterns and/or kinematics may have enabled detectable changes in gait patterns (Bailes et al, 2011) and thus a more thorough understanding of the validity of the suit-intervention.

1.5 An axial loading "SkinSuit"

1.5.1 Conceptual theory and design

Initially designed as a countermeasure to mitigate spinal elongation associated with microgravity exposure, the "SkinSuit" builds upon the concept of the "The Gravity-loading Countermeasure Skinsuit" [GLCS]), which imposes z- axial body loading by gradually increasing tension in elastic-material z-axis fibres (Waldie and Newman, 2011) from the shoulders to the feet. Compared to the Penguin Suit, such a design allows a significantly finer stepwise resolution in simulating the 1Gz loading regime on the body by continuously increasing in material tension distally to match the proportion of BW load that the segment should be experiencing (Churchill et al, 1978). As the arms are not normally subject to any weight bearing, the SkinSuit supplies loading only to the torso and legs as a sleeveless garment.

A bi-directional elastic weave material achieves the different longitudinal and lateral tensile requirements, where fibres are orientated with high modulus in the z-axis, so that substantial BW forces could be created without over stretching the weave, particularly in the lower body. Conversely, low stiffness fibres are used circumferentially, each of which is used as a 'belt' to produce many vertical stages, to facilitate easy donning/doffing, prevent suit slippage and so that the tension would not vary significantly due to changes in body shape (such as through movement). Nominally, the suit acts to apply the full BW at the feet via stirrups to spread the load over the entire sole to mimic 1Gz standing; the securing of these stirrups essentially creates an elastic band-like loop from the shoulders to the feet. In this manner, axial loading is intended to provide a passive load during both static and dynamic activity. The SkinSuit requires no

power, creates no noise or vibration, and has minimal volume and mass. Those wearing it may be able to exercise, work normally or sleep (Waldie and Newman, 2011).

1.5.2 Evolution of the SkinSuit

The evolution of the Mk VI SkinSuit – the current version – began with the creation of the GLCS at Massachusetts Institute of Technology by Dr J Waldie and Prof D Newman. The first prototype (Mk I) was purported to be accurate at simulating graduated 1Gz loads during parabolic flight – where bouts of weightlessness of ~25s are generated via an aeroplane flying in a ballistic trajectory (n=2; Waldie and Newman, 2011). This study also performed modelling simulations, which suggested that the Mk I required less than 10 mmHg of circumferential compression. Furthermore, practical aspects of the suit (such as mobility, comfort and material performance) were determined, which demonstrated negligible mobility restriction and excellent comfort properties with the absence of operational criticisms, unlike the Penguin suit. Iterations from this version to both Mk II and III (Fig. 1.4a) included textile and design improvements (e.g. a 2-way central zipper and a non-elastic ankle closure with a zipper).

Figures 1.4 a-d: Evolution of the Mk III Gravity-Loading Countermeasure SkinSuit (GLCS; a) to the European Space Agency's SkinSuit current Mk VI (d). F = front view; B = back view. Image credit – European Space Agency and King's College London; taken and adapted from Carvil, 2017.

To understand the interactions between movement and subjection to an additional 1Gz axial body load, pilot, ground-based studies were conducted whereby the Mk III GLCS was worn during cycling, running, resistance exercise and ambulatory tasks (Carvil et al, 2013; Attias et al, 2014; Carvil et al, 2016; Attias et al, 2017; Carvil et al, 2017). Findings from this body of work revealed that the loading was in fact 0.8Gz – as measured by TekScan pressure insoles (and thus ~1.8Gz when worn on Earth; Carvil et al, 2013). Such a magnitude of additional loading precipitated $\dot{V}O_2$ and HR dissociation without curtailing aerobic performance ability (Attias et al, 2017) and reduced the total work required to achieve $\dot{V}O_2$Max during cycling (Attias et al, 2014). Moreover, during running with additional 0.8Gz, augmented oxygen cost (Carvil et al, 2016), unimpeded ambulatory, mobility and strength performance (Carvil et al, 2013) and reduced shoulder-joint ROM (Carvil et al, 2017) were observed compared to 1Gz.

Although no thermoregulatory issues were noted despite exercising to 75% $\dot{V}O_2$Max (Attias et al, 2017), some participants described discomfort whilst performing the tasks, albeit remaining superior to anecdotal reports from the Penguin suit. Participants reported having sore shoulders from the pressure of the non-stretch material, and that the backward extension required by the shoulders to don the GLCS due to a zipper at the front, invoked concern over shoulder dislocation or unnatural range of movement. Thus, the Mk IVb GLCS (Fig. 5b) offered extra padding under the shoulders and a back zipper instead of a front zipper for ease of donning. The remaining primary issue was the fact that the GLCS could still not be donned alone, and without the need to anchor oneself. In order for this concept to be applicable for spaceflight crew, it was essential that the garment could be donned and doffed, with relative ease, without the assistance of another. Thus, shortly after came the evolution of the Mk V “SkinSuit” (Fig. 1.4c), where the material changed to a black woven spandex – a reportedly more comfortable material – which was easier to don, had further-increased padding under the shoulders, thicker

stirrups to avoid discomfort on the soles of the feet, and improved durability and loading consistency (Kendrick and Newman, 2014). The compromise of these improvements was a dramatic reduction in axial load provision to ~20% BW (0.2Gz).

Ahead of SkinSuit integration into European Space Agency's astronaut Andreas Mogensen's flight to the ISS in September 2015, a parabolic flight campaign was pursued to ensure that postures and movements associated with working in microgravity (i.e. hand walks) were feasible in the MK V. Investigated tasks included lateral arm raises, squats and sit and reach motions – with use of goniometry measuring joint ROM – alongside subjective ratings of thermal and movement comfort, body control and perceived exertion. The results showed no hindrances to ROM and the subjective ratings suggested that the Mk V SkinSuit was comfortable and tolerable enough to wear as an adjunct to activity in a microgravity environment, which was don- and doff-able quickly and without assistance (Green et al, 2014). The Mk VI is the current model (Fig. 1.4d; Fig. 1.5), which has no load-function differences to the Mk V; it was adapted purely to add ankle buckles that better adjusted the stirrups to the desired height to ensure necessary loading, marginally redesign the shoulder-padding elements and integrate a method for male toilet usage in line with pending day-long unloading studies.

Figure 1.5: The Mk VI SkinSuit application through the human body. The securing of the stirrups around the ankle ensures graduated 1Gz-like loading from the shoulders to the feet. Material up to the armpit-line is non-stretch; beneath this point, material is made of a bi-directional weave, where the tension in the vertical material increases from the shoulders to the feet, creating an additional axial load in proportion with the % BW load each segment should be experiencing.

Although the axial load provision is lower than originally intended, which is equivalent to ~20% BW loading by virtue of the Mk VI SkinSuit, such a magnitude of additional load in 1Gz is capable of inducing alterations to both the cardiorespiratory and neuromuscular systems (e.g. Borghols, 1978; Ghori and Luckwill, 1985; Martin, 1985; Quesada, 2000; Puthoff et al, 2006; McGowan et al, 2008; Simpson et al, 2011b; Simpson et al, 2012).

1.6 General summary of the literature

Locomoting bipedally against the force of gravity on Earth (1Gz) is capacitated via evolutionary mechanisms pertaining primarily to the autonomic nervous system for hemodynamic and cardiovascular regulation and sensory receptors (i.e. Ib afferents from Golgi

Tendon organs that stimulate leg extensor muscle activation). As such, the provision of additional bodyweight loading during locomotion precipitates physiological adaptations such as altered kinematics, increased oxygen cost and lower-limb neuromuscular activation. These adaptations can be desirable in those that seek an additional exercise stimulus, and, in such cases, additional loading is deliberately applied. However, the methods that are typically employed for this use (e.g. weighted vests) can disturb optimal biomechanics leading to increased musculoskeletal injury risk; particularly if worn for long periods. Moreover, the physiological deconditioning experienced by individuals exposed to partial gravity can be partially ameliorated by exercise which can be facilitated by additional loading, but the aforementioned approaches are rendered insufficient in weightlessness. Therefore, the provision of Earth-like axial body loading may induce beneficial augmentations to both the cardiorespiratory and neuromuscular systems whilst tackling the inappropriateness of mass-loading body segments during movement in ≤1Gz.

1.7 Aims of the thesis

The aims of this thesis were to assess the influence of 0.2Gz axial body load (via the Mk VI SkinSuit) on:

1. Cardiorespiratory responses during movement in 1Gz;
2. Neuromuscular activity and biomechanics during movement in 1Gz;
3. Cardiorespiratory and neuromuscular responses to exercise in partially-loaded environments, to evaluate the efficacy of axial-load as a means of "artificially creating" gravity exposure.

Five experimental Chapters are presented, each of which addresses one or more of the thesis aims. Chapters 3 and 5 will address aim 1 by focusing purely on the cardiorespiratory responses during movement, whereas Chapters 4 and 6 will focus on the neuromuscular and

biomechanical adaptations (aim 2). Chapters 5 and 6 will also target the third aim by introducing and implementing partial-gravity paradigms whilst examining the range of physiological variables. Chapter 7 is dedicated purely to the third aim, investigating only the neuromuscular system.

Chapter 2: General experimental and analytical methodologies

2.1 Ethics

All experiments performed were conducted to the standards set by the latest revision of the Declaration of Helsinki (2000), and procedures were approved by the King's College London **(**BDM/14/15-38; LRS15/161944**)**, London South Bank University (1563) and German Aerospace Centre ethics committees.

2.2 Participants

Nineteen healthy, recreationally active male individuals were recruited to participate in the studies within this thesis; Table 2.1 displays participant n numbers and anthropometrics for each. Only male volunteers were sought since the SkinSuits were fabricated to enable toilet usage for male users only. Although they all had differing levels of physical fitness, each were recreationally active to a moderate intensity ≥3 times per week and had previous experience in physiological testing, and $\dot{V}O_2$Max tests. All participants reported taking no medication and having no current or chronic ill-health, namely neurological, cardiorespiratory or musculoskeletal disorders, that may affect them taking part in this study. Participants were instructed to consume a similar diet and hydrate 2h before all studies whilst avoiding caffeine & nicotine for 12 h and alcohol for 24h prior to experimentation.

Table 2.1: Participant n numbers and anthropometrics for each experimental study.

Study 1 (Chapters 3 & 4)	
n	8
Age (yr)	29.6±5.6
Height (cm)	177.1±6.8
Mass (kg)	74.2±7.1
Study 2 (Chapters 4 & 5)	
n	9
Age (yr)	29.4±5.2
Height (cm)	176.4 ± 6.7
Mass (kg)	78.6 ± 6.8
Study 3 (Chapter 6)	
n	8
Age (yr)	31.88±4.7
Height (cm)	178.38±5.7
Mass (kg)	73.54±7.3

Due to time and logistical constraints, not all participants took part in all studies. Out of the 19 participants, 12 had a custom-made SkinSuit (refer to section 2.3.2); hence recruitment of 7 alternative subjects with similar anthropometric measurements, namely height and weight, was pursued. Each "substitute" was initially instructed to try on multiple appropriately-sized SkinSuits for ~1 hour and provide an anecdotal comfort report. Based on a positive report, a loading assessment was performed (section 2.4.1) and if adequate ABL was ensured (~15-20%; they were deemed an appropriate participant.

2.3 Experimental methods/calibration procedures

2.3.1 General protocol paradigms

As mentioned briefly in Chapter 1, five experimental Chapters were served by the employment of three separate repeated measures studies, which revolved around two modes of motion; cycling and running. Each study investigated the main and interaction effects of intensity (i.e.

cycling power or running speed) and condition (i.e. load) on cardiorespiratory, neuromuscular and/or biomechanical variables. Two of the studies (1 and 2) evaluated the effect of additional 20% axial body loading (ABL) in normal gravity (thus 1.2Gz) vs. 1Gz ("HYPERLOAD"). Furthermore, two of the studies (2 and 3) evaluated the effect of simulated partial gravity (0.8Gz and 0.16Gz [lunar gravity]) vs. a matched equivalent – created via a combination of unloading and reloading via ABL – at sub-maximal, steady-speed intensities ("EQUIVALENCE"). With all studies except the one that served Chapter 7, multiple visits were required, which were separated by a minimum of 24 hours, considering the incorporation of maximal voluntary performance amongst them.

2.3.2 SkinSuit fitting

Custom-fabricated Mk VI SkinSuits were made (Dainese, Italy) for each participant and were used for all studies. The creation of certain reference points on the body first and foremost were necessary which were formed using tape (Fig 2.1a). These reference lines were: around the base of the neck; yoke line; around the shoulders and neck from yoke front to yoke back; waist (belly button); fullest part of the hip; thigh at crotch line; fullest part of the thigh; above the knee; centre knee; below the knee; fullest part of the calf; and the narrowest part of the ankle. From these reference lines, necessary circumferential and vertical measurements could be made, alongside total height and weight (Fig 2.1b). As well as the circumferences around the references, marker pen was used to measure every cm of height, from the narrowest part of the ankle, to the yoke line; where circumferences were also taken from. These figures were then sent to engineering colleagues to calculate the material strains needed before being sent for fabrication.

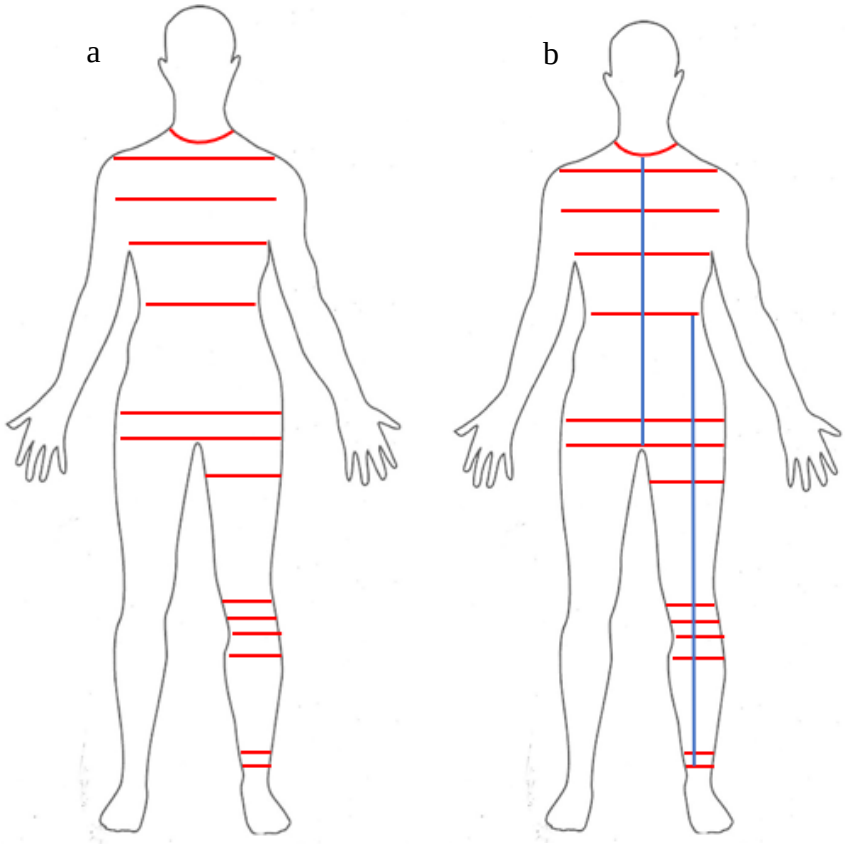

Figures 2.1 a and b: Schematic depicting procedures for SkinSuit fitting prior to fabrication. a) represents the reference lines created which resulted in circumferential measurements; b) represents two vertical lines that were measured longitudinally. Taken and adapted from from Liz Pearlman (permission received), original tailors at CostumeWorks, Boston, MA, USA.

2.3.3 Cardiopulmonary testing

Metabolic carts measure the oxygen consumed ($\dot{V}O_2$) and the carbon dioxide produced ($\dot{V}CO_2$) by an individual. Such data can be collected on a breath-by-breath basis by using a Hans Rudolf Oro-nasal mask (Shawnee, USA) which attaches to a mouthpiece with a sample line, where the other end connects to the cart. Two different metabolic carts were utilised within this thesis, with data collected employing the same breath-by-breath principles.

Prior to each session, calibration of the metabolic cart (both an Oxycon Pro [CareFusion, Germany; Chapter 3] and a Cosmed Quark CPET [Shepperton, UK; Chapter 5]) was performed

following a 15min system preparation. Automated calibration of gases was performed through removal of the sample line from the mouthpiece, which enabled alternate sampling of room air and known gas concentrations of 15.9% Oxygen and 4.93% Carbon Dioxide. The user was alerted of a successful calibration or otherwise, in which case it was repeated. Volume calibration was performed manually using a 3L volume syringe to continually pump air through the mouthpiece. This was performed until the software was satisfied with the consistency of the flow-volume loops.

2.3.4 Heart rate monitoring

2.3.4.1 Electrocardiography (ECG)

Electrocardiography is the process of recording the electrical activity of the heart over a period of time using electrodes placed on the skin. A 3-lead ECG allows for 3 major "viewpoints" of the heart. Lead I represents the voltage between the (positive) left arm (LA) electrode and right arm (RA) electrode, Lead II the voltage between the (positive) left leg (LL) electrode and the right arm (RA) electrode and Lead III the voltage between the (positive) left leg (LL) electrode and the left arm (LA) electrode (Fig.2.2). The electrodes that form these signals are located on the limbs—one on each arm and one on the left leg. These limb leads form the points of what is known as Einthoven's triangle (Jin et al, 2012). Alternatively, these can be placed on each clavicle, and under the left-hand side 6^{th} intercostal space in line with the mid-clavicular line. This configuration was adopted in the study that served Chapter 3 (HME LifePulse, UK; Chapter 3) and lead II continuously monitored with hypo-allergenic adhesive electrodes placed on each site, prior to attachment of the ECG cables. Heart rate (HR) was derived by the intervals between consecutive R-waves. Heart rate data were collected through an A-D converter

(PowerLab 26T, AD Instruments, Castlehill, Australia) and automatically derived from R-R intervals.

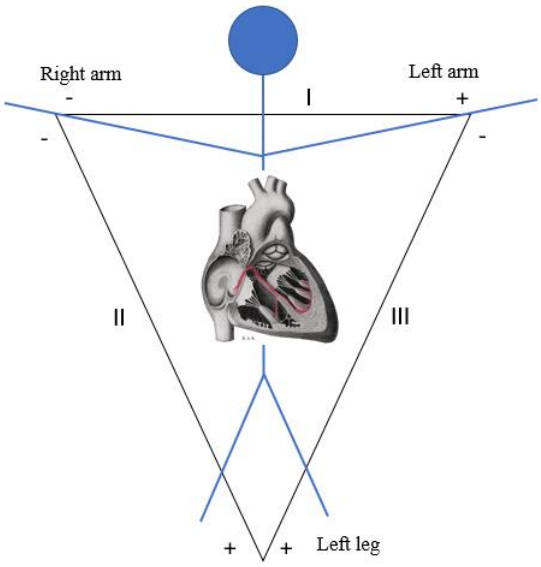

Figure 2.2: "Einthoven's triangle", depicting 3 "viewpoints of the heart via Leads I, II and III. Lead 2 was utilised for the studies within this thesis, with the positive electrode on the 6th intercostal space on the left side, the negative electrode on the right clavicle and the Earth electrode on the left clavicle. The heart image is by Henry Vandyke Carter - Henry Gray (1918) Anatomy of the Human Body. Bartleby.com: Gray's Anatomy, Plate 501, available for the public domain, https://commons.wikimedia.org/w/index.php?curid=567268.

2.3.4.2 Heart rate strap

Wearable HR monitors are also routinely used within exercise settings due to the minimal space they occupy and limited invasiveness. These monitors maintain the principles of electrocardiography to record the electrical activity of the heart. Most are made of a long, belt-like elastic band which wraps around the chest, composed of a small electrode pad that sits against the skin, which require moisture i.e. water to pick up the electrical signal. In Chapter 5, a Polar HR strap (Warwick, UK) was used to assess heart rate throughout experimentation, in the absence of a 3-lead ECG. When this method was utilised, the data were synchronised and recorded within the respective metabolic cart alongside all respiratory variables.

2.3.5 Neuromuscular function

To evaluate the effects of the studied factors on neuromuscular functions, surface electromyography (EMG) was used as an experimental technique to record and evaluate the electrical potentials produced by skeletal muscles (Kamen, 2004) during activation. Historically, EMG has been a useful assessment tool for detecting the electrical activity of specific muscles and assessing their contribution to movement (DeLuca, 1997).

Two major types of EMG are used in experimental studies: surface EMG and intramuscular EMG. The latter involves insertion of a fine wire into a muscle with a surface ground electrode placed above an electrically neutral body tissue as a reference, or two fine wires inserted into muscle referenced to each other (Konrad, 2006). Although this method is superior to surface EMG in terms of acquiring activity from deeper muscle fibres and motor units, it is extremely invasive and requires specialised advanced training. Surface EMG can be used in a number of settings and was, therefore, more appropriate for these enquires. It can be recorded with monopolar or multipolar electrodes; the studies within this thesis utilised bipolar electrodes, as they have shown good selectivity and noise stability (Lynn et al, 1978).

Muscle activity was always recorded from the dominant leg only, quantified based on participants' verbal report of which limb they would use to kick a football (Brown et al, 2014a). For all participants this was the right leg. Muscles investigated throughout all studies included the vastus lateralis (VL), rectus femoris (RF), biceps femoris (BF), tibialis anterior (TA), lateral gastrocnemius (GL), medial gastrocnemius (GM) gluteus maximum (GMAX) and soleus (SOL). Fig. 2.3a-h shows the electrode placement for all muscles, which adhered to the recommendations for Surface Electromyography for the Non-invasive Assessment of Muscles (SENIAM; Hermens et al, 2000). Furthermore, participants were asked to perform muscle

function-specific movements to accurately select the electrode location, confirmed by palpation. These included: knee flexion for identification of hamstring muscles (i.e. BF); knee extension for quadricep muscles (i.e. VL, RF); plantarflexion for calf muscles (i.e. SOL, GM, GL); dorsiflexion for shin muscles (i.e. TA) and a deliberate contraction of the gluteal muscles, where the instruction was given to squeeze the buttocks, for GMAX. Once the muscle was clearly identified, bipolar surface EMG electrodes (1mm width, 10mm pole spacing; CMRR>80dB; model DE2.1, Delsys Inc, USA) were attached to the skin above the muscle belly with double-sided adhesive interfaces (Delsys Inc, USA). Visual inspection of the strength of the EMG signal confirmed the electrode placement for each muscle. Prior to sampling, the EMG signals were pre-amplified x100 for VL, RF, GMAX and BF and x1000 for TA, GL and SOL, and band-pass filtered (20-450 Hz) at the main unit (Bagnoli-8, Delsys Inc., USA).

Figures 2.3 a-h: Electrode placement for the nine studied muscles within the thesis studies in accordance with Surface Electromyography for the Non-invasive Assessment of Muscles recommendations; a) Vastus Lateralis (VL); b) Rectus Femoris (RF); c) Biceps Femoris (BF); d) Gastrocnemius Lateralis (GL); e) Gastrocnemius Medialis (GM); f) Soleus (SOL); g) Tibialis Anterior (TA) and h) Gluteus Maximum (GMAX).

The skin area under each electrode was shaved, exfoliated and cleaned with an alcohol swab (ethyl propanol) prior to placement. The grounding electrode was placed over the patella in all studies (Dermatrode, Biosence Medical LTD, UK). Transpore and zinc oxide medical tape was

placed over each electrode for extra security and to minimise movement over the skin. During all non-SkinSuit conditions, self-adherent elastic wrap (Coban ^{TM,} 3M PLC, UK) was applied around the leg above the EMG electrodes to additionally secure their stability and to replicate the compression applied while wearing the SkinSuit. The skin impedance condition was evaluated at rest prior to the start of the experimental procedures and was considered of good quality when the average rectified EMG baseline level for each muscle was below 2 µV (Huigen et al, 2002). For consistent EMG placement across days when the study required multiple laboratory visits (as per Chapters 4 and 6), a rectangle was drawn around the sensor with a semi-permanent marker.

2.3.6 Knee joint angular movement

An electrogoniometer (SG110; accuracy ± 2°; Biometrics Ltd., UK) was positioned to measure sagittal plane motion about the knee joint during running (Chapter 4). The electrogoniometer was fixed with double-sided tape to the skin laterally alongside the line between the greater trochanter and the lateral malleolus and centred around the right lateral epicondyle of the femur as per the manufacturers' instructions (Fig. 2.4). The position of the sensor was reaffirmed with zinc oxide tape. Calibration of the electrogoniometer was performed using Datalink V7.1 Analysis Software (Biometrics Ltd, UK) by ensuring the participant firstly maintained a position of full knee extension, which was subsequently set as 0°, after which the participant was asked to flex the knee to 90°, as confirmed by a manual goniometer, which was then set on the software. Signals were pre-amplified via a conditioning unit (DLK900; Biometrics Ltd., UK) mounted on a belt around the waist of each participant.

Figure 2.4: An electrogoniometer fixed laterally on the right side alongside the line between the greater trochanter and the lateral malleolus and centred around the right lateral epicondyle.

2.3.7 Pedoped® pressure-sensitive foot insoles

Pedoped® (Novel GmbH, Germany) are pressure-sensitive shoe-insoles (Fig. 2.5) which accurately measure the normal plantar force detected inside the shoe during all static and dynamic activities. The Loadsol® software provides total load from the foot at a frequency of 83.33Hz via a combination of three separate sensors; heel force, mid-foot force, and front-foot force. This technology has a matchbox-sized electronics and communicates wirelessly with a smartphone/tablet via Bluetooth. The usage involved transmitting the data to an Ipad application in realtime (Pedoped loadsol, version 1.4.74). The insoles were calibrated for each participant individually prior to the experiment, taking into account the weight of their clothing and equipment required for the protocol. The resulting forces in Newtons were used in order to conduct the calibration procedure, where each foot was completely unloaded whilst zeroing the insole, placing the entire bodyweight load on the other foot. This process was repeated for both feet. These data were used only to identify heel strike, for the purpose of the EMG analysis during the study that served Chapter 7 (refer to section 2.4.3.1).

Figure 2.5: Pedoped® pressure-sensitive foot insoles, which allow continuous detection of plantar ground reaction force at a sampling frequency of 83.33Hz. This image is adapted from http://novel.de/novelcontent/newsflash-2015; copyright Novel GmbH.

2.3.8 ForceShoe™

The loading characteristics of each SkinSuit are unique and depend on the tightness of the ankle stirrups, though there are material "notches" that the stirrups should be pulled over, that act almost like a one-way valve, to ensure the load provision does not change during movement. Loading was quantified prior to each study using the XSENS ForceShoe™ worn on each foot (XSENS Technologies, Enschede, The Netherlands; Fig. 2.6). Each ForceShoe™ consists of 2 force-sensitive resistor sensors (front and back) located on a flexible printed circuit board, a wireless circuit and an accelerometer located at the back of the shoe. Continuous recordings of the axial body loading in three axes (anteroposterior [x], mediolateral [y] & longitudinal [z]) was taken from each ForceShoe™ while the participant stood quietly for 10s with the stirrups undone to record their standing "unloaded" weight, followed by further 10s of quiet standing

once the researcher had fixed the stirrups around the participant's feet to determine the additional load provided by the SkinSuit.

Data from both ForceShoes™ were digitised with a sample frequency of 50Hz and wirelessly transmitted via Bluetooth to a laptop using the XSENS Xbus Master device. Data were visualised and analysed in real-time using the MT SDK software (Xsens Technologies, Enschede, The Netherlands). A calibration procedure was automatically performed by the software before any participant measurements.

Figures 2.6a-c: XSENS a) Wireless Receiver (WR-A) b) set of ForceShoes™ with two load cells (front and back) each, and c) the XBus Master. This image is adapted from http://www.popdiatry.com/?p=264; copyright XSENS Technologies B.V.

2.4 Analytical methods

2.4.1 Skinsuit-induced axial body load (ABL) quantification

The SkinSuit-induced ABL was quantified for each participant using only the z-axis data collected. This occurred prior to participation in the respective study, with the exception of the

study that served Chapter 4, where due to equipment unavailability, was quantified on the same day but after the experimental trial.

The time series (F_z) obtained from all four sensors (two from each foot; [F_{zI}, F_{zII}, F_{zIII},F_{zIV}]) in the ForceShoes were exported into text files to derive the Gz-load using the following calculations:

First, the corresponding lapsed time (t, s) for each data point was calculated using the standard Nyquist sampling theorem (equation 1):

$$t = \frac{n}{f} \quad \textbf{(1)}$$

where n is the number of data points and f is the sampling frequency of 50Hz used during data acquisition.

The corresponding loading force (N) at each time point (t) was calculated as the sum of values from all four sensors (I, II, III, IV) thus forming a time series of force data points $F_{Z,TOT}(t)$ (equation 2):

$$F_{Z,TOT}(t) = F_{Z,I}(t) + F_{Z,II}(t) + F_{Z,III}(t) + F_{Z,IV}(t) \quad \textbf{(2)}$$

The axial force ($\bar{F}_{Z,TOT}(t), N$) acting on the body during each 10s period was calculated as the average of the force $F_{Z,TOT}(t)$ recorded at each data point within this period (equation 3):

$$\bar{F}_{Z,TOT}(t) = \frac{1}{n}\sum_{i=1}^{n} F_{Z,TOT}(t_i) \quad \textbf{(3)}$$

The $\bar{F}_{Z,TOT}(t)$ was then converted to a ratio of gravity (G_z; *equation 4*):

$$G_z = \frac{\bar{F}_{Z,TOT}(t)}{w \cdot g} \quad \textbf{(4)}$$

where **w** is the subject's body mass in kg and ***g*** is the Earth's gravitational acceleration constant (9.80665 $m.s^{-2}$).

Throughout all experimental Chapters, the ABL inclusive of SkinSuit-loading data is reported. Furthermore, loading for all body segments was also calculated, according to conventional body segment mass data (Churchill et al, 1978). For the purpose of this thesis, only the thigh and shank segments are reported.

2.4.1.1 SkinSuit-induced axial body load in static postures and walking

Prior to the assumption of any experimental work and using the procedures outlined above, the ABL provided by the SkinSuit (AL) was quantified by 6 participants to understand between-posture differences – standing, foetal, prone and supine. Furthermore, participants were also required to walk both in AL and in loose-fitting clothes (CONTROL). All activities were assumed for 30s and repeated three times, and the results display an average of the three trials for each posture and activity; walking also included the calculation of maximum ABL. Average values for all four static positions were 0.12Gz, 0.17Gz, 0.19Gz and 0.11Gz for standing, supine, prone and foetal, respectively. Fig. 2.7a portrays an excerpt from one of the three walking trials from a representative participant. Average and maximum load during walking were 0.97Gz & 1.06Gz and 1.75Gz vs. 1.82Gz for CONTROL and SkinSuit, respectively (Fig. 2.7b).

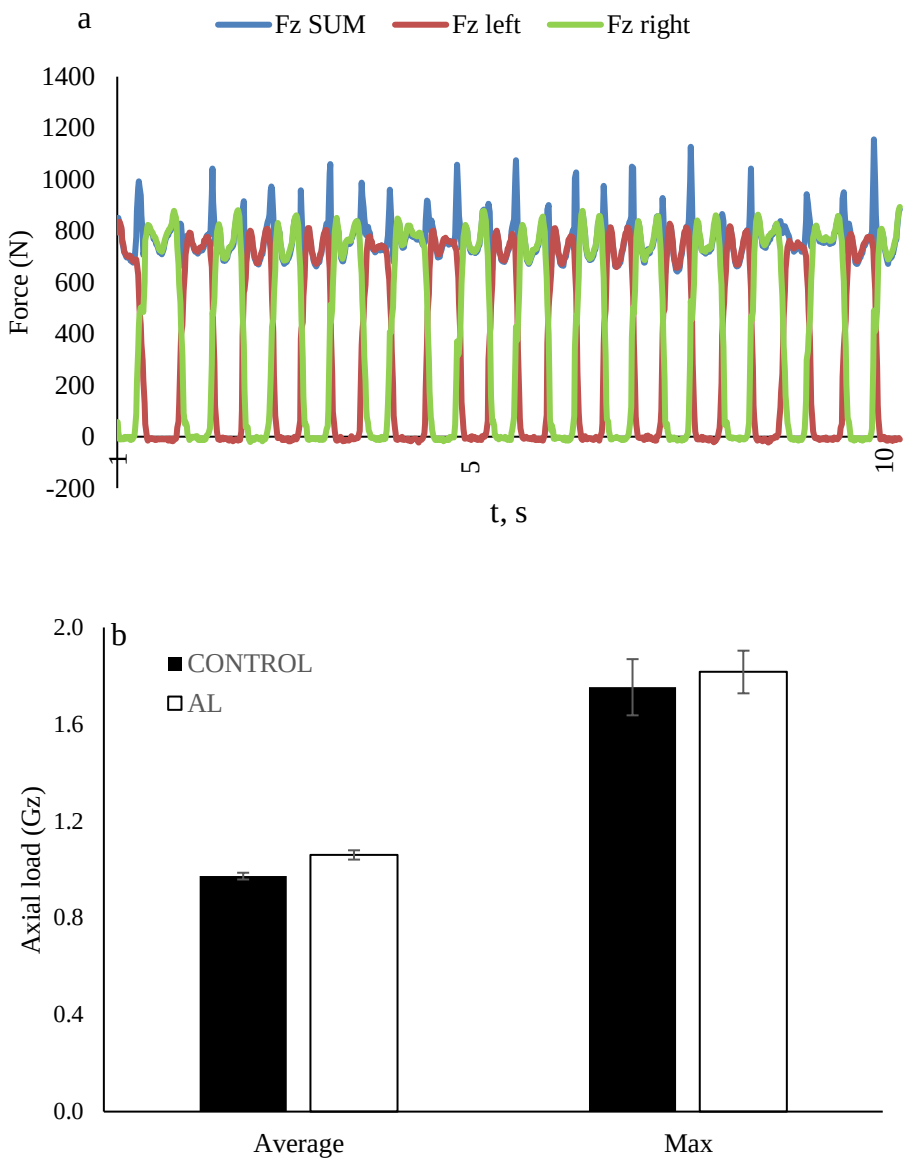

Figures 2.7 a and b: a) exemplar data from one of the three walking trials for one representative participant in the SkinSuit, depicting left and right foot forces separately as well as total force in the Z-axis; b) average and maximum Gz from an average of three walking trials per participant, in both AL and CONTROL.

2.4.2 Cardiorespiratory variables

As well as HR data from either acquisition method detailed above (section 2.3.4), the following respiratory variables were extracted from the metabolic cart for analysis: minute ventilation

($\dot{V}_E$; L/min^{-1}), tidal volume ($\dot{V}_T$; L), $\dot{V}O_2$ (ml.kg.min^{-1}), $\dot{V}CO_2$ (ml.kg.min^{-1}), breathing frequency (BR; breaths/min) and RER.

Expired gas concentrations ($\dot{V}O_2$ & $\dot{V}CO_2$) were automatically corrected for standard temperature and pressure, dry (STPD), and expiratory flow volumes ($\dot{V}_E$ & $\dot{V}_T$) for body temperature and pressure saturated (BTPS).

2.4.3 Analysis of the EMG data

All of the following EMG variables were extracted for all three Chapters involving the investigation of neuromuscular function, except for the cross-correlation function, which was undertaken only for HYPERLOAD comparisons.

2.4.3.1 Signal conditioning

Data were analysed off-line using standard and custom written scripts developed in Spike2 version 7 (Cambridge Electronic Design, UK). A set of time-amplitude and spectral parameters were extracted from the recorded EMG signals and compared across the respective conditions to investigate their effects on muscle activation levels and patterns. Prior to parameter extraction, a high pass IIR filter with a 10 Hz cut-off frequency and a Butterworth 4th order band stop notch filter between 49 and 51 Hz were applied to each EMG signal to improve the signal-to-noise ratio.

The extraction of the EMG parameters was performed on a motion cycle-by-cycle basis. The start of each revolution within the continuous cycling protocol reported in Chapter 4 was identified from the rectified VL EMG signal, since the peak knee extensor activity during cycling occurs near top dead centre (TDC) of the revolution (Baum and Li, 2003, Hug et al,

2006, Shinohara et al, 1997). The start of each stride during running was identified as the point of peak knee extension as measured by the electrogoniometry (Chapter 6), or as the start of heel force development (heel strike) measured via the Pedoped foot insoles (Chapter 7). The identified consecutive revolutions/strides were automatically labelled with event markers using a standard script (Spike2, CED, UK; Fig. 2.8) based on a double threshold-crossing method within pre-defined time intervals based on the cycling/running speed.

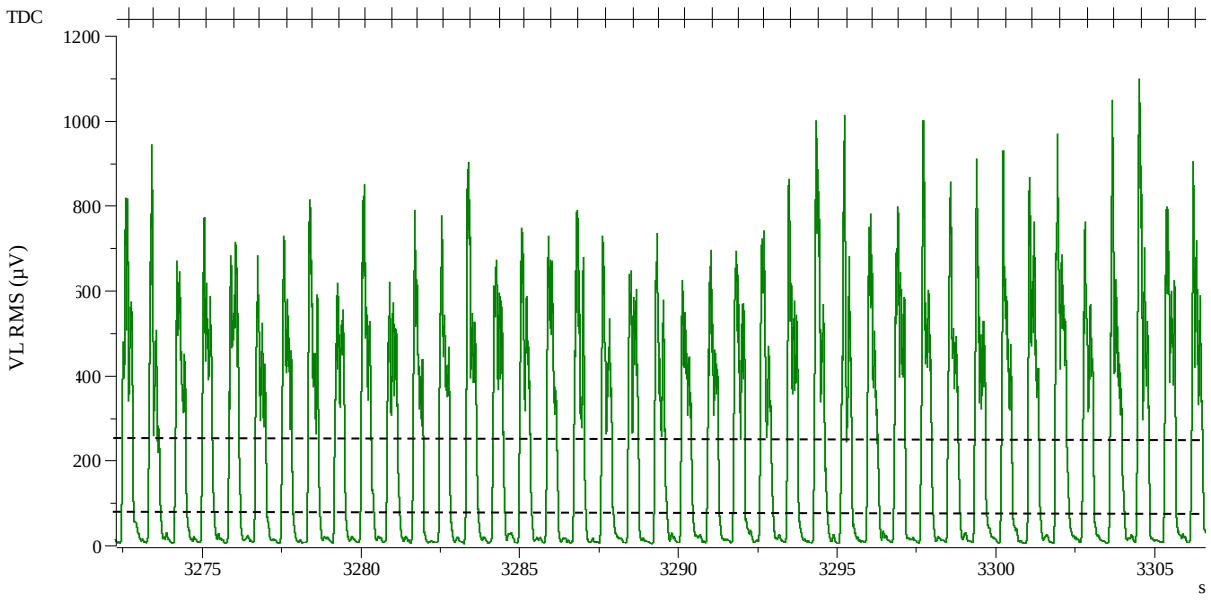

Figure 2.8: Illustration of the procedure for identifying of the consecutive revolutions within the cycling trial. The VL EMG activity was extracted from the CONTROL trial of a representative participant during 50W cycling. VL EMG was rectified and then smoothed with a time constant of 0.025s. Dashed horizontal cursors illustrate the thresholds for recognition of the consecutive peaks. The script automatically generates a channel (TDC) which stores the vertical markers (events) for each peak identified within a specified search time period.

2.4.3.2 Time-amplitude EMG parameters

The EMG signals were full-wave rectified and smoothed using a moving average method with a time constant of 0.025s. The baseline level of the EMG signal for each muscle was evaluated by the mean and standard deviation of the rectified record within a specified rest period

preceding activity. Regardless of the activity mode, participants were instructed to have the right leg fully extended and relaxed for baseline EMG data acquisition. The rectified EMG time series between two consecutive event markers within a stage of the exercise (study-dependent on cycling power or running speed) were extracted for each muscle from the records of the individual participants. These series were recalculated to an arbitrary time scale (from 0 to 100% relative stride for the running studies and from 0-360° for the cycling study) to allow for calculation of the average EMG pattern representing the individual power output/speed stages within a trial (Kleissen et al, 1989). A horizontal line visualised the mean+2*SD baseline EMG level for determination of the onset and offset of muscle activity from each average EMG pattern (Fig. 2.9a). The crosspoints between the EMG profile and the baseline level were automatically recognised to identify the onset and offset EMG points, although the script allowed for manual adjustment to avoid erroneous timing determination (Fig. 2.9a). The period elapsed between them identified the overall duration of EMG activity within a revolution/stride (Fig. 2.10). The EMG root mean square (RMS) amplitude was computed between the onset and offset points using the calculation below, in the case of a set of *n* values (equation 5):

$$\sqrt{\frac{x_1^2 + x_2^2 + \ldots + x_N^2}{N}} \quad \textbf{(5)}$$

Due to the timing of muscle activities during both cycling and running, most muscles began their activity close to TDC/heel-strike. Thus, the calculation of RMS in this case was the sum of the latter segment (i.e. the onset cursor to the end of the revolution or stride), added to the segment starting at 0 until the offset cursor – indicative of a new stride; this process is depicted for both muscles in Fig 2.9a.

2.4.3.3 Spectral EMG parameters

The EMG signals were filtered and non-rectified to conduct spectral analysis of the signal. Power spectral density of the EMG profile for each muscle was calculated using Fast Fourier Transform with a block size of 2048ms using a Hanning window function and presented between 0 and 500 Hz in 1024 bins at a resolution of 0.4883 Hz (Fig. 2.9b). The Fourier Transform was performed using a standard procedure using the generated events marking the revolutions/strides within the preselected analysis stage at each power output/speed as gates (Spike2, CED UK). The Median Frequency (MDF) is a frequency at which the EMG power spectrum is divided into two regions with equal amplitude, also defined as a half of the total power. The MDF is used in the assessment of muscle fatigue, represented as a downward shift of the frequency spectrum of the EMG signal (Phinyomark et al, 2012) and was calculated for each muscle using the following formula (equation 6):

$$\int_{o}^{f_{med}} S_m(f)\, df = \int_{f_{med}}^{\infty} S_m(f)\, df \qquad \textbf{(6)}$$

Where $S_m(f)$ is the power density spectrum of the EMG signal (Basmajian, 1985).

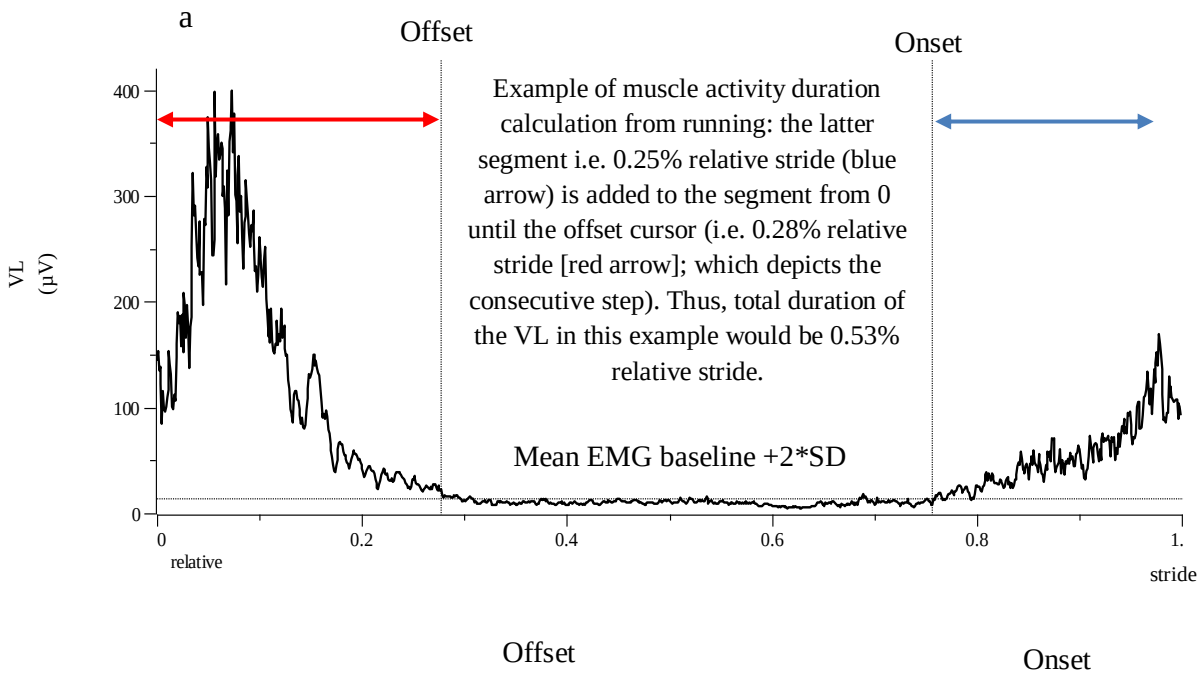

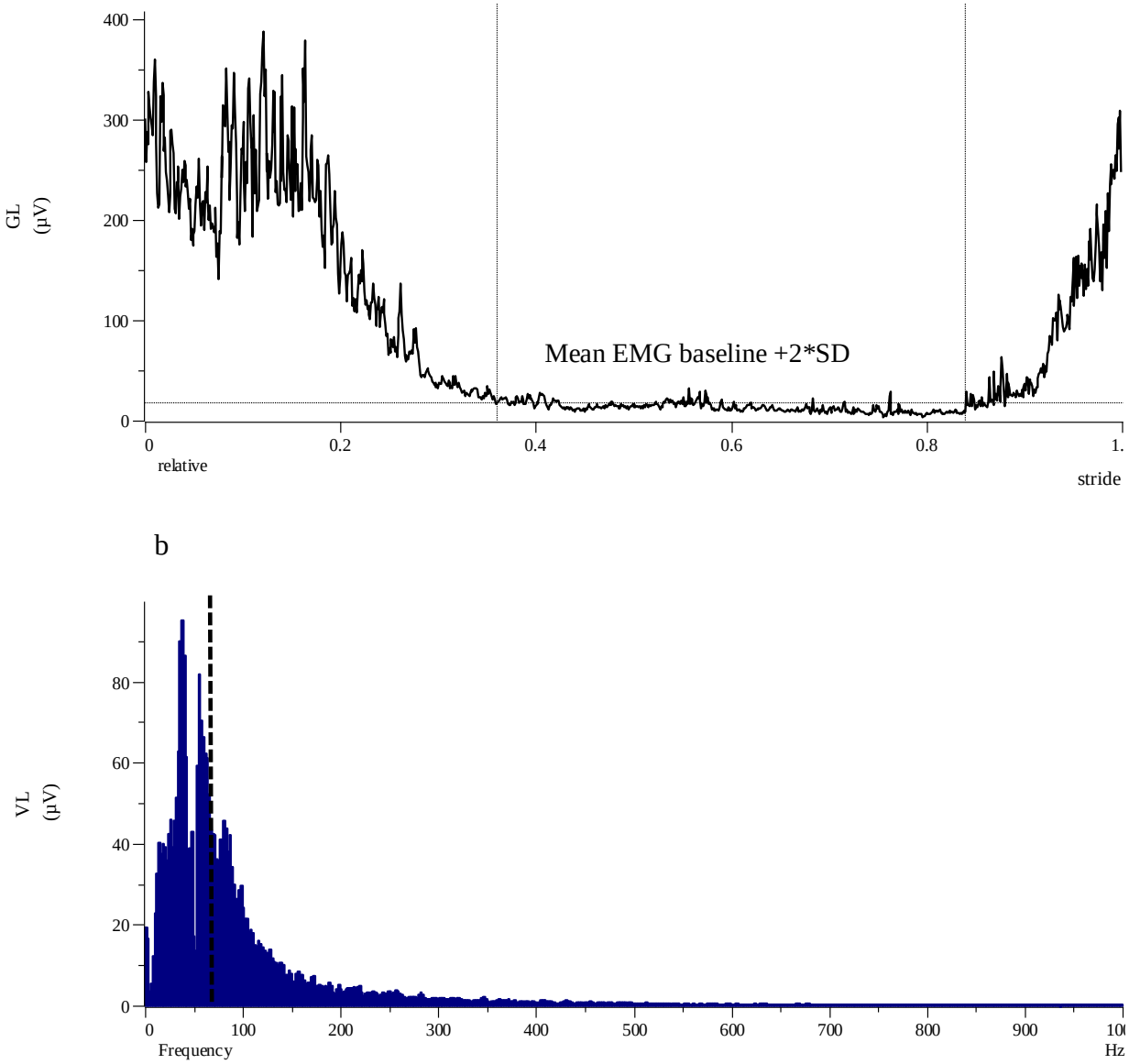

Figures 2.9 a and b: Example from a representative participant running at 9km·h^{-1} at 1Gz of a) EMG ensemble envelope from the VL (top image) and GL (bottom image) muscles. Figure 2.9a also contains a description of how the muscle activity duration was calculated. Vertical cursors signify onset and offset times (right and left respectively); horizontal cursor represents mean EMG baseline +2*SD. b) the total power spectrum for the VL, where- - - - - indicates the median frequency.

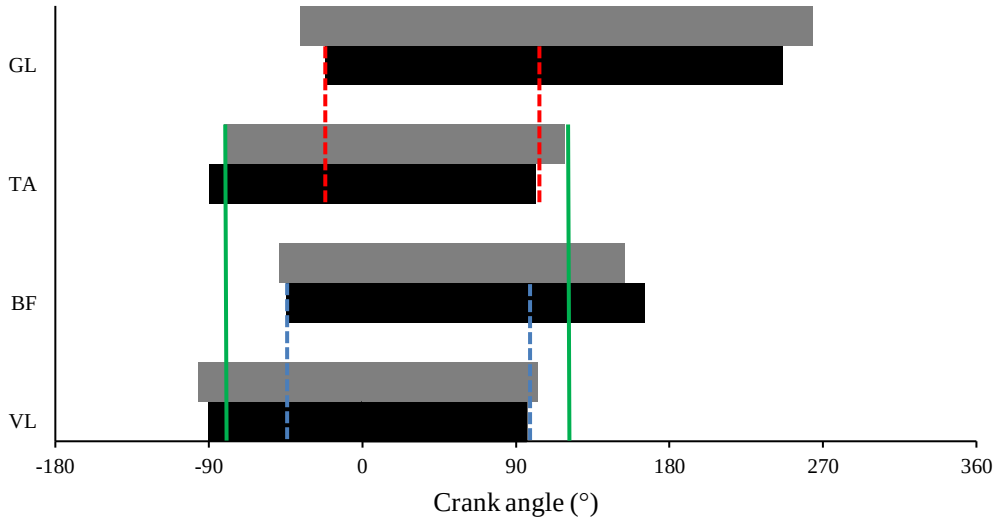

Figure 2.10: An example of the method undertaken to analyse duration of muscle activity and muscle pair co-contractions. This graph is an extract from Chapter 4, which shows EMG RMS for 4 studied muscles for two loading conditions during 50W cycling. The solid green lines show an example of the calculation of muscle activity duration from the TA muscle in the axial loading condition, which is the sum of the onset and offset crank angle i.e. 118° + (0--80°), resulting in a duration of ~198°. The dashed blue and red lines show the period of co-contraction (the length of a revolution they overlap for) for the VL/BF and the TA/GL muscle pairs during the CONTROL condition (black bars) respectively.

2.4.3.4 Analysis of muscle activation patterns

As well as the aforementioned muscle activity onset, offset and duration variables computed from the time-amplitude signal, a number of other analyses were undertaken to provide information about muscle activity patterns.

2.4.3.4.1 EMG pattern similarity

Comparison of the correlation coefficient (r) to identify similarities in muscle activity patterns between conditions was employed in all studies. Furthermore, the cross-correlation function between a pair of time series representing the average rectified muscle EMG profile within a stride/revolution at different conditions were computed using a standard iterative procedure

(Origin, ver. 6, MicroCal™ Inc, USA; Li and Caldwell, 1999). The lag time that corresponds to the maximal value of cross-correlation function was calculated to determine the phase shift between the two EMG profiles (Dorel et al, 2008), expressed as a mean lag ± 95% confidence interval – with significance defined as $p<0.05$ if the lag and/or its confidence interval range does not pass through 0° (Li and Caldwell, 1999). The left panel in Fig. 2.11 presents an example of two EMG patterns for which the cross-correlation function was calculated. The relative lag in the cross-correlation function was extracted to quantify condition- and power/speed-induced displacement in muscle activation within a revolution/stride. The maximal correlation coefficient within the cross-correlation function evaluated the strength of the relationship between the compared EMG patterns. To allow comparison between the conditions tested during separate visits each EMG profile was normalised to the mean EMG RMS from 50W (for Chapter 4), 9km·h^{-1} (for Chapter 6) and 1Gz CONTROL (Chapter 7) stages, for each muscle within a condition (Winter and Yack, 1987).

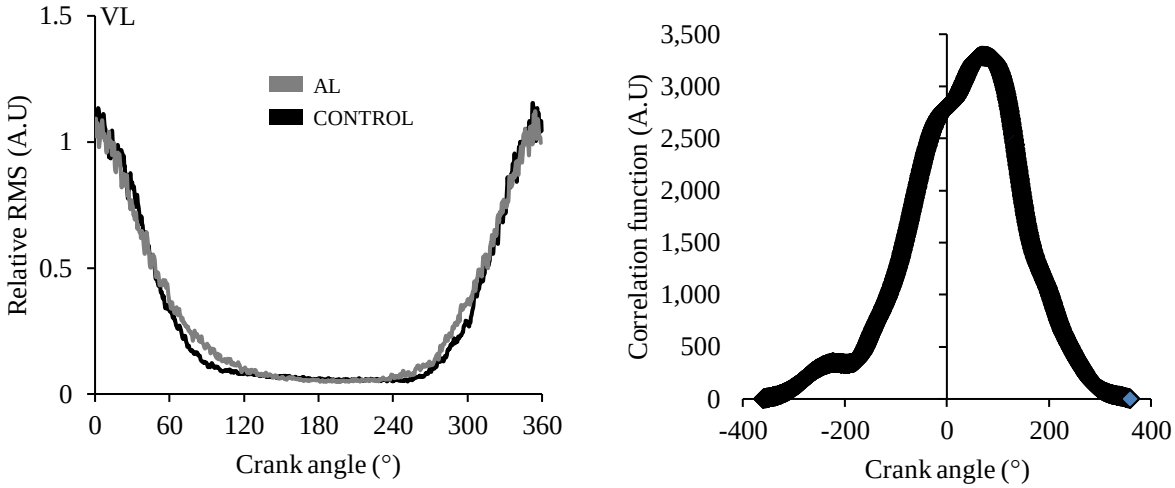

Figure 2.11: Example from the VL muscle of a representative participant cycling at 50W of ensemble of the EMG RMS envelope in AL and CONTROL (left image) and the cross-correlation function between 9km·h^{-1} and 13km·h^{-1} in CONTROL (right image).

2.4.3.4.2 Muscle co-contractions timing

Co-contractions of the antagonistic (VL/BF & TA/GL) and synergistic flexor (BF/TA) and extensor (VL/GL) muscle pairs were quantified by calculating the duration of the overlap in the EMG activation timing (Fig. 2.10).

2.4.4 Kinematic variables

As with the EMG data, an averaged right knee angle profile within a revolution or stride from the selection data portion was computed from the electrogoniometer (Fig. 2.12). Cursors were automatically pre-configured to identify heel strike (HS), toe-off and maximum flexion as per the procedures set out in James et al (2013). This enabled the computation of knee angle at all of these points and thus total knee ROM. Furthermore, stance ratio – defined as the relative duration from heel strike to toe-off (% stride) and stride duration – defined as the time taken from heel strike to the following heel strike (s) – were also calculated.

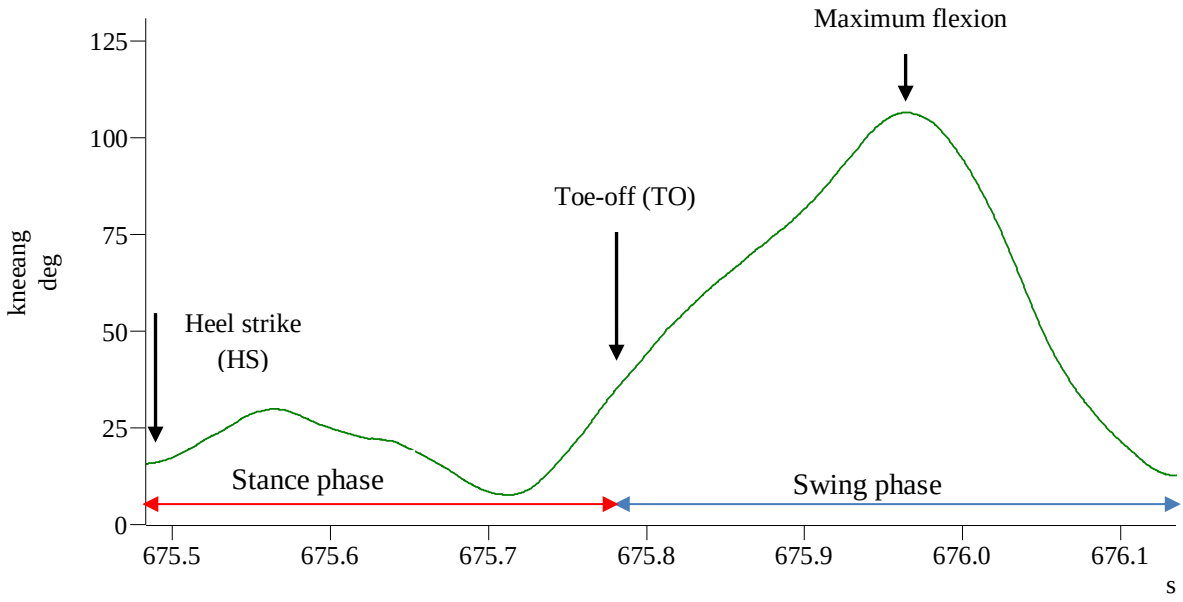

Figure 2.12: Example knee profile during a gait cycle, from heel strike to the following heel strike. The red arrow denotes approximately the timing and duration of the stance phase; the blue arrow denotes approximately the timing and duration of the swing phase.

2.5 Statistical analysis

With the exception of the correlation coefficient and the cross-correlation function, all variables are displayed as means ± standard error mean (SEM) and were statistically analysed in SPSS statistical software (IBM, version 24), with significance set to $p<0.05$. For all Chapters, repeated measures ANOVA was used, though with differences in the number of factors and levels with post-hoc tests utilised where necessary. Specific details can be found on a Chapter-by-Chapter basis. The correlation coefficient was assessed with a Pearson's test where a significant result was defined as different from $r=0$ ($p<0.05$). Strong correlations were stipulated as an r value of between 1-0.7; moderate as 0.7-0.3 and weak as 0.3-0.

Chapter 3: The influence of additional axial body loading on cardiorespiratory responses during cycling in 1Gz

3.1 Introduction

3.1.1 Chapter 3 & 4 collective introduction

Stationary cycle ergometers induce standardised workloads that are almost completely unrelated to our joints. Furthermore, biomechanical constraints of the cycling motion render minimal postural disturbances (Brown et al, 2005). Thus, cycle ergometry facilitates the study of movement patterns under controlled conditions (Hug and Dorel, 2009) and is suitable for training and rehabilitation scenarios (Fonda and Sarabon, 2010).

During cycling, total mechanical work is achieved by a combination of external work (to push the legs against external resistance) and internal work (to accelerate and decelerate the leg segments with changes in speed [cadence]; Kautz & Neptune, 2002). The saddle stabilises the body in the vertical plane, and the pedals transform the alternate action of the limbs into a continuous forward motion, minimising the amount of energy wasted against gravitational and inertial forces with each pedal cycle (Di Prampero, 2000). Virtually no external work is performed on the body centre of mass, and the measurement of the net metabolic rate is representative of the metabolic energy required to impart rotary motion to a predefined mechanically loaded crank.

Despite cycling requiring leg movement in a predefined circular trajectory (Hug & Dorel, 2009), it involves complex coordinated neuromuscular effort. Studies of muscle activity patterns in 1Gz have shown that co-activation between single- and two-joint antagonists, results

in a synchronous transfer of mechanical energy between joints (Wakeling et al, 2010). Mono-articular muscles, such as the vastus lateralis (VL) and tibialis anterior (TA), play a relatively invariant role as primary power producers (Hug et al, 2004a) and elevate activation with increasing workload to a greater extent than bi-articular muscles, such as the biceps femoris (BF) and gastrocnemius lateralis (GL; Fonda and Sarabon, 2010). In contrast, bi-articular muscles act during the upstroke (i.e. bottom dead centre [BDC] to top dead centre [TDC]) to improve the efficiency of energy transfer between the segments and can also act during the downstroke to contribute to extension of the knee, as seen in the rectus femoris for example (RF; Raasch and Zajac, 1999).

3.1.2 Chapter 3-specific introduction

As pedalling rate accelerates beyond approximately 60 rpm during constant mechanical power pedalling, $\dot{V}O_2$ is elevated (Hagberg et al, 1981), presumably as a result of increased internal work to move the legs faster (Kautz and Neptune, 2002). The energy required to sustain a given bicycle workload has been also shown to correlate with power output (Banister and Jackson, 1967) and bodyweight (i.e. load; Lafortuna et al, 2005; Lafortuna et al, 2008). In a study investigating the metabolic responses to cycling in normal weight vs. obese women at a range of metabolic intensities, the latter were shown to consume more energy (~23%) at all of them (Lafortuna et al, 2008). This suggested an increase in internal work; the energy involved in moving heavier legs (Cotes et al, 1969), possibly including also the energy to stabilise the trunk while pedalling on the ergometer (Lafortuna et al, 2005).

However, investigation of the influence of bodyweight on cycling in varying-weight individuals is confounded by factors, such as fitness level, body composition, i.e. fat mass (Goran et al, 2000), and obesity-related changes (i.e. autonomic impairment of cardiac

regulation; Liatis et al, 2004). Thus, investigation of the effects of additional imposed load on the metabolic cost during cycling have been attempted. Moreover, based on the positive correlation between $\dot{V}O_2$ and bodyweight during cycling (Adams, 1967), it is unsurprising that these methods have also been used to potentiate training stimuli. Kamon et al (1973) observed additional $\dot{V}O_2$ (367±41ml.min^{-1}) in healthy participants who pedalled at 75rpm with 10kg ankle weights, at a resistance of 500-600kilopond.min^{-1}. The addition of lower extremity weights (3% bodyweight initially then increased by the same amount each week for 8 weeks) during cycle ergometry have also been utilised in clinical populations, such as stroke patients, where significant elevation of peak $\dot{V}O_2$ were observed (Jin et al, 2011). Although the provision of axial body load (ABL) by the SkinSuit is through elastic tension rather than the addition of mass, it is unknown whether the requirement to overcome the ABL would result in similar cardiorespiratory responses during cycling compared to those which have utilised the latter.

The Penguin suit, which provided forces equivalent to ~25kg and ~ 16kg for males and females, respectively through elastic strain, was worn during incremental cycling in 10 Cosmonauts aboard the ISS, increasing metabolic cost by 20-30% (Barer et al, 1998). Interestingly cycling with a greater magnitude of additional loading in microgravity via the Penguin suit induced similar augmentation in metabolic cost as with a lighter load in 1Gz (Kamon et al, 1973). However, no performance data are available from the Barer et al study; it is likely that participants' power output was greater than that in the Kamon et al study. Moreover, Barer et al's study was performed in weightlessness and at present it is unknown how the addition of a small axial loading "dose" within a simulated reduced-gravity environment affects cardiorespiratory responses to exercise.

Subjective perceptions have been shown to have a profound impact on performance metrics (Marcora and Staiano, 2010). Ratings such as thermal comfort and perceived exertion (RPE) have been utilised as surrogate measures of core temperature and cardiovascular strain (i.e. heart rate respectively; Tikuisis et al, 2002). Performance decrements related to these perceptions have been observed in tasks involving 120min light to moderate treadmill-walking whilst wearing additional firefighter ensemble ranging from ~2-20kg (Borg et al, 2017). Furthermore, performing tasks which require a sustainable cognitive aspect, as demanded in numerous sporting endeavours can also contribute to increased RPE, with a negative impact on performance (Smith et al, 2015). It is of additional relevance to understand how such perceptions and any interactions with performance, are affected by ABL.

3.1.3 Aims & hypotheses

The aim of this study was to test the hypotheses that 0.12Gz additional ABL would: increase cardiorespiratory variables; affect performance metrics, by reducing $\dot{V}O_2$Max and total work/time to exhaustion; and worsen subjective perception of exertion and comfort, compared to those observed during 1Gz cycling.

3.2 Methods

3.2.1 Participants

Eight healthy male participants (29.6±5.6 yr; 177.1±6.8 cm and 74.2±7.1 kg; Table 3.1) gave written informed consent to participate in the study.

3.2.2 Experimental Protocol

This study was a pseudo-randomised, counterbalanced repeated measures HYPERLOAD (refer to Chapter 2, section 2.3.1) design (Fig. 3.1). Participants firstly came to the laboratory for a familiarisation session, during which their individual cycling configuration was defined. The height of the saddle was adjusted to obtain a hip joint angle of 90° upon full knee flexion. This session was also used to quantify the individual ABL produced by wearing the SkinSuit (refer to Chapter 2, section 2.4.1) and to familiarise the participants to cycling whilst wearing it.

The population average total ABL was quantified prior to the experiment while standing in the SkinSuit with the stirrups fixed around the ankles, which was 1.12 ±0.01 Gz (Table 3.1). The loading was individual-specific and varied between 1.07Gz and 1.16Gz within the studied population. The estimated average loading across the thigh thus ranged between 1.08 and 1.10Gz and across the lower leg – between 1.10-1.12Gz.

Following the familiarisation session, participants attended the laboratory on two days, separated by at least 24 hours. Each day comprised a $\dot{V}O_2$Max test in either loose-fitting clothing ("CONTROL") or with their SkinSuit, providing 0.12Gz additional axial loading ("AL").

$\dot{V}O_2$Max was determined via performance of a stepwise incremental exercise test on an upright cycle ergometer (Lode Corival, Groningen, The Netherlands) whereby participants were asked to maintain 70RPM for the duration of the test. Participants initially sat on the ergometer for 2 min (REST) before starting a 2 min warm up at a power output of 50 Watts (W), after which workload was automatically increased in 50W increments (using JLAB software from the

metabolic cart) every 3 min (Keren et al, 1980; Fig. 3.1a) until voluntary exhaustion. At the beginning of each experiment, the height of the saddle was adjusted accordingly to obtain each participants' preconfigured cycling posture.

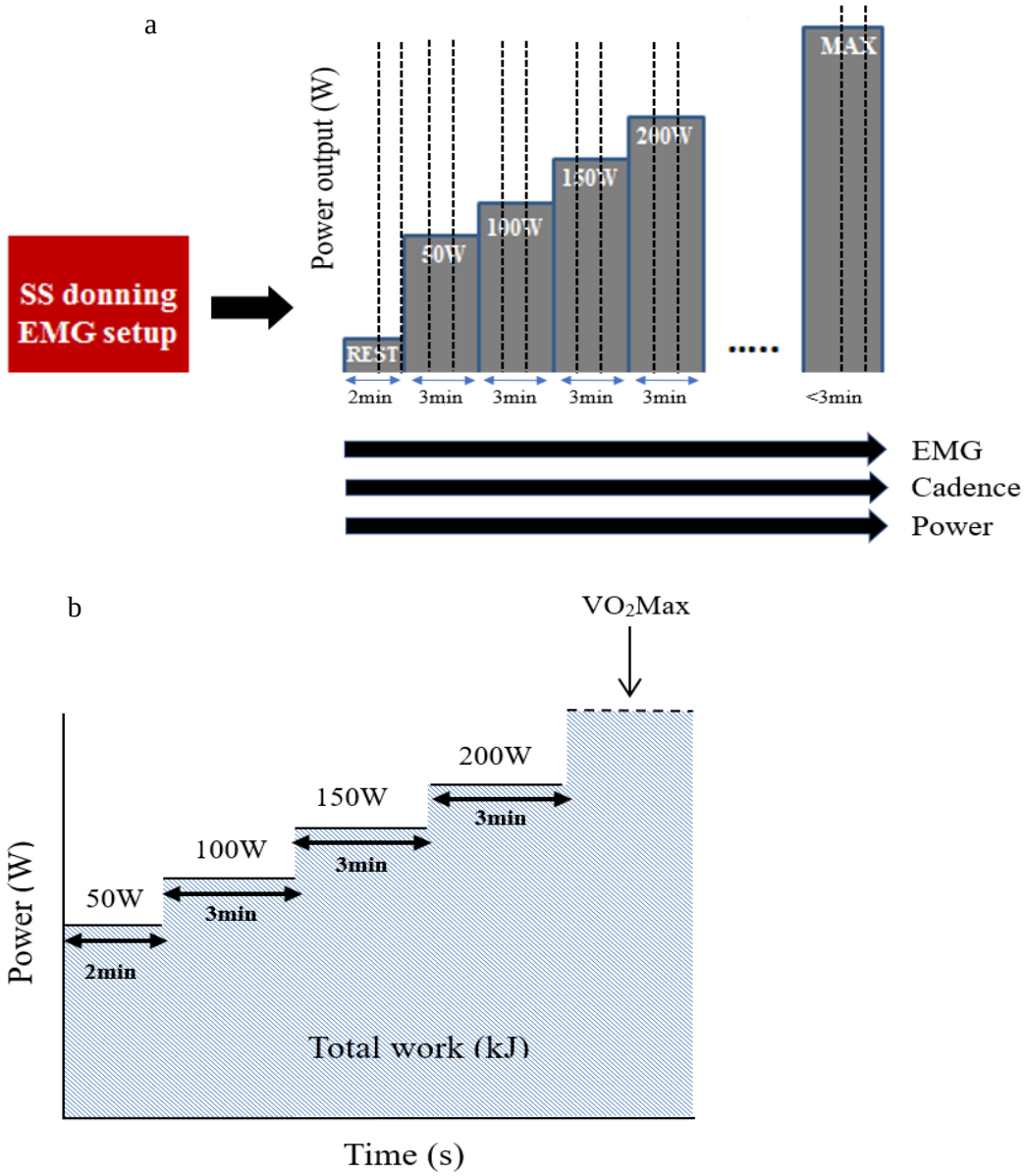

Figures 3.1 a and b: a) Schematic illustration of the experimental design and muscle EMG activity identification. During the main trials the participants were wearing either a MK VI SkinSuit or loosely-fitting gym clothes and performed a stepwise incremental cycling test to exhaustion (MAX). The dashed lines per power output stage are indicative of the portion whereby data was extracted from and analysed. b) Schematic depicting calculation of total work. Final power output is variable owing to differing $\dot{V}O_2$Max-attainment workloads.

The cycling cadence was continuously recorded during the trials using the JLAB software. Breath-by-breath expiratory flow (via an oro-nasal mask secured to the head) and expired gas concentrations (Oxycon Pro, Care Fusion, USA) were recorded continuously in addition to heart rate (HR; 3 lead ECG; HME LifePulse, UK). ECG data were sampled at 1kHz via a digital to analogue converter (Powerlab ADC, AD Instruments, Australia) and recorded in LabChart7.1. Subjective ratings of perceived exertion (RPE; Borg, 1982), thermal comfort (ASHRAE 7-point scale; Zhang and Zhao, 2008), body control (Modified Cooper-Harper scale; Cooper and Harper, 1969) and movement discomfort (Modified Corlett and Bishop scale; Corlett and Bishop, 1976) were obtained at REST and during the second minute of each stage until $\dot{V}O_2$Max.

3.2.3 Data Analysis

HR data were analysed at REST (mean over the second minute) and over the third minute of every power output. Breath-by-breath respiratory data were sampled directly from the metabolic cart (Oxycon Pro, Carefusion, California, USA), providing 10s means of breathing frequency (BR; breaths.min), expiratory tidal volume ($\dot{V}_T$; l), minute ventilation ($\dot{V}_E$; l.min^{-1}), mass-corrected oxygen consumption ($\dot{V}O_2$; ml.kg.min^{-1}), carbon dioxide production ($\dot{V}CO_2$; l.min^{-1}) and RER. These parameters were calculated at REST (mean of all breaths over the second minute), 50-200W stages (mean of all breaths over the final min) and at $\dot{V}O_2$Max (which included data from the 10s prior to and following $\dot{V}O_2$Max) in CONTROL and AL. The mean cadence during each 3min power output stage was also calculated for both conditions at 50W and MAX. Maximal Oxygen consumption ($\dot{V}O_2$Max), total test duration and consequential total work (kJ; Fig 3.1b) and the maximum power (W) required to achieve $\dot{V}O_2$Max were determined at $\dot{V}O_2$Max. The ventilatory breakpoint, indicative of the anaerobic

threshold, was determined by the Oxycon Pro software, and the $\dot{V}O_2$ at the ventilatory breakpoint computed.

3.2.4 Statistical Analysis

Having determined data normality (Shapiro-Wilk test) two-way repeated measures ANOVA was utilised to determine the effect of POWER (6 levels: REST, 50W, 100W, 150W, 200W & MAX), CONDITION (CONTROL & AL) and POWER*CONDITION interactions on cardiorespiratory variables and cadence. $\dot{V}O_2$Max, total work, the maximum power required to achieve $\dot{V}O_2$Max and $\dot{V}O_2$ at the ventilatory breakpoint were compared between CONTROL and AL with paired t-tests. Wilcoxon tests were used to compare subjective data (mean ± 95% CI) between CONTROL and AL at REST and $\dot{V}O_2$Max. All statistics were performed using SPSS (19.0, SPSS Inc., Chicago, IL, USA) with significance defined as $p<0.05$.

3.3 Results

3.3.1 Cadence

There were no significant main or interaction effects of CONDITION or POWER on the cadence of cycling (all $p>0.05$; Table 3.1). The participants maintained consistent cycling cadence at both 50W (CONTROL: 70±0.6RPM; AL: 70.3±0.7rpm) and MAX (CONTROL: 72.2±2.1RPM; AL: 72.8±0.8rpm) power output stages in both experimental conditions.

Table 3.1: Mean (±SEM) anthropometric data, SkinSuit-induced axial load and cadence at 50W and MAX in CONTROL and AL. n=8 for all metrics except axial load. n=7.

Height (cm)	177.1	2.4
Mass (kg)	74.2	2.5
Age	29.6	2
Axial load (Gz)	1.12	0.01
Cadence 50W CONTROL (RPM)	70	0.6
Cadence 50W AL (RPM)	70.3	0.7
Cadence MAX CONTROL (RPM)	72.2	2.3
Cadence MAX AL (RPM)	72.8	0.8

3.3.2 Cardiorespiratory variables during incremental exercise

POWER induced increases in $\dot{V}_E$ [F(5,35) = 83.363; p<0.001], $\dot{V}O_2$: [F(5,35) = 237.180; p<0.001], $\dot{V}CO_2$: [F(5,35) = 162.096; p<0.001], $\dot{V}_T$: [F(2,14) = 114.800; p<0.001], HR [F(2,14) = 301.739; p<0.001], RER: [F(2,14) = 117.482; p<0.001] and BR: ([F(2,14) = 135.415; p<0.001]; Fig. 3.2a-g). Post-hoc pairwise comparisons for can be found in Table 3.2.

Although no variable differed with CONDITION ($\dot{V}_E$: [F(1,7) = 1.434; p=0.270]; $\dot{V}O_2$: [F(1,7) = 2.398; p=0.165]; $\dot{V}CO_2$: [F(1,7) = 1.986; p=0.202]; $\dot{V}_T$: [F(1,7) = 0.707; p=0.428], HR: [F(1,7) = 142.228; p=0.330], BR: [F(1,7) = 3.647; p=0.098]; RER: [F(1,7) = 2.070; p=0.193], there were significant POWER*CONDITION interactions for HR [F(5,35) = 2.547 p<0.05], $\dot{V}_E$ [F(1.709,11.961) = 4.804; p<0.05], $\dot{V}O_2$ [F(5,35) = 3.120; p<0.05], $\dot{V}CO_2$ [F(5,35) = 3.459; p<0.05]; $\dot{V}_T$ [F(2,14) = 8.768; p<0.01] and BR [F(5,35) = 4.173; p<0.05]. Interestingly, within these parameters, it appeared as though AL was greater than CONTROL at REST-200W and

lower by MAX; most markedly in $\dot{V}_E$ and BR (Fig. 3.2b & g). There was no POWER*CONDITION interactions for RER [F(1,7) = 0.339; p=0.579] (Fig. 3.2f).

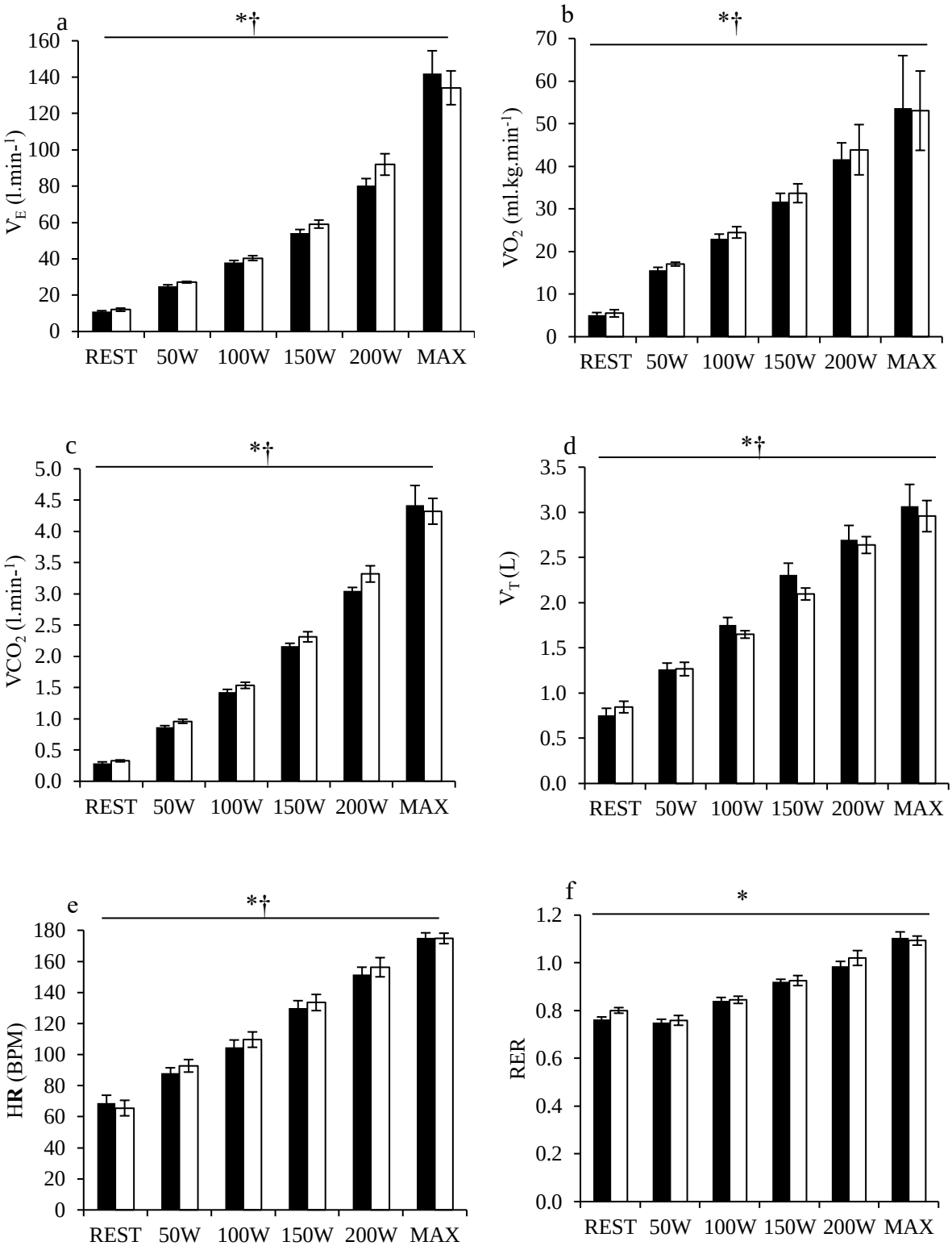
a
*†
V_E (l.min-1)
160
140
120
100
80
60
40
20
0
REST 50W 100W 150W 200W MAX
b
*†
VO_2 (ml.kg.min-1)
70
60
50
40
30
20
10
0
REST 50W 100W 150W 200W MAX
c
*†
VCO_2 (l.min-1)
5.0
4.5
4.0
3.5
3.0
2.5
2.0
1.5
1.0
0.5
0.0
REST 50W 100W 150W 200W MAX
d
*†
V_T (L)
3.5
3.0
2.5
2.0
1.5
1.0
0.5
0.0
REST 50W 100W 150W 200W MAX
e
*†
HR (BPM)
180
160
140
120
100
80
60
40
20
0
REST 50W 100W 150W 200W MAX
f
*
RER
1.2
1.0
0.8
0.6
0.4
0.2
0.0
REST 50W 100W 150W 200W MAX

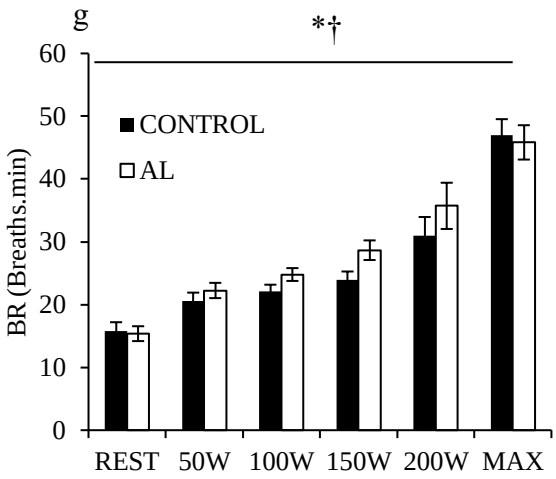

Figures 3.2 a-g: Mean (±SEM) $\dot{V}_E$, $\dot{V}O_2$, $\dot{V}CO_2$, $\dot{V}_T$, HR, RER & BR from rest, 50-200W and MAX, in CONTROL and AL.* = main effect of POWER; ANOVA; $p<0.05$. † = POWER*CONDITION interaction; ANOVA; $p<0.05$. n=8.

Table 3.2: post-hoc pairwise comparisons for $\dot{V}_E$, $\dot{V}O_2$, $\dot{V}CO_2$, $\dot{V}_T$, HR, RER & BR during rest, 50-200W and MAX; $p<0.05$. n=8.

$\dot{V}_E$						
	REST	50W	100W	150W	200W	MAX
REST		p=0.000	p=0.000	p=0.000	p=0.000	p=0.000
50W	p=0.000		p=0.000	p=0.000	p=0.000	p=0.000
100W	p=0.000	p=0.000		p=0.000	p=0.000	p=0.001
150W	p=0.000	p=0.000	p=0.000		p=0.003	p=0.003
200W	p=0.000	p=0.000	p=0.000	p=0.003		p=0.132
MAX	p=0.000	p=0.000	p=0.001	p=0.003	p=0.132	
$\dot{V}O_2$						
	REST	50W	100W	150W	200W	MAX
REST		p=0.000	p=0.000	p=0.000	p=0.000	p=0.000
50W	p=0.000		p=0.000	p=0.000	p=0.000	p=0.000
100W	p=0.000	p=0.000		p=0.000	p=0.000	p=0.000
150W	p=0.000	p=0.000	p=0.000		p=0.000	p=0.002
200W	p=0.000	p=0.000	p=0.000	p=0.000		p=0.117
MAX	p=0.000	p=0.000	p=0.000	p=0.002	p=0.117	
$\dot{V}CO_2$						
	REST	50W	100W	150W	200W	MAX
REST		p=0.000	p=0.000	p=0.000	p=0.000	p=0.000
50W	p=0.000		p=0.000	p=0.000	p=0.000	p=0.000
100W	p=0.000	p=0.000		p=0.000	p=0.000	p=0.000
150W	p=0.000	p=0.000	p=0.000		p=0.000	p=0.002
200W	p=0.000	p=0.000	p=0.000	p=0.000		p=0.109
MAX	p=0.000	p=0.000	p=0.000	p=0.002	p=0.109	
$\dot{V}_T$						
	REST	50W	100W	150W	200W	MAX
REST		p=0.008	p=0.000	p=0.000	p=0.000	p=0.000
50W	p=0.008		p=0.000	p=0.000	p=0.000	p=0.000
100W	p=0.000	p=0.000		p=0.001	p=0.000	p=0.003
150W	p=0.000	p=0.000	p=0.001		p=0.001	p=0.015
200W	p=0.000	p=0.000	p=0.000	p=0.001		p=0.224
MAX	p=0.000	p=0.000	p=0.003	p=0.015	p=0.224	
HR						
	REST	50W	100W	150W	200W	MAX
REST		p=0.052	p=0.010	p=0.000	p=0.000	p=0.000
50W	p=0.053		p=0.002	p=0.000	p=0.000	p=0.000
100W	p=0.010	p=0.002		p=0.000	p=0.000	p=0.000
150W	p=0.000	p=0.000	p=0.000		p=0.000	p=0.001

200W	p=0.000	p=0.000	p=0.000	p=0.000		p=0.039
MAX	p=0.000	p=0.000	p=0.000	p=0.001	p=0.039	
RER						
	REST	50W	100W	150W	200W	MAX
REST		p=1.000	p=0.199	p=0.002	p=0.001	p=0.000
50W	p=1.000		p=0.001	p=0.000	p=0.000	p=0.000
100W	p=0.119	p=0.001		p=0.000	p=0.000	p=0.000
150W	p=0.002	p=0.000	p=0.000		p=0.005	p=0.001
200W	p=0.001	p=0.000	p=0.000	p=0.005		p=0.071
MAX	p=0.000	p=0.000	p=0.000	p=0.001	p=0.071	
BR						
	REST	50W	100W	150W	200W	MAX
REST		p=0.110	p=0.025	p=0.006	p=0.009	p=0.000
50W	p=0.110		p=0.035	p=0.001	p=0.046	p=0.000
100W	p=0.025	p=0.034		p=0.021	p=0.162	p=0.001
150W	p=0.006	p=0.001	p=0.021		p=0.342	p=0.002
200W	p=0.009	p=0.046	p=0.162	p=0.342		p=0.109
MAX	p=0.000	p=0.000	p=0.001	p=0.002	p=0.109	

3.3.3 Performance metrics at $\dot{V}O_2Max$

No significant differences in $\dot{V}O_2Max$ (Fig. 3.3a), nor the power output required to achieve it (Fig. 3.3b) were observed in AL vs. CONTROL. However, in 5/8 participants, $\dot{V}O_2Max$ tended to decrease slightly with AL (denoted by the solid grey lines).

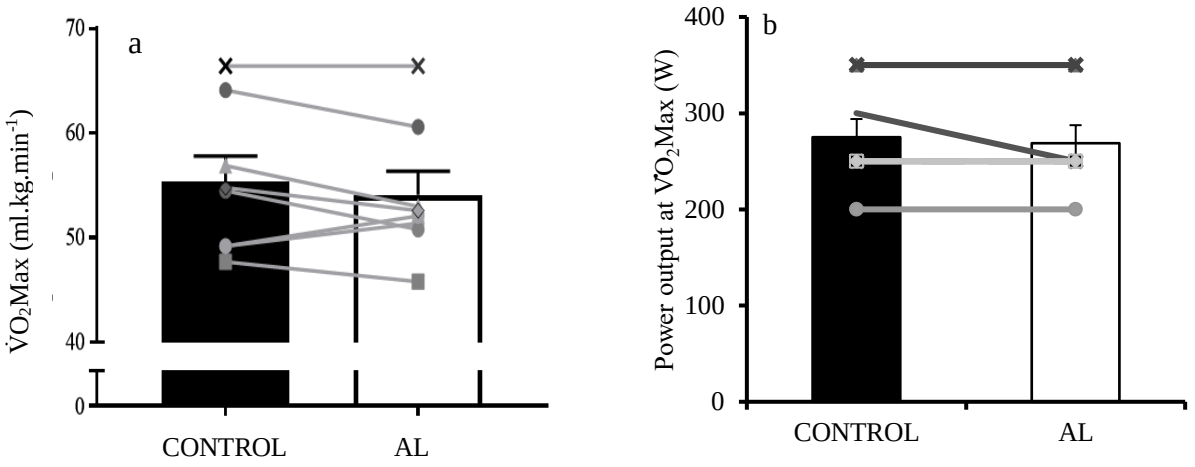

Figures 3.3 a and b: Individual (lines) and mean (bars; ± SEM) a) $\dot{V}O_2Max$ (ml.kg.min^{-1}) and b) power output (W) required to achieve $\dot{V}O_2Max$), in CONTROL and AL. n=8.

In contrast, there was a 12.6±3% reduction in the total work required to achieve $\dot{V}O_2Max$ in AL vs. CONTROL (P=0.001; Table 3.2), as a result of reduced total test duration (CONTROL: 453±56.7; AL: 395.98±55.3s; p=0.002), with 7/8 participants experiencing this reduction (Fig. 3.4). The most marked reduction was 29.25kJ in participant 5.

No difference in $\dot{V}O_2$ at the ventilatory breakpoint were observed between CONTROL and AL (Fig. 3.5), although displays a relatively even split in increases and decreases (3 and 5 participants respectively) between the two conditions (mean increase from CONTROL to AL: 23±0.03%; mean decrease from CONTROL to AL: 11±0.03%). Furthermore, there was no difference between the power output stage at which the ventilatory breakpoint was reached between AL and CONTROL (193.8±20W and 212.5±12.5W respectively). RER was >1 in both CONTROL and AL at $\dot{V}O_2Max$ (Fig. 3.2f), confirming that the lactate threshold was exceeded. In fact, RER was >1 in AL at 200W, but was not significantly different from CONTROL (0.99; Fig. 3.2f).

Table 3.3: Individual and mean (± SEM) total work (power [W] x time [s]) needed to reach $\dot{V}O_2Max$ in CONTROL and AL, and % difference between the conditions. *= paired t-test; $p<0.05$. n=8

Participant	Total work (kJ)		% reduction in total work in AL vs. CONTROL
	CONTROL	AL	
1	150	132.5	13.2
2	117.5	107.5	9.3
3	227.5	210	8.3
4	211.8	192.5	10
5	135	105.8	27.7
6	137.7	117.5	17.1
7	92.5	92.5	0
8	112.5	97.5	15.4
Mean (±SEM)	**148.1 ± 16.9**	**132 ± 15.8**	**12.6 ± 3***

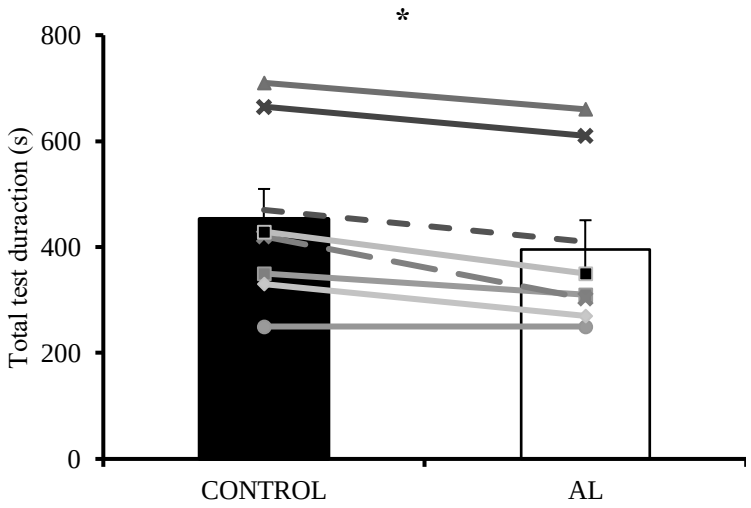

Figure 3.4: Individual (lines) and mean (bars; ±SEM) total test duration (s) in AL and CONTROL. * = paired t-test; $p<0.05$. n=8.

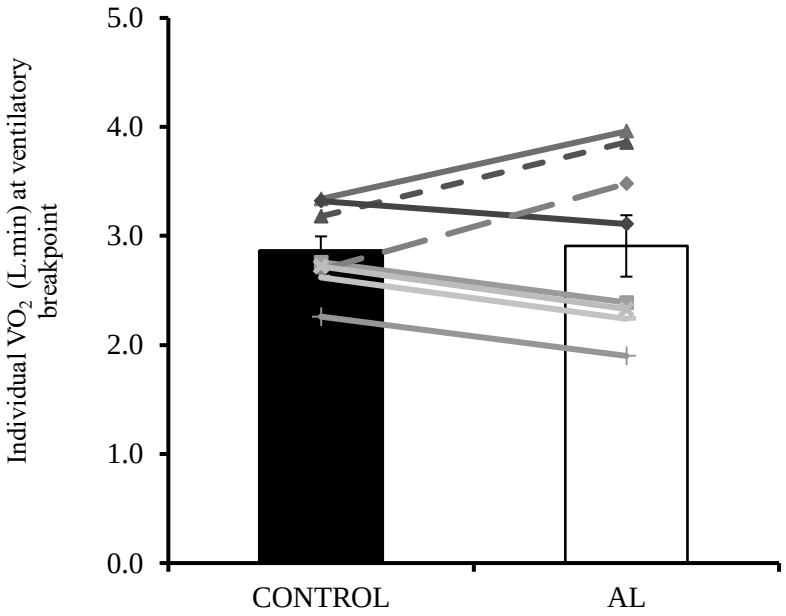

Figure 3.5: Individual (lines) and mean (bars; ±SEM) $\dot{V}O_2$ at point of ventilatory breakpoint ($l.min^{-1}$) in AL and CONTROL. n=8.

3.3.4 Subjective ratings

Thermal comfort, body control and RPE all increased with POWER from REST to $\dot{V}O_2Max$ in both conditions ($p<0.05$; Table 3.3). Movement discomfort ($p=0.041$) and requirement for body control ($p=0.041$) were significantly increased at REST in AL vs. CONTROL but did not differ between conditions at $\dot{V}O_2Max$. RPE was the only subjective rating to differ between CONDITIONs at $\dot{V}O_2Max$, being lower in AL vs. CONTROL ($p=0.026$).

Table 3.4: Mean subjective ratings (± 95% CI) at rest, and $\dot{V}O_2$Max in CONTROL and AL. † = Wilcoxon test between STAGE; $p<0.05$. * = Wilcoxon test between CONDITON at the respective workload; $p<0.05$. n=8.

	Rest CONTROL	**Rest AL**	**$\dot{V}O_2$Max CONTROL**	**$\dot{V}O_2$Max AL**
Thermal Comfort (-3 - +3)	0.3 (-0.1-0.8)	0.0 (-0.5-0.5)	2.8 (2.5-3.2)†	2.3 (1.7-3)†
Movement Discomfort (0-10)	2.2 (1.8-2.5)	3.7 (2.7-4.6)*	2.5 (1.8-3.2)	4.2 (3.2-5.1)
Body Control (0-10)	1.5 (0.8-2.2)	3.2 (2-4.3)*	2.3 (1.8-3.1)†	4.2 (3.2-5.1)†
RPE (7-20)	7.2 (6.8-7.5)	7.0 (7-7)	17.5 (16.4-18.7)†	15.8 (14.8-16.9)†*

3.4 Discussion

The aim of this study was to investigate the cardiorespiratory responses to incremental cycling with the addition of 0.12Gz axial body loading in 1Gz. The main finding was that despite cardiorespiratory responses during submaximal exercise, $\dot{V}O_2$Max, the ventilatory breakpoint and the power required to achieve it remaining unchanged between conditions, a reduction in test duration and consequential reduced total work when cycling with AL was observed.

All cardiorespiratory variables increased with each power output in both CONTROL and AL conditions, which is likely related to increased muscle activity serving to meet increased power output demands (Bigland-Ritchie & Woods, 1976). Muscle activity would need to be quantified in order to confirm this however. As expected, the presence of the ventilatory breakpoint at ~70% $\dot{V}O_2$Max and RER >1 by $\dot{V}O_2$Max in both conditions suggests that anaerobic metabolism had a significant contribution at high intensities (McArdle et al, 2010). Most subjective parameters increased from rest to $\dot{V}O_2$Max in both conditions. Additionally,

although remaining moderate, movement discomfort and body control ratings were worse in AL at REST. In contrast, RPE and thermal comfort were unaffected by CONDITION.

Contrary to the hypothesis that cardiorespiratory parameters would increase in accordance with 0.12Gz additional ABL, the absence of significant differences in cardiorespiratory variables with CONDITION suggests that such a provision was insufficient to modulate the response to sub- and maximal cycling. Although the load provided by the Mk VI SkinSuit is somewhat unconventional compared to that of mass-imposed loading approaches (i.e. ankle weights), it was hypothesised that cycling with an additional 0.12Gz ABL would induce an elevated cardiorespiratory demand compared to 1Gz cycling by virtue of having to overcome the resistance imparted by it. $\dot{V}O_2$ has been shown to increase when cycling with additional ankle weights in both healthy individuals (Kamon et al, 1973) and stroke patients (Jin et al, 2012). Increased cardiorespiratory demand was also observed in the Penguin suit in microgravity (Barer et al, 1998). However, although the provision of axial load in the Penguin suit is via elastic strain of bungee cords, it applies absolute load in two stages equivalent to ~25kg. This is contrasting to the imposition of graduated Earth-like loading that is tailored to be 12% additional relative body mass, as yielded by the SkinSuit.

The results in this Chapter are consistent with previous work where imposition of 0.8Gz additional ABL, via donning the Mk III SkinSuit had no effect upon any cardiorespiratory parameter, $\dot{V}O_2Max$, nor the power required to achieve it during cycling (Attias et al, 2014). The fact that the results between these two studies are practically identical is interesting considering only a slightly greater magnitude of test duration reduction (~5%) arising from an additional 0.7Gz ABL in the Attias et al (2014) study. However, sub-optimal ABL-

measurement techniques within the latter study renders their data not entirely conclusive and thus a comparison with such should be treated with caution.

A similar $\dot{V}O_2$Max was achieved, albeit with reduced test duration, whilst cycling with 0.12Gz ABL. Thus, total work required to achieve $\dot{V}O_2$Max was reduced by 12.6% compared to CONTROL. These results are consistent with studies that report reduced exercise tolerance with little hindrance to cardiorespiratory variables during maximal cycle exercise (Attias et al, 2014). Peoples et al (2016) suggested that such intolerances can be explained by increased work of breathing due to chest wall restriction imposed by the loading approach. Although the imparting of ABL would not induce chest wall restriction in the same manner as backpacks, i.e. through an inertial contribution, work of breathing has also been shown to increase with chest-wall strapping (CWS; O'Donnell et al, 2000). A decrease of 28±3% in total cumulative work performed was shown to be related to a 75% reduction in $\dot{V}_T$ and a 25% increase in respiratory rate at peak cycle exercise, indicative of mechanical breathing constraints (O'Donnell, 1998). Such a manifestation in these ventilatory variables may also be a factor in the significant POWER*CONDITION interactions evident for all variables except RER and $\dot{V}$CO2. Such interactions could have been a result of the respective variable appearing higher in AL vs. CONTROL from 50-200W, before becoming lower than CONTROL by $\dot{V}O_2$Max. Thus, the effect of ABL on ventilatory perturbations, and their potential indication of altered breathing mechanics, should be investigated.

It has been argued that the tolerable duration of aerobic exercise is limited by central and/or peripheral muscle fatigue (McKenna and Hargreaves, 2008). Incremental cycling to a maximal power output, as commanded in this study requires powerful activation and coordination of numerous lower-limb muscles (Fonda and Sarabon, 2010). A major limitation of this study was

the lack of biomechanical analysis employed. In an attempt to evaluate the effect of ABL on cycling biomechanics and its interplay with the findings discerned within this Chapter, inclusion of neuromuscular and kinematic analyses should be incorporated into further research.

Subjective ratings of worsened movement discomfort and body control in AL vs. CONTROL before cycling even commenced could be related to literature published from the exercise-with-compression-garments domain. Some authors suggest that increased time to exhaustion may be linked to improved perceptions (Ali et al, 2007) and sensations of vitality (Kraemer et al, 1998). Such awareness's may serve as ergogenic aids for improving performance, regardless of physiological effects (Duffield et al, 2007). It would not be entirely unforeseen if the converse was true for this study; negative connotations associated with wearing the SkinSuit for the first time could have reduced exercise tolerance. No effects of ABL on thermal comfort either at rest or at $\dot{V}O_2$Max were observed, which concurs with data from the wearing of other spandex-based garments during exercise (Belluye, 2006). However, in contrast to the Penguin Suit, where cosmonauts have cut the bungee cords as the 1- or 2-stage loading is highly uncomfortable (Waldie & Newman, 2011), the Mk VI SkinSuit-induced ABL is well tolerated. The reduction in RPE with AL at $\dot{V}O_2$Max is in contrast to studies involving load carriage (Gao et al, 2016; Simpson et al, 2011b) and are also more consistent with perceptions of exertion related to compression garments, reported on with regards to the upper leg muscles after a bout of 10 sprints (Born et al, 2013). The actual circumferential compression generated by the SkinSuit has yet to be quantified, though is designed to be no more than 5-8mmHg (a similar pressure to tight socks; Waldie & Newman, 2011).

3.5 Conclusion

Cardiorespiratory and subjective responses during cycling with 0.12Gz additional ABL were not entirely consistent with conventional load-imposed approaches. Nonetheless, $\dot{V}O_2$Max was unchanged and thus maximal aerobic exercise performance unimpeded, albeit with a reduction in total work necessary to achieve it. This reduction may be linked to altered mechanics either of the lower limbs, and/or breathing. Future work should therefore consider additional ventilatory analyses such as investigating the relationship between both tidal volume and breathing rate and minute ventilation, to understand potential disruptions to ABL-induced breathing mechanics. Further research should also include assessment of biomechanical variables during ABL exposure, particularly of the lower limbs.

Chapter 4: The influence of additional axial body loading on neuromuscular function during cycling in 1Gz

4.1 Introduction

In Chapter 3, a reduction in exercise tolerance without detriment of maximal aerobic performance (which was reached at ~272W) was observed when cycling with an additional 0.12Gz ABL. However, it was not possible to fully interpret these findings without understanding the interaction between the addition of ABL and cycling biomechanics.

It is well known that during cycling, mono-articular muscles such as the VL increase their activity to a greater extent than the RF – a bi-articular muscle from the same muscle group (Ericson, 1986). These findings are in keeping with the distinguishing tasks between these two muscle types; the RF propels the pedal crank anteriorly through its top dead centre (TDC) position while the VL produces torque during the extension phase (Ryan and Gregor, 1992). In addition to the muscle activity level (intensity), the patterns of activity (coordination) of mono- and bi-articular muscles play a significant role in the generation of a smooth pedalling revolution (Raasch,1996). So much so, that nearly equal cycling performance – maximum-speed start-up forward pedalling – can be achieved when lower limb muscles are classified into two groups, compared to when each muscle works independently on its own (Raasch and Zajac, 1999). One pair produces the energy needed to propel the crank through limb extension (mono-articular hip and knee extensor muscles) and flexion (mono-articular hip and knee flexor muscles), whilst the other pair facilitates the transfer of energy to propel the crank produced by the other muscles and also produces energy for crank propulsion from extension to flexion (hamstring and dorsiflexor muscles; BF/GL) and vice versa (RF and TA). This co-activation

of agonist/antagonist and synergistic muscle pairs results in a coordinated transfer of mechanical energy between joints (Fonda and Sarabon, 2010), reducing muscle stress and mechanical energy expenditure (Hug and Dorel, 2009).

Muscle activity of the leg and ankle extensors has been shown to increase with faster cycling cadences at a constant power output (Ericson et al, 1986; Dorel et al, 2012). Ericson et al, (1986) observed increased activity in five lower limb muscles (VL, VM, SOL, GMAX and semimembranosus) when cycling from 40 to 100rpm at 120W. Furthermore, Dorel et al (2012) observed increased peak EMG RMS activity in all 11 studied right lower limb muscles when sprint-cycling (cadence: 60-140% of optimal pedalling rate) compared to submaximal cycling (cadence: 80% of optimal pedalling rate). Significant shifts of EMG activity to an earlier cycling phase with faster cadences were also reported (Dorel et al, 2012) in addition to VL, RF, BF, SOL and GM in a different study undertaken by Marsh and Martin (1995). This is likely a strategy to compensate for the electromechanical delay between the onset of EMG and the force generation so that the torque is applied to the crank arm at a consistent position within each pedal cycle despite the cadence (Li and Baum, 2004).

Increases in power output have also been shown to require elevated muscle activity levels in the knee extensors during constant-cadence cycling at intensities >60% maximal aerobic power (Sarre et al, 2003), from 120-140W (Ericson, 1986) and from 150W to ~300W (Dorel et al, 2012; Enders et al, 2015). Enders et al (2015) observed that with higher mechanical demand (from 150W to 300W), the activation of the muscles operating around the knee joint increased substantially, whereas the demand for a stiff ankle joint necessary for efficient energy transfer to the crank was similar at both workloads. For example, GM activity has been shown to remain unchanged during cycling at power outputs of up to ~70% maximal aerobic power (Hug et al,

2004b). Few studies have focused on the effects of power output on muscle activation patterns due to the nervous system using adaptations related to the muscle EMG magnitude, rather than the timing (Jorge and Hull, 1986; Neptune and Hertzog, 1999).

Additional BW load has also been shown to precipitate muscle activity level and pattern adjustments during cycling (Baum and Li, 2003; Barer et al, 1998). Masses as light as 1-2kg, attached around the distal portion of each thigh during cycling have been shown to alter the timing more profoundly than the activity level in the extensor muscles (Baum and Li, 2003). Only the BF EMG activity significantly increased its peak magnitude by ~5% with additional loading of 2kg compared to no load. However, earlier RF onset and offset-timings and earlier SOL activation and lengthened duration were observed (Baum and Li, 2003).

Modifications to muscle activity levels have also been observed during cycling in microgravity when wearing the Penguin Suit, providing ~25kg additional body load via elastic strain, where 10min spent at 60rpm caused an increase in RF, BF and GAS EMG activity (Barer et al, 1998). As previously suggested by Dorel et al (2012) such adaptations seem to imply a coordination strategy between intensity and timing of muscle activation to further enhance the total quantity of EMG activity over the complete crank cycle.

4.1.1 Aims and hypotheses

The aim of this study was to determine the individual and combined effects of cycling power and additional 0.12Gz ABL – equivalent to ~9kgs – on lower-limb neuromuscular activity levels and patterns. It was hypothesised that increasing power output during incremental cycling would be achieved via increased activity levels of all studied muscles, especially of the mono-articular power-generating muscles such as VL. The addition of 0.12Gz ABL was

hypothesised to result in relatively small increases of muscle activity to overcome the additional body loading and modifications to muscle activity patterns i.e. timing of activity, particularly in the extensors. Hypotheses upon the interactions between power output and ABL were not possible due to a lack of literature.

4.2 Methods

4.2.1 Experimental design

The experiment followed the protocol previously described in section 3.2 of Chapter 3 (Fig. 4.1). Incremental cycling was performed at incremental power outputs of 50W every 3min until voluntary exhaustion (MAX) in both AL (i.e. the addition of 0.12Gz axial body loading) and CONTROL (without any added load i.e. 1Gz). The degree of ABL ranged from 0.07-0.16Gz (5.2-11.9kgs) between participants, with an average of 0.12Gz (~9kgs).

4.2.2 Data collection

Electromyographic activity of VL, BF, TA and GL muscles were simultaneously and continuously recorded throughout the protocol (Bagnoli-8, Delsys Inc., USA) following the methodology reported in Chapter 2, section 2.3.5. EMG signals were sampled at 2kHz via an analog-to-digital converter (Powerlab, AD Instruments, Castlehill Australia) using LabChart 7.1 software and stored on a PC for off-line analyses.

4.2.3 Data Analysis

As reported in the previous Chapter, the power output-related outcomes from the experimental protocol were not significantly different at any stage of the AL and CONTROL trials. Therefore, to test the hypotheses formulated in this Chapter only the EMG parameters from the

50W and MAX stages were analysed and compared statistically. Data from one subject from the TA muscle was omitted due to technical error.

Kinetic parameters: Cycling cadence and power output at both 50W and MAX between AL and CONTROL were analysed and reported in Chapter 3 but are re-stated below to interpret the EMG outcomes in light of the underlying motion paradigm.

EMG parameters. The approach for extraction and analysis of the characteristic parameters of the recorded EMG signals is presented in Chapter 2, sections 2.4.3.2-2.4.3.4. These are: EMG amplitude and spectral parameters (RMS and MDF), and EMG pattern parameters (onset, offset and duration of muscle activity, muscle-pair co-contractions and muscle activity similarity/displacement). The start of each revolution within the continuous cycling protocol was identified from the rectified VL EMG signal and marked as outlined in Chapter 2, section 2.4.3.1. The rectified EMG time series between the event markers within the middle 1min portion of each power output stage were extracted for each muscle from the records of the individual participants. The average EMG pattern for the last power output stage resulting in exhaustion (MAX) was constructed from the data during the penultimate 60s of the record. Onset and offset activation times and duration (deg) of each muscle within a revolution were identified for both power outputs at the crosspoints between the averaged EMG patterns and the respective baseline as previously described in section 2.4.3.2 of Chapter 2 (Fig. 4.1).

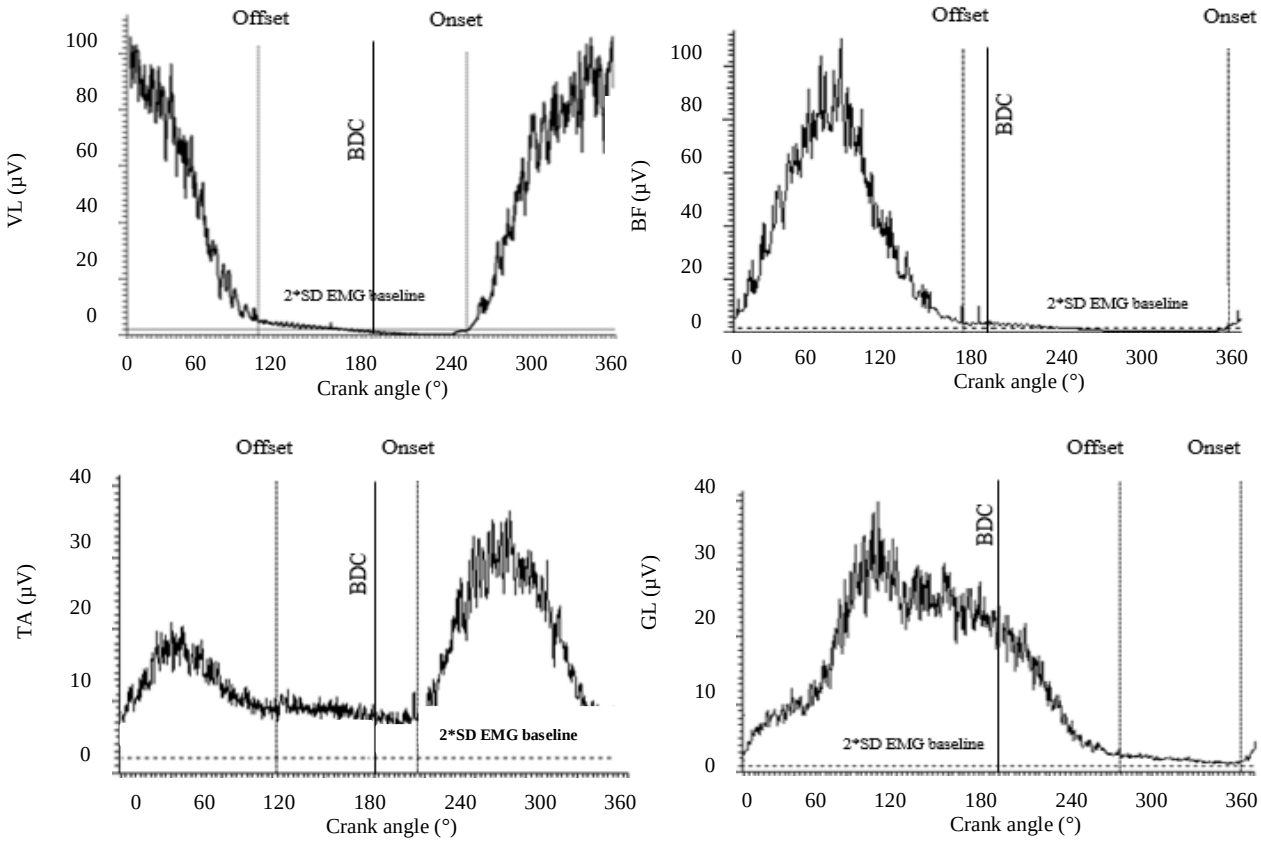

Figure 4.1. The onset and offset (vertical dashed lines) of the right VL, BF, TA and GL muscle activation during the revolution were identified as the times when the rectified EMG signal exceeded the mean EMG baseline level by more than 2*SD. X-axis uses a time-normalised scale as described in Chapter 2. Solid vertical line denotes bottom dead centre (BDC).

4.2.4 Statistical Analysis

All data were found to be normally distributed (Shapiro-Wilk test). EMG RMS, MDF, onset, offset and duration of muscle activity and muscle-pair co-contractions were statistically analysed by two-way repeated measures ANOVA with POWER (50W vs. MAX) and CONDITION (CONTROL vs. AL) as main factors. POWER*CONDITION interactions were also discerned. Pearson's correlation coefficient and the cross-correlation analysis of the relationships between the EMG envelopes was conducted across the cycling intensities (50W

and MAX) and experimental conditions (CONTROL and AL) for each muscle using SPSS ver. 21 (IBM Corp, 2012) and Origin ver. 6 (Microcal Software Inc, 1999), respectively.

4.3 Results

4.3.1 Cycling kinetics

As noted in Chapter 3 section 3.4.1, similar cycling cadence was maintained at 50W and MAX stages in both experimental conditions (CONTROL: 70±0.6rpm; AL: 70.3±0.7rpm). The power output achieved at MAX also did not differ between the conditions (CONTROL: 275±18.9W; AL: 268.8±18.8W; p=0.351).

4.3.2 Effect of cycling POWER on EMG activity

4.3.2.1 EMG amplitude and frequency parameters

A main effect of SPEED was observed in all muscles (VL [$F(1,7) = 36.996$; $p<0.001$], BF [$F(1,7) = 14.289$; $p<0.01$], TA [$F(1,7) = 13.297$; $p<0.01$] and GL [$F(1,7) = 10.171$; $p<0.05$]; Fig. 4.2a), where post-hoc pairwise comparisons revealed greater RMS amplitude at MAX compared to 50W (VL: p=0.001; BF: p=0.007; TA: p=0.008 & GL: p=0.016). The VL showed the greatest increase from 50W to MAX in both conditions by 269.2 ± 40.6% and 371.6 ± 53.5% in CONTROL and AL, respectively. Spectral analysis of the EMG signals within the revolutions revealed a main POWER effect on MDF of VL EMG power spectrum [$F(1,7) = 23.004$; $p<0.01$] with post-hoc tests evidencing an increase at MAX vs. 50W (p=0.02). In contrast, BF [$F(1,7) = 0.225$; p=0.650], TA [$F(1,7) =0.008$; p=0.930] and GL [$F(1,7) = 3.636$; p=0.0981] MDF were unchanged with POWER (Fig. 4.2b).

a) RMS

b) MDF

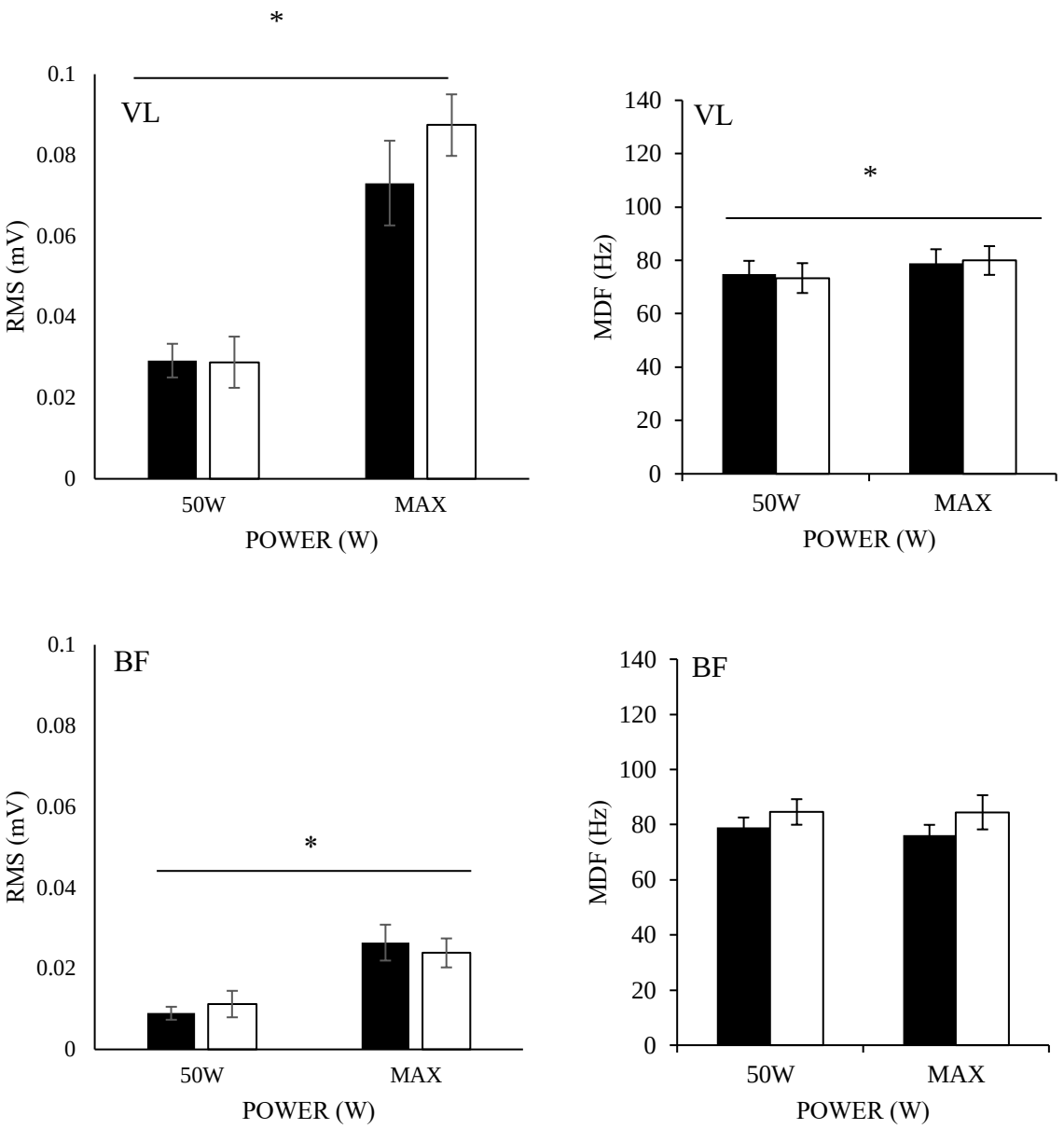
*
VL
RMS (mV)
0.1
0.08
0.06
0.04
0.02
0
50W
MAX
POWER (W)
VL
MDF (Hz)
140
120
100
80
60
40
20
0
*
50W
MAX
POWER (W)
BF
RMS (mV)
0.1
0.08
0.06
0.04
0.02
0
*
50W
MAX
POWER (W)
BF
MDF (Hz)
140
120
100
80
60
40
20
0
50W
MAX
POWER (W)

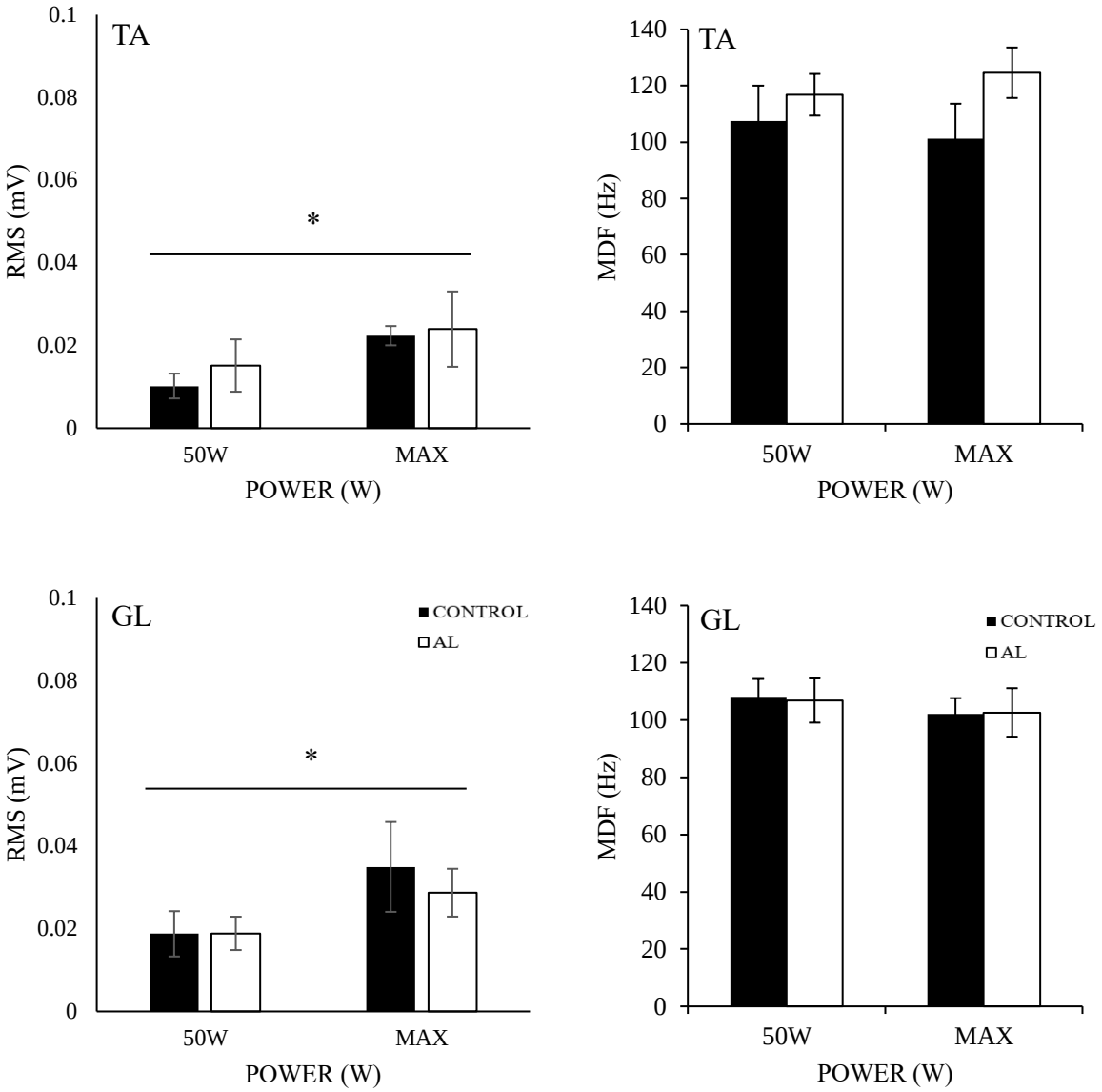

Figures 4.2 a and b: Mean (±SEM) a) root mean square (RMS) EMG amplitude (left column) and b) median frequency (MDF; right column) of the EMG power spectrum density for VL, BF, TA and GL muscles during cycling at low (50W) and high (MAX) POWER in two conditions - CONTROL and AL. * = main effect of POWER; ANOVA; $p<0.05$. n=8 for all muscles except TA (n=7).

4.3.2.2 Muscle activity patterns

The EMG activity onset of all studied muscles occurred prior to the TDC (0°). At 50W the VL activity in the CONTROL trial was observed on average between -90.6±6.4° and 96.3±6.7° but was shifted to a later onset (-61.5±2.1°) and offset (132±6.2°) by MAX (Fig. 4.3a). The onset

of the BF activity occurred later than that of VL at both 50W (-44.7±7.1°) and MAX (-40.4±4.8), though its offset was delayed at higher power outputs in (50W: 165.7±14.9 vs. MAX: 223.8±6.2°). TA activity ended later in MAX (150.6±.2°) than at 50W (101.8±12.6). GL was active on average from -22.1±6.3° at 50W and similar to VL and BF muscle activations, had a later offset at MAX (293.1±11.1°) vs 50W (246.3±10.3°).

Fig. 4.3a&b illustrates the muscle activity duration, onset and offset times within the cycling revolution for all muscles at 50W and MAX cycling POWER in both conditions (CONTROL and AL). Increasing cycling POWER had a main effect on the duration of the BF [$F(1,7) = 11.974$; $p<0.05$] and TA [$F(1,7) = 7.597$; $p<0.05$] but not of VL [$F(1,7) = 0.150$; $p=0.710$] or GL [$F(1,7) = 4.176$; $p=0.080$]. Post-hoc pairwise comparisons illustrate a lengthened duration at MAX vs. 50W (BF: $p=0.033$; TA: $p=0.011$). This was achieved mainly by delaying the EMG activity offset within the revolutions completed at higher power outputs. A significant main effect of POWER on the EMG activity offset was observed for VL [$F(1,7) = 21.852$; $p<0.01$], BF [$F(1,7) = 12.565$; $p<0.01$], TA [$F(1,6) = 56.720$; $p<0.001$] and GL [$F(1,7) = 14.886$; $p<0.01$]. Post-hoc pairwise comparison show the EMG activity offset in all studied muscles to be shifted significantly later at MAX vs 50W (VL: $p=0.002$; BF: $p=0.009$; TA: $p=0.000$ & GL: $p=0.06$) by 35° (VL), 58° (BF), 49° (TA) and 47° (GL) in CONTROL and by 29° (VL), 44° (BF), 27° (TA) and 26° (GL) in AL. A main effect of POWER was also observed for onset of the VL [$F(1,7) = 10.739$; $p<0.05$], where it was shifted earlier at MAX vs. 50W (post-hoc test: $p=0.014$). BF [$F(1,7) = 0.978$; $p=0.356$], TA [$F(1,7) = 0.882$; $p=0.384$] and GL [$F(1,7) = 3.044$; $p=0.125$] onset were not affected by POWER.

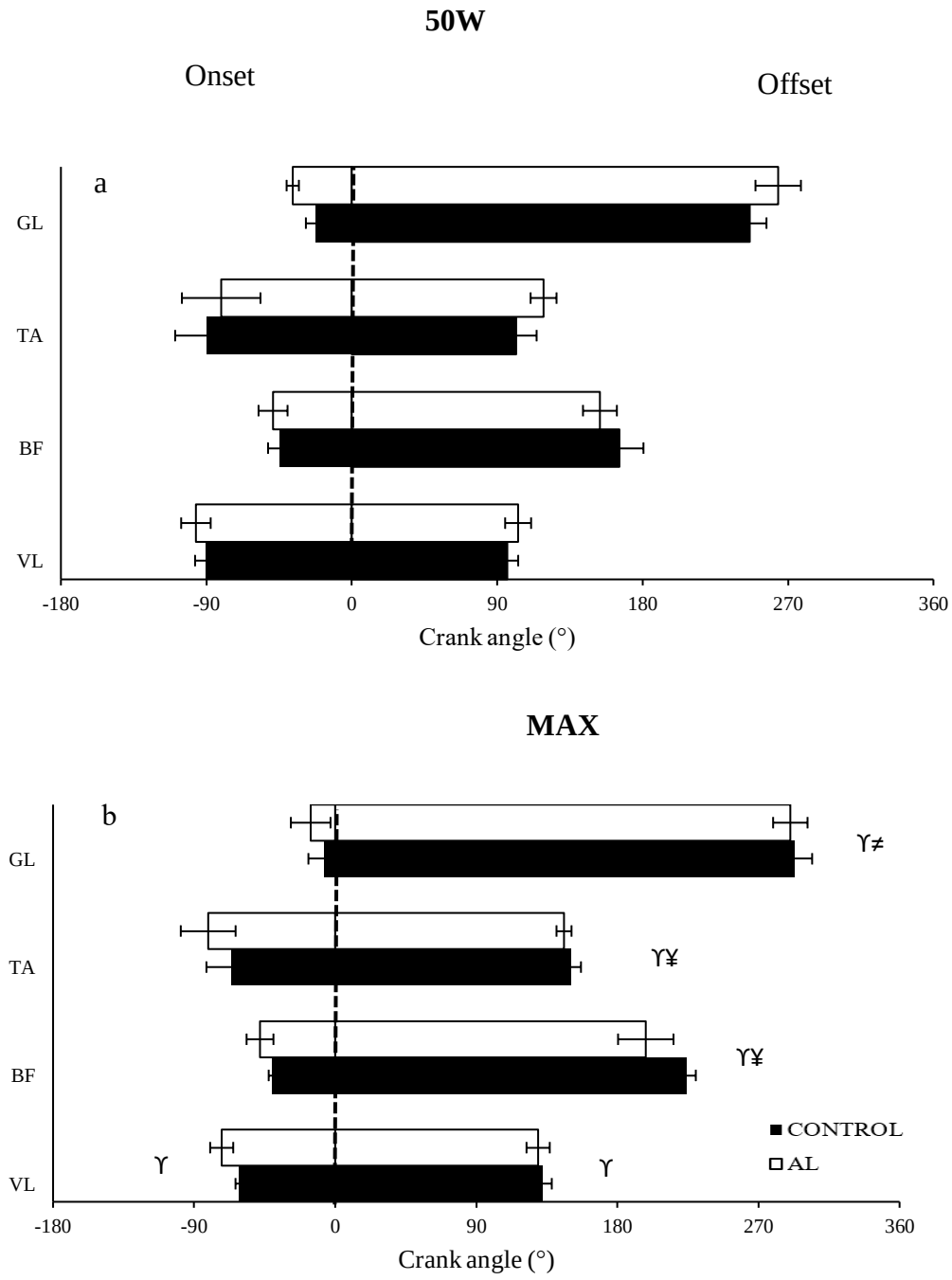

Figures 4.3 a and b: Mean (±SEM) EMG activity onset, offset and duration for VL, BF, TA & GL at a) 50W and b) MAX. --- = TDC. Main effect of POWER (50W vs. MAX): ϒ = for onset (left side of the graph) and offset (right side of the graph); ¥ = $p<0.05$ for duration with POWER; $p<0.05$; ≠ = main effect of CONDITON for duration; $p<0.05$. n=8 for all muscles except TA (n=7).

The population average EMG activity patterns across the revolution for all studied muscles during cycling at 50W and MAX in both conditions are represented with ensemble linear envelopes (Fig. 4.4). Significant correlations were found between the activity patterns at low and high cycling POWER for all muscles in both conditions (r = 0.65 to 0.89; $p<0.01$; Table 4.1 top panel). The lag of the cross-correlation functions between the EMG envelopes at 50W and MAX was negative for all muscles for both conditions, indicative of muscle activity shifts to significantly later periods in the cycling revolution at MAX compared to 50W. For example, the average lag of the cross-correlation function between the VL patterns at low and high intensity cycling was established at -28.3° (range between -47.8° and -19.6° for individual participants) and -22.7° (range between -38.4° and -7°) for CONTROL and AL respectively, indicative of a significantly later overall VL activation period at MAX vs. 50W.

A main effect of POWER was observed for the duration of the co-contraction period of the antagonist VL/BF pair [$F(1,7) = 21.623$; $p<0.01$], lasting longer at MAX vs. 50W (post-hoc test: $p=0.002$) by 62% in CONTROL and by 71% in AL (Table 4.2). The duration of the co-contraction period of the synergist VL/GL pair with POWER also reached significance [$F(1,7) = 7.064$; $p<0.05$], which also lengthened at MAX compared to 50W (post-hoc test: $p=0.033$) by 39% (CONTROL) and 21% (AL). Although not reaching significance, the co-contractions of the TA/GL [$F(1,7) = 0.935$; $p=0.371$] and BF/TA [$F(1,7) = 3.806$; $p=0.099$] muscle pairs tended to directly relate to cycling POWER in CONTROL, which was in contrast to AL, where the TA/GL pair had an inverse relationship with POWER (258.1±27.1 235.3±23.7 & BF/TA: 243.4at 50W and MAX respectively).

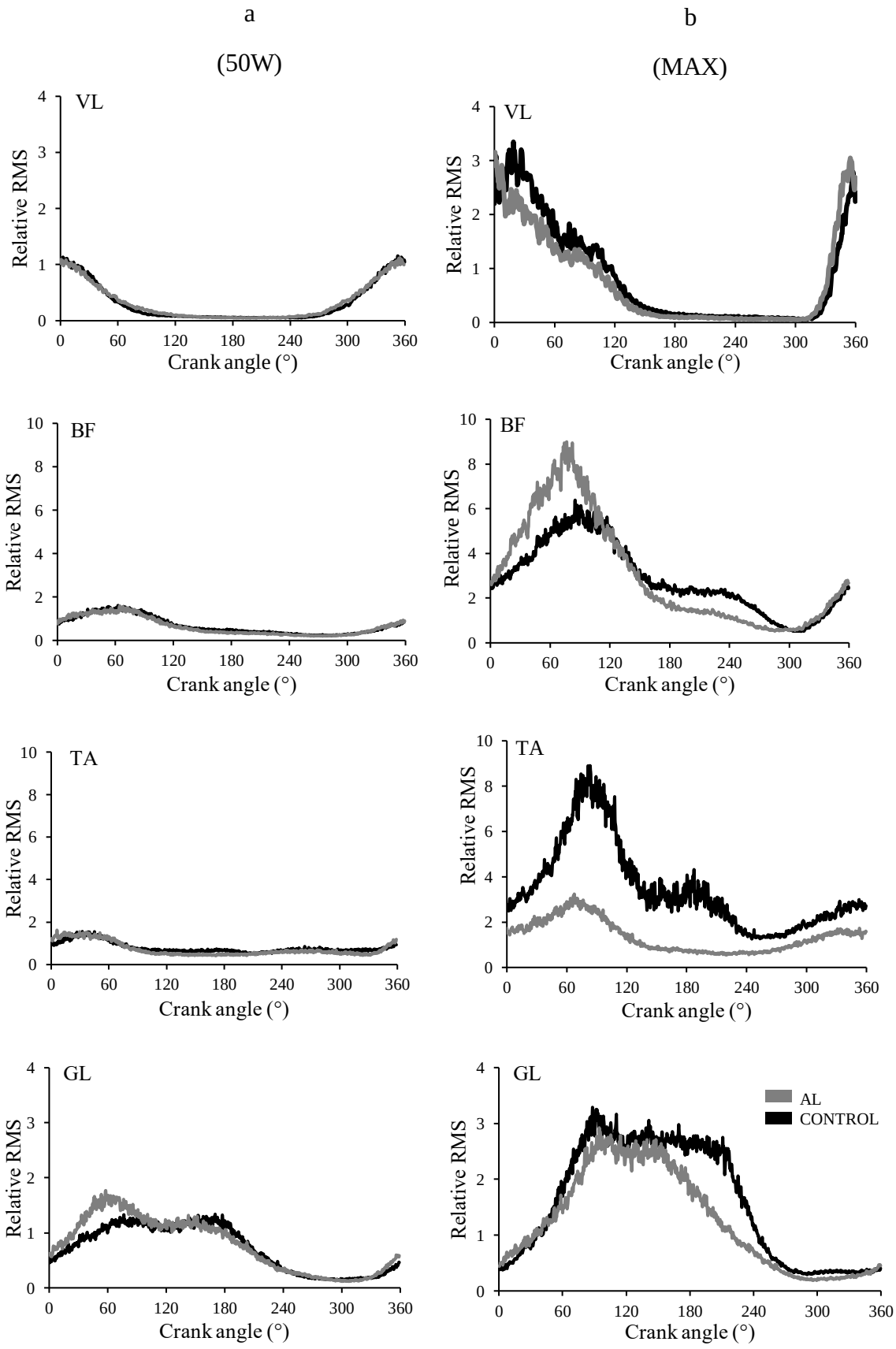
a
(50W)
b
(MAX)
VL
BF
TA
GL
Relative RMS
Crank angle (°)
AL
CONTROL

Figures 4.4 a and b: Mean ensemble curve of EMG RMS envelopes for each muscle at a) 50W and b) MAX in CONTROL and AL. Envelopes were averaged over all consecutive revolutions captured within the middle minute of each power output across all participants. Magnitudes were normalised to the mean RMS (averaged over all consecutive revolutions captured within the middle minute) of the 50W power output stage for each participant per muscle. TDC = 0°. n=8 for all muscles except TA (n=7).

Table 4.1: Pearson's correlation coefficients and cross-correlation lags (±95% confidence intervals) between ensemble EMG curves at 50W and MAX within each CONDITION (top panel; r_1 = 50W; r_2 = MAX) and in CONTROL and AL conditions within each POWER stage (bottom panel; r_1 = CONTROL; r_2 = AL). * significantly different from r=0. † = significant phase shift. n=8 for all muscles except TA (n=7).

	CONTROL		AL	
Muscle	50W (*r*)	Lag	MAX (*r*)	Lag
Vastus Lateralis	0.76*	-28.3 (-19.6, -47.8°)†	0.83*	-22.7 (-38.4, -7°)†
Biceps Femoris	0.79*	-17.8 (-30.2, -5.5°)†	0.89*	-23.9 (-40.4, -7.3°)†
Tibialis Anterior	0.66*	-21.9 (-38.1, -5.7°)†	0.65*	-31.3 (-54.5, -8.1°)†
Gastrocnemius Lateralis	0.87*	-6.9 (-11.6, -2.1°)†	0.8*	-12.4 (-20.9, -3.8°)†

	50W		MAX	
Muscle	CONTROL (*r*)	Lag	AL (*r*)	Lag
Vastus Lateralis	0.99*	-0.5 (-0.82, -0.15)†	0.98*	5.5 (1.7, 9.4)†
Biceps Femoris	0.98*	5.3 (1.63, 9)†	0.93*	6.9 (2.1, 11.6)†
Tibialis Anterior	0.92*	16.4 (4.2, 28.6)†	0.95*	16.8 (4.4, 29.2)†
Gastrocnemius Lateralis	0.93*	0.6 (0.2, 1)†	0.94*	1 (0.3, 1.6)†

Table 4.2: Mean (±SEM) muscle activity co-contractions between antagonistic muscle pairs (VL/BF & TA/GL), extensor muscle pairs (VL/GL) & flexor muscle pairs (BF/TA) across CONDITION at 50W and MAX. Values are means of degrees in crank angle ± SEM. * = main effect of POWER; $p<0.05$. n=8 for all muscles except TA (n=7).

	50W		MAX	
	CONTROL	AL	CONTROL	AL
VL/BF*	147±12.9	172.6±20.2	235.7±22.2	236±27.1
TA/GL	202±23.3	258.1±27.1	271.82±24.9	235.3±23.7
VL/GL*	125.7±8.5	162.5±16.3	206.7±20.7	206.9±25.6
BF/TA	220.5±21.7	243.4±16.1	297.9±26.3	269.7±24

4.3.3 Effect of CONDITION on EMG activity

4.3.3.1 Muscle amplitude and frequency parameters

Neither the RMS amplitude of the EMG signal (VL: [$F(1,7) = 3.751$; $p=0.094$]; BF: [$F(1,7) = 0.009$; $p=0.926$]; TA: [$F(1,7) = 0.167$; $p=0.695$] & GL: [$F(1,7) = 0.456$; $p=0.521$]) nor the MDF of the EMG power spectral density (VL: [$F(1,7) = 0.004$; $p=0.949$]; BF: [$F(1,7) = 3.563$; $p=0.101$]; TA: [$F(1,7) = 2.569$; $p=0.153$] & GL: [$F(1,7) = 0.011$; $p=0.920$]) differed significantly between CONTROL and AL in any muscle (Figs. 4.2a&b). There were also no POWER*CONDITION interactions (RMS: VL: [$F(1,7) = 3.769$; $p=0.093$]; BF: [$F(1,7) = 1.827$; $p=0.219$]; TA: [$F(1,7) = 1.092$; $p=0.331$] & GL: [$F(1,7) = 1.442$; $p=0.269$]; MDF: VL: [$F(1,7) = 0.416$; $p=0.539$] BF: [$F(1,7) = 0.411$; $p=0.542$] TA: [$F(1,7) = 1.249$; $p=0.301$] & GL: [$F(1,7) = 0.345$; $p=0.576$]).

4.3.3.2 Muscle activity patterns

During the AL trial, the VL activity onset was similar at MAX and 50W (-72.4 vs. -96.5±9.1°) but the offset at MAX was later than at 50W (129.4±7.4 vs 103.0±8°). BF activity onset occurred later than that of VL at both 50W (-48.7±9°) and MAX (-48±8.6°) though its offset was delayed at higher power outputs (50W: 153.6±10.5°; MAX: 198.1±17.7°). TA activity ended later at MAX than 50W (50W: 118.7±8°; MAX: 145.9±4.8°). The GL was active from -36.5±3.8° to 263.4±14.1° at 50W, both of which shifted later to -15.65±12.6° to 290.3±11° (Fig 4.3b).

The addition of 0.12Gz [~9kgs] (range 0.07 – 0.16Gz [5.2-11.9kgs]) load applied to the body by the SkinSuit did not significantly change the mean onset (VL: [$F(1,7) = 2.226$; $p=0.179$]; BF: [$F(1,7) = 0.684$; $p=0.436$]; TA: [$F(1,7) = 0.057$; $p=0.820$] & GL: [$F(1,7) = 3.046$; $p=0.124$]) and offset (VL: [$F(1,7) = 0.104$; $p=0.756$]; BF: [$F(1,7) = 3.570$; $p=0.101$]; TA: [$F(1,7) = 0.397$; $p=0.552$] & GL: [$F(1,7) = 0.826$; $p=0.394$]) times of the studied muscles (Fig. 4.3). Nevertheless, the GL encountered a main CONDITION effect [$F(1,7) = 8.071$; $p<0.05$] with regards to its duration, being significantly longer in AL vs. CONTROL (post-hoc test: $p=0.025$). The duration of all other muscles was unaffected by CONDITION (VL: [$F(1,7) = 1.576$; $p=0.250$]; BF: [$F(1,7) = 1.006$; $p=0.349$] & TA: [$F(1,7) = 0.229$; $p=0.650$]). There were no POWER*CONDITION interaction effects for onset (VL: [$F(1,7) = 0.211$; $p=0.660$]; BF: [$F(1,7) = 0.066$; $p=0.805$]; TA: [$F(1,7) = 1.083$; $p=0.338$] & GL: [$F(1,7) = 0.432$; $p=0.532$]), offset (VL: [$F(1,7) = 1.471$; $p=0.264$]; BF: [$F(1,7) = 0.200$; $p=0.668$] TA: [$F(1,7) = 1.490$; $p=0.268$] & GL: [$F(1,7) = 3.504$; $p=0.103$]) and duration (VL: [$F(1,7) = 0.122$; $p=0.737$]; BF: [$F(1,7) = 0.127$; $p=0.732$]; TA: [$F(1,7) = 0.004$; $p=0.951$] & GL: [$F(1,7) = 5.319$; $p=0.054$]) for all muscles.

The muscle activity patterns were highly and significantly correlated between the two conditions (range from 0.88 to 0.99; Table 4.1 bottom panel) at both 50W and MAX power outputs for all muscles (Fig. 4.4). For both 50W and MAX, the activation periods were shifted to significantly earlier times in the cycling revolutions for all muscles, except VL at 50W in AL compared to CONTROL (Table 4.1). The largest lag between the EMG envelopes in AL vs. CONTROL was registered for the TA (50W: 16.4° ± (4.2, 28.6); MAX: 16.8 ± (4.4, 29.2°).

The durations of the co-contraction periods were not significantly different between the AL and CONTROL trials for any examined synergistic or antagonist muscle pair (VL/BF: [$F(1,7) = 0.882$; $p=0.379$]; VL/GL: [$F(1,7) = 2.194$; $p=0.182$]; TA/GL: [$F(1,7) = 0.131$; $p=0.729$] & BF/TA: [$F(1,7) = 0.882$; $p=0.379$]; Table 4.2). On average, co-contraction periods for the TA/GL (AL: 258.1±27.1°; CONTROL: 202±23.3°) and BF/TA (AL: 243.4±16.1°; CONTROL: 220.5±21.7°) pairs tended to be longer at lower cycling power outputs but shorter at MAX in AL compared to CONTROL (TA/GL: 235.3±23.7° and 271.8±24.9°, respectively and BF/TA: 269.7±24° and 297.9±26.3°, respectively), but did not reach statistical significance due to high inter-individual variability. There were no POWER*CONDITION interactions in relation to the duration of co-contraction periods in any of the studied muscle pairs (VL/BF: [$F(1,7) = 0.685$; $p=0.435$]; VL/GL: [$F(1,7) = 5.494$; $p=0.052$]; TA/GL: [$F(1,7) = 2.246$; $p=0.185$] & BF/TA: [$F(1,7) = 0.730$; $p=0.426$].

4.4 Discussion

The main findings of this study were that increased cycling power output and the addition of 0.12Gz ABL caused differential modulation of the activation and coordination patterns of lower limb muscle activations. Increased cycling power was achieved by greater and longer EMG activity in all muscles, accompanied by increased median spectral frequency only in the

VL. Delayed EMG activity offset, an overall displacement of the main muscle energy generation to later periods within the cycle and an increased co-contraction of the thigh muscle antagonists (VL/BF) defined the major muscle coordination changes manifested at higher cycling power. The addition of ABL induced earlier activation of all but VL muscles at both low and high-power output and an increased GL activity duration. Axial body loading (ABL) also tended to reverse (albeit non-significantly) the relationship between cycling power and antagonist muscle pair co-contractions.

4.4.1 Neuromuscular responses during 1Gz cycling

The cycling patterns observed in this study were in concurrence with typical biomechanical cycling patterns. At 50W, VL activity occurred between -93° and 99°, with peak activity occurring at approximately TDC, consistent with the mono-articular role of this muscle, providing power to extend the knee and propel the leg downwards (Hug and Dorel, 2009). BF activity occurred at -46° to 160°, peaking prior to BDC in preparation for knee flexion during the upstroke. TA activity is usually throughout the pedal cycle, as it acts to dorsiflex the ankle but also provides stability to the talocrural joint (Raasch and Zajac, 1999); there was most inter-participant variability with TA activity, but generally activity started and ended at -85° to 110°, respectively. GL activity was also observed for the majority of the pedalling revolution from approximately 30° to 270°, consistent with its role as a talocrural joint stabliliser and an ankle plantarflexor. These activity patterns remained strongly correlated with POWER in the VL, BF and GL though less so in the TA, which may be related to differences in cycling technique between participants i.e. keeping the ankle dorsiflexed vs. plantarflexed (Fonda and Sarabon, 2010).

4.4.2 Effect of power output

4.4.2.1 Muscle activity levels

Consistent with the hypothesis, higher cycling POWER increased EMG RMS activation level in all muscles. VL EMG amplitude increased in AL and CONTROL by 3.7 and 2.7 times when cycling at MAX compared to 50W power (Fig. 4.3a), in line with the previously observed four-fold increases in VL activity at 80% peak power output (Macdonald et al, 2008). Dorel et al (2012) also observed increases in EMG RMS activity in 7 out of 11 studied right lower limb muscles, with most being mono-articular power producing extensors. These findings are consistent with the role of the VL as a primary power producer in cycling, which increase their activity more so than the bi-articular muscles (Blake et al, 2012). Increases in muscle activity levels are associated with decreases in MDF, indicative that both central and peripheral mechanisms are activated, to achieve greater power generation (Bigland-Ritchie and Woods, 1984). The contrary finding that MDF increased in the VL across POWER was, thus, not entirely anticipated.

4.4.2.2 Muscle activity patterns

Differential coordination strategies appear to have manifested between muscles in order to maintain pedalling cadence at 70Rrpm with increasing power output. The studied muscles exhibited a later offset or increased duration of muscle activity as well as activity shifts to a later phase with higher cycling power outputs, which were consistent across conditions. These results are in contrast to the notion proposed by Neptune and Hetzog (1999) that increases in power output are modulated to a greater degree by muscle activity amplitude rather than timing. However, longer durations of muscle activation can serve as an alternative strategy to generate energy and sustain the cadence at higher cycling load (Blake et al, 2012). Only the VL/GL and

VL/BF muscle pairs increased their co-contractions with POWER, which supports the argument that if the plantarflexors were not co-excited with the knee extensors during the downstroke, the energy would go towards accelerating the limbs rather than transferred to accelerate the crank (Raasch et al, 1997).

The muscle activity pattern adaptations exhibited with increased POWER may be one of many strategies to preserve and achieve maximal cycling performance. Hug et al (2008) observed a large amount of variation in the muscle activity between different participants which was not accompanied by significant amounts of variation in the pedal forces, implying that different strategies of muscle activity can produce similar forces on the pedals. Such strategies may be selected preferentially in an attempt to minimise fatigue and perceived effort (Prilutsky and Gregor, 2000). Nonetheless, because the left and right crank arms are mechanically linked, the assessment of unilateral coordination patterns and the extrapolation to bilateral patterns may be insufficient to fully understand the muscle coordination modulations illustrated here.

4.4.3 Effect of ABL

4.4.3.1 Muscle activity levels

Additional ABL of 0.12Gz (~9kg) during cycling did not induce significant increases in muscle activity level to those already elicited during CONTROL, contrary to the hypothesis.

Although the provision of ABL is low, findings from previous studies involving cycling with similar magnitudes of load support the notion that EMG burst scale by an increase in the number of motor units and firing rate as load increases (Baum and Li, 2003). Typical thigh weight is ~10% of total BW (Tözeren, 1999); thus, in the case of the study by Baum and Li (2003), where mean BW was 85 ± 10kg, each thigh would experience ~9.5-10.5kg to be

overcome with the addition of 1-2kg per thigh. SkinSuit-induced ABL over the thigh are intended to be ~70-85% of its total, adding ~3-4kg to each thigh, therefore amplifications in EMG activity were anticipated.

4.4.3.2 Muscle activity patterns

Although muscle-pair co-contractions were not affected by low-level ABL, it is interesting to note the trend that co-contractions in AL were higher than in CONTROL at 50W but lower than during CONTROL by MAX. Experienced cyclists have less coactivation of leg agonist/antagonist pairs during pedalling than novice cyclists (Chapman et al, 2008), implying an improvement in efficiency as the task is mastered. This may suggest that the addition of ABL renders the wearer's muscles more efficient at higher workloads and less so at lower workloads during cycling. The observation that EMG RMS from most muscles appeared lower in AL vs. CONTROL at MAX compared to 50W might support this argument.

Furthermore, cycling with 0.12Gz ABL did not modulate the power output-related onset and offset shifts in muscle activity compared to CONTROL; instead, it was shown to inflict earlier activity phase-shifts at both low and high-intensity power outputs – as evidenced by the lag induced by the cross-correlation function over the entire EMG ensemble. These results are congruent with that of Baum and Li (2003) who also noted significantly earlier activity in the RF and SOL and later activity in SOL with limb weights of 1-2kg's at the distal end of the thigh compared to unloaded cycling. Shifted EMG ensembles that have strong similarity in pattern – as corroborated by the correlation coefficient – may function to minimise muscle fatigue (Prilutsky and Gregor, 2000).

GL duration was lengthened in AL vs. CONTROL by prolonging its activation offset for a further ~15% at 50W in the transition from BDC to TDC, where its primary role is to aid in flexing the knee in preparation for the downstroke and ensure sufficient energy transfer to the pedal. These results are in concurrence to the lengthened duration of the SOL observed in the Baum and Li (2003) study. Although cycling has its biomechanical constraints, it can be questioned whether ABL induces ankle joint restrictions imposed by the securing of the stirrups underneath the feet. Such explanations may help to clarify some of the results observed within this study, particularly those pertaining to the ankle musculature. Raasch (1996) proposed a number of ankle-control strategies during cycling, one of which was a "locking" of the ankle in the plantarflexed position which prevents knee hyperextension, prolonging plantarflexor muscle activity. Kinematic assessment of lower-extremity joint angles should therefore be included in future investigations. Furthermore, during cycling, the saddle stabilises the body in the vertical plane, and the pedals transform the alternate action of the limbs into a continuous forward motion, thus the amount of energy to overcome gravitational and inertial forces with each pedal cycle is minimal (Di Prampero, 2000). Thus, load receptor feedback triggers may be attenuated (Dietz and Duysens, 2000), which might also contribute to the observation that muscle activity levels were not significantly increased with ABL at low or high-power outputs. It is, therefore, necessary to explore the effects of ABL in postures that require control of centre of mass.

4.5 Conclusion

Provision of 0.12Gz BW via ABL is sufficient to produce subtle but significant effects on muscle activation patterns during cycling. Specifically, lengthened duration of extensor muscle activity (GL) and earlier phase-shifts point to the significant interactions between body loading and coordination in leg extensor muscles. These results suggest an effect of ABL upon

neuromuscular control, despite the biomechanical constraints of cycling. In an attempt to more accurately interpret the effect ABL has on neuromuscular function during movement, investigation of such during free running exercise, posing an additional requirement to control centre-of-body mass, is warranted.

Chapter 5: The influence of additional axial body loading on cardiorespiratory responses during running in 1Gz and simulated partial gravity

5.1 Introduction

5.1.1 Chapters 5-7 collective introduction

In Chapter 3, cardiorespiratory variables during maximal aerobic cycling were unaffected by the addition of 0.12Gz ABL, though exercise tolerance was reduced by 12.6%. It was proposed that these results be partly related to biomechanical modulations. Chapter 4 reported muscle activity levels to remain similar to those elicited during 1Gz cycling, albeit with activity pattern modulations. Collectively, these findings may have been related to the fact that cycling requires minimal BW support and control of COM. Contrarily, running necessitates both components, permitting further exploitation of ABL-provision during human movement and is therefore the chosen exercise modality in the remaining experimental Chapters.

Treadmill running is an extremely common activity modality, utilised primarily for athletic/recreational training, rehabilitation and countermeasure exercise in 1Gz and <1Gz simulations on the ground (Bosch and Klomp, 2005; Sainton et al, 2015; Silder & Delp, 2015). Due to gravity, the ground can be hit without losing contact with it, though work must be done with each step to lift the body (Cavagna et al, 2000).

The gait cycle can be described as a series of movements of the lower extremities between initial contact, or heel-strike (HS), with the ground, until it regains contact with it (Nicola &

Jewison, 2012). It can be categorised into two main phases: the stance phase (where the foot is in contact with the ground) and the swing phase (where the foot is airborne). During running, stance makes up less than 50% of the cycle (Dugan & Bhat, 2005), whereas swing accounts for greater than 50%, causing an overlap of swing phases between lower extremities, generating a characteristic aerial phase (Dicharry, 2010). During HS – the beginning of stance– dorsiflexion, accompanied by knee flexion and hip motion are involved in distributing the force of impact through the closed kinetic chain (i.e. ankle to knee to hip), resulting in maximal ground reaction forces (GRFs). As the stance phase progresses, the HAM shortens and contract, enhanced by the contraction and push-off motion aided by the GAS and SOL, causing plantar flexion of the ankle and enabling toe-off (Nicola and Jewison, 2012). As toe-off occurs, the leg enters the swing phase, where the RF and TA are the most active. The HAM, GAS, SOL and hip extensors activate from late swing to the middle of stance, whereas the QUAD becomes active during late swing. The HAM lengthen as the lower leg extends where the foot's descent to the running surface begins.

5.1.2 Chapter 5-specific introduction

The following study, spanning this Chapter and the next, by design, aimed to focus on all three thesis objectives. The continuation of understanding how ABL affects both cardiorespiratory and neuromuscular responses during movement (objectives 1 and 2), and the introduction of objective 3 – understanding the efficacy of ABL as a means of "artificially creating" gravity exposure during exercise in partially-loaded environments are met by the creation of two sub-studies.

5.1.2.1 Factors affecting cardiorespiratory adaptations during running

Running requires a combination of joint stiffness and enhancement of muscle forces resulting from segmental stretch reflexes (Kuitunen et al, 2002), which changes muscle spindle sensitivity (Matthews & Stein, 1969). This promotes increased type Ia afferent activity (Matthews, 1984), subsequent facilitation of motor output due to increased EMG activity (Kram and Taylor, 1990), and consequential metabolic expenses (Chang et al, 2000). Thus, it is generally accepted that the relationship between running speed and $\dot{V}O_2$ is linear at speeds ranging from as low as $8km \cdot h^{-1}$ to as fast as $24km \cdot h^{-1}$ (Mayhew, 1977). Previous research has also observed that added (Inman et al, 1981; Teunissen et al, 2007; Walker et al, 2015) and reduced (Sainton et al, 2015; Raffalt et al, 2013; McNeill et al, 2015) load increase and decrease the energetic cost of running in humans, respectively.

5.1.2.2 Cardiorespiratory adaptations to increasing BW load during running

The energy cost of running has been shown to increase by 3.5-5% when running with an additional ~10% BW (Inman et al, 1981; Teunissen et al, 2007), likely attributed to the increased energy demand involved in maintaining speed, related to necessary greater vertical and horizontal forces to accelerate and decelerate an increased total inertial mass, respectively (Liew et al, 2016). However, Taylor et al (2012) found no calculable impediments in cardiorespiratory variables when running with ~20kg firefighting ensemble, though participants reached exhaustion 56% earlier and at a lower external work rate.

The addition of loads placed high up(e.g. backpacks), presents a challenge to normal breathing mechanics and predisposes the respiratory system as a limiting factor of exercise tolerance (Dominelli et al, 2012; Faghy and Brown, 2016). This has been postulated as the cause of reduced exercise tolerance denoted by a $5.5ml.kg.min^{-1}$ decline in $\dot{V}O_2peak$ when running with a 30kg

weighted vest (Walker et al, 2015). Such perturbations have been observed during exercise with circumferential chest wall strapping (CWS; Mendonca et al, 2013), which elicit similar pressures to that of intended Skinsuit pressures. A study by O'Donnell et al (2000) observed marginal changes in $\dot{V}O_2Max$ and cardiometabolic variables when cycling with and without CWS (49.21±2.12 vs. 50.96±2.01ml.kg.min^{-1}, respectively), accompanied by reduced exercise tolerance (~5%), $\dot{V}_E$ and $\dot{V}_T$ with a concurrent increase in BR, indicative of mechanical breathing constraints. The compressional nature of the SkinSuit is designed to be no greater than that of tight socks (~5-8mmHg; Waldie and Newman, 2010), but might be greater around the chest, where there is negligible elastic material stretch. The notion of increased work of breathing was proposed as a likely contributor to the POWER*CONDITION interactions in most respiratory variables in Chapter 3, though no analyses were undertaken to evaluate this.

5.1.2.3 Cardiorespiratory adaptations to decreasing BW load during running

Energy requirements for locomotion are significantly less when in partial gravity compared to 1Gz (Newman & Alexander, 1993); this pertains most obviously to astronauts, hence efforts to recreate a 1Gz stimulus through the Subject Loading Device (SLD) attached to the T2 treadmill on the ISS (Gosseye et al, 2010). Moreover, this concept has recently been incorporated into rehabilitation regimes for those recovering from a wealth of injuries (Hicks & Ginis, 2008; Farina et al, 2017). The idea that one can exercise at a reduced BW to attenuate loading on an offended area is intuitive given this principle and is enhanced further by the conception that the same individual can perform such an activity at reduced BW whilst being subjected to a full-BW stimulus, often accomplished by increases in speed (Grabowski & Kram, 2008). However, there are no data to support the use of ABL as a "reloading" stimulus during BW-supported running in such scenarios.

The most commonly utilised methods of BW removal during running are those that incorporate a treadmill with a lower body positive pressure (LBPP) device or a body suspension system. With the former, the individuals' lower body is enclosed by a waist-high pressure chamber, which increases such that the pressure difference around the waist seal produces an upward force, unloading individuals' BW. The latter supports individuals' in a harness that applies a controlled upwards force typically via pneumatics, i.e. pressurised air.

Numerous studies have observed the finding that metabolic cost reduces during running with BW support (Teunnisen et al, 2007; Grabowski & Kram, 2008; Raffalt et al, 2013; McNeill et al, 2015), primarily linked to a reduced mechanical power output requirement and thus a decreased need for ATP production (Farina et al, 2017). When running at speeds of 10.8-12km·h^{-1}, $\dot{V}O_2$, RER and HR have all been shown to decrease significantly at 0.7-0.8Gz, but in indirect proportion to the magnitude of BW support (Ruckstuhl et al, 2010; Kline et al, 2015; McNeill et al, 2015). In contrast, Teunissen et al (2007) and Grabowski and Kram (2008) observed almost linear decrements in metabolic rate (19±1.7% and ~33%, respectively, with 25% BW support) when running at 10.8km·h^{-1} compared to 100% BW. The discrepancies within these studies are likely related to the methods of BW support-application. Lower-body positive pressure treadmills have been shown to reduce HR in comparison to body suspension systems, possibly due to facilitation of venous return and reduced GRFs. Furthermore, these treadmills have been criticised for generating horizontal assistance which may overestimate metabolic cost reductions (Grabowski & Kram, 2008). Body suspension systems are beneficial because a purely vertical force can be applied (Teunissen et al, 2007).

5.1.3 Aims & hypotheses

The general aim of this study was to determine the effect of 0.2Gz ABL on cardiorespiratory variables during running. Specifically, there were three main objectives each of which sought to determine whether ABL: (1) affected these variables during slow, up to maximum-speed running and the interactions between them compared to 1Gz; (2) can elicit cardiorespiratory responses equivalent to those during 1Gz running when a simulated 1Gz scenario is created using a combination of vertical BW support and axial body reloading; (3) induces ventilatory dysfunction via the non-elastic material around the chest, in light of previous findings with CWS. It was hypothesised that all cardiorespiratory variables would increase when running with 0.2Gz ABL compared to without, at slow and faster running speeds; that cardiorespiratory variables would reduce proportionally with 0.2Gz BW unloading compared to 1Gz, which would restore to those witnessed at 1Gz when created via a combination of 0.8Gz BW support and 0.2Gz ABL and that subtle, but significant ventilatory perturbations would be present.

5.2 Methods

5.2.1 Participants

This study involved nine healthy male participants (29.4±5.2yr; 78.6 ± 6.8kg; 176.4 ± 6.7cm), each of whom provided written informed consent prior to participation in this study.

5.2.2 Overall Study Design

This study was a pseudo-randomised, counterbalanced repeated measures design and involved two sub-studies. The first study involved investigating cardiorespiratory responses during a) incremental treadmill running to volitional exhaustion at 1Gz vs. 1.2Gz (HYPERLOAD) and the second involved sub-maximal, speed-specific treadmill running during 1Gz, 0.8Gz, and

simulated 1Gz – created via a combination of 0.2Gz unloading and the addition of 0.2Gz ABL (EQUIVALENCE). Participants were required to attend the laboratory on two consecutive days; once for a $\dot{V}O_2$Max test in gym clothes (1Gz; "CONTROL") and the other in the SkinSuit (1.2Gz; "AL"). If the visit was for the former, they completed two, 3min runs for the second sub-study; if the visit was for the latter, they completed one 3min run (Fig. 5.1). Regardless of the visit, each 3min run was performed at a set-speed of $10km \cdot h^{-1}$.

5.2.3 Experimental protocol

5.2.3.1 Familiarisation

Owing to the fact that participants were required to run at <1Gz during parts of the EQUIVALENCE protocol, they were weighed upon arrival to the laboratory on both days to enable calculations of required BWs. Full BW was acquired in underwear, after which derivations of 80% were made. They were also made familiar with the support harness that was to be worn for both protocols, allowing customisation to fit for maximum comfort. Once in the harness, extra thin bathroom scales were placed underneath the participants' feet and BW removed until they were at the required BW for the condition they were trialling. Even with the 1Gz trials, BW removal to subtract the weight of the harness and equipment was undertaken. Starting with 1Gz, participants were asked to start the treadmill belt and increase the speed until they perceived themselves to be running at ~65-70% maximal effort – deemed to be challenging but enabled them to maintain a conversation. This was repeated for the 0.8Gz condition and replicated for familiarisation of the set-speed ($10km \cdot h^{-1}$).

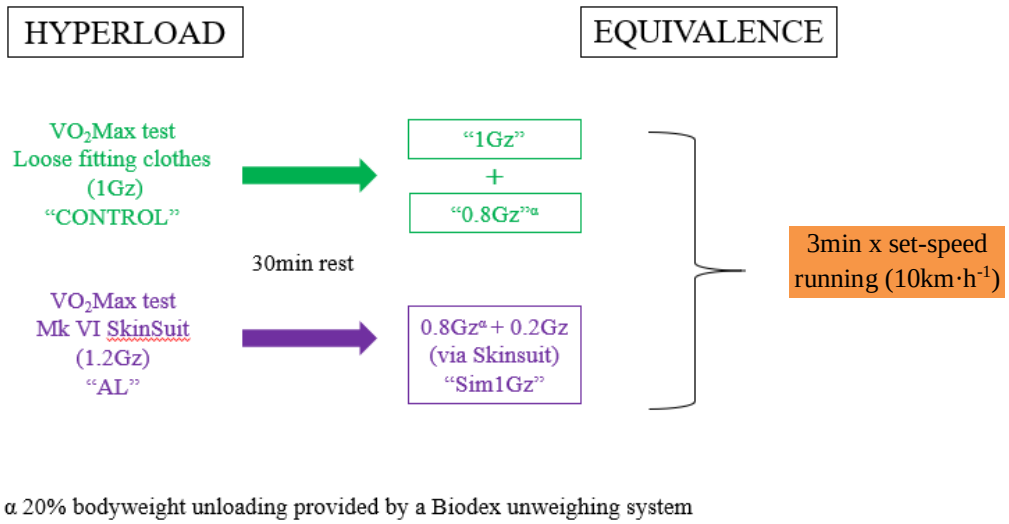

Figure 5.1: A schematic depicting the two parts of the experimental protocol. Participants completed a repeated measures design, which began with a treadmill test to exhaustion with speed increments of 1km·h^{-1} every min preceded by a 2min warm up at 9km·h^{-1}. After a 30min rest, participants ran for 3min at a set speed of 10km·h^{-1}. This was repeated twice, at both 1Gz and 0.8Gz – with the latter accomplished by 0.2Gz BW removal from the Biodex system – if performing the CONTROL condition. If the visit was for the AL condition, participants only performed one, 6min run, at a simulated 1Gz environment, invoked via 0.2Gz BW removal, and 0.2Gz axial body reloading via the SkinSuit.

5.2.3.2 HYPERLOAD protocol

Participants were required to run on a treadmill (h/p/cosmos pulsar 3p, Munich, Germany) starting at 9km·h^{-1} for 2min, followed by speed increments of 1km·h^{-1} every min, until volitional exhaustion. This was performed on two consecutive days in CONTROL and AL, in a pseudo-randomised order. SkinSuit-induced ABL was 0.1-0.24Gz across participants (Fig. 5.2).

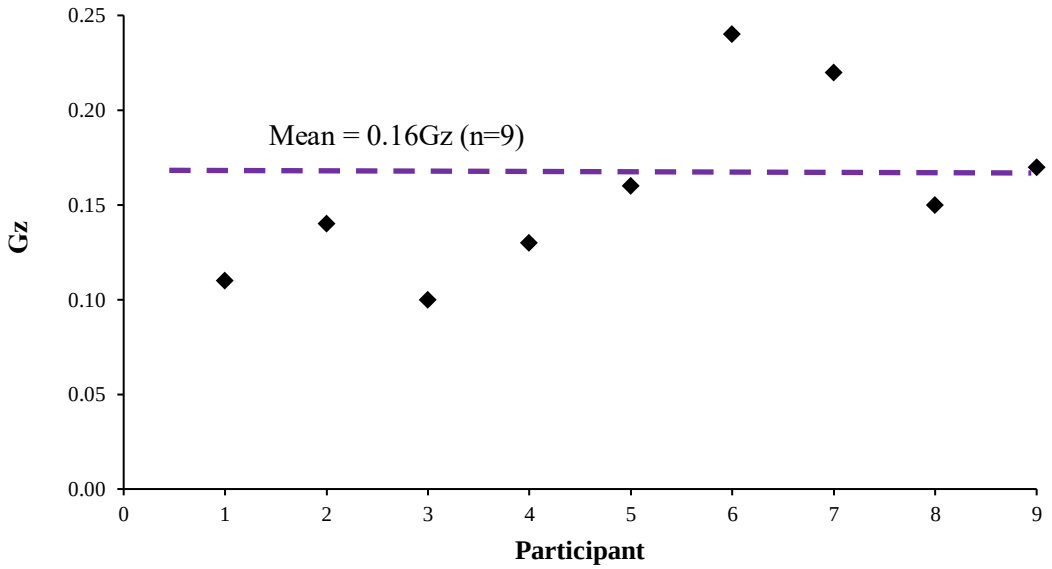

Figure 5.2: Individual and mean Skinsuit-induced Δ axial load (Gz) when standing. Dashed line is indicative of the mean across all nine participants. n=9.

The Biodex Unweighing System (Biodex Co., Shirley, NY, USA; Fig. 5.3) was attached to the treadmill providing unloading through using an h/p/cosmos unweighting harness strapped around the thorax and legs of each participant. A JUN/AIR (Michican, USA) compressor provided lift through compression of room air and application of upward pressure to lift the harness, removing the percentage of BW required. A standard operating procedure was performed ensuring the two compressor dials measured 10 and 7 bar, respectively. Systems providing BW support using harnesses attached to a vertical pulley have been shown to preserve normal walking kinematics during Gz levels close to 1Gz (Van Hedel et al, 2006). Their study showed that cadence, stride length and trajectories of the knee and ankle joint remained largely unaffected until a BW support of 75%. Thus, there was reassurance that there would not be an influence of the equipment on kinematic variables at 0.8Gz, and that any observed alterations on such variables can be attributed to the provision of unloading itself.

Figure 5.3: The H/P Cosmos treadmill with a Biodex Uweighting system equipped with a body harness attached around the shoulders and thighs. BW unloading is provided through compression of room air which permits upward force application.

The treadmill was connected to a base computer, allowing the belt to commence at 9km·h^{-1}, after which speeds were automatically adjusted. A 2min cool down at 4km·h^{-1} was enforced upon the participant signalling by a wave gesture that they had reached maximum effort.

5.2.3.3 EQUIVALENCE protocol

Because BW and speed interact (Raffalt et al, 2013), this sub-study employed sustainable, sub-maximal intensity running so that any response variations could be attributed to the ABL. A speed of 10km·h^{-1} was chosen because it undoubtedly defined a run – determined as presence of an aerial phase – which was confirmed visually during the familiarisation session for each participant. After 30min rest from the $\dot{V}O_2$Max test, participants undertook the

EQUIVALENCE protocol either once or twice. If the participant performed their $\dot{V}O_2$Max test in CONTROL, they performed two further 3min running bouts; one at 1Gz and one at 0.8Gz. If performed in AL, they performed the 3min run only at 0.8Gz with the extra 0.2Gz being provided by the SkinSuit, forming a simulated 1Gz condition ("Sim1Gz").

5.2.4 Data Collection

Continuous breath-by-breath respiratory data were acquired using a Cosmed Quark CPET metabolic cart (Rome, Italy), which was set-up and calibrated as per Chapter 2, section 2.3.3. The collected respiratory variables are also previously listed in Chapter 2 section 2.4.2. HR data was acquired via a heart rate strap as previously described (Chapter 3, section 2.3.4.2).

5.2.5 Data Analysis

Regarding both protocols, data was extracted for $\dot{V}_E$, $\dot{V}_T$, $\dot{V}O_2$, $\dot{V}CO_2$, BR, RER and HR during the final 30s of the rest period and for each speed before being averaged per participant. Regarding the HYPERLOAD protocol, data was extracted at speeds of 9-13km·h^{-1}, seeing as all participants achieved completion of these stages. Furthermore, a number of performance metrics were computed: $\dot{V}O_2$Max - defined as the highest $\dot{V}O_2$ value plus two breaths prior, the maximum speed achieved (km·h^{-1}), time to exhaustion (s) and the ventilatory breakpoint using the V-slope method (Beaver et al, 1986). Additional ventilatory analyses, permitting a more thorough representation of breathing mechanics (O'Donnell et al, 2009), were also undertaken, where BR and $\dot{V}_T$ were compared against $\dot{V}_E$ across running speeds in both conditions. Three out of the nine participants did not have either a visible ventilatory breakpoint or reliable HR data due to technical error of the HR strap and thus were excluded from analysis in case of data-confoundment.

Owing to the different loading witnessed between individuals and their SkinSuits, a linear regression analysis was first performed per parameter, speed and participant, in order to correct the variable value, had the loading have been 0.2Gz.

5.2.6 Statistical Analysis

All data were normally distributed (Shapiro-Wilk test). Two-way repeated measures ANOVA with SPEED (5 levels: 9km·h^{-1}, 10km·h^{-1}, 11km·h^{-1}, 12km·h^{-1} & 13km·h^{-1}) and CONDITION (2-levels: CONTROL vs. AL) as main factors as well as SPEED*CONDITION interactions were used to statistically analyse all variables for the HYPERLOAD protocol. With regards to the performance metrics, one-way repeated measures ANOVA was performed, using only the CONDITION comparison. EQUIVALENCE protocol analysis used a one-way repeated measures ANOVA with CONDITION as the main factor within the ANOVA, with 3 levels (0.8Gz, 1Gz and Sim1Gz). Due to multiple comparisons, post-hoc tests with Bonferroni correction were utilised to assess the location of between-CONDITION differences, in the event of significance. For BR and $\dot{V}_T$ comparisons against $\dot{V}_E$, a linear regression analysis was performed to evaluate potential differences in the slopes between CONTROL and AL.

5.3 Results

5.3.1 Effect of ABL during running at different speeds (HYPERLOAD protocol)

5.3.1.1 Cardiorespiratory variables

Figs. 5.4a-g show that all variables increased with SPEED: $\dot{V}_E$ [$F(5,40) = 156.571$; $p<0.001$]; $\dot{V}O_2$: [$F(5,40) = 1201.308$; $p<0.001$]; $\dot{V}CO_2$: [$F(5,40) = 305.593$; $p<0.001$]; $\dot{V}_T$: [$F(5,40) = 63.323$; $p<0.001$]; HR [$F(5,40) = 196.697$; $p<0.001$]; RER: [$F(5,40) = 16.048$; $p<0.001$]; & BR

: [F(5,40) = 62.140; p<0.001]. Post-hoc pairwise comparisons can be found in Table 5.1. HR [F(1,7) = 10.342; p<0.01] and $\dot{V}_T$ [F(1,8) = 6.292; p<0.05] were also affected by CONDITION, with the former increasing (p=0.015) and the latter decreasing (p=0.036) in AL vs. CONTROL, respectively. $\dot{V}_E$ [F(1,8) = 0.540; p=0.484]; $\dot{V}O_2$: [F(1,8) = 0.311; p=0.592]; $\dot{V}CO_2$: [F(1,8) = 1.211; p=0.303]; RER: [F(1,8) = 0.076; p=0.789]; & BR: [F(1,8) = 4.903; p=0.058] did not encounter a CONDITON effect. There were no SPEED*CONDITION interactions in any cardiorespiratory variable ($\dot{V}_E$ [F(5,40) = 0.359; p=0.873]; $\dot{V}O_2$: [F(5,40) = 0.770; p=0.577]; $\dot{V}CO_2$: [F(5,40) = 0.324; p=0.896]; $\dot{V}_T$ [F(5,40) = 0.445; p=0.814], HR [F(5,40) = 0.766; p=0.581], RER: [F(5,40) = 0.744; p=0.595] and BR: [F(5,40) = 1.159; p=0.346]. Linear regression analysis revealed no significant differences in $\dot{V}_E/\dot{V}_T$ between CONDITION (Fig. 4.5a), though a significantly steeper slope (p=0.044) in AL vs. CONTROL was observed with $\dot{V}_{E/}$ BR (Fig. 4.5b).

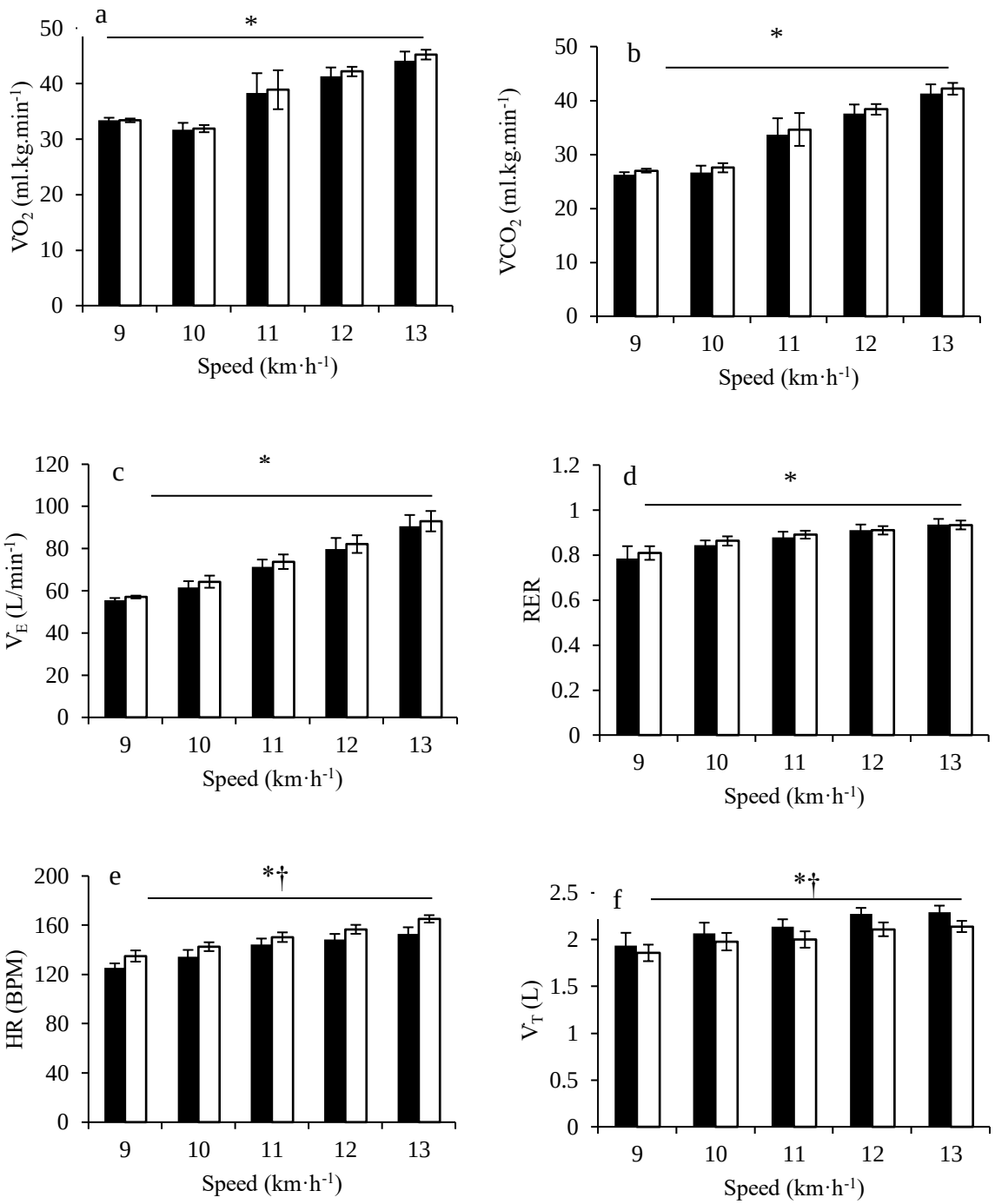
a
*
VO_2 (ml.kg.min^{-1})
50
40
30
20
10
0
9
10
11
12
13
Speed (km·h^{-1})
b
*
VCO_2 (ml.kg.min^{-1})
50
40
30
20
10
0
9
10
11
12
13
Speed (km·h^{-1})
c
*
V_E (L/min^{-1})
120
100
80
60
40
20
0
9
10
11
12
13
Speed (km·h^{-1})
d
*
RER
1.2
1
0.8
0.6
0.4
0.2
0
9
10
11
12
13
Speed (km·h^{-1})
e
*†
HR (BPM)
200
160
120
80
40
0
9
10
11
12
13
Speed (km·h^{-1})
f
*†
V_T (L)
2.5
2
1.5
1
0.5
0
9
10
11
12
13
Speed (km·h^{-1})

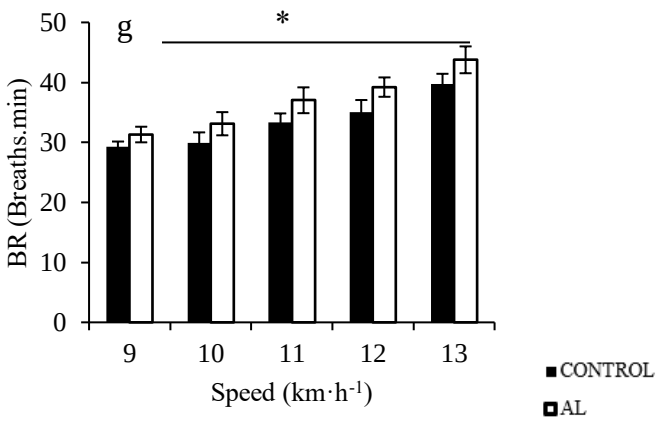

b

Figures 5.4a-g: Population average (±SEM) $\dot{V}_E$, $\dot{V}O_2$, $\dot{V}CO_2$, $\dot{V}_T$, HR, RER & BR from 9-13km·h^{-1}, in CONTROL and AL.* = main effect of SPEED; $p<0.05$. † = main effect of CONDITION; $p<0.05$. n=9, except for HR, where n=6.

Table 5.1: post-hoc pairwise comparisons for $\dot{V}_E$, $\dot{V}O_2$, $\dot{V}CO_2$, $\dot{V}_T$, HR, RER & BR during running at 9-13km·h^{-1}; p<0.05. n=9.

$\dot{V}_E$					
	9km·h^{-1}	10km·h^{-1}	11km·h^{-1}	12km·h^{-1}	13km·h^{-1}
9km·h^{-1}		p=0.000	p=0.000	p=1.000	p=0.019
10km·h^{-1}	p=0.000		p=0.000	p=0.015	p=1.000
11km·h^{-1}	p=0.000	p=0.000		p=0.000	p=0.000
12km·h^{-1}	p=1.000	p=0.015	p=0.000		p=0.000
13km·h^{-1}	p=0.019	p=1.000	p=0.000	p=0.000	
$\dot{V}O_2$					
	9km·h^{-1}	10km·h^{-1}	11km·h^{-1}	12km·h^{-1}	13km·h^{-1}
9km·h^{-1}		p=0.000	p=0.000	p=0.000	p=0.000
10km·h^{-1}	p=0.000		p=0.000	p=0.000	p=0.000
11km·h^{-1}	p=0.000	p=0.000		p=0.000	p=0.000
12km·h^{-1}	p=0.000	p=0.000	p=0.000		p=0.000
13km·h^{-1}	p=0.000	p=0.000	p=0.000	p=0.000	
$\dot{V}CO_2$					
	9km·h^{-1}	10km·h^{-1}	11km·h^{-1}	12km·h^{-1}	13km·h^{-1}
9km·h^{-1}		p=0.001	p=0.000	p=0.000	p=0.000
10km·h^{-1}	p=0.001		p=0.000	p=0.000	p=0.000
11km·h^{-1}	p=0.000	p=0.000		p=0.000	p=0.000
12km·h^{-1}	p=0.000	p=0.000	p=0.000		p=0.000
13km·h^{-1}	p=0.000	p=0.000	p=0.000	p=0.000	
$\dot{V}_T$					

	9km·h^{-1}	10km·h^{-1}	11km·h^{-1}	12km·h^{-1}	13km·h^{-1}
9km·h^{-1}		p=0.395	p=0.169	p=0.037	p=0.079
10km·h^{-1}	p=0.395		p=1.000	p=0.102	p=0.612
11km·h^{-1}	p=0.169	p=1.000		p=0.062	p=0.557
12km·h^{-1}	p=0.037	p=0.102	p=0.062		p=1.000
13km·h^{-1}	p=0.079	p=0.612	p=0.557	p=1.000	
HR					
	9km·h^{-1}	10km·h^{-1}	11km·h^{-1}	12km·h^{-1}	13km·h^{-1}
9km·h^{-1}		p=0.001	p=0.000	p=0.001	p=0.001
10km·h^{-1}	p=0.001		p=0.000	p=0.002	p=0.013
11km·h^{-1}	p=0.000	p=0.000		p=0.616	p=0.159
12km·h^{-1}	p=0.001	p=0.012	p=0.616		p=0.056
13km·h^{-1}	p=0.001	p=0.013	p=0.159	p=0.056	
RER					
	9km·h^{-1}	10km·h^{-1}	11km·h^{-1}	12km·h^{-1}	13km·h^{-1}
9km·h^{-1}		p=0.002	p=0.000	p=0.000	p=0.000
10km·h^{-1}	p=0.002		p=0.001	p=0.000	p=0.000
11km·h^{-1}	p=0.000	p=0.001		p=0.007	p=0.000
12km·h^{-1}	p=0.000	p=0.000	p=0.007		p=0.000
13km·h^{-1}	p=0.000	p=0.000	p=0.000	p=0.000	
BR					
	9km·h^{-1}	10km·h^{-1}	11km·h^{-1}	12km·h^{-1}	13km·h^{-1}
9km·h^{-1}		p=0.054	p=0.029	p=1.000	p=0.077
10km·h^{-1}	p=0.054		p=0.001	p=1.000	p=1.000

11km·h^{-1}	p=0.029	p=0.001		p=0.000	p=0.000
12km·h^{-1}	p=1.000	p=1.000	p=0.000		p=0.025
13km·h^{-1}	p=0.077	p=1.000	p=0.000	p=0.025	

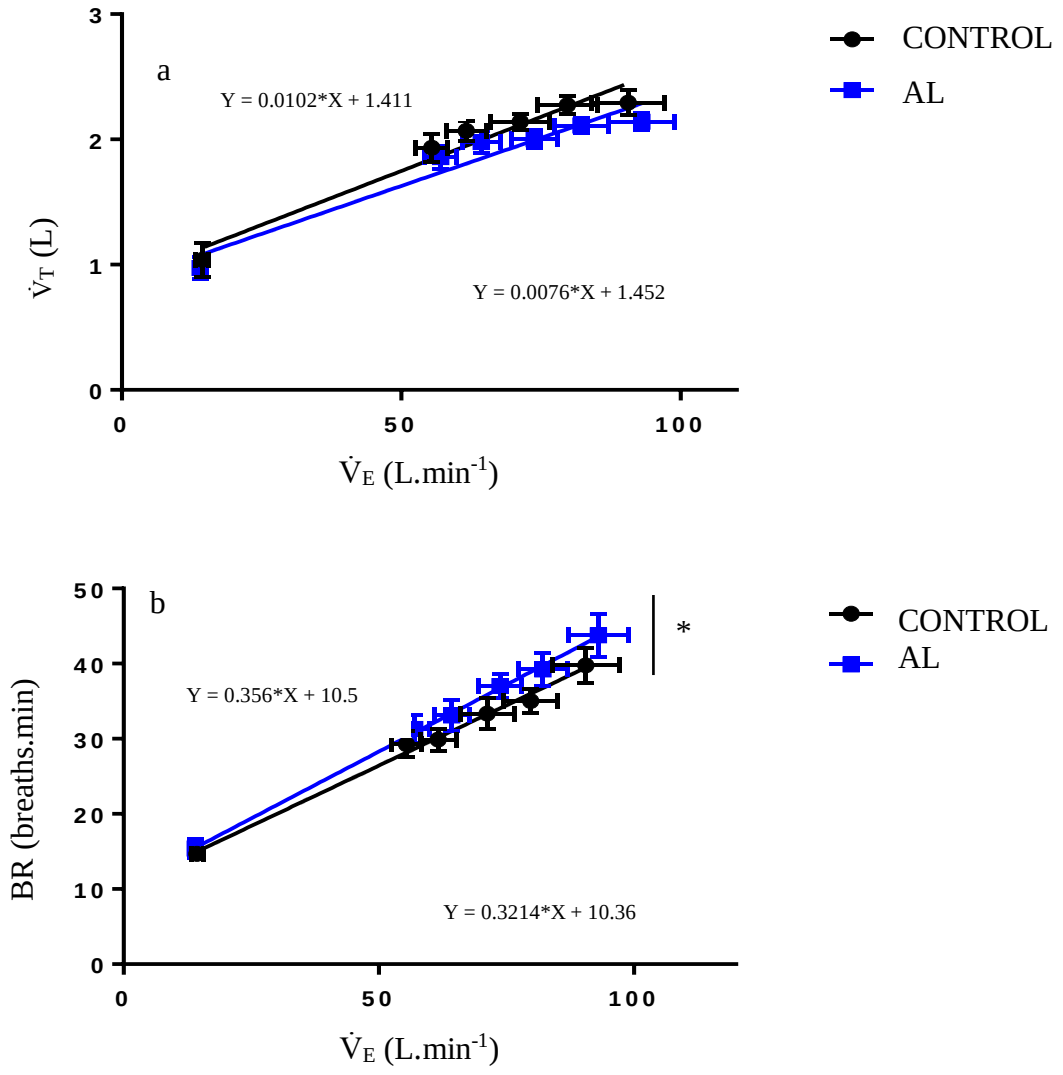

Figures 5.5 a and b: Population average (±SEM) scatter plots of (a) $\dot{V}_E$ vs. $\dot{V}_T$ and (b) $\dot{V}_E$ vs. BR in CONTROL and AL. * = significantly different regression slope between CONTROL & AL ($p<0.05$). n=9.

5.3.1.2 Performance metrics

There were no significant differences in $\dot{V}O_2Max$ in AL vs. CONTROL ([$F(1,8) = 1.047$; $p<0.05$]; Fig. 5.6a). However, CONDITION affected max speed [$F(1,8) = 7.2$; $p<0.05$] with reductions in AL vs. CONTROL ($15.8\pm0.5 km \cdot h^{-1}$ vs. $16.8\pm0.5 km \cdot h^{-1}$, respectively, Fig. 5.6c [$p=0.028$]) and thus a consequent reduction in the total test duration required to achieve $\dot{V}O_2Max$ in AL vs. CONTROL by 63.7s [$F(1,8) = 22.669$; $p<0.01$]; Fig. 5.6b [$p=0.001$]). The ventilatory breakpoint – determined as the % $\dot{V}O_2Max$ where the rise in $\dot{V}CO_2$ exceeded the rise in $\dot{V}O_2$ – was no different between CONDITION ([$F(1,8) = 0.063$; $p=0.808$]; AL: 83.1±6.6 & CONTROL: 73.9±5.6; Fig. 5.6d).

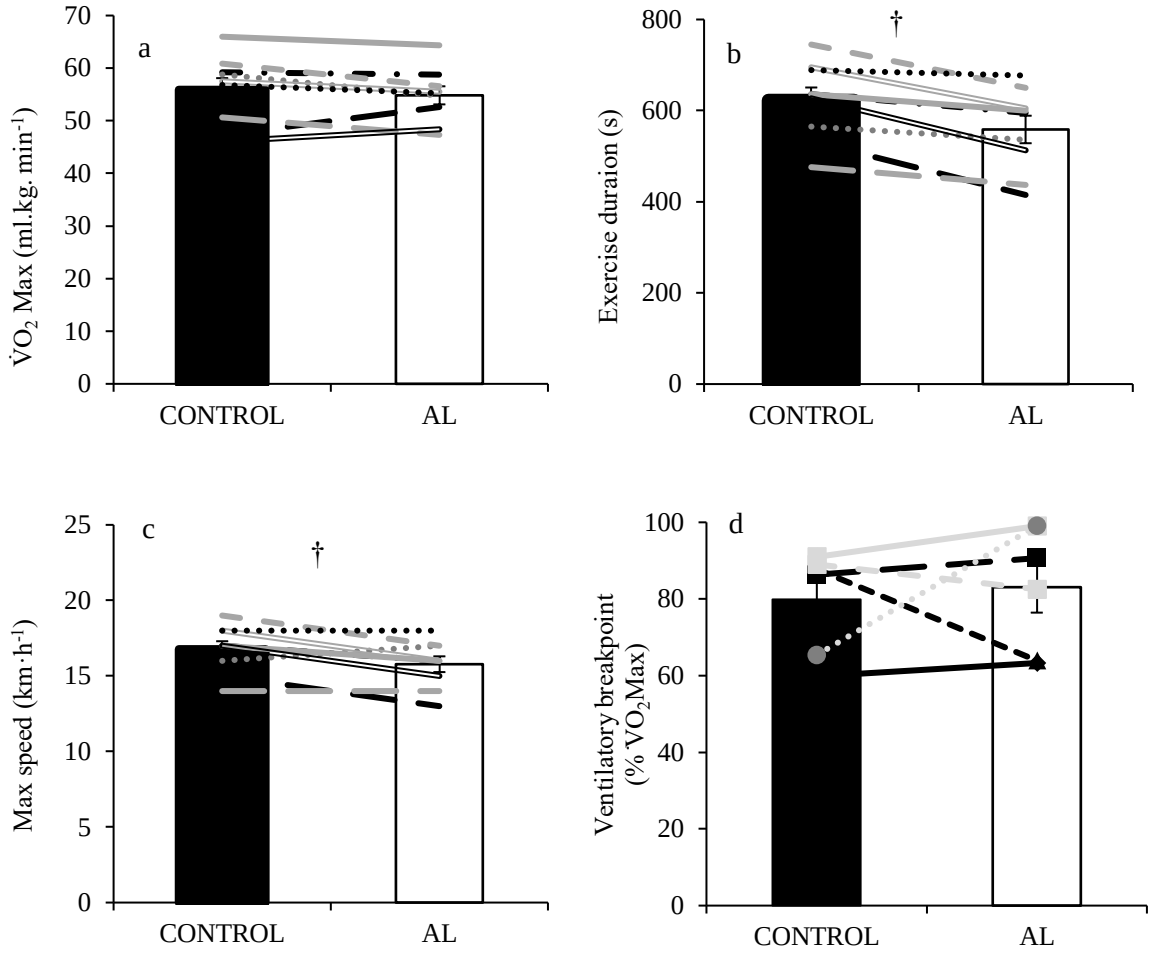

Figures 5.6 a-d: Population average (represented by the bars; ±SEM) and individual (lines) a) $\dot{V}O_2$Max (mean = thick black line) b) exercise duration (mean = thick black line), c) speed at $\dot{V}O_2$Max and d) ventilatory breakpoint in CONTROL and AL. † = main effect of CONDITION; $p<0.05$. n=9 except for d), where n=6.

5.3.2 Effect of 0.2Gz unloading and 0.2Gz axial body reloading (EQUIVALENCE protocol)

$\dot{V}O_2$ [$F(2,16) = 17.702$; $p<0.001$], $\dot{V}CO_2$ [$F(2,16) = 17.408$; $p<0.001$], $\dot{V}_E$ [$F(2,16) = 13.229$; $p<0.001$], $\dot{V}_T$ [$F(2,16) = 19.869$; $p<0.001$] and BR [$F(2,16) = 7.430$; $p<0.01$] were all affected by CONDITON (Fig. 5.7 and Table 5.2), whereas HR [$F(2,10) = 1.581$; $p=0.253$] and RER [$F(2,16) = 2.178$; $p=0.146$] were not. The reduction in $\dot{V}O_2$ and $\dot{V}CO_2$ at 0.8Gz vs. 1Gz were consistent with 0.2Gz BW unloading (19% and 22% respectively) and were also reduced at Sim1Gz vs. 1Gz (Table 5.3). $\dot{V}_T$ was lower at 0.8Gz vs. 1Gz (Table 5.2) and was also lower at

Sim1Gz vs. 1Gz (Table 5.3). Both $\dot{V}_E$ and BR were reduced at 0.8Gz vs. 1Gz, but not between 1Gz and Sim1Gz. However, BR was the only variable to differ with Sim1Gz vs. 0.8Gz, where it was greater in the former compared to the latter (Table 5.3).

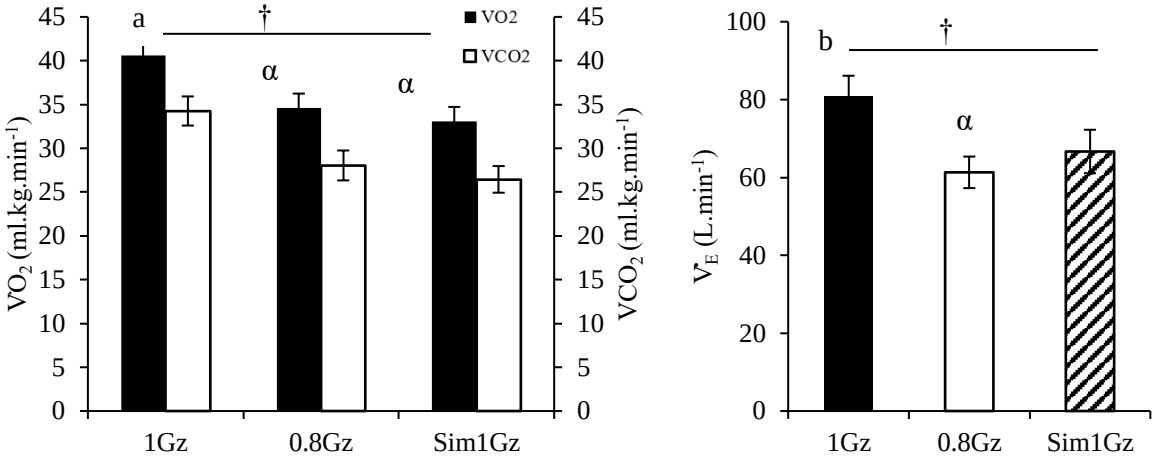

Figures 5.7 a and b: Population average (±SEM) a) $\dot{V}O_2$ & $\dot{V}CO_2$ and b) $\dot{V}_E$ during 1Gz, 0.8Gz & Sim1Gz during set-speed running at 10km·h^{-1}. † = main effect of CONDITION; p<0.01. α = significantly lower than 1Gz; post-hoc tests; p<0.05. n=9.

Table 5.2: Mean (±SEM) $\dot{V}_T$, BR , RER & HR during 1Gz, 0.8Gz & Sim1Gz during set-speed running at 10km·h^{-1}. † = main effect of CONDITION; p<0.01. α = significantly lower than 1Gz; post-hoc tests; p<0.05. n=9.

	1Gz	0.8Gz	Sim1Gz
$\dot{V}_T$ (L) †	2 ± 0.1	1.7 ± 0.1$^{\alpha}$	1.5 ± 0.1$^{\alpha}$
BR †	41.6 ± 2.4	37.4 ± 1.4$^{\alpha}$	45.3 ± 3
RER	0.84 ± 0.02	0.80 ± 0.02	0.80 ± 0.02
HR (BPM)	161 ± 4	157 ± 12	141 ± 9

Table 5.3: post-hoc pairwise comparisons for $\dot{V}_E$, $\dot{V}O_2$, $\dot{V}CO_2$, $\dot{V}_T$, HR, RER & BR during 1Gz, 0.8Gz and Sim1Gz during set-speed running at 10km·h^{-1}; $p<0.05$. n=9.

	1Gz vs. 0.8Gz	1Gz vs. Sim1Gz	0.8Gz vs. Sim1Gz
$\dot{V}O2$	P=0.000	P=0.009	p=0.823
$\dot{V}CO2$	P=0.000	P=0.024	p=0.780
$\dot{V}_E$	P=0.000	p=0.064	p=0.526
$\dot{V}_T$	P=0.011	P=0.001	p=0.138
HR	p=1.000	p=0.164	p=1.000
RER	p=0.052	p=0.645	p=1.000
BR	P=0.049	p=0.296	p=0.046

5.4 Discussion

This was the first study to determine the effect of 0.2Gz ABL on cardiorespiratory variables during incremental running and to ascertain whether 0.2Gz axial body reloading during sub-maximal running at 0.8Gz could elicit cardiorespiratory responses equivalent to those during 1Gz running. The main findings show that the addition of 0.2Gz ABL did not alter $\dot{V}O_2$Max, nor the associated cardiorespiratory variables, though reduced the time required to achieve it by 10.3%. Supplementary analyses allowed for a better understanding of ABL-induced breathing mechanics, suggesting an augmented work of breathing, manifested as a steeper BR/$\dot{V}_E$ relationship in AL compared to CONTROL. Additionally, axial body reloading lowered respiratory responses comparable to those elicited at 0.8Gz.

5.4.1 Effect of 0.2Gz axial body loading on cardiorespiratory responses during speed-incremented running in 1Gz

Increases in all cardiorespiratory variables when running from 9-13km·h^{-1} in 1Gz (Fig. 5.4a-g) were entirely foreseen, in agreement with previous literature (Mayhew, 1977; Grabowski and Kram, 2008), with $\dot{V}_E$ incurring the greatest increase (~39%). Increased running speed augments the requirement for joint stiffness and enhancement of muscle forces resulting from segmental stretch reflexes (Kuitunen et al, 2002). Such an adaptation i.e. the stretched muscle will change muscle spindle sensitivity (Matthews & Stein, 1969) and thus promote increased type Ia afferent activity (Matthews, 1984; Kram and Taylor, 1990), which consequentially increases metabolic cost (Chang et al, 2000).

Consistent with previous data presented in Chapter 3 (Attias et al, 2015), the ability to achieve maximal aerobic performance as well as most respiratory variables (excluding $\dot{V}_T$ and HR) were not affected by the provision of additional 0.2Gz ABL during incremental running. These findings are in contrast to an anticipated reduction in Max and induced greater cardiorespiratory "cost" when running at faster speeds. However, these results are consistent with Taylor et al (2012) who observed unimpeded respiratory variables during running with evenly-distributed firefighter ensemble, in contrast to hindrances when wearing heavy boots. Although maximal aerobic running performance was undisrupted by the provision of 0.2Gz ABL, it was accomplished 10.3% quicker. Reduced exercise tolerance has also been reported with the addition of load during running (Taylor et al, 2012; 56%). One explanation of these findings is said to reside in the way of disrupted ventilatory mechanics (Phillips et al, 2016). One of the aims within this study was to explore this concept further, in light of the possible interactions with performance metrics.

It was discerned in the results that the relationship between BR/$\dot{V}_E$ was disrupted when participants were subjected to additional 0.2Gz ABL during incremental running, whereby a greater BR was associated with the same $\dot{V}_E$ compared to CONTROL, as corroborated by a steeper regression slope (Fig. 5.5b). These findings are congruent with that of Phillips et al (2016), who noted increased BR (by 2%) and decreased $\dot{V}_T$ (by 6%) when carrying a 25kg backpack compared to without, which is characteristic of a rapid and shallow breathing pattern, likely to maintain alveolar ventilation. The fact that this data also showed a reduced $\dot{V}_T$ in AL vs. CONTROL – which appeared slightly magnified at faster speeds (9km.h: 1.86±0.09 vs. 1.93±0.01 [~4%] & 13km.h: 2.14±0.07 vs. 2.29l±0.1 [~6%], respectively) – supports the contention that 0.2Gz ABL may have induced altered ventilatory mechanics. Furthermore, such alterations may have been responsible for the exacerbated HR values evidenced with AL compared to CONTROL, particularly at faster speeds.

5.4.2 Effect of 0.2Gz unloading and 0.2Gz axial body reloading on cardiorespiratory responses during steady-state sub-maximal running

5.4.2.1 Body unloading

In concurrence with the hypotheses, some – primarily $\dot{V}O_2$, $\dot{V}CO_2$ and $\dot{V}_E$ – but not all respiratory responses were reduced with 0.2Gz unloading. Furthermore, such reductions were relatively linear considering the degree of BW unloading ($\dot{V}O_2$: 19%; $\dot{V}CO_2$: 22%, respectively). These are consistent with previous reports from Teunissen et al (2007) and Grabowski & Kram (2008) who observed proportional decrements in metabolic rate (19±1.7% and ~33%, respectively) when running with 0.25Gz BW unloading at 10.8km·h^{-1} compared to 1Gz. An interesting finding was that HR and RER did not fall significantly with 0.8Gz, in contrast to previous literature (Ruckstuhl et al, 2009; McNeill et al, 2015). However, both of

these studies utilised LBPP devices, which are known to provide additional horizontal assistance (Grabowski and Kram, 2008), which may further attenuate HR and RER responses during 0.8Gz running. Such assistance is not an identified feature of body-suspension devices, which may account for the discrepancies between the results presented and that of these aforementioned studies. Moreover, the absence of data from three participants due to technical error could be a likely cause of the large standard error mean, contributing to a lack of statistically-significant changes.

5.4.2.2 Axial body reloading

Contrary to the hypothesis, most cardiorespiratory variables were lower at Sim1Gz compared to 1Gz. With respect to variables that did not encounter a reduction at 0.8z compared to 1Gz (i.e. RER and HR), this isn't entirely unforeseen, as there was no decline to be regained. However, ventilatory variables subjected to a decrease during 0.8Gz were not offset by equivalent axial body reloading. For example, $\dot{V}O_2$ and $\dot{V}CO_2$ reduced from 40.6±1.6 and 34.3±1.7ml.kg.min^{-1} to 33.08±1.6 and 26.5±1.5ml.kg.min^{-1} with 0.2Gz unloading, which restored only to 34.8±1.7 and 28±1.7ml.kg.min^{-1}, respectively, during Sim1Gz.

Although merely a speculation, these findings could be related to the contribution of inadvertent circumferential compression around the lower extremities. Previous research has reported reductions in oxygen cost of 12.5% when running with compression tights (Bringard et al, 2006), attributed these reductions to assisted motion patterns by improved proprioception and muscle coordination. This argument may also help to explain the general indifferences in cardiorespiratory variables with CONDITION during the HYPERLOAD protocol. Nonetheless, investigation involving wearing the SkinSuit without securing the stirrups to

provide a compression-only comparison should be incorporated into future work to evaluate an effect of circumferential compression around the lower limbs.

5.5 Conclusion

Overcoming the resistance imposed by the SkinSuit was not metabolically equivalent to 20% BW when added to 1Gz or 0.8Gz running, as corroborated by indifferent maximal aerobic performance and associated cardiorespiratory variables compared to the respective control conditions. Nonetheless, as previously observed, 0.2Gz ABL reduced exercise tolerance, which could be related to disrupted breathing mechanics (i.e. a shallower yet more rapid pattern) as verified by supplementary ventilatory analyses. An inability for ABL to serve as a reloading stimulus during 0.8Gz running may be linked to inadvertent SkinSuit circumferential compression which future work should look to explore.

Chapter 6: The influence of additional axial body loading on neuromuscular and biomechanical responses during running in 1Gz and simulated partial gravity

6.1 Introduction

The previous Chapter presented the rationale and motivations for introducing a running exercise modality, to further explore the effects of ABL on the cardiorespiratory and neuromuscular systems. The experimental design outlined two separate protocols, to firstly continue the understanding of the influence of 0.2Gz ABL on intensity-incremented exercise in 1Gz (HYPERLOAD) and secondly to assume a comprehension of the ability of ABL to act as a reloading stimulus during BW-unloaded running (EQUIVALENCE). Cardiorespiratory data from both protocols were presented in Chapter 5 whereas the purpose of this Chapter is to present the neuromuscular and biomechanical data from this experimental study.

6.1.1 Effects of increasing speed

As running speed increases, the requirement for force production is greater, which is accomplished by changes in intra- and inter-muscle activation and pattern strategies. Furthermore, time spent in stance and stride duration reduce coupled with greater knee flexion to absorb shock and clear the limb into the swing phase (Dicharry, 2010). To achieve this the knee extensors (e.g. VL) elicit an earlier onset of activation and higher EMG amplitudes during the contact phase (Komi et al, 1987; Nilsson et al, 1985), which aid in preventing unnecessary yielding of the runner during the braking phase and regulate leg stiffness upon landing. Subsequently, the knee flexors (e.g BF) enhance force production in the contact phase when

extending the hip joint, by releasing elastic energy stored during the swing phase (Simonsen et al, 1985) before powerfully propelling the body forward into swing (Kyröläinen et al, 2005).

6.1.2 Effects of BW loading

Loading of the limb has been proposed to enhance activity of the antigravity (i.e. extensor) muscles during stance (Ivanenko et al, 2002), evidenced by Silder et al (2013), who found muscle activity across the entire gait cycle to increase when running with weight-vest loads of 10-30% BW for the SOL, GAS, lateral hamstrings, VM, VL and RF. Studies involving the addition of hand weights, belts and backpacks in the range of 20-30% BW have also reported muscle activity pattern modulations during walking and running, specifically increased duration (Stephens and Yang, 1999; Silder et al, 2013), later offset (Ghori and Luckwill, 1985) and earlier onset of the leg and hip extensors (Stastny et al, 2014). Such demonstrations were also observed in Chapter 4, where muscle activity patterns rather than levels were modulated in response to 0.12Gz additional ABL during cycling. Quantification of the effect of ABL during running on neuromuscular activity levels and patterns has not been attempted.

It is also established that the addition of low-moderate loads (10-40% BW) profoundly impacts lower-limb kinematics during walking and running. Concurrence amongst authors exists, where decreased step length (Stephens & Yang, 1999; Seay et al, 2014; James et al, 2015) and a shortened time spent in swing (Ghori & Luckwill, 1985; Brown et al, 2014b) have been observed. These kinematic adaptations result in a greater proportion of the step cycle with both feet on the ground, which aid in stabilising the individual against imparted COM-displacement. Conflicting results with regards to knee joint ROM have been reported when running sub-maximally with loads of 10-45% BW, where reductions (Kendrick et al, 2016), unchanged

(Brown et al, 2014b) and increases (Silder et al, 2015) have been observed, in comparison to the no load condition. These discrepancies may be related to the loading methodologies, suboptimal data interrogation (i.e. comparisons only being undertaken at initial contact) and a lack of neuromuscular activity analysis, leaving little clarity on a more thorough biomechanical picture. Analysis of both kinematic and neuromuscular activity of the lower-limb during running with load would, therefore, be appreciated.

6.1.3 Effects of BW unloading

In accordance with their antigravity function, the hip, knee and ankle extensor muscles show reduced activity with BW unloading. Studies offering running with BW unloading via treadmills equipped with lower-body positive pressure (LBPP) devices have reported reductions in the range of 5-35% in hip, knee and ankle extensor activity when running between 100-60% BW (Liebenberg et al, 2011, Hunter et al, 2014 and Sainton et al, 2015). Furthermore, these studies have shown contrasting findings with regards to the knee flexors, where the BF has been shown to reduce its activation – albeit to a lesser degree – alongside the extensors or remain unchanged. These findings are likely related to the reduced requirement of lower-limb musculature activation to serve ~5-8% decreases and increases in step frequency and swing time, respectively, observed with 20-25% BW unloading during running at 9-11km·h-1 (Grabowski & Kram, 2008; Raffalt et al, 2013 and Sainton et al, 2015). Minimal information exists on neuromuscular activity patterns with BW unloading. As aforementioned with regards to assessing the effects of ABL on running in 1Gz, analysis and interpretation of both kinematic and neuromuscular variables would allow for a more complete understanding of the biomechanical adaptations during running with BW unloading and thus during subsequent reloading.

6.1.4 Aims & hypotheses

The aim of this study was to investigate the effect of 0.2Gz ABL on neuromuscular and biomechanical variables during running. As with Chapter 5, there were specific objectives each of which sought to determine whether ABL: 1) affected these variables during slow, up to maximum-speed running and the interactions between them compared to 1Gz; (2) could elicit neuromuscular/kinematic responses equivalent to those during sub-maximal running at 1Gz when a simulated 1Gz scenario is created using a combination of vertical BW unloading and axial body reloading. The first objective was addressed via the HYPERLOAD protocol and the second via the EQUIVALENCE protocol (refer to Chapter 5, section 5.2.2-5.2.3).

It was hypothesised that all muscles' activity would increase with speed and that 0.2Gz ABL would magnify such – particularly in the extensors – with concomitant reductions in stride duration, compared to 1Gz. It was also anticipated that 0.2Gz unloading would reduce neuromuscular activity primarily in the extensor muscles, whilst also decreasing stride frequency i.e. increasing stride duration. It was also hypothesised that 0.2Gz axial body reloading would elicit equivalent responses to those seen during a comparative 1Gz running condition. Due to the ambiguous findings in the literature (aforementioned), hypotheses related to lower limb kinematics and muscle activity patterns could not be generated.

6.2 Methods

6.2.1 Experimental Protocol

The experimental protocol was previously defined in Chapter 5 section 5.2.3.

6.2.2 Data collection

VL, RF, BF, TA, GL, SOL, GMAX from the right leg were simultaneously recorded as per the methods outlined in Chapter 2, section 2.3.5. Sagittal plane kinematics were assessed using an electrogoniometer placed laterally to the right knee, as outlined in Chapter 2, section 2.3.6.

6.2.3 Data Analysis

As reported in the previous Chapter (5), the speed-related outcomes from the experimental protocol were not significantly different between the AL and CONTROL trials. Therefore, to test the hypotheses formulated in this Chapter only the EMG parameters from the 9km·h-1 and 13km·h^{-1} speeds were analysed and compared statistically.

The lowest knee angle within each stride representing maximal knee extension during heel strike was marked with events (Fig. 6.1). With reference to these event markers an average EMG ensemble profile of the rectified EMG signal was calculated for each muscle from all strides captured within the final 30s of running at each speed. Running at 13km·h^{-1} was used to represent a fast and 9km·h^{-1} a slow running speed; 13km·h^{-1} was the final speed that all participants completed in both conditions and 9km·h^{-1} was the starting speed implemented in the running protocol. All neuromuscular activity level and pattern variables extracted from the HYPERLOAD protocol have been described in Chapter 2, section 2.4.3 together with the approach for their analysis. The same variables were extracted from the EQUIVALENCE protocol with the exception of the cross-correlation function. Kinematic variables were analysed for both protocols as following the methods presented in Chapter 2 section 2.4.4-5.

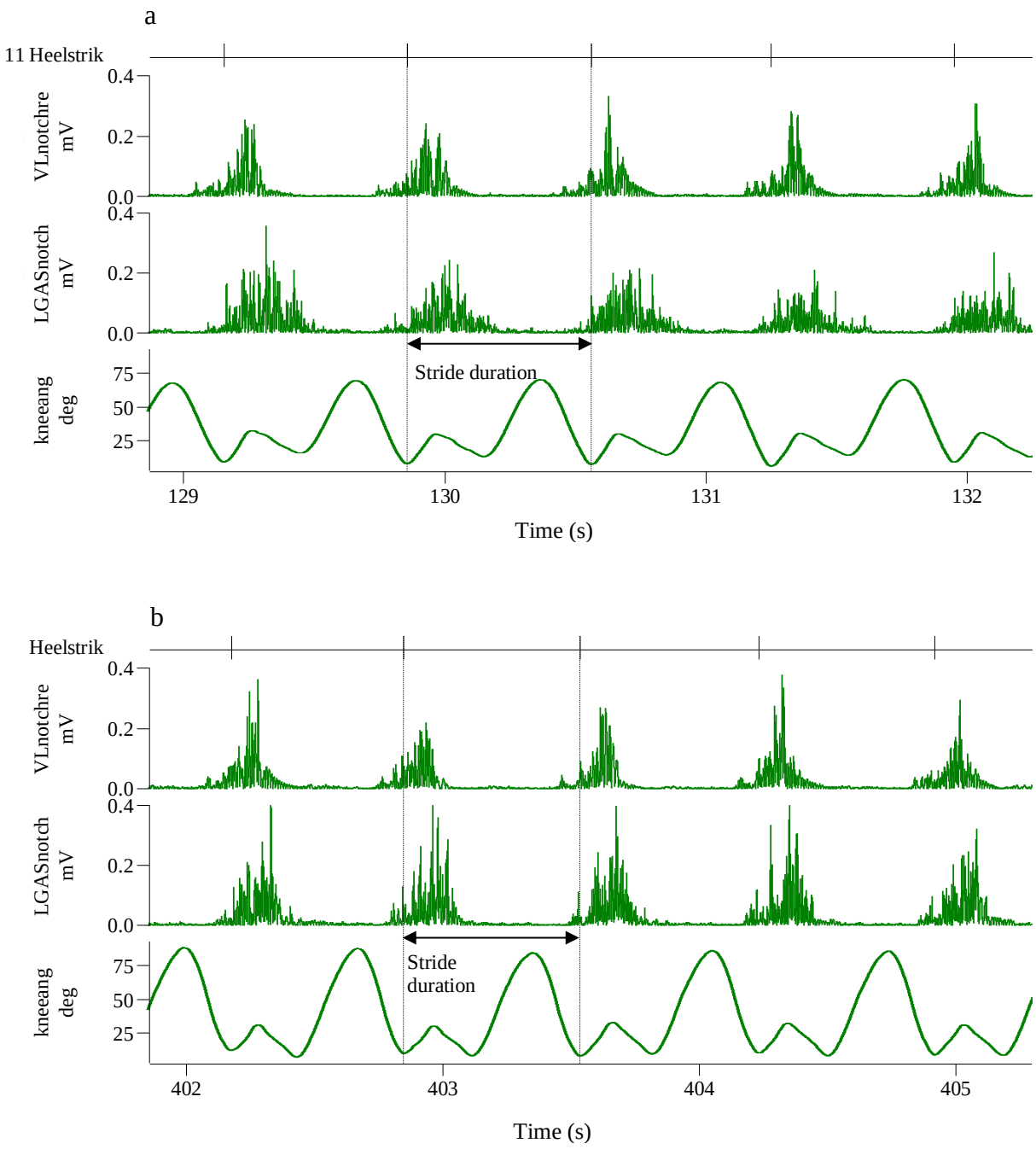

Figure 6.1: a sample trace of the GL and VL muscles, knee angle, and identification of heel strike with event markers from a) 9km·h^{-1} and b) 13km·h^{-1}. The period in between the dashed cursors signifies stride duration and all data is analysed with respect to this i.e. heel strike to heel strike.

6.2.4 Statistical analysis

All data were normally distributed (Shapiro-Wilk test). Two-way repeated measures ANOVA with SPEED (9km·h^{-1} vs. 13km·h^{-1}) and CONDITION (CONTROL vs. AL) as main factors were used to statistically analyse EMG and kinematic variables. Analysis for the

EQUIVALENCE protocol used a one-way repeated measures ANOVA with CONDITION as the main factor (0.8Gz, 1Gz and Sim1Gz); post-hoc tests with Bonferroni correction were employed to assess any between-CONDITION differences. Pearson's correlation coefficient and the cross-correlation function were calculated as explained in Chapter 2 section 2.4.3.3 to compare similarities of muscle activity patterns and displacement, respectively, between SPEED and CONDITION.

6.3 Results

6.3.1 Effect of ABL during running at different speeds (HYPERLOAD protocol)

6.3.1.1 EMG amplitude and frequency parameters

Electromyographic RMS increased with SPEED in all muscles except RF ([$F(1,8) = 3.350$; $p=0.105$]): TA [$F(1,8) = 6.959$; $p<0.05$]; SOL: [$F(1,8) = 10.188$; $p<0.05$]; GL: [$F(1,8) = 14.770$; $p<0.01$]; VL: [$F(1,8) = 42.680$; $p<0.001$]; BF [$F(1,8) = 7.140$; $p<0.05$] and GMAX: [$F(1,8) = 32.397$; $p<0.001$] (Fig. 6.2), where it increased from km.h to 13km.h (post-hoc tests; Table 6.1). A main effect of CONDITION was found for RMS amplitude of the VL ([$F(1,8) = 5.656$; $p<0.05$] -where CONTROL was higher compared to AL ($p=0.045$) – whereas TA [$F(1,8) = 3.525$; $p=0.097$], SOL [$F(1,8) = 1.518$; $p=0.253$], GL [$F(1,8) = 1.389$; $p=0.272$], BF [$F(1,8) = 1.799$; $p=0.217$], RF [$F(1,8) = 0.430$; $p=0.530$] and GMAX [$F(1,8) = 0.001$; $p=0.975$] were no different between conditions. BF RMS amplitude increased to a greater extent in AL vs. CONTROL at faster speeds compared to $9 km \cdot h^{-1}$ ([$F(1,8) = 5.5408$; $p<0.05$]; SPEED*CONDITION interaction effect), whereas no other muscle encountered a SPEED*CONDITION interaction (TA: [$F(1,8) = 2.334$; $p=0.165$]; SOL: [$F(1,8) = 1.619$;

p=0.239]; GL: [F(1,8) = 0.082; p=0.782]; VL: [F(1,8) = 2.263; p=0.171] RF: [F(1,8) = 0.014; p=0.910] and GMAX: [F(1,8) = 1.743; p=0.223]).

Table 6.1: post-hoc pairwise comparisons for EMG RMS amplitude of the TA, SOL, GL, VL, BF and GMAX during running at 9 and 13km·h^{-1}; p<0.05. n=9.

RMS amplitude	9km·h^{-1} vs. 13km·h^{-1}
TA	p=0.030
SOL	p=0.013
GL	p=0.005
VL	p=0.000
BF	p=0.028
GMAX	p-0.000

MDF of all lower-limb muscles was unaffected by SPEED (TA: [F(1,8) = 1.922; p=0.203]; SOL: [F(1,8) = 0.232; p=0.643]; GL: [F(1,8) = 0.031; p=0.866; VL: [F(1,8) = 3.173; p=0.113]; BF: [F(1,8) = 1.804; p=0.216]; RF: [F(1,8) = 1.209; p=0.303]; and GMAX: [F(1,8) = 1.615; p=0.239]). A main effect of CONDITION was observed for the MDF of the SOL [F(1,8) = 7.918; p<0.05], where CONTROL was greater than AL (p=0.023), whereas no other muscle encountered a CONDITION effect (TA: [F(1,8) = 0.042; p=0.843]; SOL: [F(1,8) = 1.922; p=0.203]; GL: [F(1,8) = 0.002; p=0.968]; VL: [F(1,8) = 1.799; p=0.217]; BF: [F(1,8) = 0.000; p=1.000]; RF: [F(1,8) = 4.917; p=0.057]; and GMAX: [F(1,8) = 0.196; p=0.669]). There were no SPEED*CONDITION interaction effects in any muscle (TA: [F(1,8) = 1.885; p=0.207]; SOL: [F(1,8) = 0.923; p=0.365]; GL: [F(1,8) = 2.418; p=0.159]; VL: [F(1,8) = 0.199; p=0.667]; BF: [F(1,8) = 0.310; p=0.593]; RF: [F(1,8) = 0.274; p=0.615]; and GMAX: [F(1,8) = 0.087; p=0.776]).

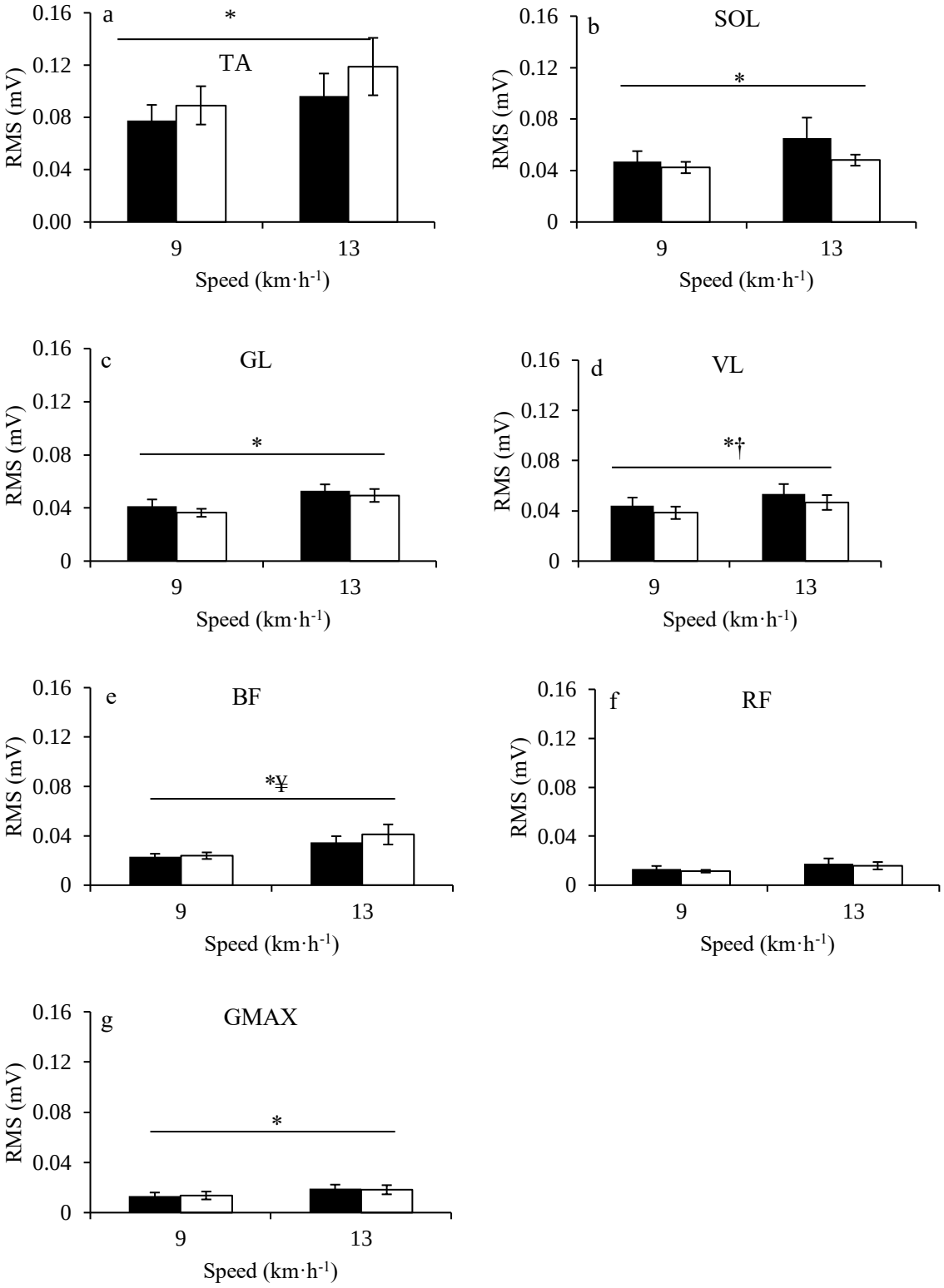

Figures 6.2 a-g: Population average (± SEM) RMS amplitude of TA, SOL, GL, VL, BF, RF & GMAX muscle EMG activity during running at 9 and 13km·h^{-1} in CONTROL (black bars) and AL (white bars). * = main SPEED effect; $p<0.05$. † = main CONDITION effect $p<0.05$. ¥ = SPEED*CONDITION interaction; $p<0.05$. n=9.

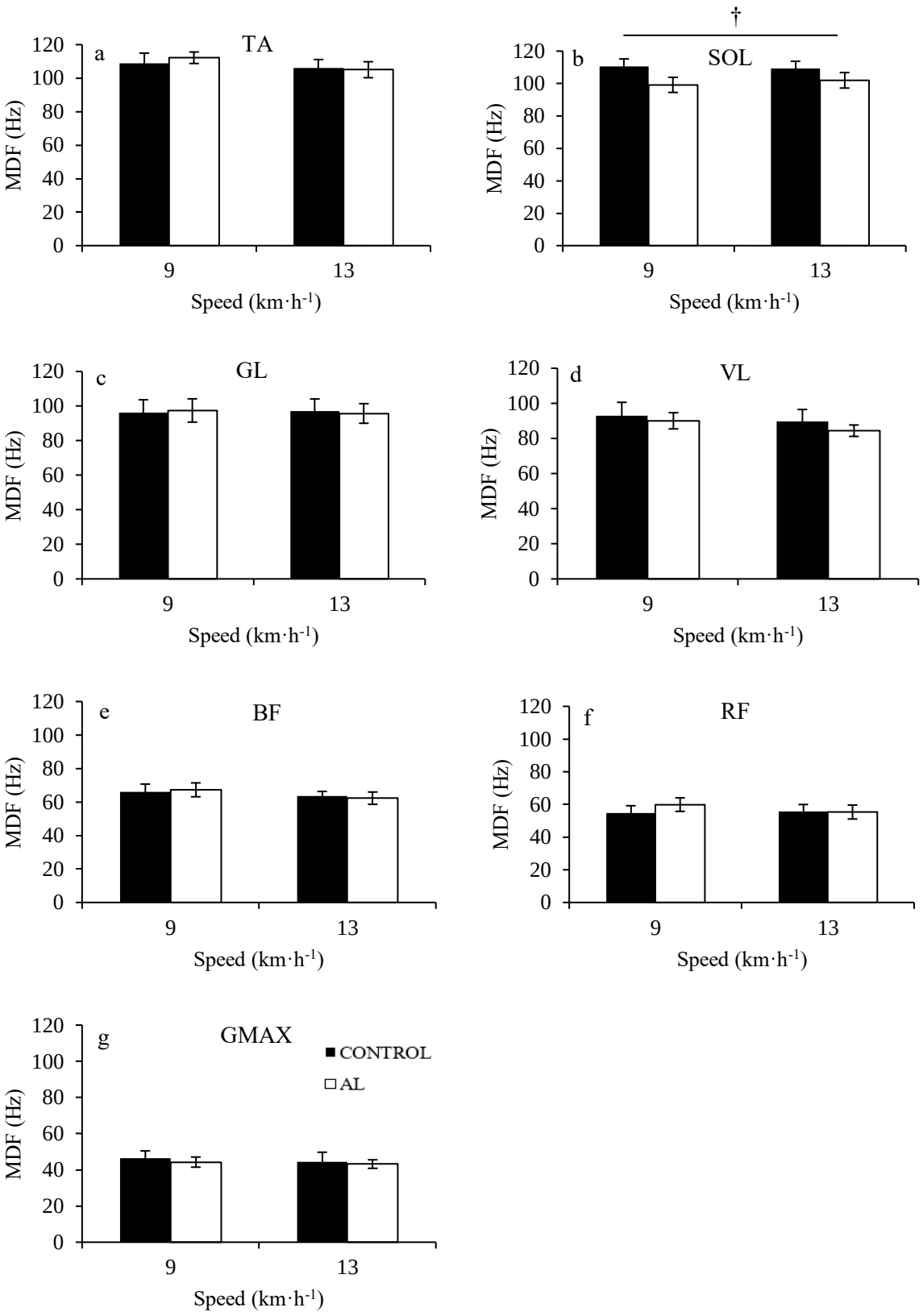

Figures 6.3 a-g: Population average (± SEM) MDF of TA, SOL, GL, VL, BF, RF & GMAX muscle EMG activity during running at 9 km·h^{-1} and 13 km·h^{-1} in CONTROL (black bars) and AL (white bars). † = main CONDITION effect; $p<0.05$. n=9.

6.3.1.2 Muscle activity patterns

At 9km·h^{-1} in CONTROL, the activity of the TA started ~60% prior to heesltrike (HS) with its offset slightly after heel strike (5%; Fig. 6.4a). The plantarflexor muscles (SOL and GL) operated with an activity onset at ~10% prior to HS through to about 40% of stance. VL activity began at a comparable time to the plantarflexors (~14% before HS) and was active for a similar duration (offset: ~36% after HS). RF onset was similar to the VL, GL and SOL, but its offset was deferred to ~70% after HS. The activity of the BF started 10% earlier (~45% prior to HS) and ended slightly later than that of the knee extensors/plantarflexors (~43% into stance). The GMAX started its activity at ~17% prior to HS, similar to the onset of the BF, but with an offset ~30% into stance.

The onset and offset of the TA (onset: [$F(1,8) = 0.184$; $p=0.679$]; offset: [$F(1,8) = 4.302$; $p=0.072$]), GMAX (onset: [$F(1,8) = 0.464$; $p=0.515$]; offset: [$F(1,8) = 1.728$; $p=0.225$]) and RF (onset: [$F(1,8) = 0.268$; $p=0.619$] offset: [$F(1,8) = 5.294$; $p=0.050$]) were unaffected by SPEED (Figs. 6.4a&b). In contrast, SOL EMG activity onset [$F(1,8) = 14.533$; $p<0.01$] and offset [$F(1,8) = 27.366$; $p<0.05$] were influenced by SPEED, both of which were earlier at 9km·h^{-1} vs. 13km·h^{-1} ($p=0.005$ and $p=0.001$, respectively). SPEED did not affect the onset of the GL [$F(1,8) = 1.525$; $p=0.252$], VL [$F(1,8) = 1.131$; $p=0.319$], or BF [$F(1,8) = 0.037$; $p=0.852$] but an effect on offset was observed (VL: [$F(1,8) = 56.272$; $p<0.001$]; BF [$F(1,8) = 15.650$; $p<0.01$]; GL: [$F(1,8) = 7.897$; $p<0.05$]), which were earlier at 13km·h^{-1} vs. 9km·h^{-1} ($p=0.000$; $p=0.004$ & $p=0.023$, respectively). BF onset [$F(1,8) = 6.737$; $p<0.05$] and GMAX offset [$F(1,8) = 5.434$; $p<0.05$] were subject to CONDITION effects, where both were later in AL vs. CONTROL ($p=0.016$ and $p=0.025$, respectively; Figs. 6.4a&b). The offset of the BF [$F(1,8) = 1.942$; $p=0.201$], onset of the GMAX [$F(1,8) = 1.597$; $p=0.242$] and both onset and

offset of all other muscles did not observe a CONDITION effect (TA: [F(1,8) = 0.463; p=0.516 & [F(1,8) = 4.302; p=0972]; SOL: [F(1,8) = 0.213; p=0.657] & F(1,8) = [3.601; p=0.094]; GL: [F(1,8) = 0.278; p=0.612] & [F(1,8) = 5.295; p=0.050]; VL: [F(1,8) = 0.20; p=0.892] & [F(1,8) = 0625; p=0.452] and RF: [F(1,8) = 2.455; p=0.156] & [F(1,8) = 0.027; p=0.873] for onset and offset, respectively]. There were no SPEED*CONDITION interactions in the onset or offset of any muscle (TA: [F(1,8) = 0.243; p=0.635] & [F(1,8) = 0.160; p=0.700]; SOL: [F(1,8) = 0.669; p=0.437] & [F(1,8) = 0.226; p=0.647]; GL: [F(1,8) = 1.605; p=0.241] & [F(1,8) = 0.399; p=0.545]; VL: [F(1,8) = 0.249; p=0.631] & [F(1,8) = 9.768; p=0.052]; BF: [F(1,8) = 0.528; p=0.488] & [F(1,8) = 3.352; p=0.097]; RF: [F(1,8) = 3.720; p=0.090] & [F(1,8) = 0.208; p=0.660] and GMAX: [F(1,8) = 0.031; p=0.865] & [F(1,8) = 0.282; p=0.610] for onset and offset, respectively).

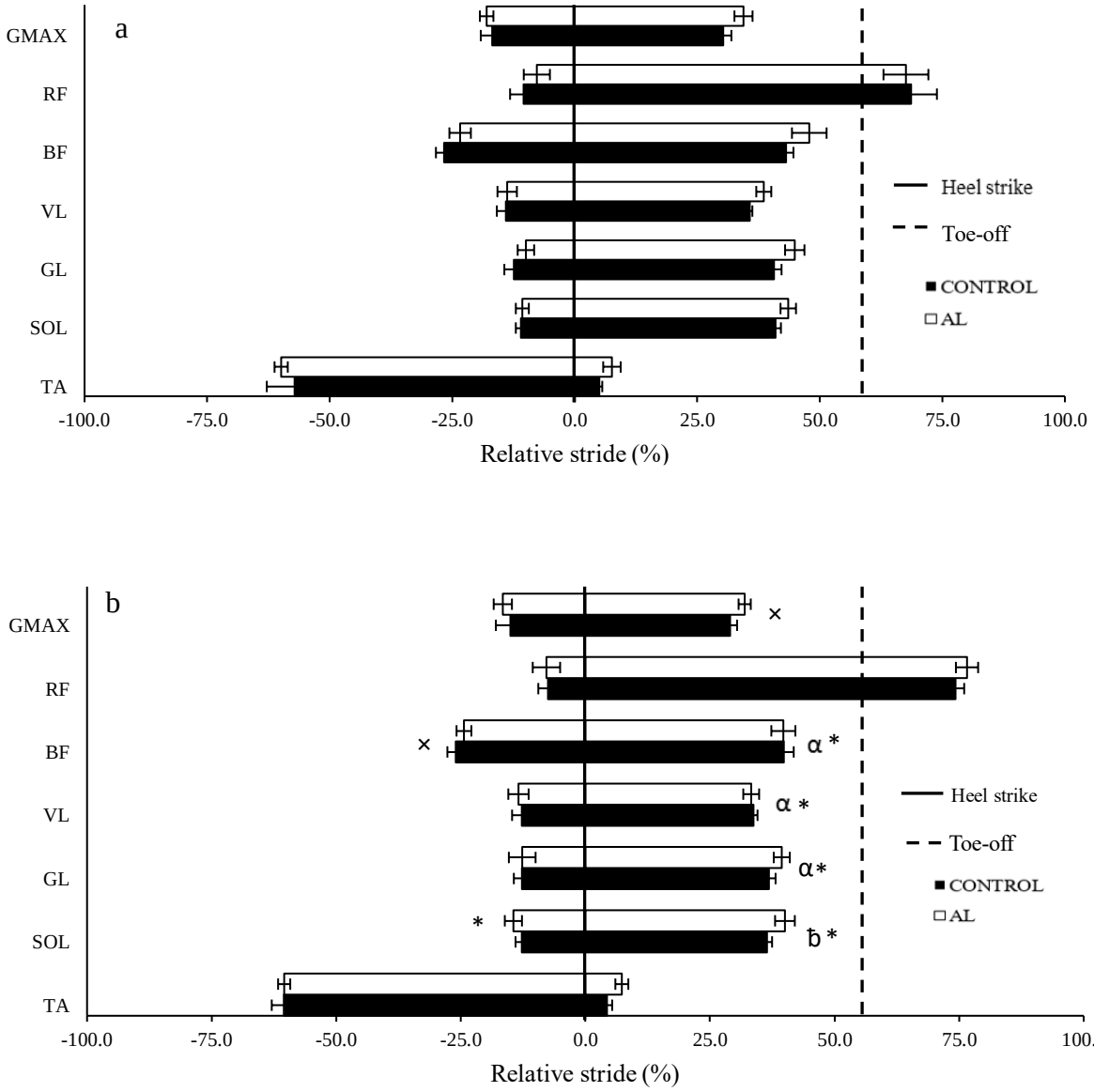

Figures 6.4 a and b: Population average (± SEM) muscle activity duration, onset and offset of TA, SOL, GL, VL, BF, RF & GMAX at a) 9km·h^{-1} and b) 13km·h^{-1} in CONTROL and AL.α = main effect of SPEED with duration; $p<0.05$. ƀ = main effect of CONDITION with duration; $p<0.05$. * = main effect of SPEED with onset (left side of the graph) and offset (right side of the graph); $p<0.05$. × = main effect of CONDITION with onset (left side of the graph) and offset (right side of the graph); $p<0.05$. The solid and dashed lines signify heel strike and toe-off respectively; these are collective for AL & CONTROL owing to the absence of difference in stance ratio between them. n=9.

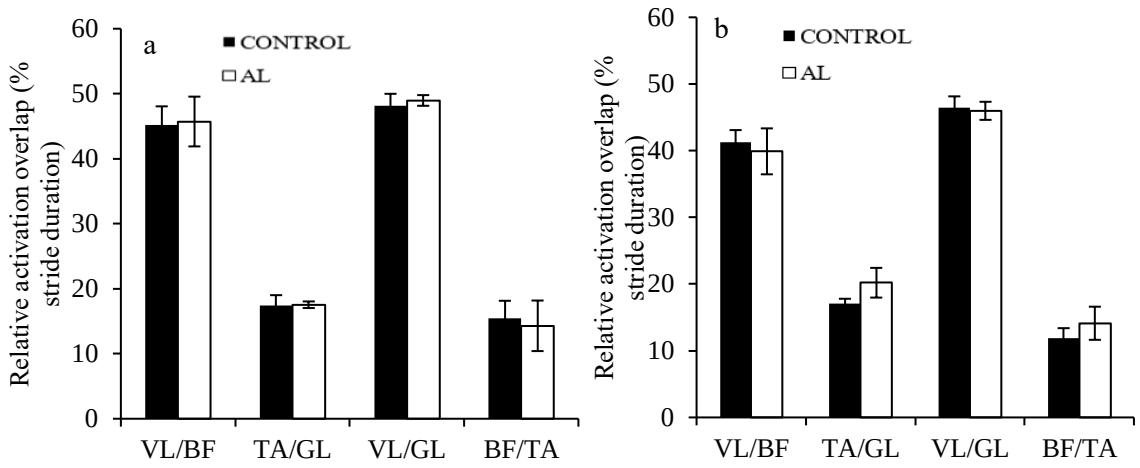

Figures 6.5 a and b: Population average (± SEM) co-contraction time between antagonistic and synergistic muscle pairs VL/BF, TA/GL, VL/GL, & BF/TA at 9km·h^{-1} (top) and 13km·h^{-1} (bottom) in CONTROL and AL. n=9.

There were no significant SPEED (VL/BF: [F(1,8) = 17.786; p=0.051]; TA/GL: [F(1,8) = 0.601; p=0.460]; VL/GL: [F(1,8) = 4.181; p=0.075] & BF/TA: [F(1,8) = 2.616; p=144]), CONDITION (VL/BF: [F(1,8) = 0.141; p=0.717]; TA/GL: [F(1,8) = 0.620; p=0.454]; VL/GL: [F(1,8) = 0.001; p=0.974] & BF:TA: [F(1,8) = 1.579; p=0.244]) or SPEED*CONDITION interaction effects (VL/BF: [F(1,8) = 1.504; p=0.255]; TA/GL: [F(1,8) = 1.873; p=0.208]; VL/GL: [F(1,8) = 0.221; p=0.651] & BF:TA: [F(1,8) = 0.329; p=0.582]) on co-contraction time of any muscle pair (Fig. 6.5).

Comparison of muscle activity patterns using average EMG ensembles (Fig. 6.6) showed very strong positive correlations for all muscles with SPEED in CONTROL and AL (Table 6.2). All muscles activity patterns also display very strong positive correlations between CONDITION at 9km·h^{-1}, with negligible differences at 13km·h^{-1} (Table 6.2). Lag analysis of the cross correlation shows activity for SOL, GL and RF to be shifted significantly earlier in both CONTROL and AL and VL and BF only in AL with SPEED (Table 6.3). In contrast to SPEED,

a CONDITION effect was observed only in the GL, where activity started later in AL vs. CONTROL at 9km·h^{-1}.

GL [F(4,32) = 5.776; p<0.01], VL [F(4,32) = 9.656; p<0.01] and BF [F(1.997,15.975) = 6.410; p<0.01] duration were affected by SPEED, unlike TA ([F(1,8) = 0.314; p=0.591], SOL: [F(1,8) = 1.792; p=0.217], RF [F(1,8) = 3.647; p=0.093] and GMAX: [F(1,8) = 2.897; p=0.127]). Both the GL (p=0.001) and BF (p=0.009) decreased from 9km·h^{-1} to 13km·h^{-1} in contrast to VL duration, which increased from 9km·h^{-1} to 13km·h^{-1} (p=0.000). SOL [F(1,8) = 12.303; p<0.01] was the only muscle to elicit a CONDITION effect (TA: [F(1,8) = 1.685; p=0.230]; GL: [F(1,8) = 1.009; p=0.344]; VL: [F(1,8) = 1.141; p=0.317]; BF: [F(1,8) = 0.014; p=0.907]; RF: [F(1,8) = 0.056; p=0.820] and GMAX: [F(1,8) = 3.992; p=0.081], attributed to a longer duration in AL vs. CONTROL (p=0.008; Fig. 6.4). There were no SPEED*CONDITION interaction effects on the duration of activity in any muscle (TA: [F(1,8) = 0.233; p=0.642]; SOL: [F(1,8) = 0.580; p=0.468]; GL: [F(1,8) = 0.066; p=0.804]; VL: [F(1,8) = 0.743; p=0.414]; BF: [F(1,8) = 10.263; p=0.052]; RF [F(1,8) = 0.985; p=0.350] and GMAX: [F(1,8) = 0.069; p=0.799]).

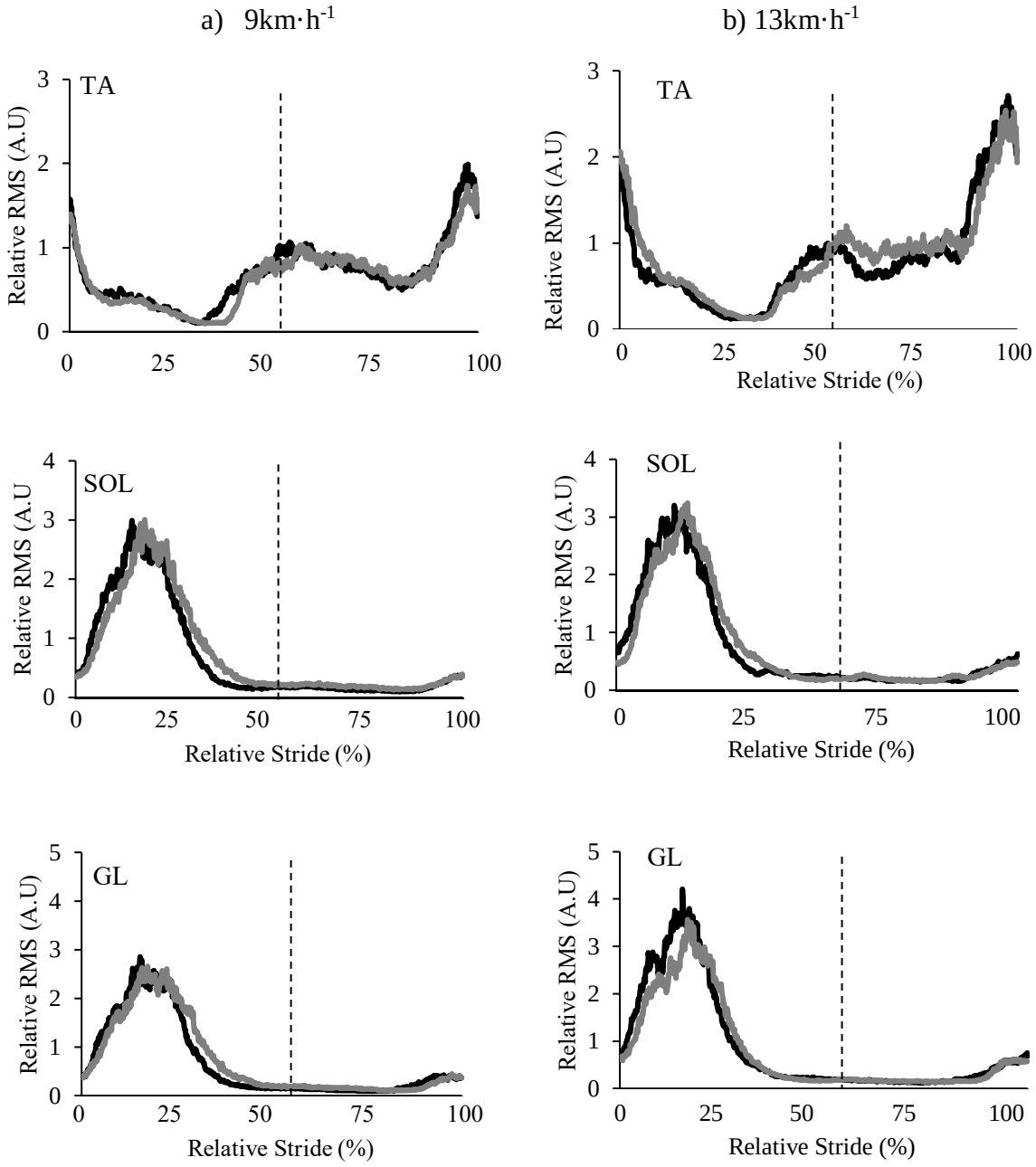
a) 9km·h-1
b) 13km·h-1
TA
SOL
GL
Relative RMS (A.U)
Relative Stride (%)
0
25
50
75
100

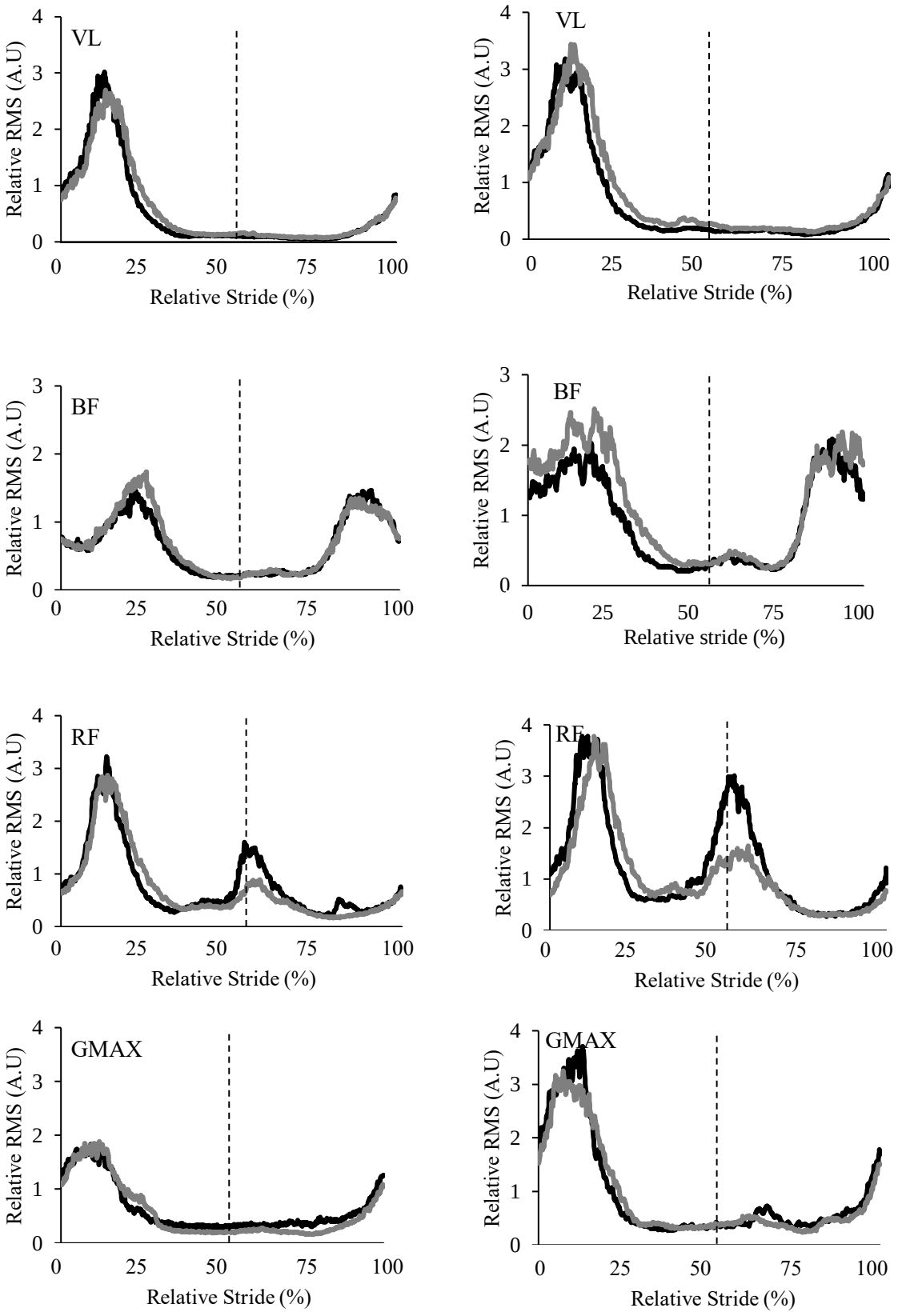

Figures 6.6 a and b: Population average ensemble curve of EMG RMS envelopes for each muscle at a) 9km·h^{-1} (left panel) and b) 13km·h^{-1} (right panel) for all participants. Magnitudes were normalised to the mean RMS from

9km·h^{-1} during the respective condition for each participant per muscle. Heel strike = 0% relative stride. Dashed line = beginning of the swing phase (~55% stride as denoted by stance ratio at both 9km·h^{-1} and 13km·h^{-1} in CONTROL and AL; Fig. 6.8). n=9.

Table 6.2: Pearson correlation coefficients between ensemble EMG curves across CONDITION at 9km·h^{-1} & 13km·h^{-1} (1st and 2nd columns), and SPEED in CONTROL & AL (3rd and 4th columns); * = significant correlation; $p<0.01$. n=9.

CONTROL vs AL: 9km·h^{-1}	CONTROL vs AL: 13km·h^{-1}	9km·h^{-1} vs. 13km·h^{-1}: CONTROL	9km·h^{-1} vs. 13km·h^{-1}: AL
TA			
r = .974*	*r* =.973*	*r* =.922*	*r* =.946*
SOL			
r =.971*	*r* =.976*	*r* =.970*	*r* =.965*
GL			
r = .968*	*r* = .973*	*r* =.962*	*r* =.956*
VL			
r =.968*	*r* =.967*	*r* =.971*	*r* =.968*
BF			
r =.943*	*r* =.921*	*r* =.901*	*r* =.866*
RF			
r =.923*	*r* =.949*	*r* =.933*	*r* =.912*
GMAX			
r =.973*	*r* =.986*	*r* =.982*	*r* =.957*

Table 6.3: Cross-correlation lags (± 95% confidence intervals) between ensemble EMG curves across SPEED in CONTROL and AL and CONDITION at 9km·h^{-1} and 13km·h^{-1}. * = significantly earlier activity at 13km·h^{-1} vs. 9km·h^{-1}. † = significantly later activity in AL vs. CONTROL. n=9.

CONTROL	AL	9km·h^{-1}	13km·h^{-1}
TA		<u>TA</u>	
0.55 (-0.52, 1.62)	0.27 (-0.09, 0.63)	-2.42 (-4.88, 0.02)	-1.29 (-3.01, 0.43)
GL		<u>GL</u>	
4.88 (0.76, 9.01)*	8.28 (3.63, 12.94)*	-8.36 (-15.14, -1.58)†	-6.7 (-14.52, 1.08)
BF		<u>BF</u>	
2.89 (-2.40, 8.18)	2.89 (0.41, 6.78)*	-1.68 (-3.68, 0.33)	-2.3 (-5.18, 0.5)
GMAX		<u>GMAX</u>	
0.12 (-0.81, 1.04)	0.2 (-0.79, 1.18)	-0.7 (-1.55, 0.15)	-2.7 (-7.1, 1.8)
SOL		<u>SOL</u>	
5.90 (1.15, 10.62)*	7.97 (3.53, 12.41)*	-8.09 (-18.3, 2.13)	-6.8 (-15.55, 1.87)
VL		<u>VL</u>	
3.09(-0.11, 6.28)	4.57 (1.39, 7.75)*	-5.6 (-12.08, 0.83)	-4.7 (-11.91, 2.46)
RF		<u>RF</u>	
3.28 (0.22, 6.35)*	4.10 (1.53, 6.67)*	-6.29 (-13.62, 1.05)	-5.9 (-12.26, 0.46)

6.3.1.3 Kinematic parameters

Knee angle at HS did not change with SPEED [$F(1,8) = 0.841$; $p=0.386$], whereas it was significantly reduced ($p=0.025$) in AL vs. CONTROL ([$F(1,8) = 60.744$; $p<0.001$], main CONDITION effect, Fig. 6.7). A SPEED*CONDITION interaction [$F(1,8) = 8.635$; $p<0.05$] was also observed, where knee angle decreased and increased in CONTROL and AL, respectively, from 9-13km·h^{-1}. Maximum knee flexion differed with both SPEED [$F(1,8) = 146.956$; $p<0.001$] and CONDITION ([$F(1,8) = 13.828$; $p<0.01$]; Fig. 6.7), by increasing from 9km·h^{-1} to 13km·h^{-1} ($p=0.000$) and reducing in AL vs. CONTROL ($p=0.006$), but a SPEED*CONDITION interaction wasn't observed [$F(1,8) = 2.293$; $p=0.168$]. Total knee ROM increased with SPEED [$F(1,8) =142.173$;.$p<0.001$], but did not encounter an effect of

CONDITION [F(1,8) = 0.006; p=0.941] or SPEED*CONDITION interaction [F(1,8) = 0.016; p=0.901].

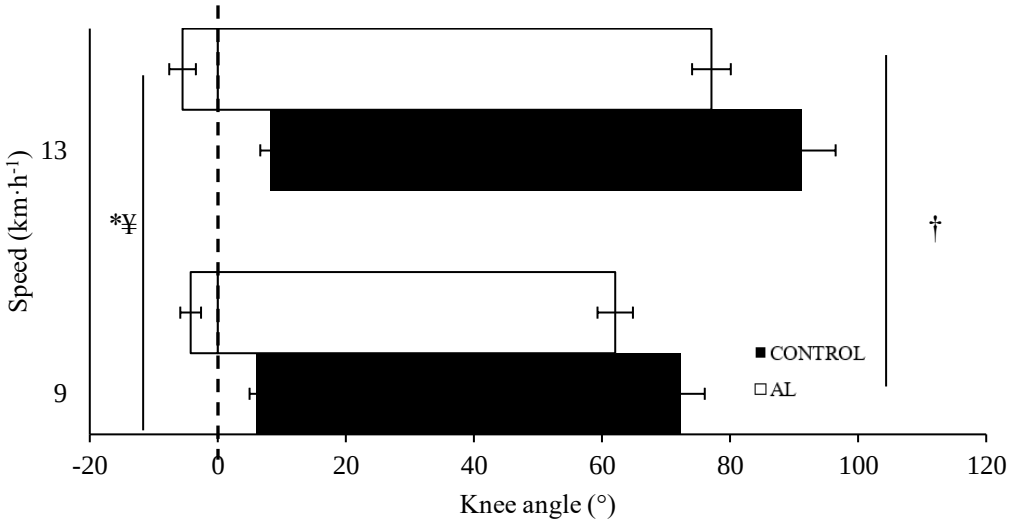

Figure 6.7: Population average (± SEM) knee joint angle at heel strike (°; left side of bar), toe-off (°; right side of bar) and resulting total knee ROM (°) at 9km·h^{-1} & 13km·h^{-1} in CONTROL and AL.* = main effect of SPEED; p<0.05. † = main effect of CONDITION; p<0.05. ¥ = SPEED*CONDITION interaction effect; p<0.05. - - - = knee at full extension (0°). n=9.

A main effect of SPEED was observed for stance ratio [F(1,8) = 19.675; p<0.01], where it decreased from 9km.h to 13km.h (p=0.002) but a CONDITION effect was not observed ([F(1,8) = 0.007; p=0.934]; Fig. 6.8a). Stride duration also encountered a SPEED effect [F(1,8) = 195.844; p<0.001], which became shorter at faster speeds (p=0.000). In contrast to stance ratio, a CONDITION effect [F(1,8) = 27.502; p<0.01] was observed for stride duration, which was longer in CONTROL vs. AL (p=0.001; Fig. 6.8b). There were no significant SPEED*CONDITION interaction effects for either variable (stance ratio: [F(1,8) = 0.342; p=0.575]; stride duration: [F(1,8) = 0.828; p=0.390]).

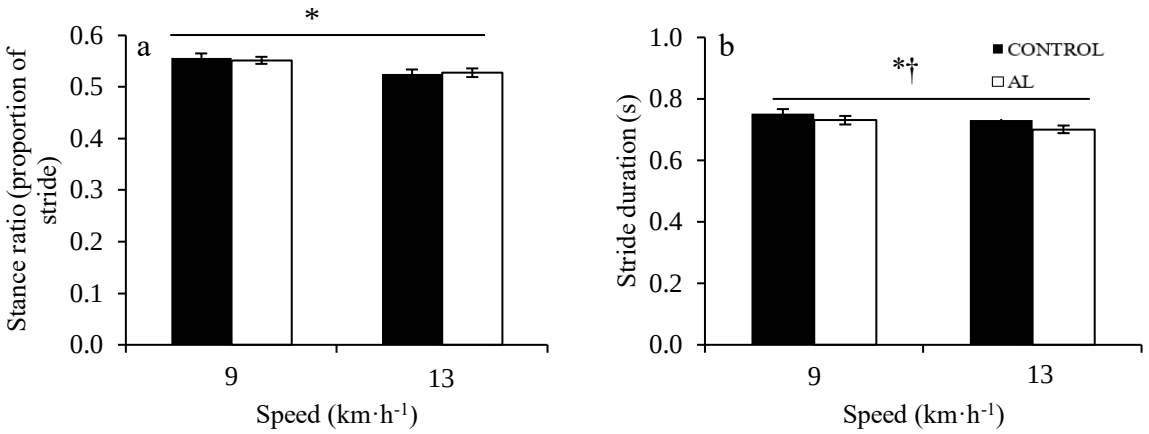

Figures 6.8 a and b: Population average (± SEM) a) stance ratio (left) and b) stride duration (right) at 9km·h^{-1}-13km·h^{-1} in CONTROL and AL.* = main effect of SPEED; p<0.01. † = main CONDITION effect; p<0.01. n=9.

6.3.2 Effect of BW unloading and ABL reloading (EQUIVALENCE protocol)

6.3.2.1 EMG amplitude and frequency parameters

There were no significant differences in EMG RMS amplitude (TA: [F(2,16) = 0.051; p=0.950]; SOL: [F(2,16) = 1.832; p=0.192]; GL: [F(2,16) = 2.280; p=0.134]; VL: [F(2,16) = 0.989; p=0.394]; BF: [F(2,16) = 2.208; p=0.142]; RF [F(2,16) = 0.703; p=0.510] and GMAX [F(2,16) = 1.480; p=0.257]) or MDF (TA: [F(2,16) = 0.415; p=0.667]; SOL: [F(2,16) = 0.123; p=0.885]; GL: [F(2,16) = 0.396; p=0.679]; VL: [F(2,16) = 1.792; p=0.198]; BF: [F(2,16) = 0.828; p=0.455]; RF: [F(2,16) = 1.763; p=0.203] and GMAX; [F(2,16) = 1.696; p=0.215]) with CONDITION in any muscle (Table 6.4).

Table 6.4: Population average (± SEM) EMG RMS amplitude (left) and MDF (right) of TA, SOL, GL, VL, BF, RF & GMAX muscle EMG activity during running at 1Gz, 0.8Gz and Sim1Gz. n=9.

EMG RMS amplitude			**EMG MDF**		
1Gz	0.8Gz	Sim1Gz	1Gz	0.8Gz	Sim1Gz
TA					
0.076±0.014	0.08±0.013	0.089±0.17	110.9±11.5	114.8±10.1	113.1±8.3
SOL					
0.043±0.005	0.036±0.004	0.043±0.004	95.5±11.5	101.1±10.1	95.7±8.3
GL					
0.042±0.007	0.037±0.009	0.028±0.004	90.5±10.8	97.2±12.8	99±7.1
VL					
0.05±0.01	0.035±0.007	0.04±0.006	89.8±8.1	82.7±8.4	73.6±5.9
RF					
0.025±0.003	0.02±0.002	0.022±0.002	68.1±2.5	69.7±2.5	71.2±3.4
BF					
0.011±0.002	0.014±0.007	0.012±0.004	55.8±3.3	59.7±4.3	54.3±4.7
GMAX					
0.013±0.002	0.01±0.001	0.013±0.003	43.4± 6.1	49.7±7.7	53.2±4.3

6.3.2.2 Muscle activity patterns

Muscle activity patterns had very strong positive correlations between all three load conditions (Table 6.5). There were no differences in any muscle activities' onset (TA: [$F(2,16) = 1.182$; $p=0.332$]; SOL: [$F(2,16) = 0.313$; $p=0.736$]; GL: [$F(2,16) = 2.070$; $p=0.159$]; VL: [$F(2,16) = 0.177$; $p=0.839$]; BF: [$F(2,16) = 0.786$; $p=0.472$]; RF: [$F(2,16) = 0.520$; $p=0.604$] and GMAX; [$F(2,16) = 1.449$; $p=0.264$]) or offset (TA: [$F(2,16) = 0.588$; $p=0.567$]; SOL: [$F(2,16) = 3.112$; $p=0.072$]; GL: [$F(2,16) = 1.208$; $p=0.325$]; VL: [$F(2,16) = 0.505$; $p=0.613$]; BF: [$F(2,16) = 1.128$; $p=0.348$]; RF: [$F(2,16) = 1.032$; $p=0.379$] and GMAX: [$F(2,16) = 2.686$; $p=0.099$]) with CONDITION (Fig. 6.9).

Furthermore, only TA duration differed with CONDITION [$F(2,16) = 4.398$; $p<0.05$], though no between-load differences could be distinguished (1Gz vs.0.8Gz: $p=0.285$; 1Gz vs. Sim1Gz:

p=0.081 & 0.8Gz vs. Sim1Gz: p=1.000; Fig. 6.9). All other muscles did not encounter a CONDITION effect (SOL: [F(2,16) = 1.841 p=0.191]; GL: [F(2,16) = 0.193; p=0.827]; VL: [F(2,16) = 0.578; p=0.572]; BF: [F(2,16) = 0.012; p=0.988]; RF [F(2,16) = 0.710; p=0.506] and GMAX: [F(2,16) = 1.709; p=0.212]).

A CONDITON effect was not observed for the co-contraction period in any muscle pair (VL/BF: [F(2,16) = 0.007; p=0.993]; TA/GL: [F(2,16) = 2.885; p=0.085]; VL/GL: [F(2,16) = 0.237; p=0.639] and BF/TA: [F(2,16) = 1.777; p=0.201]; Fig. 6.10).

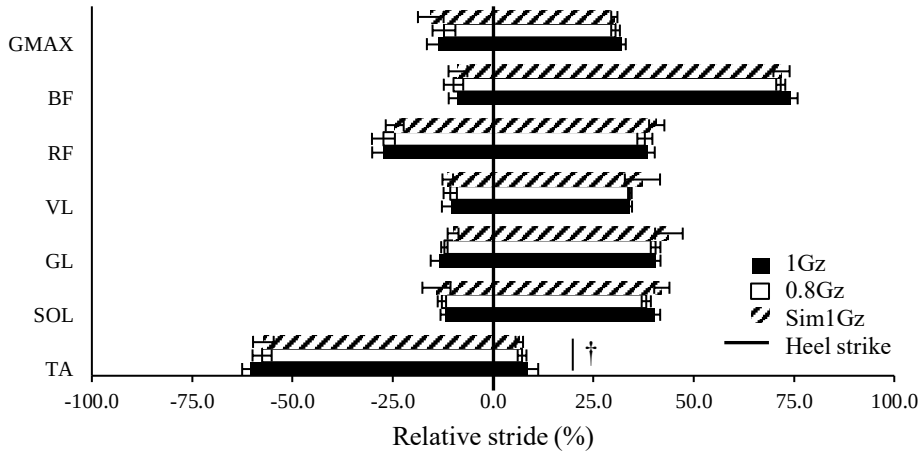

Figure 6.9: Population average (± SEM) muscle activity duration, onset and offset of TA, SOL, GL, VL, BF, RF & GMAX during set-speed running at 1Gz, 0.8Gz & Sim1Gz. † = main effect of CONDITION for duration; $p<0.05$. n=9.

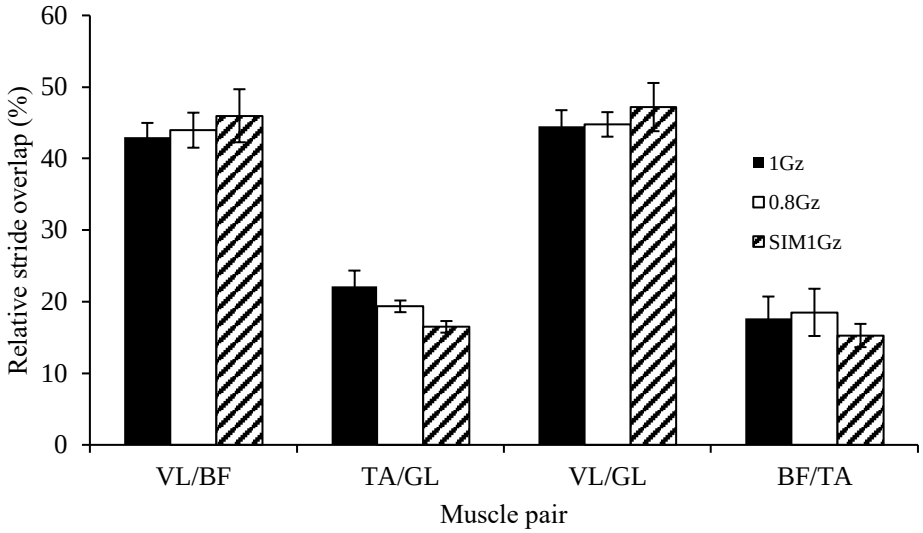

Figure 6.10: Population average (± SEM) co-contraction time between antagonistic and synergistic muscle pairs VL/BF, TA/GL, VL/GL, & BF/TA during set-speed running at 1Gz, 0.8Gz & Sim1Gz. n=9.

Table 6.5: Pearson's correlation coefficients (*r*) from EMG ensemble curves between 1Gz, Sim1Gz & 0.8Gz whilst running at set speed. * = significant correlation; $p<0.01$. n=9.

1Gz vs. 0.8Gz	1Gz vs. Sim1Gz	0.8Gz vs. Sim1Gz
TA		
.986*	.989*	.990*
SOL		
.976*	.972*	.977*
GL		
.992*	.971*	.963*
VL		
.992*	.979*	.987*
BF		
.915*	.924*	.981*
RF		
.894*	.926*	.937*
GMAX		
.964*	.962*	.994*

6.3.2.3 Kinematic parameters

Knee angle at HS [F(2,16) = 19.679; p<0.001] and toe-off [F(2,16) = 5.949 p<0.05] was influenced by CONDITION (Fig. 6.11). Post-hoc analysis revealed reduced knee angle at HS during Sim1Gz vs. both 0.8Gz (p=0.003) and 1Gz (p=0.001), with no differences observed between 1Gz and 0/8Gz (p=0.406). Regarding knee angle during toe-off, post-hoc tests could not determine between-condition differences (1Gz vs. 0.8Gz: p=1.000; 1Gz vs. Sim1Gz: p=0.145 & 0.8Gz vs. Sim1Gz: p=0.073). Total knee ROM [F(2,16) = 0.827; p=0.455] and maximum knee flexion [F(2,16) = 3.218; p=0.067] as well as stance ratio [F(2,16) = 0.018; p=0.982] and stride duration [F(2,16) = 3.047; p=0.076] were unaffected by CONDITION (Figs. 6.11 & 6.12).

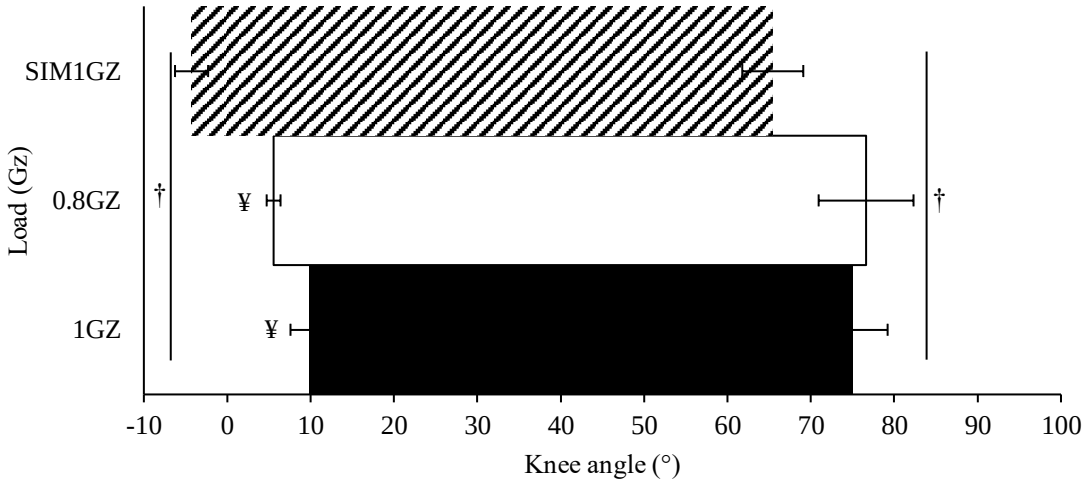

Figure 6.11: Population average (± SEM) knee joint angle at heel strike (°; left side of bar), toe-off (°; right side of bar) and total knee ROM during set-speed running at 1Gz, 0.8Gz & Sim1Gz. † = main effect of CONDITION; p<0.05. ¥ significantly different from Sim1Gz; post-hoc tests; p<0.05. n=9.

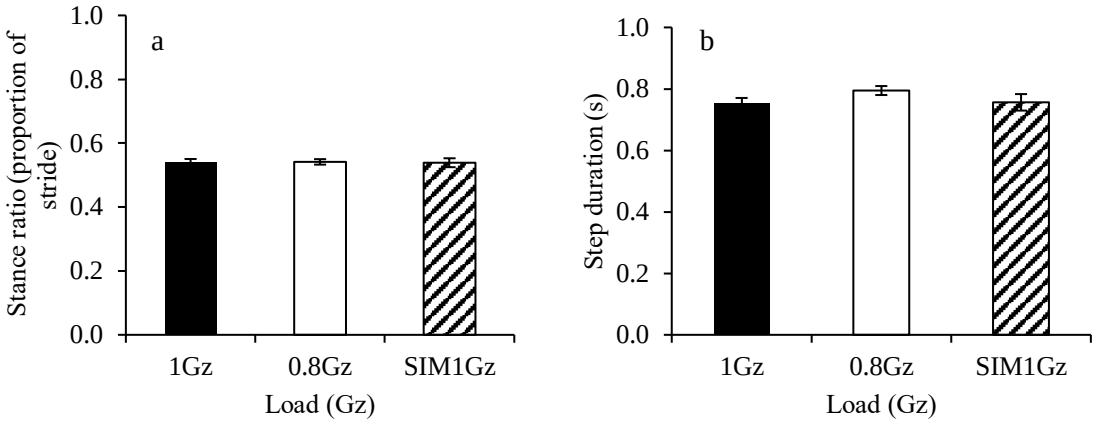

Figures 6.12 a and b: Population average (± SEM) a) stance ratio and b) stride duration during set-speed running at 1Gz, 0.8Gz & Sim1Gz. n=9.

6.4 Discussion

The objectives of this study were twofold: to determine the effect of additional 0.2Gz ABL on neuromuscular and kinematic variables during: a) slow and faster-speed running compared to 1Gz and b) submaximal steady-speed running whilst at 0.8Gz. The main findings were that contrary to the hypotheses, running with 0.2Gz ABL – whether as an addition to 1Gz, or as a reloading stimulus during running at 0.8Gz – did not significantly increase muscle activity levels. However, 0.2Gz ABL caused muscle activity pattern modulations, evidenced by lengthened duration of the SOL and a displaced knee joint.

6.4.1 Neuromuscular responses during 1Gz running

For all leg extensors (VL, RF, GL, & SOL), regardless of speed, pre-activity prior to heel strike (HS; Fig. 6.4a) is pre-programmed (Dietz et al, 1979) and generated on a spinal and/or a brainstem level (Dietz et al, 1992). The ~10% longer activity duration of the RF in comparison to the other extensors is most likely related to its contribution to two functions: as a knee extensor at the beginning of foot contact and as a powerful hip flexor at the beginning of the swing phase (Nicola & Jewison, 2012). Upon toe-off, increased TA activity functions to

provide clearance in swing (Novacheck, 1998), whereas BF activity was evidenced both in the latter part of the swing phase – approximately 10% earlier than the extensors – and continued into the foot contact phase. These results are consistent with those of Kyröläinen et al (2005), where BF EMG activity increased both in the latter part of swing and in the contact phase. This is in keeping with the notion suggested by Simonsen et al (1985), that the BF enhances force production in the contact phase when extending the hip joint, by releasing elastic energy stored during the swing phase and drive the body more powerfully in the forward direction during the propulsive phase.

6.4.2 Effect of 0.2Gz axial body loading on neuromuscular and kinematic responses during speed-incremented running in 1Gz

The observed earlier GL offset coupled with earlier activation of VL, BF, SOL & GL at 13km·h^{-1} compared to 9km·h^{-1} supports the contention that the aforementioned pre-activity of the leg extensors increases with speed (Nilsson et al, 1985). Kinematic analysis showed that with faster speeds, stance ratio and stride duration decreased and knee flexion increased, likely to attenuate the shock from increased ground reaction forces (GRFs) accompanying faster speeds (Hof et al, 2002). Consequently, the activity levels of all muscles increased from 9km·h^{-1} to 13km·h^{-1}, despite their activity profiles remaining similar. Moreover, it has been suggested that EMG amplitudes in calf and quadriceps muscles increase little with speed and to a slightly greater extent in the hip flexors and extensors (GMAX, BF and RF), implying that speed increases are accomplished mainly by a larger leg swing (Gazendam & Hof, 2007). The results observed in the present study are consistent with this finding, where TA activity increased to a greater extent than the GL, VL, RF and SOL (Fig. 6.2a). Although the BF did not increase with speed to the same magnitude as the TA, the delta increase from 9-13km·h^{-1} (~62%) remained

greater than that observed in leg extensors. A greater swing phase with speed is further supported by the decreased stance ratio and GL duration at 13km·h^{-1} compared to 9km·h^{-1}.

A shorter stride duration without a change in stance ratio as observed in AL vs. CONTROL is indicative of a shorter swing (Figs. 6.12 a&b), consistent with previous literature investigating similar loading magnitudes (Ghori & Luckwill, 1985; Brown et al, 2014b). Furthermore, running with additional 0.2Gz ABL reduced knee angle at HS, toe-off and during swing (maximum flexion). The same degree of flexion-reduction was apparent at each of the aforementioned gait phases (~10%), resulting in displaced knee movement rather than a reduction of its range. Increased GRFs are unlikely with 0.2Gz ABL during running, thereby dissuading the need for increased flexion. However, this argument would only satisfy the observation that knee angle was indifferent to CONTROL, as opposed to significantly lower (i.e. less flexed).

The addition of 0.2Gz ABL did not modify speed-related activity levels in most muscles, contrary to previously observed increases with moderate loads (Pamukoff et al, 2016; Silder et al, 2015). In fact, EMG RMS level increased in the VL to a greater extent in CONTROL compared to AL yet decreased in CONTROL vs. AL at faster speeds (SPEED*CONDITION interaction) in the BF. Similar findings have been observed by Kendrick (2016) whilst running at 0.75Gz with additional 0.75Gz ABL (~1.5Gz). Knee extensor muscles reduced their activity during stance, owing to the elastic material around the knee acting as a stabilising force, whereas flexor muscle activity increased during swing in an attempt to overcome the forces of the elastic loading elements as they stretched around the joint.

Despite similar levels and patterns of muscle activation, 0.2Gz ABL prolonged SOL activity. Similar findings have been reported when carrying 30% BW loads, where SOL duration increased by 7% (Stephens & Yang, 1999); lengthened activity of other plantarflexor muscles (GL & GM) have also been observed when walking with an extra 20% BW (Ghori & Luckwill, 1985). An effect of 0.2Gz ABL on SOL duration that is unapparent with its amplitude and MDF is consistent with the lengthened GL duration coupled with unchanged activity levels during cycling with 0.12Gz ABL (Chapter 4).

6.4.3 Neuromuscular and biomechanical responses to 0.2Gz BW unloading

Unlike running in 1.2Gz vs.1Gz, most kinematic variables were generally unchanged between 1Gz and 0.8Gz, consistent with studies using similar magnitudes of BW-unloading on the same apparatus (Fischer & Wolf, 2015). However, knee angle was decreased at Sim1Gz compared to both 1Gz and 0.8Gz (Fig. 6.11). Seeing as this cannot be related to the influence of unweighting – as there was no change in knee angle between 1Gz vs. 0.8Gz – the likely explanation must be related to ROM restrictions imposed by the SkinSuit, which is a liable contributor to the reduced knee flexion observed when running in 1.2Gz vs. 1Gz.

Muscle activity levels were not reduced when loading was reduced from 1Gz to 0.8Gz. These results are in contrast to the reductions in lower-limb neuromuscular activity evidenced during 0.8Gz running using LBPP (Liebenberg et al, 2011; Sainton et al, 2015). However, the horizontal assistance offered by these devices has been proposed as the source of the reduced neuromuscular expenditure (Grabowski and Kram, 2008). Although not entirely comparable owing to a ~55% difference in BW unloading, the results obtained from this study are consistent with Ferris et al (2001), who utilised similar apparatus to that used in this study. Only decreases in VL (58%) and SOL (32%) activity were observed; extrapolating these results

to the current study would imply that there would be negligible decreases in VL, and potentially non-existent decrements in SOL with only 0.2Gz BW unloading. Moreover, the maintained kinematics would not necessitate a greater activation of the lower-limb musculature.

The body-suspension system utilised in this study applies vertical unloading force only to the trunk; these systems cannot aid the swing movements of the limbs and thus they remain subject to full gravity during swing (Lacquaniti et al, 2017). Moreover, the resultant forces were scaled by the cosine of the angle relative to the vertical (Graham et al, 2009). Deviations to this alignment i.e. standing slightly forward or backwards would result in a greater provision of unloading than when directly underneath (Frey et al, 2006). Although care was taken to ensure that participants were directly underneath the harness attachment at the time of BW removal, this was not meticulously verified. Thus, participants could have been running >0.8Gz, which may have contributed to these findings. Owing to the fact that very little differences were observed between neuromuscular and kinematic parameters during running at 1Gz and 0.8Gz, it is not possible to fully evaluate the reloading capabilities of ABL to the neuromuscular system.

6.5 Conclusion

Speed-related neuromuscular activation levels during running at 1Gz or 0.8Gz were not enhanced with 0.2Gz ABL possibly related to the absence of load-associated GRF augmentations, although increased plantarflexor (SOL) duration suggests load-dependant activation strategies of the anti-gravity muscles. Concomitant with reduced knee angle, these findings might imply mechanical alterations during 1Gz running with low-level ABL. Bodyweight unloading of 0.2Gz did not offer a stimulus profound enough to induce neuromuscular or kinematic adaptations, and thus the reloading capabilities of ABL cannot be

fully concluded, likely due to limitations of the unweighting method used. Future work should look to investigate the changes in running neuromechanics at greater unloading levels on the basis of which the addition of 0.2Gz ABL may present a proportionally much greater re-loading stimulus. This should be accomplished utilising an unloading system that counteracts the component of the gravity force acting on the body and limbs in the sagittal plane.

Chapter 7: The influence of additional axial body loading on neuromuscular responses during running in simulated lunar gravity (0.16Gz)

7.1 Introduction

In Chapter 6, it was shown that 0.2Gz ABL did not augment neuromuscular activity levels when added to 1Gz or 0.8Gz bodyweight (BW). Moreover, the inability of 0.8Gz to reduce muscle activity levels from those demonstrated at 1Gz rendered the reloading capability of ABL difficult to elucidate. It was concluded that these results may be due to the fact that a 0.2Gz BW reduction represents a small delta from 1Gz and may not have imposed a stimulus large enough to elicit a considerable unloading effect. A gravity load that enables a larger deviation from 1Gz and where the dosage of ABL to the unweighting stimulus could be much greater is thus desirable. The limitations of the BW-support apparatus employed may have also been a contributing factor to the findings from Chapter 6. Body-suspension systems typically apply vertical unloading force only to the trunk and thus the limbs remain subject to 1Gz during swing (Lacquaniti et al, 2017).

Differential effects of BW unloading on EMG characteristics, further confounded by changes in speed have been observed (Ferris et al, 2001; Ivanenko et al, 2002; Van Hedel et al, 2006). Ivanenko et al (2002) studied six lower limb muscles when walking from 0.7-5km·h^{-1} at BW loads ranging from 0-100% in ~25% increments. Muscle activity patterns remained similar across the BW loads during walking, although they observed the GL muscle activity to decrease monotonically with unloading at all speeds, whereas knee extensor (VL) muscle activity depended non-linearly on speed. For example, during unloading, VL activity did not

change at low speeds (0.7–1.1km·h^{-1}), increased at intermediate speeds (2–3km·h^{-1}) and decreased at faster speeds (5km·h^{-1}; $p<0.05$). In the same study, the highest BF activity occurred around HS when walking at 100-50% BW, though as gravity decreased, its activity shifted to mid- and late-stance. In contrast, TA activity was independent of BW changes regardless of speed, likely because the BW-support apparatus employed did not offload the effect of gravity from the swinging limb. Similar patterns of muscle activity profiles were observed for four lower limb muscles during running at 0.25 Gz vs. 1Gz independent of speed, albeit coupled with speed-dependant activation levels (Ferris et al, 2001). Comparable to that observed by Ivanenko et al (2002), the VL had a tendency to reduce its activity marginally when walking but decreased during running by 58% within the same gravity range. This "gravity-dependence" on neuromuscular activation during walking has not been quantified during running.

The differential functional role of muscles between locomotor tasks and BWs might have been responsible for these disparities. For example, it has been suggested that the contribution of the VL during walking lay primarily with decelerating the limb before HS to attenuate impact forces (Jefferson et al, 1990) and/or acts to balance hamstring moments about the knee to control the direction of the ground reaction force vector (Simonsen et al, 1997); if it acts to supports BW then its activity should have decreased when BW was reduced, contrary to the findings by both Ferris et al (2001) and Ivanenko et al (2002). During running however, the role of the VL in generating force to counter BW is greater and thus a greater decline in its activity is observed (Farley & McMahon, 1992). Further, the peak BF activity occurring around HS at 100-50% BW in the Ivanenko et al (2002) study likely serves to decelerate the swinging limb (Winter, 1991), whereas the shift to late stance at lower BW is presumably related to the need to assist vaulting over an inverted pendulum of the stance

limb and swing initiation (Sylos-Labini et al, 2014). These adaptations likely serve in part to maintain appropriate lower body kinematics during locomotion at varying BW loads and speeds. This is supported by the observation that stride length and swing-phase duration have been shown to change only to a limited extent over a fourfold reduction in gravity during walking (Donelan and Kram, 1997). Moreover, as gravity reduces so does locomotive speed; in fact, the preferred movement on the moon (0.16Gz) relies upon variations in skipping (Pavei et al, 2015). This is due to energetic optimality under reduced gravity conditions (Rader et al, 2007) and low frictional contact forces, which are proportional to gravity (Lacquaniti et al, 2017). Taken together, investigations must control for and standardise speed so that the effect of reduced loading on the neuromuscular system can be isolated.

On the European Space Agencies' near agenda is the creation of a "moon village". Such an endeavour is planned not only to consider scientific and technological activities, but also activities based on exploiting resources or even tourism (Woerner, 2016). Furthermore, the Moon Village could also act as the perfect springboard and testing ground with the objective in mind that in the future, humans will take part in crewed flights farther into the Solar System. Thus, it is of necessity to better understand not only how humans may locomote, but to also investigate and develop countermeasures in an attempt to preserve physiological function at this Gz (0.16 of Earths'). Experimentally, such a gravity level would also allow an ABL reloading dose of ~100%.

The data acquired from the abovementioned studies was gathered using body suspension devices exposing the individual to a Gz vector. Horizontal suspension coupled with verticalised treadmill systems have allowed locomotion in simulated partial unloading by equally removing gravity from the trunk and the swing leg (Ivanenko et al, 2011). Moreover, such

systems have been shown to produce negligible differences in lower limb kinematics and neuromuscular activity levels during running at simulated 1Gz vs. actual 1Gz and during partial gravity exposure compared to actual weightlessness, determined through parabolic flight (Genc et al, 2006; De Witt et al, 2014; Jordan et al, 2017). These findings imply that horizontal suspension is a robust platform to investigate locomotion with or without load replacement in partial gravity.

7.1.1 Aims and hypotheses

The aims of this study were to assess the effects of bodyweight unloading to lunar gravity level and the reloading capability of ABL on lower-limb neuromuscular activity levels and patterns during speed-standardised submaximal running. Horizontal suspension was used to simulate and compare running at: 1) 0.16 Gz vs. 1Gz and 2) 0.16 Gz with the addition of 0.2Gz ABL versus a matched equivalent.

Based on previous evidence, it was hypothesised that EMG activity patterns of major lower limb muscles would remain similar across gravities, albeit with the leg extensors reducing their activity levels to a greater extent than the flexors at 0.16Gz vs. 1Gz. Secondly, it was hypothesised that the addition of 0.2Gz ABL during running at 0.16Gz would partially reload the neuromuscular system and achieve muscle activity levels: (i) greater than those observed at 0.16Gz, particularly in the knee and ankle extensors, and (ii) equivalent to those evoked when running at a matched gravity load.

7.2 Methods

7.2.1 Participants

Eight healthy male participants (31.88±4.67yr; 73.54±7.33kg; 178.38±5.68cm) provided written informed consent to participate in this study.

7.2.2 Overall study design

This study adopted a pseudo-randomised, counterbalanced repeated measures EQUIVALENCE (refer to Chapter 2, section 2.3.1) design (Fig. 7.1) and was conducted in a laboratory at the German Aerospace Centre (DLR) in Cologne, Germany. Participants were required to attend the laboratory on two occasions; once for a pre-study medical examination and once for the experimental trial. The trial involved recording neuromuscular activity during submaximal, steady-state treadmill running in 4 conditions: at 1Gz (CONTROL), 0.16Gz ("016"), 0.16Gz+participant-specific ABL ("016SS") and an equivalent Gz to that created by 016SS (MATCHED). The ABL ranged from 0.13-0.23Gz, thus the Gz during the MATCHED trial ranged from 0.29-0.39Gz. To control for speed a set percentage (>25%) from the preferred walk-run transition speed (PTS) was used.

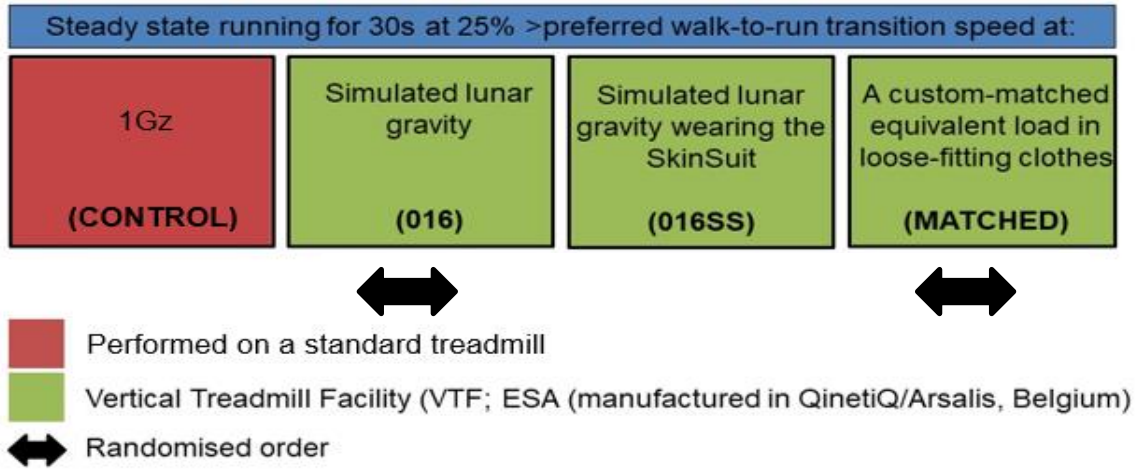

Figure 7.1: Experimental design. Participants ran at 25% greater speed than their walk to run transition on each of 4 separate occasions: 1Gz ("CONTROL), simulated lunar gravity (0.16Gz; "016"), simulated lunar gravity plus their SkinSuit ("016SS") and a custom-matched equivalent load to 016SS in loose-fitting clothes ("MATCHED"). The trials started with CONTROL, performed on a standardised treadmill and continued with the three <1Gz on a verticalised treadmill facility with the first two in a randomised order.

7.2.3 Experimental protocol

7.2.3.1 Pre-protocol examination and familiarisation

All participants attended the laboratory prior to the study for recording a resting 12-lead ECG. All ECGs were read and reported on by a qualified clinician, before being cleared to participate. The participants also visited the on-site physician for a medical examination on the day of the study, which consisted of conducting resting blood pressure, heart (rate and sounds) and anthropometric tests. All medical documentation was written either in English or translated into English for understanding. Upon attending the laboratory for familiarisation, participants trialled running on the two treadmills used in the study (refer to section 7.2.3.3 for treadmill setup). Regardless of the condition, the treadmill belt was always started automatically, and the participants were asked to maintain a default body position in between

running trials. This involved holding on to the bars located to the side of the treadmill and ensuring their feet were adjacent to the treadmill belt (Fig. 7.2b) unless instructed otherwise. The recording software was triggered by a pedal for synchronisation, the activation of which was preceded in each condition by an instruction to: "stamp your foot on the pedal, keep holding the bars whilst you move your feet on to the belt and begin running. Please remove your hands from the bars after your first few strides". Participants practiced running at >25% of their previously-determined PTS integrated with the commands for all four gravity levels. They were visually inspected by the experimenters to ensure the presence of an aerial phase, which, combined with anecdotal feedback, implied that they could no longer sustain a walk.

7.2.3.2 Experimental procedures

Each running trial comprised 30s running at >25% PTS estimated for each participant individually (refer to 7.2.3.4 for derivation) on the verticalised treadmill facility (VTF; Fig. 7.2b). The purpose for the 016SS condition was to provide an equivalent load to MATCHED, therefore, participants used the PTS derived for the 016 trial to prevent potential influence of kinematic variability that may have manifested at MATCHED compared to 016. The aim was to assess the effect of 016SS compared to pure lunar gravity considering that regardless of speed, ABL does not affect kinematic variables with reductions of 0.2Gz (Chapter 6 Fig. 6.12).

Before any of the running trials commenced, participants were fitted with all the necessary equipment (refer to section 7.3 for data collection). The conditions within the experimental trial always began with CONTROL and ended with 016SS, for practical reasons. CONTROL was the only trial that required a different treadmill, whereas 016SS was the only trial that required

the participant to wear their SkinSuit. Therefore, it was the least time-consuming to perform CONTROL first, so that once the participant was set up on the VTF, they only needed to be released to don their SkinSuit and be re-set the once. All conditions except 016SS were performed in loose-fitting clothes due to the nature of this study being part of a larger collaborative endeavour, where access to the skin surface of the left lower limb was required for ultrasound assessment, which was not possible with the SkinSuit donned. For each trial, the individual PTS was programmed into the treadmill software whilst participants assumed the default position, stamped the pedal and began running. At the end of the 30s run, participants were asked to resume the default position by holding on to the bars and swiftly jumping their feet to the side of the treadmill (as the belt continued to run throughout all trials for practical reasons i.e. to avoid lengthy start-up procedures in between trials) and rested before assuming the next trial (~60s).

7.2.3.3. The Verticalised Treadmill Facility (VTF)

The Verticalised Treadmill Facility (VTF)/Subject Loading System (SLS) is owned by the European Space Agency but is housed at the DLR institute via a loan agreement. It has been manufactured by Arsalis/QinetiQ (Belgium) and consists of the following components:

1. *A verticalized treadmill*. Its main component is a customized, commercially available treadmill (Woodway) that is almost identical to the one used on board the International Space Station. It is mounted into a chassis that helps to withstand contact forces during VTF running.
2. *A body suspension system.* The VTF uses an innovative suspension system that uses springs to provide the suspension force for each body segment which mounted into a chassis that is connected to the treadmills' chassis. The subject body is supported by 5 independent suspension units: one unit for the thorax and head, one for the abdomen,

one for the arms, one for the thighs and one for the shanks and feet; all of which support bilateral limbs (Fig. 7.2a). Each suspension unit is actuated by a tension spring located in the spring rack. Each unit has a trolley, mounted on the suspension beam, supporting a dual pulley that reduces the change in length of the springs due the movements of the runner, hence reducing the variation of the suspension force. The tension in each unit is adjusted with a spool that controls the length of a wire pulling at the bottom of the spring (Gosseye et al, 2011).

3. *The subject loading system*. The SLS consists of two pneumatic pistons attached to a harness on either side of the subject's trunk at the level of the hip (Fig. 7.2b). The harness comprises a large belt and adjustable straps, distributing the pull-down force between the hips and the shoulders and does not constrain any movements of the lower and upper limbs (Gosseye et al, 2010). By virtue of these pressurisable pistons, a pull-down-force is generated equivalent to the product of piston pressure and piston cross-section. The high-pressure reserve provides the pressure necessary for the 2 SLS actuators and is pressurized by the compressor (Gosseye et al, 2011). Because the piston's cross section is small in relation to its volume, the force variation during a normal running cycle with displacement ≤ 10cm is approximately 5%. Piston pressure is servo-controlled and can be set between 180 and 990 N. One can accordingly set the pull-down force to values equivalent to body weight, and also to fractions of it or to values that are slightly greater. In order to measure the forces exerted by the subject on the treadmill while running or walking, the treadmill contains four Arsalis Mini-3D force transducers.

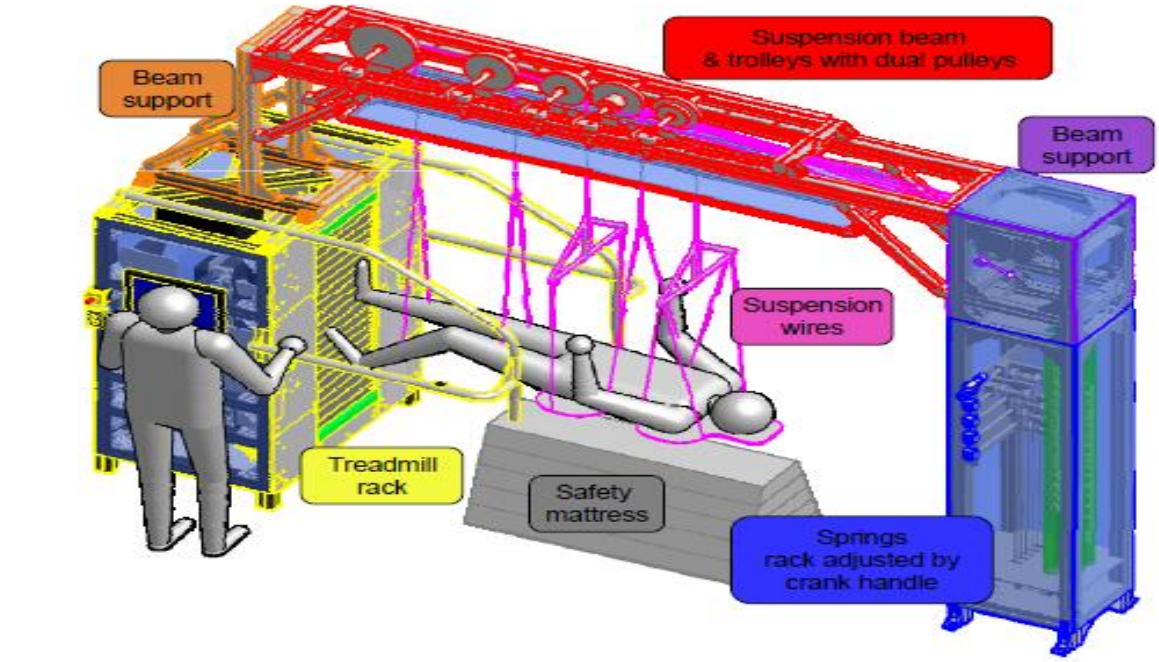

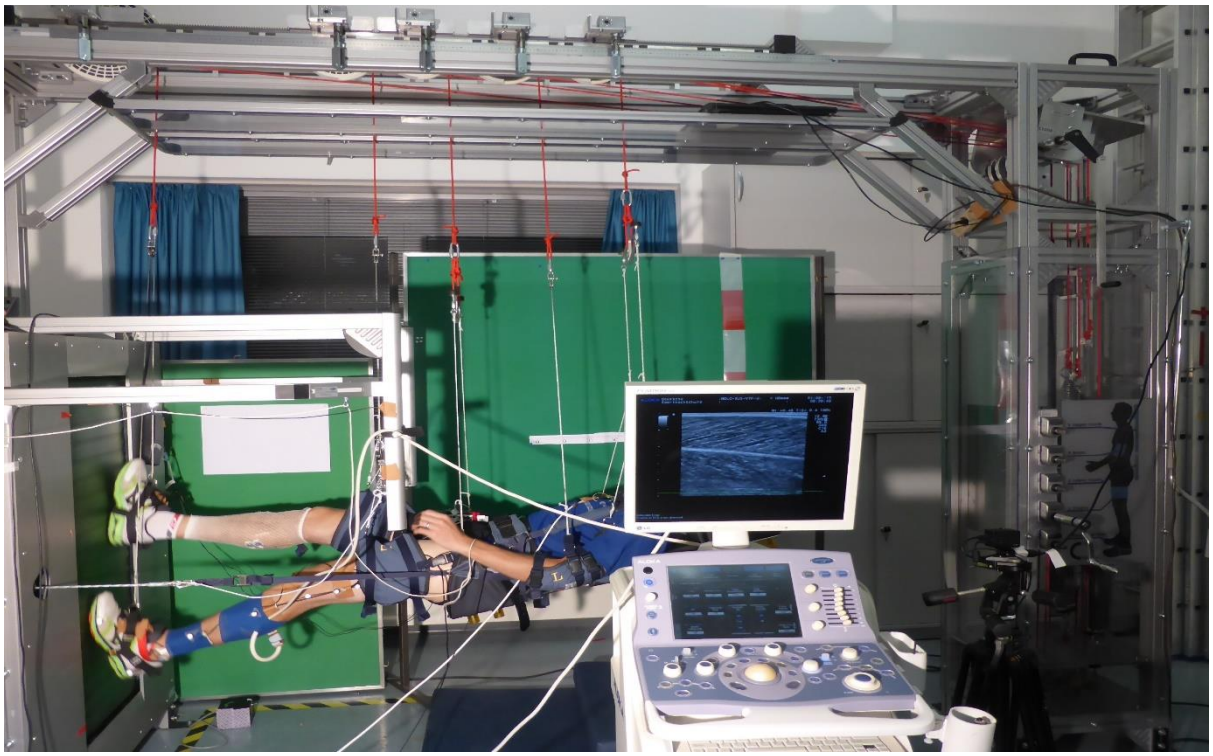

Figures 7.2 a and b: a): main components of the body suspension system (taken and adapted from Gosseye te al, 2011); b) the Verticalised Treadmill Facility (VTF) providing graded partial gravity exposure through horizontal suspension and the use of a subject-loading system. This equipment is owned by the European Space Agency, based at the German Aerospace Centre in Cologne, Germany.

7.2.3.4 Derivation of the preferred walk-to-run transition speed (PTS)

The individual PTS was derived using the Froude number (Fr); a dimensionless speed, defined as the ratio between the centripetal force and the gravitational force (Alexander, 1989) and was calculated as follows (equation 7):

$$Fr=\frac{V^2}{g.l} \quad \textbf{(7)}$$

Where V is treadmill speed, g is loading equivalent to a reduced gravitational acceleration and l is leg length.

Humans have been shown to transition from walking to running at varying Fr depending on gravity (Kram et al, 1997). Therefore, the results obtained from Kram et al (1997; Fig. 7.3) were utilised and extrapolated the Fr to derive the PTS for this study (Table 7.1). The treadmill speed ($m.s^{-2}$) was then calculated for each participant and condition based on the following equation (8) (Kram et al, 1977) before being converted to $km \cdot h^{-1}$:

$$V = Fr\sqrt{}.g.l \quad \textbf{(8)}$$

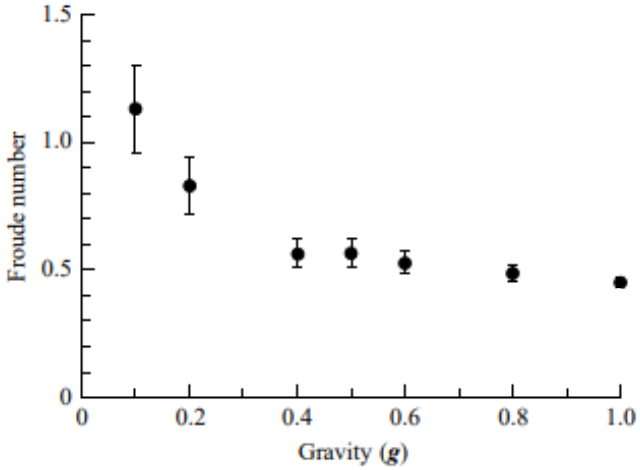

Figure 7.3: The Froude number (Fr) at which the preferred walk-run transition speed (PTS) occurred in relation to the gravity level. Adapted and modified from Kram et al, 1997.

Table 7.1: Froude numbers utilised in the study using an extrapolation from the findings (Fig.7.3) of Kram et al (1997).

Gravity level (Gz)	Gravitational acceleration (m/s^2)	Estimated PTS (Froude number)
0.16	1.57	0.93
0.38	3.73	0.60
MATCHED i.e. 0.35	3.43	0.62
1	9.81	0.48

7.2.4 Data Collection

Muscle activity of the VL, RF, BF, TA, GL, GM and SOL from the right leg were simultaneously recorded using bipolar surface EMG electrodes (1mm width, 10mm pole spacing; Ambu LTD, Cambridgeshire, UK) during the study and following the procedures set out in Chapter 2, section 2.3.5. EMG signals were continuously sampled throughout the

protocol (wired system; Noraxon Inc, Arizona, USA) at a frequency of 1500Hz and pre-amplified x1000 before being stored on a PC for off-line analyses.

For identification of foot contact during each stride, wireless foot insoles (Pedoped, Novel GmbH, Munich, Germany) were placed into both shoes of each participant (Chapter 2 section 2.3.7). Each insole had sensors measuring heel, midfoot and forefoot plantar force, resulting in total force applied from each foot. Such forces were collected through software in real time via an iPpad application (Pedoped loadsol, version 1.4.74) communicating with the insoles via Bluetooth.

7.2.5 Data Analysis

Prior to analysis of EMG signals, the Pedoped records were merged with the EMG records for synchronicity, according to the beginning of the trigger signal. Following this, the EMG signals were rectified before being split into consecutive strides from heel strike to heel strike – as identified by the initial rise in right heel force preceding its peak. These events were automatically marked to generate the profile of the rectified EMG signal, averaged across all strides captured within the middle 20s of every 30s activity bout for each muscle.

The analysed parameters from the EMG signals included analysis of activation levels (RMS and MDF) and patterns (onset, offset, duration, muscle pair co-contractions and assessment of the correlation coefficient between muscle activity profiles). The respective analytical methods were undertaken as described in Chapter 2 section 2.4.3.

7.2.6 Statistical Analysis

All data were normally distributed (Shapiro-Wilk test). One-way repeated measures ANOVA with CONDITION as the main factor (4 levels: CONTROL, 016, 016SS and MATCHED) was used to statistically analyse all variables ($p<0.05$) except the correlation coefficient (Pearson's test). Post-hoc tests with Bonferroni correction were used to ascertain the location of significant between-CONDITION differences.

7.3 Results

7.3.1 Performance metrics

A CONDITION effect was observed for running speed [$F(3,21) = 3214.202$; $p<0.001$]. During CONTROL, participants ran at 9.45±0.1km·h^{-1} (25% >PTS), which was significantly faster than all <1Gz running speeds (1Gz vs. MATCHED: p=0.000; 1Gz vs. 016SS: p=0.000; 1Gz vs. 016: p=0.000; Fig. 7.4). Running speed during 016 and thus 016SS was 5.4±0.1km·h^{-1}, which was significantly lower than the speed ran at MATCHED (6.3±0.1km·h^{-1}; p=0.000).

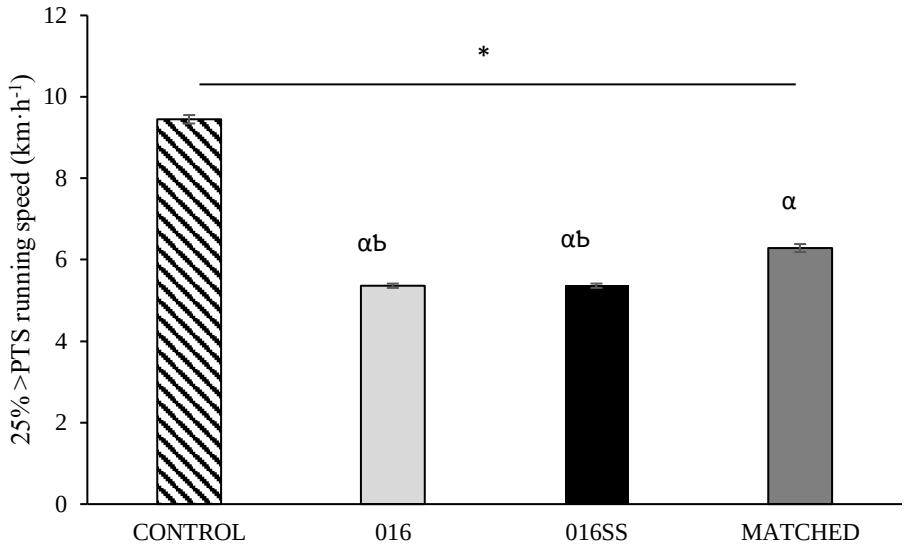

Figure 7.4: Mean (±SEM) running speed – determined as 25% >PTS – performed during 1Gz, 016Gz, 016SS & MATCHED. * = main effect of CONDITION; p<0.001. α = significantly lower than CONTROL and ƀ = significantly lower than MATCHED; p<0.001; post-hoc tests. n=8.

7.3.2 EMG amplitude and frequency parameters

Eelectromyographic RMS amplitude was significantly different across the conditions in all muscles (VL: [F(3,21) = 255.711; p<0.001]; RF: [F(3,21) = 52.627; p<0.001]; BF [F(3,21) = 45.189; p<0.001]; GL: [F(3,21) = 50.895; p<0.001]; GM: [F(3,21) = 19.068; p<0.001]; SOL: [F(3,21) = 18.356; p<0.001]; TA [F(3,21) = 32.822; p<0.001]). For all muscles, post-hoc tests demonstrated reductions in EMG RMS amplitude in 016 vs. CONTROL (Table 7.2 & Fig 7.5a-g; p<0.05). EMG RMS amplitude in all muscles was equivalent between 016SS and 016 (p<0.05), which were also comparable to MATCHED (p<0.05) in all but the VL and GL muscles. VL and GL EMG RMS amplitude was equivalent between 016SS and 016 but was lower in both compared to MATCHED (p=0.04 & p=0.01, respectively), whereas GL EMG RMS amplitude was reduced only in 016SS vs. MATCHED (p=0.047; Table 7.2).

Table 7.2: post-hoc pairwise comparisons for EMG RMS amplitude and MDF of the VL, RF, BF, GL, GM, SOL and TA during running at 25% >PTS in CONTROL, 016, 016SS and MATCHED conditions; $p<0.05$. n=8.

	CONTROL vs. MATCHED	CONTROL vs. 016SS	CONTROL vs. 016	MATCHED vs. 016SS	MATCHED vs. 016	016SS vs. 016
RMS						
VL	p=0.000	p=0.000	p=0.000	p=0.040	p=0.010	p=1.000
RF	p=0.000	p=0.000	p=0.001	p=0.131	p=0.946	p=1.000
BF	p=0.000	p=0.000	p=0.001	p=1.000	p=1.000	p=1.000
GL	p=0.000	p=0.001	p=0.000	p=0.047	p=0.323	p=1.000
GM	p=0.000	p=0.033	p=0.011	p=0.053	p=1.000	p=0.254
SOL	p=0.000	p=0.016	p=0.001	p=1.000	p=1.000	p=1.000
TA	p=0.000	p=0.024	p=0.000	p=0.207	p=0.115	p=1.000
MDF						
RF	p=0.012	p=0.076	p=0.014	p=1.000	p=1.000	p=1.000
GL	p=0.147	p=0.179	p=0.271	p=1.000	p=1.000	p=1.000
GM	p=0.292	p=1.000	p=0.128	p=1.000	p=1.000	p=0.355
SOL	p=0.002	p=0.021	p=0.032	p=1.000	p=1.000	p=1.000

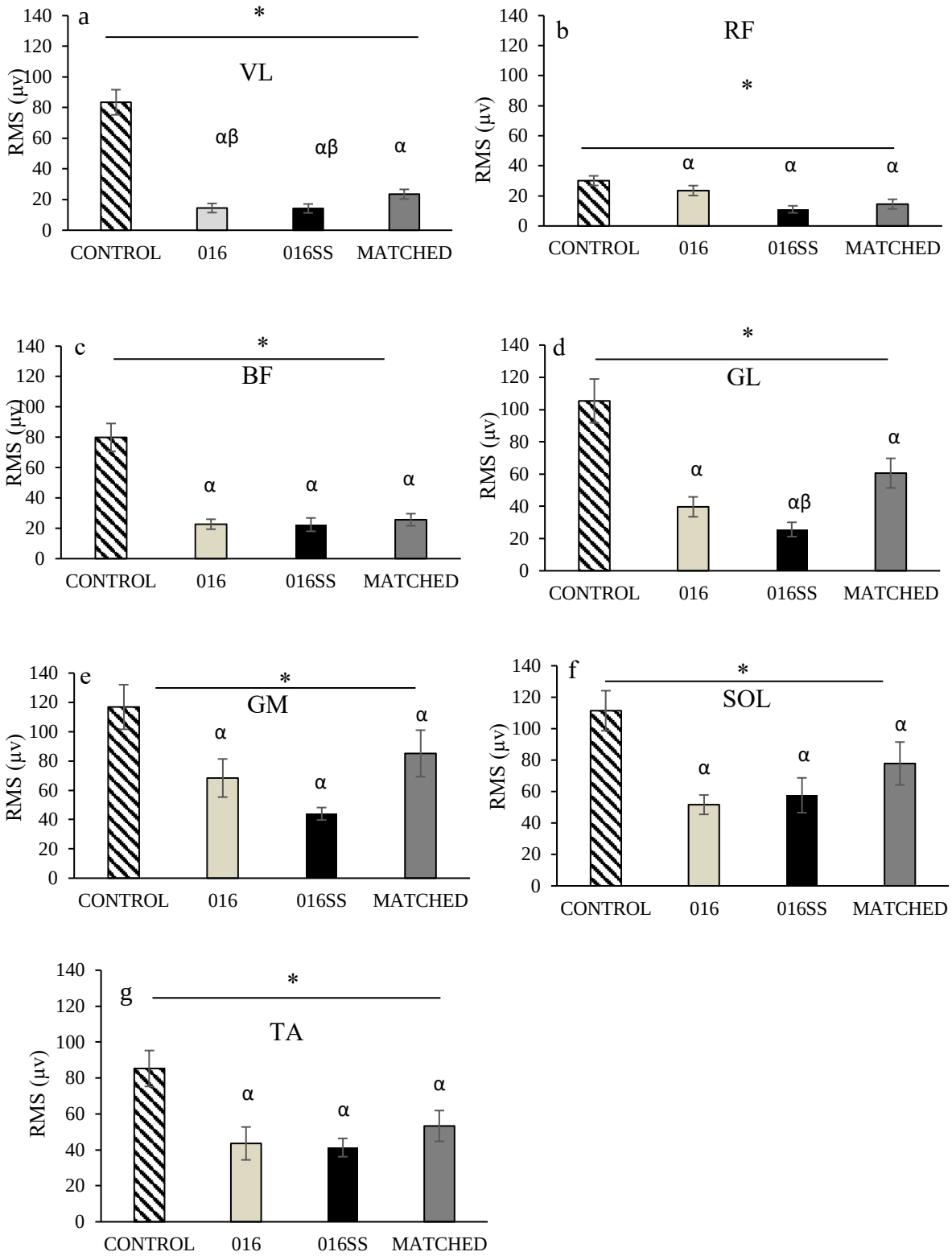

Figures 7.5 a-g: Mean (± SEM) EMG RMS amplitudes of VL, RF, BF, GL, GM, SOL & TA during running at 25% >PTS in CONTROL, 016, 016SS and MATCHED conditions (taken during the middle 20s of each condition). * = main effect of CONDITION; $p<0.001$; α = significantly lower than CONTROL. ƀ = significantly lower than MATCHED; $p<0.05$; post-hoc tests. n=8.

In contrast to RMS, EMG MDF was significantly influenced by CONDITION only in RF [$F(3,21) = 12.170$; $p<0.001$], GL [$F(3,21) = 5.050$; $p<0.01$], GM [$F(3,21) = 4.146$; $p<0.01$] and SOL [$F(3,21) = 6.876$; $p<0.01$] (Figs. 7.6b, d-f). Post-hoc tests were only obtained in RF and SOL, where MDF was greater in CONTROL vs. 016 in the RF ($p=0.014$) and SOL ($p=0.032$; Table 7.2). EMG MDF was equivalent in all muscles between 016 vs. 016SS, which was also comparable to MATCHED. A CONDITION effect was not observed in the EMG MDF of the VL [$F(3,21) = 1.859$; $p=0.168$], BF [$F(3,21) = 1.578$; $p=0.224$] and TA [$F(3,21) = 0.831$; $p=0.492$].

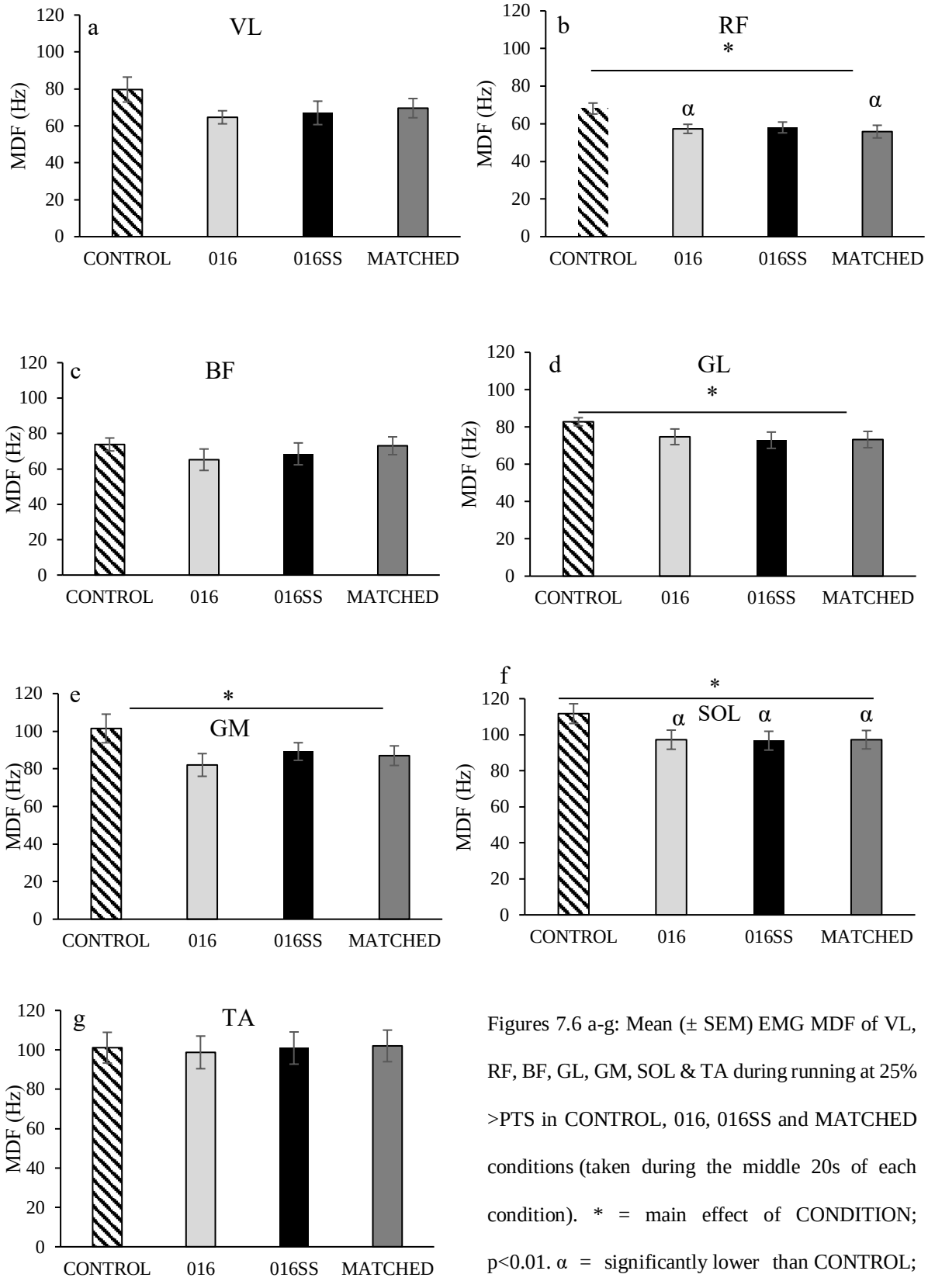

Figures 7.6 a-g: Mean (± SEM) EMG MDF of VL, RF, BF, GL, GM, SOL & TA during running at 25% >PTS in CONTROL, 016, 016SS and MATCHED conditions (taken during the middle 20s of each condition). * = main effect of CONDITION; $p<0.01$. α = significantly lower than CONTROL; $p<0.05$; post-hoc tests. n=8.

7.3.3 Muscle activity patterns

In CONTROL, the activity of the TA started ~60% prior to heelstrike (HS) with its offset ~12% after HS (Fig. 7.6a). The plantarflexor muscles (GL, GM and SOL) operated with an activity onset at ~10-15% prior to HS through to about 40% of stance. VL activity began slightly earlier than the plantarflexors (~20% before HS) and was active for a similar duration (offset: ~26% after HS). RF onset was similar to the knee and ankle extensors, but its offset was prolonged to ~70% after HS. The activity of the BF started ~30% prior to HS and ended simultaneously with the VL, GL, GM and SOL (~37% after HS).

The onset of the GL [$F(3,21) = 3.196$; $p<0.05$] and TA [$F(3,21) = 4.705$; $p<0.05$] demonstrated a CONDITION effect, though post-hoc tests could not discern any differences between the pairs (CONTROL vs. MATCHED: $p=0.495$ & $p=1.000$; CONTROL vs. 016SS: $p=1.000$ & $p=0.24$; CONTROL vs. 016: $p=0.398$ & $p=0.398$; MATCHED vs. 016SS: $p=0.610$ & $p=0.188$; MATCHED vs. 016: $p=1.000$ & $p=0.494$ and 016SS vs. 016: $p=0.204$ & $p=1.000$ for GL and TA respectively). A CONDITION effect was not observed for the VL [$F(3,21) = 1.929$; $p=0.156$], RF [$F(3,21) = 1.955$; $p=0.152$], BF [$F(3,21) = 1.181$; $p=0.341$], GM [$F(3,21) = 2.789$; $p=0.066$] and SOL [$F(3,21) = 2.522$; $p=0.085$]. In none of the recorded muscles was activity offset influenced by CONDITION (VL: [$F(3,21) = 2.973$; $p=0.055$]; RF: [$F(3,21) = 0.635$; $p=0.601$]; BF: [$F(3,21) = 2.122$; $p=0.128$]; GL: [$F(3,21) = 2.725$; $p=0.070$]; GM: [$F(3,21) = 1.775$; $p=0.183$]; SOL [$F(3,21) = 1.153$; $p=0.351$] and TA [$F(3,21) = 1.425$; $p=0.264$]; Fig. 7.7a).

In contrast, the duration of plantarflexor muscle activities were modified by CONDITION (GL [$F(3,21) = 3.847$ $p<0.05$]; GM [$F(3,21) = 4.825$; $p<0.05$]; & SOL [$F(3,21) = 5.374$; $p<0.01$]; Fig. 7.7b). Post-hoc tests demonstrated a reduced duration during 016 (43.1±4.7%)

vs. CONTROL in the GL (56.1±1.7%; p=0.049) but no differences in any other pair (CONTROL vs. MATCHED: p=0.602; CONTROL vs. 016SS: p=1.000; MATCHED vs. 016SS: p=1.000; MATCHED vs. 016: p=0.312 and 016SS vs. 016: p=0.380). GM duration was reduced during 016 (39.3±4.7%) vs. 016SS (45.4±5%; p=0.010) and MATCHED p=0.023) though no other between-pair differences were observed (CONTROL vs. MATCHED: p=1.000; CONTROL vs. 016SS: p=1.000; CONTROL vs. 016: p=0.140; MATCHED vs. 016SS: p=1.000). Post-hoc tests distinguished a significant difference between MATCHED and 016 for the SOL (p=0.038), though did not decipher any other between-pair differences in (CONTROL vs. MATCHED: p=1.000; CONTROL vs. 016SS: p=1.000; CONTROL vs. 016: p=0.105; MATCHED vs. 016SS: p=1.000 and 016SS vs. 016: p=0.490). All other muscles showed equivalent activity durations across all four conditions (VL: [F(3,21) = 0.247; p=0.863]; RF: [F(3,21) = 2.680; p=0.073]; BF [F(3,21) = 0.183; p=0.907] and TA: [F(3,21) = 2.713; p=0.071]).

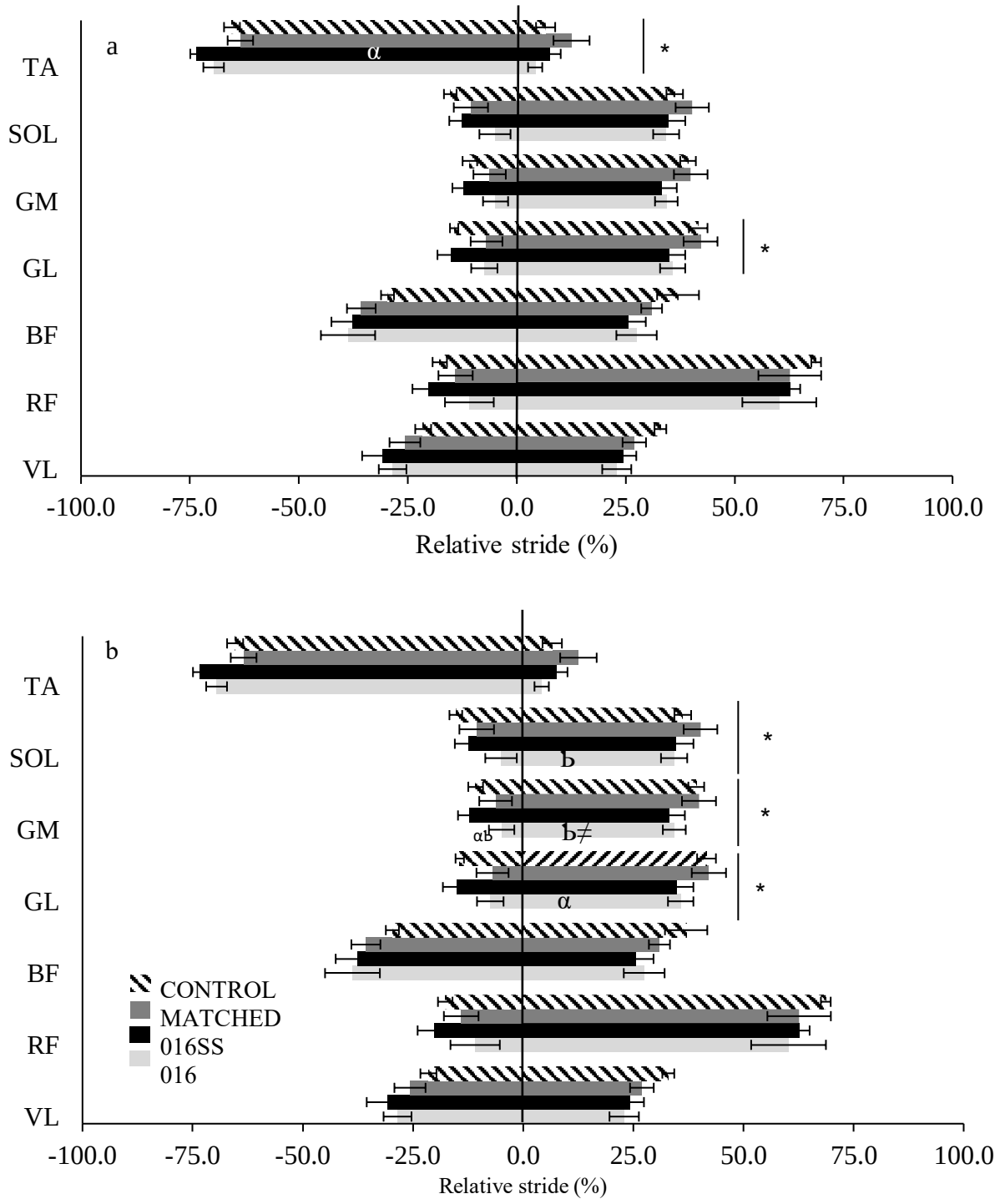

Figures 7.7 a and b: Mean (± SEM) characteristics of the pattern of muscle activity: a) onset (left hand side of the bars) and offset (right hand side of the bars) and b) duration (sum of the bars) of VL, RF, BF, GL, GM, SOL & TA during running at 25% >PTS in CONTROL, 016, 016SS and MATCHED conditions. * = main effect of CONDITION with respect to onset (located on graph a) and duration (located on graph b); $p<0.05$. Onset post-hoc tests: α = significantly earlier onset than CONTROL; $p<0.05$. Duration post-hoc tests: α = significantly

shorter than CONTROL; p<0.05. ƀ = significantly shorter than MATCHED; p<0.05. ≠ = significantly shorter than 016SS; p<0.05. Symbols are displayed on the respective trial bar. Solid line = heel strike. n=8.

The durations of co-contractions of the VL/BF [F(3,21) = 0.247; p=0.863], TA/GL [F(3,21) = 2.250; p=0.112] and BF/TA [F(3,21) = 1.376; p=0.277] muscle pairs were not modified by CONDITION (Fig. 7.8). However, the VL/GL pair demonstrated a CONDITION effect [F(3,21) = 6.197; p<0.01]. Post-hoc tests determined a significantly reduced duration at CONTROL vs. MATCHED (p=0.046), though all other between-condition differences were not detected (CONTROL vs. 016SS: p=0.883; CONTROL vs. 016: p=0.051; MATCHED vs. 016SS: p=0.882; MATCHED vs. 016: p=0.545 and 016SS vs. 016: p=1.000).

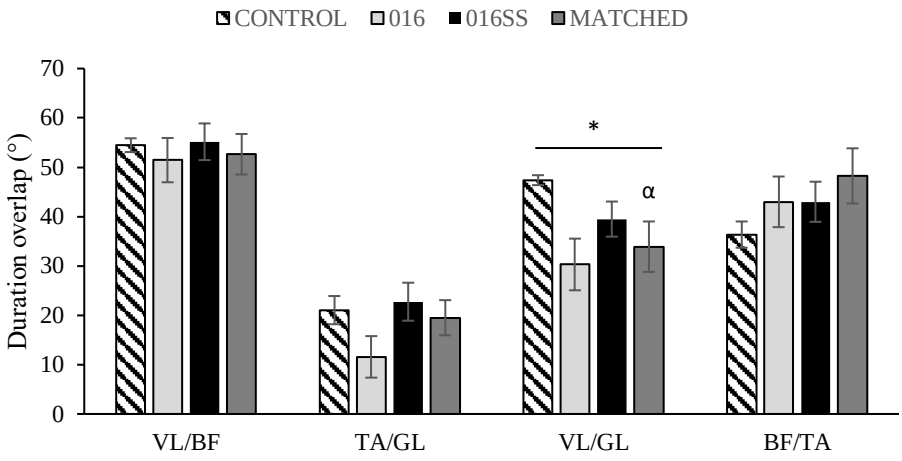

Figure 7.8: Mean (± SEM) co-contractions between antagonistic and synergistic muscle pairs VL/BF, TA/GL, VL/GL, & BF/TA during running at 25% >PTS in CONTROL, 016, 016SS and MATCHED conditions. * = main effect of CONDITION; p<0.01; ANOVA; α = significantly lower than CONTROL; p<0.05; post-hoc tests. n=8.

The population average EMG activity patterns for all studied muscles during submaximal running in all four conditions are represented with ensemble linear envelopes (Fig. 7.9a-g). When comparing CONTROL and 016, the plantarflexor muscles showed the strongest correlation (GL: *r*=0.953 GM: *r*=0.958 SOL: *r*=0.936), whereas the BF showed the weakest

(*r*=0.556). All muscles were strongly correlated during 016 vs. 016SS, which were maintained in all except the TA (*r*=0.544) when compared to MATCHED (Table 7.3).

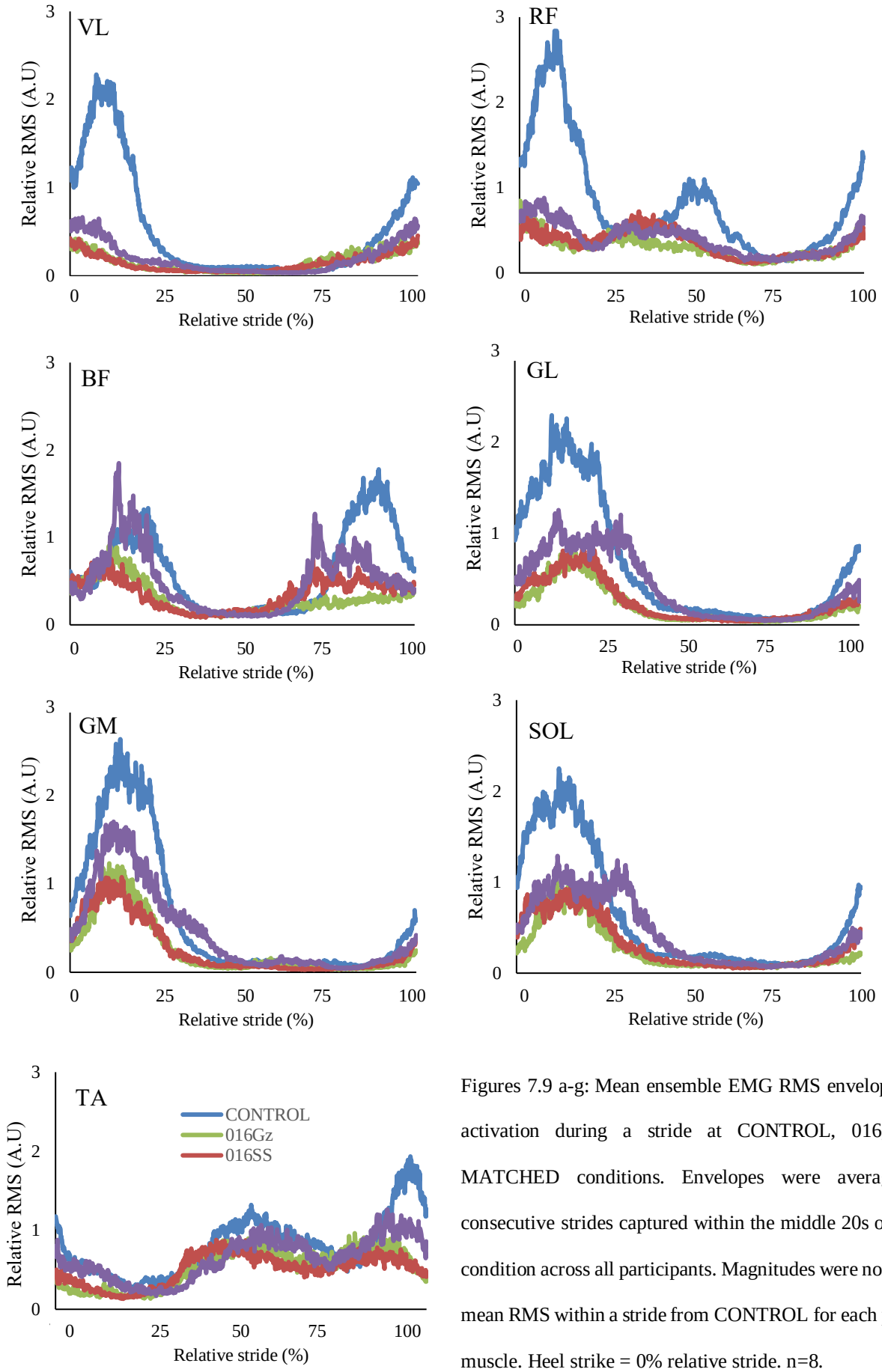

Figures 7.9 a-g: Mean ensemble EMG RMS envelopes for muscle activation during a stride at CONTROL, 016, 016SS and MATCHED conditions. Envelopes were averaged over all consecutive strides captured within the middle 20s of each running condition across all participants. Magnitudes were normalised to the mean RMS within a stride from CONTROL for each participant and muscle. Heel strike = 0% relative stride. n=8.

Table 7.3: Pearson correlation coefficients (*r*) between ensemble EMG curves across CONDITION during CONTROL, 016, 016SS and MATCHED. * significant correlation; p<0.01. n=8.

016SS VS MATCHED		016SS VS 016		MATCHED VS 016Gz	
VL	*r* =0.789*	VL	*r* =0.91*	VL	*r* =0.839*
RF	*r* =0.744*	RF	*r* =0.752*	RF	*r* =0.883*
BF	*r* =0.832*	BF	*r* =0.759*	BF	*r* =0.79*
GL	*r* =0.789*	GL	*r* =0.935*	GL	*r* =0.852*
GM	*r* =0.935*	GM	*r* =0.939*	GM	*r* =0.961*
SOL	*r* =0.823*	SOL	*r* =0.907*	SOL	*r* =0.824*
TA	*r* =0.544*	TA	*r* =0.861*	TA	*r* =0.728*

CONTROL VS. MATCHED		CONTROL VS. 016SS		CONTROL VS. 016Gz	
VL	*r* =0.835*	VL	*r* =0.544*	VL	*r* = 0.685*
RF	*r* =0.811*	RF	*r* =0.393*	RF	*r* =0.666*
BF	*r* =0.761*	BF	*r* =0.629*	BF	*r* =0.556*
GL	*r* =0.824*	GL	*r* =0.981*	GL	*r* =0.953*
GM	*r* =0.959*	GM	*r* =0.958*	GM	*r* =0.958*
SOL	*r* =0.799*	SOL	*r* =0.979*	SOL	*r* =0.936*
TA	*r* =0.834*	TA	*r* =0.615*	TA	*r* =0.669*

7.4 Discussion

These data are the first to show the effects of neuromuscular activity patterns during BW-unloaded running using horizontal suspension. The aims of this study were to assess the effect of running at a standardised submaximal speed in 0.16Gz vs. 1Gz on lower-limb neuromuscular activity and pattern parameters with the further aim to evaluate the reloading capability of 0.2Gz ABL in 0.16Gz using horizontal suspension. The main findings confirm the hypothesis that during submaximal running at simulated lunar gravity (0.16 Gz), muscle activity patterns are generally maintained, whilst activity levels decline in all lower limb muscles, compared to 1Gz. The similarities in muscle activity levels between 016 and 016SS are in conflict with the hypothesis that these would be greater during running at simulated lunar gravity with the addition of 0.2Gz ABL. Nonetheless, the plantarflexors (GM)

showed a greater duration of activity at 016SS compared to 016, equivalent to that observed during MATCHED, indicative of ABL reload-capability.

7.4.1 Neuromuscular responses during 1Gz running

The onset and offset timings during running in CONTROL (1Gz) maintain similarity to those observed in Chapter 6. Emergence of pre-heel strike activity of the leg extensors are generated on a spinal and/or a brainstem level (Dietz et al, 1992). Their deactivation prior to swing emphasises their role in BW support during stance. A longer-acting RF in comparison to both knee and ankle monoarticular extensors (by 35%), relates to its biarticular function as a hip flexor and knee extensor (Landin et al, 2016). Acting as an ankle dorsiflexor and invertor, TA activity onset prior to toe-off aids in providing clearance through swing (Novacheck, 1998) confirmed by its deactivation shortly after HS, whereas BF activity was evident in both the latter part of the swing phase (~35% prior to HS) and stance (~30% after HS), in accordance with its role in both phases (Nicola and Jewison, 2012). These results confirm that the CONTROL condition was an accurate platform from which to compare muscle activity patterns from simulated lunar running.

7.4.2 Muscle activity amplitude and frequency parameters

7.4.2.1 CONTROL vs. 016

The activity level of all muscles reduced during running at 25% >PTS in 016 (5.4km·h^{-1}) compared to CONTROL (9.45km·h^{-1}), with the greatest decline (~70%) seen in the monoarticular knee extensor (VL). These results are consistent with the observed VL activity reduction (58%) when running at 0.25Gz compared to 1Gz (Ferris et al, 2001) and 1-0.05Gz at 5km·h^{-1} (Ivanenko et al, 2002). The VL generates force to support BW in 1Gz (Farley &

McMahon, 1992); thus, GRFs necessary to overcome at such low gravity levels (Hunter et al, 2014) would limit the requirement for their activity. The significant decrease in TA activity levels at 0.16Gz compared to CONTROL implies a successful removal of gravity from the swinging limb (Lacquaniti et al, 2017) in contrast to suspension systems using body harnesses (Ivanenko et al, 2011).

Activity of the ankle extensors has been previously demonstrated to decline proportionately with BW reductions (Ivanenko et al, 2002), which was not observed within this study. For example, activity of the GL, GM and SOL were reduced by only 62%, 42% and 53%, respectively, in 016 vs. CONTROL. Ground contact forces have been shown to shift to the forefoot when locomoting <0.25Gz (Ivanenko et al, 2002; Van Hedel et al, 2006); participants may have acquired a shift in locomotive technique to "toe-running", necessitating a greater contribution of plantarflexor activity. Biomechanical assessment (i.e. 3D motion capture of the lower leg and foot) would be required to confirm this contention. Alternatively, it may be that the VTF allows a more accurate biomechanical representation of running in simulated partial gravity. The observed results from this study are similar to those observed when jumping in 0.16Gz vs. 1Gz during parabolic flight, which showed a disproportionate decrease in plantarflexor activity (Ritzmann et al, 2016). However, jumping generates greater GRFs and, thus, muscle activation than running (Ricard and Veatch, 1994) and, therefore, such a supposition could only be confirmed if compared with muscle activities during running in actual weightlessness, which to the authors' knowledge has not been investigated.

7.4.2.2 <1Gz conditions

Eleectromyographic RMS amplitude and MDF of all muscles were not significantly different between 016 and 016SS, both of which were comparable to MATCHED. Only the VL reduced

its activity during MATCHED in comparison to 016 and also 016SS, which further confirms its role in force generation to counter BW (Farley and McMahon, 1992). Nonetheless, these results show that the 0.2Gz reduction in 016 compared to MATCHED was not sensitive enough to promote further decrements in any other muscles' activity level. This was particularly surprising in the plantarflexors, considering the previously-observed proportionate decreases with 1-0.05Gz (Ivanenko et al, 2002). Moreover, further reductions in SOL and GM were reported from 0.38Gz to 0.16Gz in weightlessness during jumping (Ritzmann et al, 2016). These discrepancies could be linked to limitations of the VTF system. The loading increments/decrements are constrained to 10-15N; thus, it is possible that participants were not always at the desired loading, which would have a more profound effect the lower the gravity required. It could have been that participants were "overloaded" for 016 and "underloaded" for MATCHED, thereby decreasing the delta between them and affecting neuromuscular output. The unchanged activity levels between MATCHED and 016 leaves minimal scope for ABL to reload – an issue which arose in Chapter 6, where activity levels remained similar in all muscles between 0.8Gz and 1Gz. A larger dose of ABL (i.e. 0.84Gz) should be incorporated so that definitive reductions in activity levels can firstly be achieved by unloading from 1Gz to 0.16Gz (as accomplished in this study), whereby a more plausible attempt to reload to 1Gz can then ensue.

7.4.3 Muscle activity patterns

7.4.3.1 CONTROL vs. 016

With the exception of a few muscle- and condition-related outliers, the activity profiles of lower-limb muscles across partial gravities were strongly correlated with those in CONTROL. Together with the observed absence of change in the durations of the muscle-pair co-

contractions (except for in the VL/GL pair), these findings imply relatively maintained muscle activity patterns between CONTROL and <1Gz conditions, supporting the notion that running with BW unloading via horizontal suspension allows for normal locomotor behaviour to be preserved (Genc et al, 2006). The observation that the plantarflexors (SOL, GM and GL) decreased their activity duration during 016 compared to CONTROL was one that was absent when running at 0.8Gz compared to 1Gz in Chapter 6. Concomitant with an earlier GL activity onset, these findings are indicative of a sufficient Gz delta to induce meaningful neuromuscular pattern adaptations and scope for ABL-reloading.

7.4.3.2 <1Gz conditions

The strong correlations between muscle activity profiles during 016SS compared to 016 were marginally weaker when compared to MATCHED in most muscles. Most likely this is due to the significantly higher running speed at which MATCHED was performed (6.3km·h^{-1}) compared to 016 and 016SS (5.4km·h^{-1}). This is likely to have influenced the running kinematics in 016SS and 016 compared to MATCHED (Dicharry, 2010), despite previous data exhibiting minimal kinematic changes over a fourfold reduction in gravity (Donelan and Kram, 1997). This difference could also have contributed to the different muscle activity levels between 016SS and MATCHED discussed above. Incorporation of kinematic analyses in future studies assessing running on the VTF at varying gravities and speeds would assist in confirming or denying this contention. Nonetheless, the GM activity duration was similar in 016SS and MATCHED, but significantly greater in MATCHED versus 016. This suggests that the delta between 0.16Gz and 0.39Gz was sensitive enough to modify muscle activity patterns in the plantarflexors, contrary to those observed when using ABL to reload from 0.8Gz to 1Gz during unloading simulation achieved via a body harness system (Chapter 6).

7.5 Conclusion

Running at simulated partial gravity using horizontal suspension provides a valid method to maintain 1Gz motor patterns and unlike other simulators, enables the successful removal of gravity from the entire body, including the swinging limb. Decrements in the activity level and duration of lower limb muscles, particularly in the knee and ankle extensors, when running in 0.16Gz compared to 1Gz emphasise the role of loading in the generation of motor output. Aside from decreased plantarflexor activity duration, the preservation of muscle activity levels and patterns between 016, 016SS and MATCHED suggests that a delta of 0.2Gz on the VTF is insufficient to produce significant effects on neuromuscular output, which rendered the reloading capability of ABL implausible. Biomechanical assessment (i.e. 3D motion capture) would assist in further evaluating partial gravity-induced kinematics, which would help to improve in understanding these findings. Determination of the "optimal dose" of ABL for reloading purposes would be valuable and could be accomplished by incorporating a greater magnitude of ABL provision during simulated lunar running.

Chapter 8: General discussion

8.1 General aims and summary of findings

This thesis was aimed at determining the effect of additional low-level (0.2Gz) axial body load (ABL) on gravity-dependant physiological variables during human movement, namely aerobic exercise in 1Gz and <1Gz environments. The studies produced by means of this thesis, spread across fove Chapters, were, therefore, designed to incorporate assessment techniques that evaluated cardiorespiratory, neuromuscular and kinematic variables during conventional bipedal exercise modalities, with and without additional ABL. The concept of providing additional ABL to <1Gz running was also experimentally scrutinised, with the aim of enabling an understanding of its potential role as a reloading stimulus and consequential applicability to unloading-induced population demographics.

The three experimental studies within this thesis demonstrated a number of key findings. Despite inducing a slight, but significantly more rapid and shallow breathing pattern – possibly contributing to reduced exercise tolerance – 0.12-0.2Gz ABL did not induce functionally-meaningful alterations in cardiorespiratory responses during low to maximum-intensity exercise when cycling or running in ≤1Gz (Chapters 3 and 5). The lower limb musculature did not change their activity levels in response to this level of ABL when added to gravities in the range of 1-0.16Gz (Chapters 4, 6 and 7). Moreover, although kinematic analysis was limited to running, Chapter 6 showed that the knee joint remained less flexed when running with 1.2Gz compared to 1Gz. However, modified muscle activity patterns (i.e. increased duration), particularly in the plantarflexors were observed (Chapters 4 and 6), suggestive of load receptor (i.e. Golgi Tendon Organ) triggering, implying that alternative neuromuscular strategies – likely governed by the central nervous system – are employed to preserve the desired

movement under loaded conditions. An evaluation of the reloading capability of ABL was permitted only with respect to cardiorespiratory variables due to an absent response of the neuromuscular system to 0.2Gz unloading, regardless of where on the gravity spectrum the removal was from (1Gz vs. 0.8Gz [Chapter 6]; 0.39Gz vs. 0.16Gz [Chapter 7]). Nonetheless, cardiorespiratory variables were not reloaded by ABL to levels equivalent to 0.2Gz, despite a significant unloading effect (Chapter 5).

8.2 Cardiorespiratory adaptations to axial body loading during maximal running and cycling in 1Gz

Across Chapters 3 and 5 investigating the effect of ABL on cardiorespiratory variables, the findings were relatively synonymous in that regardless of whether participants cycled or ran, maximal aerobic capacity was unimpeded when subjected to 0.2Gz ABL. It was not anticipated that detriments to $\dot{V}O_2$Max would be evident, as body loading has not been reported to affect either central (i.e. oxygen-carrying capacity) or peripheral (i.e skeletal muscle extraction of O_2) determinants of aerobic capacity during running or cycling. However, although $\dot{V}O_2$Max has traditionally been considered the ‘‘gold standard’’ for evaluation of endurance performance (Costill, 1967), Weltman et al (1978) suggested that, regardless of an individual's $\dot{V}O_2$Max, the onset of the anaerobic threshold i.e. metabolic acidosis must be a good measure for evaluating submaximal fitness. This pertains to the theory that when oxygen supplies to the working muscle become insufficient, anaerobic metabolism is initiated, and consequently lactic acid starts to increase through a mechanism of anaerobic glycolysis (Kumagai et al, 1982). Within this thesis, the ventilatory threshold, specifically by using the V-slope method (Beaver et al, 1986), was employed to ascertain the anaerobic threshold and nonetheless remained unaffected by ABL during running (Chapter 6). In fact, studies incorporating loading into longer-term training interventions have been shown to improve $\dot{V}O_2$Max in clinical populations (Jin et al,

2012), attributed to peripheral improvements (i.e. knee muscle strength/vascular supply). The prospective use of ABL as a training intervention was not an objective of this thesis and hence cannot be speculated upon.

The fact that $\dot{V}O_2$ increased across intensity-incremented running and cycling with ABL to the same magnitude as the CONTROL comparative (Chapters 3 and 5) rejects the hypothesis that $\dot{V}O_2$ is augmented when running with additional load (i.e. 41.7±3.8ml.kg.min^{-1} vs. 43.9±5.9ml.kg.min^{-1} during cycling at 200W [Fig. 3.2b] and 41.3±1.7 ml.kg.min^{-1} and 42.1±0.9 ml.kg.min^{-1} during running at 12km·h^{-1} [Fig.5.4a], in CONTROL and AL, respectively). These findings are in contrast to previous studies observing an increased metabolic cost when using similar load magnitudes during both running and cycling in 1Gz (Kamon et al, 19873; Teunissen et al, 2007; LaFortuna et al, 2008). Teunissen et al (2007) added lead strips to a waist belt equivalent to 20% BW whilst participants ran at 10.8km·h^{-1} and observed a 24% augmented metabolic rate whereas Kamon et al (1973) observed similar increases (~26%) when cycling with 10kg ankle weights. Furthermore, LaFortuna et al (2008) observed a 23% increase in $\dot{V}O_2$ during cycling in obese individuals bearing 110kgs compared to normative controls (54kgs); this comparison is potentially confounded by numerous obesity-related factors which could have influenced their results (i.e. autonomic impairment of cardiac regulation; Liatis et al, 2004). Nonetheless, despite the methodological differences, there remains a common theme between these studies; that the additional loading has an inertial component, which would displace body COM (Whalen, 1993). Interestingly, a comparable delta $\dot{V}O_2$ increase (20-30%) was discerned by Barer et al (1998) whilst cycling in the Penguin Suit, constituting ~25kg, in microgravity. However, it is unknown how the addition of a small ABL "dose" within a reduced gravity environment affects cardiorespiratory responses to exercise.

It has been argued that the impact of load carriage on cardiorespiratory responses varies as a function of where it is distributed on the body (Soule and Goldman, 1969). Loads ranging from 1-14kg added to the head, hands or feet when walking have a greater oxygen cost than equivalent masses distributed around the torso likely related to undisturbed COM (Soule and Goldman, 1969; Myers and Steudel, 1985). Because during cycling the body is stabilised in the vertical plane without holding the body's COM over the base of support (Di Prampero, 2000), a running modality, which necessitates COM control, was implemented in Chapter 5 to permit an expanded understanding of the functionality of additional ABL. Furthermore, increased metabolic rate with additional load has been linked to greater muscle activation (Teunissen et al, 2007) and knee flexion (McMahon et al, 1987) to attenuate COM displacement and load-associated instability (Schiffman et al, 2006). However, muscle activity levels were not modulated during either cycling or running, and the angle of the knee was rendered into greater extension when running with ABL (Chapter 6; to be discussed below), thus not necessitating an increased metabolic output (McMahon et al, 1987). Therefore, the undifferentiating $\dot{V}O_2$ observed between running and cycling likely implies that the provision of shoulder-to-feet-distributed ABL does not impose COM disruptions any more than the activity itself, which might explain why these results are in contrast to previous literature.

The reduced exercise tolerance observed during both cycling (12.6%; Table 3.2) and running (10.3%; Fig. 5.6b) with additional ABL is cohesive with previous literature using comparable load magnitudes during similar tasks (Taylor et al, 2012). Such demonstrations have been related to the contention that chest-wall movement restriction is precipitated, resulting in disrupted ventilation (i.e. a more rapid and shallow breathing pattern; Peoples et al, 2016). However, such explanations are inherent predominantly with mass loading high up on the back

or around the torso due to their physical interaction with chest wall mechanics (Phillips et al, 2016). The ~40% greater magnitude of exercise intolerance in the Taylor et al (2012) study compared to ours may be explained by their breathing equipment weighing ~12kg that loaded the chest specifically, despite the entirety of their loading equipment being evenly distributed.

Nonetheless, similar ventilatory patterns have been reported in individuals wearing chest-wall strapping (CWS) during high intensity exercise (O'Donnell et al, 2000). This study observed non-significant differences in $\dot{V}O_2Max$ and cardiometabolic variables when cycling with and without CWS (49.21±2.12 vs. 50.96±2.01ml.kg.min^{-1}, respectively). This was accompanied with increased BR (~11%) and concurrent reductions in $\dot{V}_E$ (~11%), $\dot{V}_T$ (~22%) and exercise tolerance (~5%), indicative of mechanical breathing constraints. A significant POWER*CONDITION interaction effect on ventilatory variables was observed in Chapter 3 concomitant with reduced tolerance. It was suggested that the non-elastic SkinSuit material around the upper chest could be contributing to this. The presence of a significantly steeper $\dot{V}_E$/BR slope in Chapter 5 (Fig. 5.5b), indicative of a more rapid and shallow breathing pattern may corroborate this speculation. Nonetheless, the work by O'Donnell's group performed spirometry assessment to ascertain resting lung volumes to determine if CWS had an effect before exercise assumption, which was not determined in the studies that are comprised within this thesis. Thus, whether the provision of 0.2Gz ABL induces ventilatory mechanic-perturbations as a function of exercise intensity or passive-wear is unknown. Indications of such volumes (i.e. vital capacity at rest) would hence be valuable in forecasting possible ventilatory disturbances during exercise with ABL.

8.3 Biomechanical adaptations to axial body loading during running and cycling

8.3.1 Muscle activity levels

It was discerned in Chapters 4, 6 and 7 that during cycling and running in a gravity range of 1Gz-0.16Gz, workload-related increases in neuromuscular activity levels were not augmented with 0.12-0.2Gz ABL, implying that increased muscle fibre recruitment to meet the task demands was not necessitated (Figs. 4.3a, 6.2 and 7.5). These observations are in direct conflict with the hypothesis that muscle activity levels would be greater in an attempt to overcome the imparted resistance offered through ABL. Despite observations that muscle activity levels of both the leg extensors and flexors increased when cycling with additional loads of similar magnitude in ≤1Gz (Barer et al, 1998; Baum and Li, 2003), the amount of energy to overcome gravity and inertia with each pedal cycle is minimal (Di Prampero, 2000). Nonetheless, during running – where control of body COM is required, and load receptor feedback is more prevalent (Dietz and Duysens, 2000) – muscle activity levels remained unchanged with ABL.

Axial body loading imparts resistance by means of elastic bands in series along the limb which increase with proportional stiffness distally. As the muscular-tendon system represents an elastic band-like system (Shadwick, 1990), and a spring-mass model can be used to replicate the motion of the body COM during locomotion (Blickhan, 1989), stretching the muscle will cause energy to be stored (eccentric phase) and regained upon shortening (concentric phase). As such, the addition of a spring in parallel with the human leg has been proposed to reduce the force and mechanical work of the lower limb (Cherry et al, 2016). Research has recently exploited this concept via the creation of wearable elastic "exoskeletons" for gait assistance. Walking with spring-like exoskeletons at the ankle (Sawicki and Ferris, 2008; Bregman et al, 2012), or spanning multiple lower-limb joints (ankle, knee and hip; Wang et al, 2011; Mooney

et al, 2014) have been shown to reduce the energy cost of walking by 10-36%. These results are suggested to arise from reduced mechanical work at the ankle due to assisted toe-off, validated by 28-35% decreases in SOL activity (RMS; Gordon and Ferris, 2007; Sawicki and Ferris, 2008). To the authors' knowledge, although elastic exoskeletons have also been created for the purpose of running adjuncts (Elliot et al, 2013; Cherry et al, 2016), such studies have only detailed "proof-of-concept" and pilot data without thorough interrogation of cardiorespiratory or neuromuscular variables.

Although there are limited data on cycling/running with whole-body axial loading "suits", Kendrick (2016) observed that whilst running with 0.75Gz additional ABL during 75% BW running (~1.5Gz), flexor muscle activity, as quantified via static optimisation, during the swing phase was elevated, in an attempt to overcome the forces of the elastic loading elements as they stretched over the knee joint. Consequently, knee extensor muscles reduced their activity upon extension from swing to stance, owing to the "restoring" forces on offer from the stretched elastic recoil through swing. It may be that the SkinSuit accumulates energy during flexion to use during recoil from extension during cycling and running. This notion would certainly help to explain the lowered VL activation in AL vs. CONTROL during HYPERLOAD running in Chapter 6 ($9km \cdot h^{-1}$: 0.044±0.007 vs. 0.038±0.005mV; $13km \cdot h^{-1}$: 0.054±0.008 vs. 0.047±0.006mV in CONTROL and AL, respectively [Fig. 6.2d]). Here lies a paradox: if the loading properties are not capacitated without the simultaneous action of elastic properties, then differing hypotheses regarding muscle activation levels would be formulated. Whether the elastic nature of the SkinSuit offers mechanical assistance (i.e. the capacity to store and recoil elastic energy), similar to the abovementioned exoskeletons would help to clarify anticipated physiological and biomechanical outcomes and should, therefore, be investigated. This could

be accomplished by using force transducers attached to the SkinSuit stirrups to record the forces and torques produced during cycling and running (Sawicki et al, 2008).

One of the limitations within this thesis was that the ABL provided by each person's SkinSuit was not quantified during cycling or running. SkinSuit-induced ABL has previously been assessed during walking (outlined in Chapter 2), but one must take into consideration the biomechanical differences between walking and running. This would be especially pertinent if differences in loading are apparent between stance and swing phase, as the duration of these phases can alter between these two exercises (Dicharry, 2010). Previous data reported in Chapter 2, section 2.4.1.1 have shown that in a group of 6 participants with an additional ABL of 0.12Gz during standing, only a maximum of 0.07Gz of this was imparted during walking, likely during the stance phase. Running typically involves shorter stance phases than walking (Dicharry, 2010), in which case even less ABL may be imparted. Further analyses are therefore required to quantify the provision of ABL during running gait phases.

8.3.2 Muscle activity patterns

Although providing valuable information, investigating only muscle activity levels does not provide a comprehensive portrayal of neuromuscular coordination (Hug and Tucker, 2016) and obtaining information about amplitude relies heavily on factors such as electrode placement and low-pass filter choice (Farina et al, 2004). Moreover, the mean EMG amplitude over a specific part of a movement may conceal important information about coordination strategies. Thus, for a deeper understanding of muscle coordination strategies, interrogation of the linear envelope and the EMG profile is imperative (Hug and Tucker, 2016), which may enable significant effects to be revealed that are masked with amplitude analysis.

Contrary to the muscle activity level, the patterns of muscle activity were affected by ABL. This manifested primarily as a lengthened activity duration of the plantarflexors when cycling (GL; Chapter 4) and running (SOL; Chapter 6) with the addition of 0.12-0.2Gz compared to 1Gz (300.4±12.6° vs. 268.4±10.3° when cycling at 50W [Fig. 4.3b] and 54.5±1.4% relative stride vs. 49.2±1.7% relative stride when running at 13km·h^{-1} [Fig. 6.4] in AL vs. CONTROL, respectively; $p<0.05$). In Chapter 4, it was speculated that the elongated GL duration may be linked to biomechanical modulations linked to control of the ankle joint during cycling (Raasch, 1996). However, the fact that a comparable, significant trend occurred with running rendered this explanation less arguable. These findings are consistent with those of multiple authors in studies investigating cycling and running in 1Gz with the addition of both lower (Baum and Li, 2003; <5% BW) and comparable load magnitudes (20-30% BW; [Ghori and Luckwill, 1985; Stephens and Yang, 1999]).

Roy et al (1991) suggested that recruitment of additional motor units in the GM of rats with increased treadmill speed served to compensate for diminished activation time due to shorter gait cycle durations at higher speeds. The opposite phenomena of prolonged activation time serving to compensate for a lack of increased muscle activity level may thus have contributed to the aforementioned findings. Moreover, Brown and Cooke (1990) and Virji-Babul (1994) have illustrated that initial agonist burst duration in the upper arm muscles increased under load where the amplitude was held constant. Collectively, these findings are consistent with the contention that adaptations in muscle activity under load are related not to amplitude parameters but rather to the temporal characteristics of the movement. These are likely governed by the CNS, altering neuromuscular strategies to preserve similar movements under different conditions (Ghori and Luckwill, 1985; Virji-Babul, 1994). The fact that the consistent location of lengthened muscle activity across thesis studies was in the plantarflexors supports

this notion, particularly considering that this is where load-sensitive group Ib afferents providing limb load feedback reside (Gordon et al, 2009). In Chapter 4, there were also earlier phase shifts of activity evident in all recorded muscles, as verified through analysis of the cross-correlation function using the averaged EMG ensemble envelopes. These results confirm the important role of loading for the CNS in regulating phase shifts to adjust basic locomotor patterns in "altered" conditions (MacLellan & McFadyen, 2010).

8.3.3 Lower-limb kinematics

Kinematic analysis during running in Chapter 6 showed that ABL inflicted displacement in the knee angle to an extended position at both HS and maximum knee flexion (swing). Conflicting findings with regards to knee-joint kinematics have been observed when running with additional loads of similar magnitudes (Brown et al, 2014b; Silder et al, 2015); such inconsistencies are likely related to the differences in load provision in these studies (military ensemble and weighted vest, respectively) and the potential COM disruption, as discussed earlier, in comparison to ABL. The data presented concurs with the reduced knee flexion observed in two out of three participants when running with 0.75Gz ABL at 0.75Gz (thus ~1.5Gz; Kendrick, 2016). Thus, a feasible explanation for the greater degree of knee extension observed is the elastic material used in the SkinSuit affecting joint ROM during running. However, aside from the greater magnitude of ABL imparted, this study only had a sample size of three (and thus statistical analysis was lacking) and the results were obtained through modelling as opposed to biomechanical analysis, making direct comparisons challenging.

Stance ratios were unaffected by ABL during running in ≤1Gz (Fig. 6.8a and 6.12a). In contrast, substantial increases in stance time to compensate for a lack of knee joint flexion in order to attenuate loads have been observed (Brown et al, 2014), which reinforces the

contention that the extended knee with ABL is unrelated to an inertial cause. Nevertheless, it has been argued that greater knee flexion of a landing leg is responsible for energy absorption when load-carrying and a more extended knee might increase musculoskeletal injury risk (Polcyn et al, 2002; Brown et al, 2016). Moreover, increased knee flexion produces increased propulsive force by allowing the leg extensor muscles to operate at a more favourable position on the force-length curve and is thus a necessary attribute to maintain economical running (Moore et al, 2016). Further, the quantification of stance ratio and all other kinematic variables was through manual identifcation of HS – denoted by the minimum knee angle, and toe-off – denoted by the increase in angular velocity during the second knee flexion peak (Fig. 2.12). This suboptimal measurement technique renders the data susceptible to erroneous interpretation. For example, knee angle at HS during incremental running was observed to be ~6° in CONTROL at 9km·h^{-1}, and only ~2° more flexed by 13km·h^{-1} which is discrepant to the typical ~20-25° knee flexion occuring at HS to act as a shock absorber from the impact of foot-ground contact (Dicharry, 2010). Thus, a more robust assessment of knee joint angle (i.e. 3D motion analysis) should be implemented. This would aid in elucidating if the use of ABL would be contraindicated on the premise of impaired running economy or injury risk.

8.4 Reloading with axial body loading (ABL)

Recent research has focused on the use of BW unloading with increases in speed to achieve a full BW stimulus, considering the applicability to a number of rehabilitation scenarios (a review is offered by Farina et al, 2017). It can be argued that the use of loading can be utilised instead of speed to achieve this, though this has not been explored. This is likely due to the potential physiological burden (i.e. instability of COM displacement) associated with the load approach, especially considering that the population demographics requiring the unloading are likely to have some form of predisposition to/acute injury. Thus, the other primary aim of this

thesis was to attempt an understanding of ABL as a "reloading" stimulus to the cardiorespiratory and neuromuscular systems in order to determine if it has any utility in unloading-based rehabilitation scenarios.

Experimentally, a way in which to investigate the reloading potential of ABL is to firstly "unload" an individual by a desired amount (i.e. 0.2Gz) and substitute this with the same loading quantity. In the study that served Chapters 5 and 6, a body-suspension system was used to enable running at 0.8Gz, and a condition comprised of 0.8Gz plus SkinSuit-induced 0.2Gz ABL (Sim1Gz). Chapter 5 reported ventilatory variables (i.e. $\dot{V}O_2$, $\dot{V}CO_2$, $\dot{V}_E$ and $\dot{V}_T$) to reduce when running with 0.2Gz unloading to a greater extent than cardiovascular variables (HR; Fig. 5.7a&b and Table 5.1), possibly related to the between-participant variability which was further impacted by omitted data from three participants. Nonetheless, for the neuromuscular system, such an unloading effect was indistinguishable. In fact, activity levels of all lower-limb muscles remained unchanged between 1Gz and 0.8Gz (Chapter 6; Table 6.3) and 0.39Gz and 0.16Gz (Chapter 7; Fig. 7.5). These results are in contrast to the greater EMG reductions observed in the SOL (~20%), VM (~7%) and GL (~15%) when running at 80% BW on LBPP treadmills (Liebenberg et al, 2011; Sainton et al, 2015). Thus, for the neuromuscular system, the reloading potential of ABL could not be accurately assessed, as there must firstly be a significant unloading effect to enable a reloading "opportunity".

A number of factors may have influenced the failure to observe differences in lower limb activity with unloading. The horizontal assistance offered by LBPP devices as utilised in the Liebenberg et al (2011) and Sainton et al (2015) studies has been proposed as the cause of reduced neuromuscular expenditure (Grabowski and Kram, 2008) due to aided forward propulsion. This is absent in body-suspension devices and could, in part, explain the non-

existent unloading effect in the current findings in comparison to theirs. This is supported by the fact that these results are consistent with Ferris et al (2001) who observed negligible differences in neuromuscular activity levels with 0.75Gz unloading using similar apparatus to ours. Furthermore, deviations in vertical alignment from the pulley within these systems can generate inaccurate BW unloading (Frey et al, 2006; Graham et al, 2009); if participants were exposed to lower levels of unloading than intended, their muscle activity levels would have been expectedly higher. Interestingly, despite the experimental study in Chapter 7 utilising a vertical treadmill facility – which inhibits exposure of the swinging limb to a Gz vector (Lacquaniti et al, 2017) and enables a 100% delta unload from 0.39Gz to 0.16Gz – the maintenance of muscle activity levels persisted. Thus, the contribution of methodological issues to the findings reported remains ambiguous.

Some authors argue that reductions in neuromuscular activity scale nonlinearly from 1-0.8Gz during running (Ferris et al, 2001). Moreover, it appears from the data presented as though a reduction of 0.2Gz unloading during high or low portions of the gravity spectrum (from 1Gz to 0.8Gz and 0.39Gz to 0.16Gz) was not potent enough to reduce the activity required from lower-limb muscles. Although a nonlinear scaling of inter-lower-limb muscle activity levels has been observed from 1-0.05Gz, proportional declines in plantarflexor activity have been evidenced (Ivanenko et al, 2002). However, muscle activity patterns, particularly by means of plantarflexor duration decreased when running at 0.16Gz vs. 0.39Gz, but failed to do so at 0.8Gz, compared 1Gz. There may therefore be a threshold by which changes in gravity affect physiological responses during movement that is yet to be completely determined. Such information is crucial in ascertaining the optimal dose of ABL, where firstly definitive reductions in muscle activity can be achieved and subsequently a more plausible attempt at reloading can be made.

In light of the above discussion, the reloading capability of ABL could only be scrutinised with respect to respiratory variables in Chapter 5. $\dot{V}O_2$, $\dot{V}CO_2$, $\dot{V}_E$, $\dot{V}_T$ were reduced from 1Gz to 0.8Gz, which were not reinstated to 1Gz values when 0.2Gz ABL was added (Sim1Gz). Moreover, although not significant, HR values tended to be lower during Sim1Gz (141±9bpm) compared to 1Gz (161±4bpm) and even 0.8Gz (157±12bpm). Collectively, these results are congruent with studies involving the use of compression garments during running, which have observed reduced peak $\dot{V}_E$ (Rivas et al, 2017), $\dot{V}O_2$ (Bringaard et al, 2006), HR (Dascombe et al, 2011) and muscle oscillations subsequently reducing metabolic demand (Born et al, 2014). A potential effect of circumferential compression arising from the SkinSuit may explain these discrepancies, as well as the equivalent cardiorespiratory responses between AL and CONTROL during HYPERLOAD protocols; any loading effect serving to augment $\dot{V}O_2$, for example, may have been negated by a compression effect acting to reduce it.

8.5 Possible applications of axial body loading

Most of the musculoskeletal risk in military personnel is attributed to the instability of COM displacement with additional load (Schiffman et al, 2006). Attempts to reconfigure soldiers' carrying equipment in a manner that bears less of a burden on the COM is not a novel idea (Knapik et al, 2004) and has been investigated with regards to carrying double packs (Harman et al, 1994), carts (Haisman et al, 1972) and pack frames (Vacheron et al, 1999). The fact that the observed results infer that bearing additional axial load longitudinally does not impose COM displacement verifies the importance of a continual quest for optimal load-carrying. Ergonomic investigations could ratify the reconfiguring of equipment which is evenly dispersed from head to foot, albeit whilst avoiding chest/thorax load to minimise breathing-mechanic impediments.

A light-weight garment providing axial body loading that does not limit performance yet may permit muscle coordination strategies by the CNS may have some utility, particularly clinically. For example, Kourtidou-Papadeli et al (2008) suggested that a brain damaged child at birth may require a higher intensity gravity stimulus before their brain becomes programmed to respond to direction and acceleration and eventually learn to walk. A reduced firing rate and recruitment of single motor units are characteristic features in individuals with central motor lesions (Rosenfalck and Andreassen, 1980), and Parkinsonism (Dietz et al, 1974). Furthermore, reduced EMG (Berger et al, 1982) and a reduced rate of force development are attributes of those with CP (Geersten et al, 2015). Krause et al (2017) observed improved neuromuscular coordination in subjects with CP which indicated improved voluntary movement control. It may be possible, therefore, that, like the Adeli suit, longer-term ABL-wear could be used for training interventions in populations that have difficulty increasing their motor unit firing rate (Lee, 2016) and would, thus, benefit from improved intramuscular coordination. Moreover, it may be that ABL has a more profound effect on those that already suffer some debilitation; the participant cohort selected were all healthy young men, all of whom were recreationally active with no underlying motor disorder.

Preparations are already underway for human sojourns to Mars (Schwender et al, 2017). Given the practical limitations of the craft-type that will be responsible for transport, a new generation of countermeasures that require low power, volume and mass which are capable of impacting multiple physiological systems are sought (Owerkowicz et al, 2016). Furthermore, loaded exercise will need to be performed to protect bone and muscle strength (Lang et al, 2017), combined with an optimal concoction of exercise intensity, duration and frequency to optimise operational aspects (i.e. crew time, caloric expenditure). A way of meeting this objective is via

the development of means which can simulate or reproduce some effects of gravitational loads, including loading suits, which could reduce the workload and length of training sessions required (Kozlovskaya et al, 2002). On the premise that further investigations can determine an optimal ABL dose which produces a significant reloading stimulus to the cardiorespiratory and neuromuscular systems, the SkinSuit could potentially provide an effective countermeasure whilst meeting the majority of these practical requirements.

Ground reaction forces reduce linearly with BW unloading, which provides a useful training platform to reduce the risk of overuse injury or as a rehabilitation tool to speed recovery after injury or surgery (Hunter et al, 2014; Saaman et al, 2014). However, because metabolic power decreases linearly during BW unloading, weight-supported running may not accrue the same cardiovascular benefits as normal running. Increasing running speed during BW support has been implemented as a means of increasing the metabolic cost that would be offset by the unloading, to achieve the same stimulus (i.e. $\dot{V}O_2$; Farina et al, 2017). For example, with every 25% reduction in BW, an increase in speed of ~4.5km·h^{-1} would be required to achieve the same $\dot{V}O_2$ (Farina et al, 2017). However, this relationship has been based only on three datasets and with a BW ≥50%. Nonetheless, using this theory and applying it to data acquired from Thomson et al (2017), running at 75% BW at 14.5km·h^{-1} would result in similar plantar forces – a proxy for GRFs – to that of running at 100% BW at 10km·h^{-1} (2.016 BWs vs. 2.011 BWs respectively). Thus, the increased speed required to maintain the physiologic stimulus may, therefore, negate some of the desired musculoskeletal unloading. Although not investigated, it is reasonable to assume that ABL would not accentuate GRFs owing to its low mass and absence of lower-limb neuromuscular adaptations that would typically be associated with increased GRFs (i.e. increased activity levels), and thus may be a more viable alternative

combined with slower speeds (Puthoff et al, 2006), on the premise that an optimal dose has been determined.

8.6 Limitations

There are multiple limitations related to the studies that served this thesis, primarily related to methodological aspects, some of which have been previously alluded to. Due to a scarcity of biomechanical equipment, the determination of movement phases across all studies was rendered suboptimal. Identification of top dead centre (TDC) during cycling was via the selection of VL activity peaks, which has previously been used as a surrogate (Shinohara). However, although peak activity of the VL has been shown to begin just prior to TDC, such activity can remain until 30° after TDC (Fonda and Sarabon, 2010) and thus this method may provide slight inaccuracies in TDC identification. Regarding running, electrogoniometry (Chapter 6) was used to identify the lowest knee angle i.e. the most extended position of the knee as a determinant of HS. The knee is typically at its most extended as the foot strikes the ground (Nicola and Jewison, 2012), hence the justification for identifying such a knee angle for HS detection; though changes in running technique could render a more flexed knee at HS with the most extended knee position occurring at an alternative time. To ensure absolute data accuracy, future studies should incorporate more robust measures i.e. 3D motion capture to identify movement phases, which will prevent ambiguity over the data that is expressed relative to them.

The sample size within the experimental studies was small, which was somewhat uncontrollable owing to the custom-fit nature of the SkinSuits. It could have been possible to increase the sample size by having a greater number of "substitute" participants, but with the risk of jeopardising data integrity. However, numerous studies investigating EMG (Labini et

al, 2011; Park et al, 2014; Ritzmann et al, 2015), kinematic variables (Labini et al, 2011; Sylos-Labini et al, 2013; Ritzmann et al, 2015), and cardiorespiratory responses (Teunissen et al, 2007; Grabowski and Kram, 2008; Grabowski, 2010; Faghy et al, 2016) during loaded vs. unloaded movement have implemented similar, participant numbers (≤10). Moreover, power calculations (appendix. 4) were computed for all investigated variables and loading scenarios, which supported the sample size used in experimental studies. Nevertheless, future studies would be enhanced by incorporating a greater sample size to improve their statistical validity.

Although intended to be 0.2Gz, the ABL provided by each participants' SkinSuit fluctuated by as low as 0.07Gz to as high as 0.24Gz. This was a uniform issue across all participants, not only when substitutes were used. It thus could have made it difficult to distinguish the effects of the ABL as the magnitude of exposure was different between subjects. Nonetheless, attempts were made to overcome this in both analysis and methodological terms in the studies that required equivalent levels of Gz to be created. In Chapters 5 and 6, a linear regression analysis was performed per participant to predict parameter values, had the ABL had been 0.2Gz. In Chapter 7, the MATCHED level was custom-made for each participant, depending on the ABL imparted. In Chapters 3 and 4, it was deemed unnecessary to "correct" the ABL because there were no comparisons to an equivalent Gz being made.

8.7 Conclusion

Provision of 0.2Gz ABL via vertical elastic resistance in addition to Earth- or partial-gravity environments does not induce cardiorespiratory or neuromuscular responses equivalent to 20% BW loading, presumably due to the absence of centre of mass displacement, in contrast to overcoming the inertia of mass loading. Future research should investigate the influence of SkinSuit-induced compression and elastic energy-lending potential which may have masked

some of these effects. However, the significant effect of additional ABL on muscle activity patterns during both cycling and running in ≤1Gz, particularly in the plantarflexors, suggests strategic modulation of locomotor control governed by the central nervous system, which may have utility in populations suffering from neurological impairments or exposed to the detrimental effects of partial gravity. Unloading of 0.2Gz during high or low portions of the gravity spectrum was not potent enough to reduce the activity required from lower-limb muscles, making "reloading" opportunities inconceivable. Nonetheless, the use of horizontal suspension enabled an improved knowledge of how partial gravity influences neuromuscular function during submaximal running, which ultimately assists in comprehending the conception of bodyweight reloading. In the absence of performance decrements, ABL provides a safe adjunct to exercise in ≤1Gz; on the premise that an optimal reloading dose is determined, investigation into the potential assistance of ABL-integrated exercise to preserve or enhance physiological function (i.e. muscle strength) in ≤1Gz could be attempted.

References

Adams, W. C. (1967). Influence of age, sex, and body weight on the energy expenditure of bicycle riding. *Journal of Applied Physiology*, *22*(3), 539-545.

Alexander, R. M. (1989). Optimization and gaits in the locomotion of vertebrates. *Physiological reviews*, *69*(4), 1199-1227.

Ali, A., Caine, M. P., & Snow, B. G. (2007). Graduated compression stockings: physiological and perceptual responses during and after exercise. *Journal of sports sciences*, *25*(4), 413-419.

Amann, M., Subudhi, A. W., & Foster, C. (2006). Predictive validity of ventilatory and lactate thresholds for cycling time trial performance. *Scandinavian journal of medicine & science in sports*, *16*(1), 27-34.

Attias, J., Waldie, J., Evetts, S & Green, D (2014). The effect of the Gravity-Loading Skinsuit (GLCS) upon maximal aerobic performance ($\dot{V}O_2$Max) and Oxygen Kinetics. *Aviation, Space and Environmental Medicine*, 85(3), 352

Attias, J., Scott, J. P. R., Russomano, T. & Green, D. A. (2015). The effect of the MK VI Gravity-Loading Countermeasure Skinsuit (GLCS) upon maximal aerobic exercise ($\dot{V}O_2$Max). *International Congress of Aviation and Space Medicine (ICASM), Oxford, UK*.

Attias, J., Philip, A. C., Waldie, J., Russomano, T., Simon, N. E., & David, A. G. (2017). The Gravity-Loading countermeasure Skinsuit (GLCS) and its effect upon aerobic exercise performance. *Acta Astronautica*, *132*, 111-116.

Attwells, R. L., Birrell, S. A., Hooper, R. H., & Mansfield, N. J. (2006). Influence of carrying heavy loads on soldiers' posture, movements and gait. *Ergonomics*, *49*(14), 1527-1537.

Bailes, A. F., Greve, K., Burch, C. K., Reder, R., Lin, L., & Huth, M. M. (2011). The effect of suit wear during an intensive therapy program in children with cerebral palsy. *Pediatric physical therapy*, *23*(2), 136-142.

Banister, E. W., & Jackson, R. C. (1967). The effect of speed and load changes on oxygen intake for equivalent power outputs during bicycle ergometry. *European Journal of Applied Physiology and Occupational Physiology*, *24*(4), 284-290.

Barer, A. S., Kozlovskaia, I. B., Tikhomirov, E. P., Sinigin, V. M., & Letkova, L. I. (1998). Effect of loading suit" Penguin" on human metabolism during movements. *Aviakosmicheskaia i ekologicheskaia meditsina= Aerospace and environmental medicine*, *32*(4), 4-8.

Bar-Haim S, Harries N, Belokopytov M, et al. Comparison of efficacy of Adeli suit and neurodevelopmental treatments in children with cerebral palsy. *Dev Med Child Neurol.* 2006;48(5):325-330.

Basmajian, J. V. (1985). Description and analysis of the EMG signal. *Muscles Alive*, 73-90

Baum, B. S., & Li, L. (2003). Lower extremity muscle activities during cycling are influenced by load and frequency. *Journal of Electromyography and Kinesiology*, *13*(2), 181-190.

Beaver, W. L., Wasserman, K. & Whipp, B. J. (1986). A new method for detecting anaerobic threshold by gas exchange. *Journal of applied physiology*, *60*(6), 2020-2027.

Belluye, N. (2006). Aerobic energy cost and sensation responses during submaximal running exercise–positive effects of wearing compression tights. *Int J Sports Med*, *27*(5), 373-378.

Berg, H. E., Eiken, O., Miklavcic, L., & Mekjavic, I. B. (2007). Hip, thigh and calf muscle atrophy and bone loss after 5-week bedrest inactivity. *European journal of applied physiology*, *99*(3), 283-289.

Berger, W., Quintern, J., & Dietz, V. (1982). Pathophysiology of gait in children with cerebral palsy. *Electroencephalography and clinical neurophysiology*, *53*(5), 538-548.

Biewener, A. A. (1991). Musculoskeletal design in relation to body size. *Journal of Biomechanics*, *24*, 19-29.

Bigland-Ritchie, B., & Woods, J. J. (1976). Integrated electromyogram and oxygen uptake during positive and negative work. *The Journal of Physiology*, *260*(2), 267-277.

Bigland-Ritchie, B. W. J. J., & Woods, J. J. (1984). Changes in muscle contractile properties and neural control during human muscular fatigue. *Muscle & nerve*, *7*(9), 691-699.

Birrell, S. A., & Haslam, R. A. (2009). The effect of military load carriage on 3-D lower limb kinematics and spatiotemporal parameters. *Ergonomics*, *52*(10), 1298-1304.

Birrell, S. A., & Haslam, R. A. (2010). The effect of load distribution within military load carriage systems on the kinetics of human gait. *Applied ergonomics*, *41*(4), 585-590.

Blacker, S. D., Fallowfield, J. L., Bilzon, J. L., & Willems, M. E. (2013). Neuromuscular impairment following backpack load carriage. *Journal of human kinetics*, *37*(1), 91-98.

Blake, O. M., Champoux, Y., & Wakeling, J. M. (2012). Muscle coordination patterns for efficient cycling. *Medicine & Science in Sports & Exercise*, *44*(5), 926-938.

Blickhan, R. (1989). The spring-mass model for running and hopping. *Journal of biomechanics*, *22*(11-12), 1217-1227.

Blomqvist, C. G., & Stone, H. L. (1991). Cardiovascular adjustments to gravitational stress. *Comprehensive Physiology*.

Bobet, J., & Norman, R. W. (1984). Effects of load placement on back muscle activity in load carriage. *European journal of applied physiology and occupational physiology*, *53*(1), 71-75.

Borg, G. A. (1982). Psychophysical bases of perceived exertion. *Med sci sports exerc*, *14*(5), 377-381.

Borg, D. N., Costello, J. T., Bach, A. J., & Stewart, I. B. (2017). Perceived exertion is as effective as the perceptual strain index in predicting physiological strain when wearing personal protective clothing. *Physiology & behavior*, *169*, 216-223.

Borghols, E. A. M., Dresen, M. H. W., & Hollander, A. P. (1978). Influence of heavy weight carrying on the cardiorespiratory system during exercise. *European Journal of Applied Physiology and Occupational Physiology*, *38*(3), 161-169.

Born, D. P., Holmberg, H. C., Goernert, F., & Sperlich, B. (2014). A novel compression garment with adhesive silicone stripes improves repeated sprint performance–a multi-

experimental approach on the underlying mechanisms. *BMC sports science, medicine and rehabilitation*, *6*(1), 21.

Bosch, F., & Klomp, R. (2005). *Running: Biomechanics and exercise physiology in practice*. Elsevier Churchill Livingstone.

Bosco, C., Zanon, S., Rusko, H., Dal Monte, A., Bellotti, P., Latteri, F., Candeloro, N., Locatelli, E., Azzaro, E., Pozzo, R., & Bonomi, S. (1984). The influence of extra load on the mechanical behavior of skeletal muscle. *European journal of applied physiology and occupational physiology*, *53*(2), 149-154.

Bosco, C., Rusko, H., & Hirvonen, J. (1986). The effect of extra-load conditioning on muscle performance in athletes. *Medicine and science in sports and exercise*, *18*(4), 415-419.

Bregman, D. J. J., Harlaar, J., Meskers, C. G. M., & De Groot, V. (2012). Spring-like Ankle Foot Orthoses reduce the energy cost of walking by taking over ankle work. *Gait & posture*, *35*(1), 148-153.

Bringard, A., Perrey, S., & Belluye, N. (2006). Aerobic energy cost and sensation responses during submaximal running exercise-positive effects of wearing compression tights. *International journal of sports medicine*, *27*(05), 373-378.

Brown T.G. (1911). The intinsie factors in the act of progression in the mammal. Proc R Soc Lond; B84:308-19.

Brown T,G. (1912). The factors in rhythmic activity of the nervous system. Proc R Soc London Ser; B85:278—89

Brown, S. H., & Cooke, J. D. (1990). Movement-related phasic muscle activation. I. Relations with temporal profile of movement. *Journal of neurophysiology*, *63*(3), 455-464.

Brown, D. A., Nagpal, S., & Chi, S. (2005). Limb-loaded cycling program for locomotor intervention following stroke. *Physical therapy*, *85*(2), 159-168.

Brown, A. M., Zifchock, R. A., & Hillstrom, H. J. (2014a). The effects of limb dominance and fatigue on running biomechanics. *Gait & posture*, *39*(3), 915-919.

Brown, T. N., O'Donovan, M., Hasselquist, L., Corner, B. D., & Schiffman, J. M. (2014b). Body borne loads impact walk-to-run and running biomechanics. *Gait & posture*, *40*(1), 237-242.

Brown, T. N., O'Donovan, M., Hasselquist, L., Corner, B., & Schiffman, J. M. (2016). Lower limb flexion posture relates to energy absorption during drop landings with soldier-relevant body borne loads. *Applied ergonomics*, *52*, 54-61.

Carvil, P.A.T., Attias, J., Evetts, S.N., Waldie, J., & Green, D.A. (2013). The Validity, Viability & Tolerability of a Gravity Loading Countermeasure Skinsuit (GLCS) during Ambulation & Resistance Exercise. *Aviation, Space, and Environmental Medicine*, *84*(4).

Carvil, P. A., Attias, J., Evetts, S., Waldie, J., & Green, D. A. (2016). The effect of the gravity loading countermeasure skinsuit upon movement and strength. *Journal of strength and conditioning research/National Strength & Conditioning Association*.

Carvil, P.A.T. (2017). Axial loading as a countermeasure to microgravity-induced deconditioning: effects on the spine and its associated structures. Unpublished doctoral thesis.

Cavagna, G. A., Thys, H., & Zamboni, A. (1976). The sources of external work in level walking and running. *The Journal of physiology*, *262*(3), 639-657.

Cavagna, G. A., Willems, P. A., & Heglund, N. C. (2000). The role of gravity in human walking: pendular energy exchange, external work and optimal speed. *The Journal of Physiology*, *528*(3), 657-668.

Cavanagh, P. R., Licata, A. A., & Rice, A. J. (2007). Exercise and pharmacological countermeasures for bone loss during long-duration space flight. *Gravitational and Space Research*, *18*(2).

Chang, Y. H., Huang, H. W., Hamerski, C. M., & Kram, R. (2000). The independent effects of gravity and inertia on running mechanics. *Journal of Experimental Biology*, *203*(2), 229-238.

Chapman, A. R., Vicenzino, B., Blanch, P., & Hodges, P. W. (2008) Patterns of leg muscle recruitment vary between novice and highly trained cyclists. Journal of Electromyography and Kinesiology, 18(3), 359-371.

Charles, J. B., Bungo, M. W., & Fortner, G. W. (1994). Space physiology and medicine. *Cardiopulmonary Function*, 286-304.

Cherry, M. S., Kota, S., Young, A., & Ferris, D. P. (2016). Running with an elastic lower limb exoskeleton. *Journal of applied biomechanics*, *32*(3), 269-277.

Churchill, E., Laubach, L. L., Mcconville, J. T., & Tebbetts, I. (1978). Anthropometric source book. Volume 1: Anthropometry for designers.

Claremont, A. D., & Hall, S. J. (1988). Effects of extremity loading upon energy expenditure and running mechanics. *Medicine and science in sports and exercise*, *20*(2), 167-171.

Clément, G., & Bukley, A. (Eds.). (2007). *Artificial gravity* (Vol. 20). Springer Science & Business Media. p37

Convertino, V. A. (1995). *Clinical aspects of the control of plasma volume at microgravity and during return to one gravity* (No. AL/AO-JA-1995-0119). Armstrong Lab Brooks AFB TX Aerospace Medicine Directorate

Convertino, V. A. (2002). Mechanisms of microgravity induced orthostatic intolerance: implications for effective countermeasures. *Journal of gravitational physiology: a journal of the international Society for Gravitational Physiology*, *9*(2), 1-13.

Convertino, V. A. (2011). Exercise and adaptation to microgravity environments. *Comprehensive Physiology*.

Cooper, G.E., & Harper, R.P. (1969) The use of pilot rating in the evaluation of aircraft handling qualities, NASA-TN-D-5153[27] J.R. Vos, M.L. Gernhardt, L. Lee, The walkback test.

Corlett, E. N., & Bishop, R. P. (1976). A technique for assessing postural discomfort. *Ergonomics*, *19*(2), 175-182.

Costill DL. The relationship between selected physiological variables and distance running performance. J Sports Med Phys Fitness 1967: 7: 61–66.

Cotes, J. E. (1969). Relationships of oxygen consumption, ventilation and cardiac frequency to body weight during standardized submaximal exercise in normal subjects. *Ergonomics*, *12*(3), 415-427.

Crompton, R. H., Weijie, L. Y. W., Günther, M., & Savage, R. (1998). The mechanical effectiveness of erect and "bent-hip, bent-knee" bipedal walking in Australopithecus afarensis. *Journal of Human Evolution*, *35*(1), 55-74.

Cronin, J., Hansen, K., Kawamori, N., & Mcnair, P. (2008). Effects of weighted vests and sled towing on sprint kinematics. *Sports Biomechanics*, *7*(2), 160-172.

Cross, M. R., Brughelli, M. E., & Cronin, J. B. (2014). Effects of vest loading on sprint kinetics and kinematics. *The Journal of Strength & Conditioning Research*, *28*(7), 1867-1874.

Darwin, C. (1871). The descent ofman. *The Great Books ofthe Western World*, *49*, 320.

Dascombe, B. J., Hoare, T. K., Sear, J. A., Reaburn, P. R., & Scanlan, A. T. (2011). The effects of wearing undersized lower-body compression garments on endurance running performance. *International journal of sports physiology and performance*, *6*(2), 160-173.

Delcomyn, F. (1980). Neural basis of rhythmic behavior in animals. *Science*, *210*(4469), 492-498.

De Luca, C. J. (1997). The use of surface electromyography in biomechanics. *Journal of applied biomechanics*, *13*(2), 135-163.

De Witt, J. K., & Ploutz-Snyder, L. L. (2014). Ground reaction forces during treadmill running in microgravity. *Journal of biomechanics*, *47*(10), 2339-2347.

Dicharry J. Kinematics and kinetics of gait: from lab to clinic. (2010). Clin Sports Med; 29(3):347– 64.

Dietz, V., Hillesheimer, W., & Freund, H. J. (1974). Correlation between tremor, voluntary contraction, and firing pattern of motor units in Parkinson's disease. *Journal of Neurology, Neurosurgery & Psychiatry*, *37*(8), 927-937.

Dietz, V., Schmidtbleicher, D., & Noth, J. (1979). Neuronal mechanisms of human locomotion. *journal of Neurophysiology*, *42*(5), 1212-1222.

Dietz, V., Gollhofer, A., Kleiber, M., & Trippel, M. (1992). Regulation of bipedal stance: dependency on "load" receptors. *Experimental brain research*, *89*(1), 229-231.

Dietz, V., & Duysens, J. (2000). Significance of load receptor input during locomotion: a review. *Gait & posture*, *11*(2), 102-110.

Di Prampero, P. E. (2000). Cycling on Earth, in space, on the Moon. *European journal of applied physiology*, *82*(5-6), 345-360.

Di Prampero, P. E., Lazzer, S., & Antonutto, G. (2009). Human powered centrifuges on the Moon or Mars. *Microgravity Science and Technology*,*21*(1-2), 209-215.

Dominelli, P. B., Sheel, A. W., & Foster, G. E. (2012). Effect of carrying a weighted backpack on lung mechanics during treadmill walking in healthy men. *European journal of applied physiology*, *112*(6), 2001-2012.

Donelan, J. M., & Kram, R. (1997). The effect of reduced gravity on the kinematics of human walking: a test of the dynamic similarity hypothesis for locomotion. *Journal of Experimental Biology*, *200*(24), 3193-3201.

Dorel, S., Couturier, A., & Hug, F. (2008). Intra-session repeatability of lower limb muscles activation pattern during pedaling. *Journal of Electromyography and Kinesiology*, *18*(5), 857-865.

Dorel, S., Guilhem, G., Couturier, A., & Hug, F. (2012). Adjustment of muscle coordination during an all-out sprint cycling task. *Medicine & Science in Sports & Exercise*, *44*(11), 2154-2164.

Duffield, R., & Portus, M. (2007). Comparison of three types of full-body compression garments on throwing and repeat-sprint performance in cricket players. *British journal of sports medicine*, *41*(7), 409-414.

Dugan, S. A., & Bhat, K. P. (2005). Biomechanics and analysis of running gait. *Physical Medicine and Rehabilitation Clinics*, *16*(3), 603-621.

Duysens, J., & Pearson, K. (1980). Inhibition of flexor burst generation by loading ankle extensor muscles in walking cats. *Brain research*, *187*(2), 321-332.

Duysens, J., & Van de Crommert, H. W. (1998). Neural control of locomotion; Part 1: The central pattern generator from cats to humans. *Gait & posture*, *7*(2), 131-141.

Elliott, G., Sawicki, G. S., Marecki, A., & Herr, H. (2013, June). The biomechanics and energetics of human running using an elastic knee exoskeleton. In *Rehabilitation Robotics (ICORR), 2013 IEEE International Conference on* (pp. 1-6). IEEE.

Enders, H., Von Tscharner, V., & Nigg, B. M. (2015). Neuromuscular strategies during cycling at different muscular demands. *Medicine & Science in Sports & Exercise*, *47*(7), 1450-1459.

Ericson, M. (1986). On the biomechanics of cycling. A study of joint and muscle load during exercise on the bicycle ergometer. *Scandinavian journal of rehabilitation medicine. Supplement*, *16*, 1-43.

Etkin, W. (1954). Social behavior and the evolution of man's mental faculties. *The American Naturalist*, *88*(840), 129-142.

Faghy, M., Blacker, S., & Brown, P. I. (2016). Effects of load mass carried in a backpack upon respiratory muscle fatigue. *European journal of sport science*, *16*(8), 1032-1038.

Farina, D., Merletti, R., & Enoka, R. M. (2004). The extraction of neural strategies from the surface EMG. *Journal of applied physiology*, *96*(4), 1486-1495.

Farina, K. A., Wright, A. A., Ford, K. R., Wirfel, L. A., & Smoliga, J. M. (2017). Physiological and Biomechanical Responses to Running on Lower Body Positive Pressure Treadmills in Healthy Populations. *Sports Medicine*, 1-15.

Farley, C. T., & McMahon, T. A. (1992). Energetics of walking and running: insights from simulated reduced-gravity experiments. *Journal of Applied Physiology*, *73*(6), 2709-2712.

Farley, C. T., & Gonzalez, O. (1996). Leg stiffness and stride frequency in human running. *Journal of biomechanics*, *29*(2), 181-186.

Ferris, D. P., Aagaard, P., Simonsen, E. B., Farley, C. T., & Dyhre-Poulsen, P. (2001). Soleus H-reflex gain in humans walking and running under simulated reduced gravity. *The Journal of physiology*, *530*(1), 167-180.

Ferris, D. P., Bohra, Z. A., Lukos, J. R., & Kinnaird, C. R. (2006). Neuromechanical adaptation to hopping with an elastic ankle-foot orthosis. *Journal of Applied Physiology*, *100*(1), 163-170.

Fischer, C. L., Johnson, P. C., & Berry, C. A. (1967). Red blood cell mass and plasma volume changes in manned space flight. *Jama*, *200*(7), 579-583.

Fischer, A. G., & Wolf, A. (2015). Assessment of the effects of body weight unloading on overground gait biomechanical parameters. *Clinical Biomechanics*, *30*(5), 454-461.

Fonda, B & Sarabon, N. (2010). Biomechanics of cycling. *Sport Science Review, 19(1-2)*, 187-210

Frederick, E. C. (1984). Physiological and ergonomics factors in running shoe design. *Applied ergonomics*, *15*(4), 281-287.

Frey, M., Colombo, G., Vaglio, M., Bucher, R., Jorg, M., & Riener, R. (2006). A novel mechatronic body weight support system. *IEEE Transactions on Neural Systems and Rehabilitation Engineering*, *14*(3), 311-321.

Gao, Z. G., Sun, S. Q., Goonetilleke, R. S., & Chow, D. H. K. (2016). Effect of an on-hip load-carrying belt on physiological and perceptual responses during bimanual anterior load carriage. *Applied ergonomics*, *55*, 133-137.

Gazendam, M. G., & Hof, A. L. (2007). Averaged EMG profiles in jogging and running at different speeds. *Gait & posture*, *25*(4), 604-614.

Geertsen, S. S., Kirk, H., Lorentzen, J., Jorsal, M., Johansson, C. B., & Nielsen, J. B. (2015). Impaired gait function in adults with cerebral palsy is associated with reduced rapid force generation and increased passive stiffness. *Clinical Neurophysiology*, *126*(12), 2320-2329.

Gell, C. F. (1961). Table of equivalents for acceleration terminology recommended for general international use by the Acceleration Committee of the Aerospace Medical Panel, AGARD. *Aerospace medicine*, *32*, 1109-1111.

Genc, K. O., Mandes, V. E., & Cavanagh, P. R. (2006). Gravity replacement during running in simulated microgravity. *Aviation, space, and environmental medicine*, *77*(11), 1117-1124.

Ghori, G. M. U., & Luckwill, R. G. (1985). Responses of the lower limb to load carrying in walking man. *European journal of applied physiology and occupational physiology*, *54*(2), 145-150.

Glaister, D. H. (1978). Human tolerance to impact acceleration. *Injury*, *9*(3), 191-198.

Goran, M., Fields, D. A., Hunter, G. R., Herd, S. L., & Weinsier, R. L. (2000). Total body fat does not influence maximal aerobic capacity. *International journal of obesity*, *24*(7), 841.

Gordon, K. E., & Ferris, D. P. (2007). Learning to walk with a robotic ankle exoskeleton. *Journal of biomechanics*, *40*(12), 2636-2644.

Gordon, K. E., Wu, M., Kahn, J. H., Dhaher, Y. Y., & Schmit, B. D. (2009). Ankle load modulates hip kinetics and EMG during human locomotion. *Journal of neurophysiology*, *101*(4), 2062-2076.

Gordon, K. E., Wu, M., Kahn, J. H., & Schmit, B. D. (2010). Feedback and feedforward locomotor adaptations to ankle-foot load in people with incomplete spinal cord injury. *Journal of neurophysiology*, *104*(3), 1325-1338.

Gosseye, T. P., Willems, P. A., & Heglund, N. C. (2010). Biomechanical analysis of running in weightlessness on a treadmill equipped with a subject loading system. *European journal of applied physiology*, *110*(4), 709-728.

Gosseye, T.P., Andre, T., Bastien, G., & Penta, M. (2011). "Subject loading system: Vertical Treadmill Facility Design Report Reduced Version". Arsalis, Belgium.

Grabowski, A., Farley, C. T., & Kram, R. (2005). Independent metabolic costs of supporting body weight and accelerating body mass during walking. *Journal of Applied Physiology*, *98*(2), 579-583.

Grabowski, A. M., & Kram, R. (2008). Effects of velocity and weight support on ground reaction forces and metabolic power during running. *J Appl Biomech*, *24*(3), 288-297.

Grabowski, A. M. (2010). Metabolic and biomechanical effects of velocity and weight support using a lower-body positive pressure device during walking. *Archives of physical medicine and rehabilitation*, *91*(6), 951-957.

Graham, T., Harrison, M.C., Lee, S and Robinson, C.L (2009). *Force as a vector.* http://www.mathcentre.ac.uk/resources/uploaded/mc-web-mech1-5-2009.pdf

Green, D., Attias, J., Carvil, P., Fréchette, A. and Waldie, J. (2014) Gravity loading countermeasure SkinSuit (GLCS) tolerability and performance in models of weightlessness. in Charite in Space: *6th International congress of Medicine in Space and extreme Environments (ICMS)*. Berlin. Germany

Greenleaf, J. E., Simonson, S. R., Stocks, J. M., Evans, J., Knapp, C. F., Cowell, S. A., Pemberton, K.N., Wilson, H.W., Vener, J.M., & Evetts, S. N. (2001).

Hackney, K. J., Scott, J. M., Hanson, A. M., English, K. L., Downs, M. E., & Ploutz-Snyder, L. L. (2015). The astronaut-athlete: optimizing human performance in space. *The Journal of Strength & Conditioning Research*, *29*(12), 3531-3545.

Hagberg, J. M., Mullin, J. P., Giese, M. D., & Spitznagel, E. (1981). Effect of pedaling rate on submaximal exercise responses of competitive cyclists. *Journal of applied physiology*, *51*(2), 447-451.

Haisman MF, Winsmann FR, Goldman RF: Energy cost of pushing loaded handcarts. J Appl Physiol 1972; 33: 181–3.

Hamner, S. R., & Delp, S. L. (2013). Muscle contributions to fore-aft and vertical body mass center accelerations over a range of running speeds. *Journal of biomechanics*, *46*(4), 780-787.

Han, K. H., Harman, E., Frykman, P., Johnson, M., Russell, F., & Rosenstein, M. (1992). Load Carriage: the effects of walking speed on gait timing, kinetics and muscle activity.. *Medicine & Science in Sports & Exercise*, *24*(5), S129.

Harkema, S. J. (2008). Plasticity of interneuronal networks of the functionally isolated human spinal cord. *Brain research reviews*, *57*(1), 255-264.

Harman EA, Frykman PN, Knapik JJ, Han KH: Backpack vs. front-back: differential effects of load on walking posture. Med Sci Sports Exerc 1994; 26: S140.

Hay J.G. (1985). The biomechanics of sports techniques. Prentice Hall, USA

Hermens, H. J., Freriks, B., Disselhorst-Klug, C., & Rau, G. (2000). Development of recommendations for SEMG sensors and sensor placement procedures. *Journal of electromyography and Kinesiology*, *10*(5), 361-374.

Hewes, G. W. (1961). Food transport and the origin of hominid bipedalism. *American Anthropologist*, *63*(4), 687-710.

Hicks, A. L., & Ginis, K. M. (2008). Treadmill training after spinal cord injury: it's not just about the walking. *Journal of rehabilitation research and development*, *45*(2), 241.

Hof, A. L., Elzinga, H., Grimmius, W., & Halbertsma, J. P. K. (2002). Speed dependence of averaged EMG profiles in walking. *Gait & posture*, *16*(1), 78-86.

Hoffmann, U., Moore Jr, A. D., Koschate, J., & Drescher, U. (2016). \ dot {V} O2 and HR kinetics before and after International Space Station missions.*European journal of applied physiology*, *116*(3), 503-511.

Holt, K. G., Wagenaar, R. C., LaFiandra, M. E., Kubo, M., & Obusek, J. P. (2003). Increased musculoskeletal stiffness during load carriage at increasing walking speeds maintains constant vertical excursion of the body center of mass. *Journal of biomechanics*, *36*(4), 465-471.

Hug, F., Decherchi, P., Marqueste, T., & Jammes, Y. (2004a). EMG versus oxygen uptake during cycling exercise in trained and untrained subjects. *Journal of Electromyography and Kinesiology*, *14*(2), 187-195.

Hug, F., Bendahan, D., Le Fur, Y., Cozzone, P. J., & Grelot, L. (2004b). Heterogeneity of muscle recruitment pattern during pedaling in professional road cyclists: a magnetic resonance imaging and electromyography study. *European journal of applied physiology*, *92*(3), 334-342.

Hug, F., Laplaud, D., Lucia, A., & Grelot, L. (2006). EMG threshold determination in eight lower limb muscles during cycling exercise: a pilot study. *International journal of sports medicine*, *27*(06), 456-462.

Hug, F., Drouet, J. M., Champoux, Y., Couturier, A., & Dorel, S. (2008). Interindividual variability of electromyographic patterns and pedal force profiles in trained cyclists. *European journal of applied physiology*, *104*(4), 667-678.

Hug, F., & Dorel, S. (2009). Electromyographic analysis of pedaling: a review. *Journal of Electromyography and Kinesiology*, *19*(2), 182-198.

Hug, F. (2011). Can muscle coordination be precisely studied by surface electromyography? *Journal of electromyography and kinesiology*, *21*(1), 1-12.

Hug, F., & Tucker, K. (2016). Surface electromyography to study muscle coordination.

Hunter, I., Seeley, M. K., Hopkins, J. T., Carr, C., & Franson, J. J. (2014). EMG activity during positive-pressure treadmill running. *Journal of Electromyography and Kinesiology*, *24*(3), 348-352.

Inman, V.T., Ralston, H.J., & Todd., F. (1981), 'Human Locomotion', in: Human Walking, Rose, J. & Gamble, J. G., eds., Williams and Wilkins, Baltimore.

Ivanenko, Y. P., Grasso, R., Macellari, V., & Lacquaniti, F. (2002). Control of foot trajectory in human locomotion: role of ground contact forces in simulated reduced gravity. *Journal of neurophysiology*, *87*(6), 3070-3089.

Ivanenko, Y. P., Labini, F. S., Cappellini, G., Macellari, V., McIntyre, J., & Lacquaniti, F. (2011). Gait transitions in simulated reduced gravity. *Journal of Applied Physiology*, *110*(3), 781-788.

James, D. C., Mileva, K. N., & Cook, D. P. (2014). Low-frequency accelerations over-estimate impact-related shock during walking. *Journal of Electromyography and Kinesiology*, *24*(2), 264-270.

James, C. R., Atkins, L. T., Yang, H. S., Dufek, J. S., & Bates, B. T. (2015). Kinematic and ground reaction force accommodation during weighted walking. *Human movement science*, *44*, 327-337.

Jefferson, R. J., Collins, J. J., Whittle, M. W., Radin, E. L., & O'Connor, J. J. (1990). The role of the quadriceps in controlling impulsive forces around heel strike. *Proceedings of the Institution of Mechanical Engineers, Part H: Journal of Engineering in Medicine*, *204*(1), 21-28.

Jin, H., Jiang, Y., Wei, Q., Wang, B., & Ma, G. (2012). Intensive aerobic cycling training with lower limb weights in Chinese patients with chronic stroke: discordance between improved cardiovascular fitness and walking ability. *Disability and rehabilitation*, *34*(19), 1665-1671.

Jolly, C. J. (1970). The seed-eaters: a new model of hominid differentiation based on a baboon analogy. *Man*, *5*(1), 5-26.

Jones, B. H., Toner, M. M., Daniels, W. L., & Knapik, J. J. (1984). The energy cost and heart-rate response of trained and untrained subjects walking and running in shoes and boots. *Ergonomics*, *27*(8), 895-902.

Jordan, A. R., Barnes, A., Claxton, D., Purvis, A., & Fysh, M. (2017). Kinematics and neuromuscular recruitment during vertical treadmill exercise. *Journal of exercise rehabilitation*, *13*(3), 307.

Jorge, M., & Hull, M. L. (1986). Analysis of EMG measurements during bicycle pedalling. *Journal of biomechanics*, *19*(9), 683-694.

Joseph, A., Wanono, R., Flamant, M., & Vidal-Petiot, E. (2017). Orthostatic hypotension: A review. *Nephrologie & therapeutique*, *13*, S55-S67.

Kamen, G., & Kinesiology, E. (2004). Research methods in biomechanics. *Champaign, IL, Human Kinetics Publ*.

Kamon, E., Metz, K. F., & Pandolf, K. B. (1973). Climbing and cycling with additional weights on the extremities. *Journal of applied physiology*, *35*(3), 367-370.

Kautz, S. A., & Neptune, R. R. (2002). Biomechanical determinants of pedaling energetics: internal and external work are not independent. *Exercise and sport sciences reviews*, *30*(4), 159-165.

Kendrick, D. P., & Newman, D. J. (2014, July). Modeling the Gravity Loading Countermeaure Skinsuit. 44th International Conference on Environmental Systems.

Kendrick, D. P. (2016). *The gravity loading countermeasure skinsuit: a passive countermeasure garment for preventing musculoskeletal deconditioning during long-duration spaceflight* (Doctoral dissertation, Massachusetts Institute of Technology).

Keren, G., Magazanik, A., & Epstein, Y. (1980). A comparison of various methods for the determination of $\dot{V}O_2$max. *European journal of applied physiology and occupational physiology*, *45*(2-3), 117-124.

Kimura, T. (1991). Body center of gravity and energy expenditure during bipedal locomotion in humans, chimpanzees and macaques. *Primate Rep*, *31*, 19-20.

Kinoshita, H. (1985). Effects of different loads and carrying systems on selected biomechanical parameters describing walking gait. *Ergonomics*, *28*(9), 1347-1362.

Kirschmann E (1999) *Das Zeitalter der Werfer*. Hannover, Germany: Eduard Kirschmann Grünlinde 4, 30459.

Kleissen, R. F. M., Hermens, H. J., den Exter, T., de Kreek, J. A., & Zilvold, G. (1989). Simultaneous measurement of surface EMG and movements for clinical use. *Medical and Biological Engineering and Computing*, *27*(3), 291.

Kline, J. R., Raab, S., Coast, J. R., Bounds, R. G., McNeill, D. K., & De Heer, H. D. (2015). Conversion table for running on lower body positive pressure treadmills. *The Journal of Strength & Conditioning Research*, *29*(3), 854-862.

Knapik, J., Harman, E., & Reynolds, K. (1996). Load carriage using packs: a review of physiological, biomechanical and medical aspects. *Applied ergonomics*, *27*(3), 207-216.

Knapik, J. J., Reynolds, K. L., & Harman, E. (2004). Soldier load carriage: historical, physiological, biomechanical, and medical aspects. *Military medicine*, *169*(1), 45-56.

Knudson, D. (2007). *Fundamentals of biomechanics*. Springer Science & Business Media, 42.

Ko, M. S., Lee, J. A., Kang, S. Y., & Jeon, H. S. (2015). Effect of Adeli suit treatment on gait in a child with cerebral palsy: a single-subject report. *Physiotherapy theory and practice*, *31*(4), 275-282.

Komi, P. V., Gollhofer, A., Schmidtbleicher, D., & Frick, U. (1987). Interaction between man and shoe in running: considerations for a more comprehensive measurement approach. *International journal of sports medicine*, *8*(03), 196-202.

Konrad, P. (2005). The abc of emg. *A practical introduction to kinesiological electromyography*, *1*, 30-35.

Kourtidou-Papadeli, C., Papadelis, C. L., Vernikos, J., Bamidis, P. D., Hitoglou-Antoniadou, M., Perantoni, E., & Vlachogiannis, E. (2008). The therapeutic benefits of gravity in space and on earth. *Hippokratia*, *12*(Suppl 1), 28.

Kozlovskaya, I. B., Grigoriev, A. I., & Stepantzov, V. I. (1995). Countermeasure of the negative effects of weightlessness on physical systems in long-term space flights. *Acta astronautica*, *36*(8-12), 661-668.

Kozlovskaya, I. B. (2002, September). Countermeasures for long-term spaceflights. Lessons learned from the Russian space program. In *Life in Space for Life on Earth* (Vol. 501, pp. 47-51).

Kraemer, W. J., Bush, J. A., Newton, R. U., Duncan, N. D., Volek, J. S., Denegar, C. R., Canavan, P., Johnston, J., Putukian, M., & Sebastianelli, W. J. (1998). Influence of a compression garment on repetitive power output production before and after different types of muscle fatigue. *Research in Sports Medicine: An International Journal*, *8*(2), 163-184.

Kram, R., & Taylor, C. R. (1990). Energetics of running: a new perspective. *Nature*, 346 (6281), 265-267.

Kram, R., Domingo, A., & Ferris, D. P. (1997). Effect of reduced gravity on the preferred walk-run transition speed. *Journal of Experimental Biology*, *200*(4), 821-826.

Krause, A., Schönau, E., Gollhofer, A., Duran, I., Ferrari-Malik, A., Freyler, K., & Ritzmann, R. (2017). alleviation of Motor impairments in Patients with cerebral Palsy: acute effects of Whole-body Vibration on stretch reflex response, Voluntary Muscle activation and Mobility. *Frontiers in neurology*, *8*, 416.

Kreitenberg, A., Baldwin, K. M., Bagian, J. P., Cotten, S., Witmer, J., & Caiozzo, V. J. (1998). The" Space Cycle" Self-Powered Human Centrifuge: a proposed countermeasure for prolonged human spaceflight. *Aviation, space, and environmental medicine*, *69*(1), 66-72.

Krupenevich, R., Rider, P., Domire, Z., & DeVita, P. (2015). Males and Females Respond Similarly to Walking With a Standardized, Heavy Load.*Military medicine*, *180*(9), 994-1000.

Kumagai, S., Tanaka, K., Matsuura, Y., Matsuzaka, A., Hirakoba, K., & Asano, K. (1982). Relationships of the anaerobic threshold with the 5 km, 10 km, and 10 mile races. *European journal of applied physiology and occupational physiology*, *49*(1), 13-23.

Kuitunen, S., Komi, P. V., & Kyröläinen, H. (2002). Knee and ankle joint stiffness in sprint running. *Medicine and science in sports and exercise*, *34*(1), 166-173.

Kyröläinen, H., Avela, J., & Komi, P. V. (2005). Changes in muscle activity with increasing running speed. *Journal of sports sciences*, *23*(10), 1101-1109.

Labini, F. S., Ivanenko, Y. P., Cappellini, G., Gravano, S., & Lacquaniti, F. (2011). Smooth changes in the EMG patterns during gait transitions under body weight unloading. *Journal of neurophysiology*, *106*(3), 1525-1536.

Lackner, J. R., & DiZio, P. (1998). Adaptation in a rotating artificial gravity environment. *Brain Research Reviews*, *28*(1), 194-202.

Lacquaniti, F., Ivanenko, Y. P., Sylos-Labini, F., La Scaleia, V., La Scaleia, B., Willems, P. A., & Zago, M. (2017). Human locomotion in hypogravity: from basic research to clinical applications. *Frontiers in Physiology*, *8*.

Lafortuna, C. L., Maffiuletti, N. A., Agosti, F., & Sartorio, A. (2005). Gender variations of body composition, muscle strength and power output in morbid obesity. *International journal of obesity*, *29*(7), 833-841.

Lafortuna, C. L., Agosti, F., Galli, R., Busti, C., Lazzer, S., & Sartorio, A. (2008). The energetic and cardiovascular response to treadmill walking and cycle ergometer exercise in obese women. *European journal of applied physiology*, *103*(6), 707.

Laing, C., Green, D. A., Mulder, E., Goswami, N., & Rittweger, J. (2016, March). Implementation of short-arm human centrifugation with an altered rotational axis position. In *Aerospace Conference, 2016 IEEE* (pp. 1-7). IEEE.

Landin, D., Thompson, M., & Reid, M. (2016). Actions of Two Bi-Articular Muscles of the Lower Extremity: A Review. *Journal of clinical medicine research*, *8*(7), 489.

Lang, T., Van Loon, J. J., Bloomfield, S., Vico, L., Chopard, A., Rittweger, J., Kyparos, A., Blottner, D., Vuori, I., Gerzer, R., & Cavanagh, P. R. (2017). Towards human exploration of space: the THESEUS review series on muscle and bone research priorities. *npj Microgravity*, *3*(1), 8.

Laskowski, E, R. (2015). What's a normal resting heart rate? *Mayo Clinic: Healthy Lifestyle and Fitness.* Retrieved from https://www.mayoclinic.org/healthy-lifestyle/fitness/expert-answers/heart-rate/faq-20057979

LeBlanc, A., Lin, C., Shackelford, L., Sinitsyn, V., Evans, H., Belichenko, O., Kozlovskaya, I., Oganov, V., Bakulin, A., & Hedrick, T. (2000). Muscle volume, MRI relaxation times (T2), and body composition after spaceflight. *Journal of Applied Physiology*, *89*(6), 2158-2164.

Lee, C. R., & Farley, C. T. (1998). Determinants of the center of mass trajectory in human walking and running. *Journal of experimental biology*, *201*(21), 2935-2944.

Lee, B. H. (2016). Clinical usefulness of Adeli suit therapy for improving gait function in children with spastic cerebral palsy: a case study. *Journal of physical therapy science*, *28*(6), 1949-1952.

Li, L., & Caldwell, G. E. (1999). Coefficient of cross correlation and the time domain correspondence. *Journal of Electromyography and Kinesiology*, *9*(6), 385-389.

Li, L., & Baum, B. S. (2004). Electromechanical delay estimated by using electromyography during cycling at different pedaling frequencies. *Journal of Electromyography and Kinesiology*, *14*(6), 647-652.

Liatis, S., Tentolouris, N., & Katsilambros, N. (2004). Cardiac autonomic nervous system activity in obesity. *Pediatric endocrinology reviews: PER*, *1*, 476-483.

Liebenberg, J., Scharf, J., Forrest, D., Dufek, J. S., Masumoto, K., & Mercer, J. A. (2011). Determination of muscle activity during running at reduced body weight. *Journal of sports sciences*, *29*(2), 207-214.

Liew, B. X., Morris, S., & Netto, K. (2016). Joint power and kinematics coordination in load carriage running: implications for performance and injury. *Gait & posture*, *47*, 74-79.

Linnarsson, D., Hughson, R. L., Fraser, K. S., Clément, G., Karlsson, L. L., Mulder, E., Paloski, W.H., Rittweger, J., & Zange, J. (2014). Effects of an artificial gravity countermeasure on orthostatic tolerance, blood volumes and aerobic power after short-term bed rest (BR-AG1). *Journal of Applied Physiology*, *118*(1), 29-35.

Lynn, P. A., Bettles, N. D., Hughes, A. D., & Johnson, S. W. (1978). Influence of electrode geometry on bipolar recordings of the surface electromyogram. *Medical and Biological Engineering and Computing*, *16*(6), 651-660.

Macdonald, J. H., Farina, D., & Marcora, S. M. (2008). Response of electromyographic variables during incremental and fatiguing cycling.

MacLellan, M. J., & McFadyen, B. J. (2010). Segmental control for adaptive locomotor adjustments during obstacle clearance in healthy young adults. *Experimental brain research*, *202*(2), 307-318.

Marsh, A. P., & Martin, P. E. (1995). The relationship between cadence and lower extremity EMG in cyclists and noncyclists. *Medicine and science in sports and exercise*, *27*(2), 217-225.

Martin, P. E. (1985). Mechanical and physiological responses to lower extremity loading during running. *Medicine and Science in Sports and Exercise*, *17*(4), 427-433.

Marcora, S. M., & Staiano, W. (2010). The limit to exercise tolerance in humans: mind over muscle?. *European journal of applied physiology*, *109*(4), 763-770.

Martin, P. E., & Nelson, R. C. (1986). The effect of carried loads on the walking patterns of men and women. *Ergonomics*, *29*(10), 1191-1202.

Masani, K., Sayenko, D. G., & Vette, A. H. (2013). What triggers the continuous muscle activity during upright standing?. *Gait & posture*, *37*(1), 72-77.

Mathias, C. J. (2002). To stand on one's own legs. *Clinical medicine*, *2*(3), 237-245.

Matthews, P. B. C., & Stein, R. B. (1969). The regularity of primary and secondary muscle spindle afferent discharges. *The Journal of physiology*, *202*(1), 59-82.

Matthews, P. B. C. (1984). Evidence from the use of vibration that the human long-latency stretch reflex depends upon spindle secondary afferents. *The Journal of Physiology*, *348*(1), 383-415.

Maus, H. M., Lipfert, S. W., Gross, M., Rummel, J., & Seyfarth, A. (2010). Upright human gait did not provide a major mechanical challenge for our ancestors. *Nature communications*, *1*, 70.

Mayhew, J. L. (1977). Oxygen cost and energy expenditure of running in trained runners. *British journal of sports medicine*, *11*(3), 116-121.

McArdle, W. D., Katch, F. I., & Katch, V. L. (2010). *Exercise physiology: nutrition, energy, and human performance*. Lippincott Williams & Wilkins.

McDonald, J. W., & Sadowsky, C. (2002). Spinal-cord injury. *The Lancet*, *359*(9304), 417-425.

McGowan, C. P., Neptune, R. R., & Kram, R. (2008). Independent effects of weight and mass on plantar flexor activity during walking: implications for their contributions to body support and forward propulsion. *Journal of applied physiology*, *105*(2), 486-494.

McKenna, M. J., & Hargreaves, M. (2008). Resolving fatigue mechanisms determining exercise performance: integrative physiology at its finest!.

McMahon, T. A., Valiant, G., & Frederick, E. C. (1987). Groucho running. *Journal of Applied Physiology*, *62*(6), 2326-2337.

McNeill, D. K., Kline, J. R., de Heer, H. D., & Coast, J. R. (2015). Oxygen consumption of elite distance runners on an anti-gravity treadmill®. *Journal of sports science & medicine*, *14*(2), 333.

Mendonca, C. T., Schaeffer, M. R., Riley, P., & Jensen, D. (2013). Physiological mechanisms of dyspnea during exercise with external thoracic restriction: role of increased neural respiratory drive. *Journal of Applied Physiology*, *116*(5), 570-581.

Merletti, R., & Conte, L. R. L. (1997). Surface EMG signal processing during isometric contractions. *Journal of Electromyography and Kinesiology*, *7*(4), 241-250.

Mooney, L. M., Rouse, E. J., & Herr, H. M. (2014). Autonomous exoskeleton reduces metabolic cost of human walking during load carriage. *Journal of neuroengineering and rehabilitation*, *11*(1), 80.

Moore, A. D., Lynn, P. A., & Feiveson, A. H. (2015). The first 10 years of aerobic exercise responses to long-duration ISS flights. *Aerospace medicine and human performance*, *86*(12), A78-A86.

Moore, I. S. (2016). Is there an economical running technique? A review of modifiable biomechanical factors affecting running economy. *Sports Medicine*, *46*(6), 793-807.

Morey-Holton, E.R.(2000). Ground-Based Models for Studying Adaptation to Altered Gravity, NASA Ames Research Centre Report - Moffet Field, CA.

Myers, M. J., & Steudel, K. (1985). Effect of limb mass and its distribution on the energetic cost of running. *Journal of Experimental Biology*, *116*(1), 363-373.

Neptune, R. R., & Herzog, W. (1999). The association between negative muscle work and pedaling rate. *Journal of biomechanics*, *32*(10), 1021-1026.

Newman, D. J., & Alexander, H. L. (1993). Human locomotion and workload for simulated lunar and Martian environments. *Acta Astronautica*, *29*(8), 613-620.

Nicola, T. L., & Jewison, D. J. (2012). The anatomy and biomechanics of running. *Clinics in sports medicine*, *31*(2), 187-201.

Nilsson, J., Thorstensson, A., & HALBERTSMA, J. (1985). Changes in leg movements and muscle activity with speed of locomotion and mode of progression in humans. *Acta Physiologica*, *123*(4), 457-475.

Novacheck, T. F. (1998). The biomechanics of running. *Gait & posture*, *7*(1), 77-95.

O'Donnell, D. E. (1998). Exertional breathlessness in chronic respiratory disease. *Lung Biology in Health and Disease*, *111*, 97-147.

O'Donnell, D. E., Hong, H. H., & Webb, K. A. (2000). Respiratory sensation during chest wall restriction and dead space loading in exercising men. *Journal of Applied Physiology*, *88*(5), 1859-1869.

O'Donnell, D. E., Ora, J., Webb, K. A., Laveneziana, P., & Jensen, D. (2009). Mechanisms of activity-related dyspnea in pulmonary diseases. *Respiratory physiology & neurobiology*, *167*(1), 116-132.

Owerkowicz, T., Cotter, J. A., Haddad, F., Yu, A. M., Camilon, M. L., Hoang, T. N., Jimenez, D.J., Kreitenberg, A., Tesch, P.A., Caiozzo, V.J., & Adams, G. R. (2016). Exercise responses to gravity-independent flywheel aerobic and resistance training. *Aerospace medicine and human performance*, *87*(2), 93-101.

Pamukoff, D. N., Lewek, M. D., & Blackburn, J. T. (2016). Greater vertical loading rate in obese compared to normal weight young adults. *Clinical Biomechanics*, *33*, 61-65.

Park, H., Branson, D., Kim, S., Warren, A., Jacobson, B., Petrova, A., Peksoz, M., & Kamenidis, P. (2014). Effect of armor and carrying load on body balance and leg muscle function. *Gait & posture*, *39*(1), 430-435.

Paul, S., Bhattacharyya, D., Chatterjee, T., Pal, M. S., Majumdar, D., Singh, S. N., & Majumdar, D. (2015). Physiological and biochemical responses during incremental uphill load carriage. *International Journal of Industrial Ergonomics*, *50*, 26-33.

Pavei, G., Biancardi, C. M., & Minetti, A. E. (2015). Skipping vs. running as the bipedal gait of choice in hypogravity. *Journal of Applied Physiology*, *119*(1), 93-100.

Pavy-Le Traon, A., Heer, M., Narici, M.V., Rittweger, J & Vernikos, J. (2007) From space to Earth: advances in human physiology from 20 years of bed rest studies (1986–2006). *Eur J Appl Physiol*, **101** 2 pp. 143–194.

Peoples, G. E., Lee, D. S., Notley, S. R., & Taylor, N. A. (2016). The effects of thoracic load carriage on maximal ambulatory work tolerance and acceptable work durations. *European journal of applied physiology*, *116*(3),635-646.

Perhonen, M. A., Franco, F., Lane, L. D., Buckey, J. C., Blomqvist, C. G., Zerwekh, J. E., Peshock, R.M., Weatherall, P.T., & Levine, B. D. (2001). Cardiac atrophy after bed rest and spaceflight. *Journal of Applied Physiology*, *91*(2), 645-653.

Phillips, D. B., Stickland, M. K., Lesser, I. A., & Petersen, S. R. (2016). The effects of heavy load carriage on physiological responses to graded exercise. *European journal of applied physiology*, *116*(2), 275-280.

Phinyomark, A., Thongpanja, S., Hu, H., Phukpattaranont, P., & Limsakul, C. (2012). The usefulness of mean and median frequencies in electromyography analysis. In *Computational intelligence in electromyography analysis-A perspective on current applications and future challenges*. InTech.

Polcyn, A. F., Bensel, C. K., Harman, E. A., Obusek, J. P., & Pandorf, C. (2002). *Effects of weight carried by soldiers: combined analysis of four studies on maximal performance, physiology, and biomechanics* (No. NATICK/TR-02/010). Army Natick Soldier Cenre MA supporting science and technology directorate

Poole, D. C., Ferreira, L. F., Behnke, B. J., Barstow, T. J., & Jones, A. M. (2007). The final frontier: oxygen flux into muscle at exercise onset.*Exercise and sport sciences reviews*, *35*(4), 166-173.

Prilutsky, B. I., & Gregor, R. J. (2000). Analysis of muscle coordination strategies in cycling. *IEEE Transactions on rehabilitation engineering*, *8*(3), 362-370.

Puthoff, M. L., Darter, B. J., Nielsen, D. H., & Yack, H. J. (2006). The effect of weighted vest walking on metabolic responses and ground reaction forces.*Medicine and science in sports and exercise*, *38*(4), 746-752.

Quesada, P. M., Mengelkoch, L. J., Hale, R. C., & Simon, S. R. (2000). Biomechanical and metabolic effects of varying backpack loading on simulated marching. *Ergonomics*, *43*(3), 293-309.

Raasch, C. C. (1996). Coordination of pedaling: Functional muscle groups and locomotor strategies.

Raasch, C. C., Zajac, F. E., Ma, B., & Levine, W. S. (1997). Muscle coordination of maximum-speed pedaling. *Journal of biomechanics*, *30*(6), 595-602.

Raasch, C. C., & Zajac, F. E. (1999). Locomotor strategy for pedaling: muscle groups and biomechanical functions. *Journal of neurophysiology*, *82*(2), 515-525.

Rader, A. A., Newman, D. J., & Carr, C. E. (2007). *Loping: A Strategy for Reduced Gravity Human Locomotion?* (No. 2007-01-3134). SAE Technical Paper.

Raffalt, P. C., Hovgaard-Hansen, L., & Jensen, B. R. (2013). Running on a lower-body positive pressure treadmill: $\dot{V}O_2$max, respiratory response, and vertical ground reaction force. *Research quarterly for exercise and sport*, *84*(2), 213-222.

Ricard, M. D., & Veatch, S. (1994). Effect of running speed and aerobic dance jump height on vertical ground reaction forces. *Journal of Applied Biomechanics*, *10*(1), 14-27.

Rittweger, J., Bareille, M. P., Clément, G., Linnarsson, D., Paloski, W. H., Wuyts, F., Zange, J., & Angerer, O. (2015). Short-arm centrifugation as a partially effective musculoskeletal countermeasure during 5-day head-down tilt bed rest—results from the BRAG1 study. *European journal of applied physiology*, *115*(6), 1233-1244.

Ritzmann, R., Freyler, K., Weltin, E., Krause, A., & Gollhofer, A. (2015). Load dependency of postural control-kinematic and neuromuscular changes in response to over and under load conditions. *PloS one*, *10*(6), e0128400.

Ritzmann, R., Freyler, K., Krause, A., & Gollhofer, A. (2016). Bouncing on Mars and the Moon—the role of gravity on neuromuscular control: correlation of muscle activity and rate of force development. *Journal of Applied Physiology*, *121*(5), 1187-1195.

Rivas, E., Smith, J. D., & Sherman, N. W. (2017). Leg compressions improve ventilatory efficiency while reducing peak and post exercise blood lactate, but does not improve perceived exertion, exercise economy or aerobic exercise capacity in endurance-trained runners. *Respiratory Physiology & Neurobiology*, *237*, 1-6.

Rodman, P. S., & McHenry, H. M. (1980). Bioenergetics and the origin of hominid bipedalism. *American Journal of Physical Anthropology*, *52*(1), 103-106.

Roy, R. R., Hutchison, D. L., Pierotti, D. J., Hodgson, J. A., & Edgerton, V. R. (1991). EMG patterns of rat ankle extensors and flexors during treadmill locomotion and swimming. *Journal of applied physiology*, *70*(6), 2522-2529.

Rosenfalck, A., & Andreassen, S. (1980). Impaired regulation of force and firing pattern of single motor units in patients with spasticity. *Journal of Neurology, Neurosurgery & Psychiatry*, *43*(10), 907-916.

Russell, D. J., Avery, L. M., Rosenbaum, P. L., Raina, P. S., Walter, S. D., & Palisano, R. J. (2000). Improved scaling of the gross motor function measure for children with cerebral palsy: evidence of reliability and validity. *Physical therapy*, *80*(9), 873-885.

Ruckstuhl, H., Kho, J., Weed, M., Wilkinson, M. W., & Hargens, A. R. (2009). Comparing two devices of suspended treadmill walking by varying body unloading and Froude number. *Gait & posture*, *30*(4), 446-451.

Ruckstuhl, H., Schlabs, T., Rosales-Velderrain, A., & Hargens, A. R. (2010). Oxygen consumption during walking and running under fractional weight bearing conditions. *Aviation, Space, and Environmental Medicine*, *81*(6), 550-554.

Ryan, M. M., & Gregor, R. J. (1992). EMG profiles of lower extremity muscles during cycling at constant workload and cadence. *Journal of Electromyography and Kinesiology*, *2*(2), 69-80.

Sainton, P., Nicol, C., Cabri, J., Barthelemy-Montfort, J., Berton, E., & Chavet, P. (2015). Influence of short-term unweighing and reloading on running kinetics and muscle activity. *European journal of applied physiology*, *115*(5), 1135-1145.

Salem, G., Young, J., Gregor, R., Ryan, M., Abrahamse, A., & Greendale, G. (1996). Knee Extensor Moments And Knee-extensor Strength In Older Persons Wearing A Weighted Vest 655. *Medicine & Science in Sports & Exercise*, *28*(5), 110.

Samaan, C. D., Rainbow, M. J., & Davis, I. S. (2014). Reduction in ground reaction force variables with instructed barefoot running. *Journal of Sport and Health Science*, *3*(2), 143-151.

Sandbrink, F. (2012). Motor unit recruitment in emg definition of motor unit recruitment and overview. *Medscape website. Available at: http://emedicine. medscape. com/article/1141359-overview# aw2aab6b4. Accessed June*, *26*.

Sanders, J. S., Ferguson, D. W., & Mark, A. L. (1988). Arterial baroreflex control of sympathetic nerve activity during elevation of blood pressure in normal man: dominance of aortic baroreflexes. *Circulation*, *77*(2), 279-288.

Sarre, G., Lepers, R., Maffiuletti, N., Millet, G., & Martin, A. (2003). Influence of cycling cadence on neuromuscular activity of the knee extensors in humans. *European journal of applied physiology*, *88*(4), 476-479.

Sawicki, G. S., & Ferris, D. P. (2008). Mechanics and energetics of level walking with powered ankle exoskeletons. *Journal of Experimental Biology*, *211*(9), 1402-1413.

Schiffman, J. M., Bensel, C. K., Hasselquist, L., Gregorczyk, K. N., & Piscitelle, L. (2006). Effects of carried weight on random motion and traditional measures of postural sway. *Applied Ergonomics*, *37*(5), 607-614.

Scholtes, V. A., Becher, J. G., Janssen-Potten, Y. J., Dekkers, H., Smallenbroek, L., & Dallmeijer, A. J. (2012). Effectiveness of functional progressive resistance exercise training on walking ability in children with cerebral palsy: a randomized controlled trial. *Research in developmental disabilities*, *33*(1), 181-188.

Schwendner, P., Mahnert, A., Koskinen, K., Moissl-Eichinger, C., Barczyk, S., Wirth, R., Berg, G., & Rettberg, P. (2017). Preparing for the crewed Mars journey: microbiota dynamics in the confined Mars500 habitat during simulated Mars flight and landing. *Microbiome*, *5*(1), 129.

Seay, J. F., Fellin, R. E., Sauer, S. G., Frykman, P. N., & Bensel, C. K. (2014). Lower extremity biomechanical changes associated with symmetrical torso loading during simulated marching. *Military medicine*, *179*(1), 85-91.

Semenova KA. (1997) Basis for a method of dynamic proprioceptive correction in the restorative treatment of patients with residual-stage infantile cerebral palsy. *Neurosci Behav Physiol* 27: 639–643.

Severin, G. (1991). Pingvin-3: Muscle and Bone Loading Suit, Aviaexport USSR, Moscow.

Shadwick, R. E. (1990). Elastic energy storage in tendons: mechanical differences related to function and age. *Journal of applied physiology*, *68*(3), 1033-1040.

Shinohara, M., Kouzaki, M., Yoshihisa, T., & Fukunaga, T. (1997). Mechanomyography of the human quadriceps muscle during incremental cycle ergometry. *European journal of applied physiology and occupational physiology*, *76*(4), 314-319.

Silder, A., Delp, S. L., & Besier, T. (2013). Men and women adopt similar walking mechanics and muscle activation patterns during load carriage. *Journal of biomechanics*, *46*(14), 2522-2528.

Silder, A., Besier, T., & Delp, S. L. (2015). Running with a load increases leg stiffness. *Journal of biomechanics*, *48*(6), 1003-1008.

Simonsen, E. B., Thomsen, L., & Klausen, K. (1985). Activity of mono-and biarticular leg muscles during sprint running. *European Journal of Applied Physiology and Occupational Physiology*, *54*(5), 524-532.

Simonsen, E. B., Dyhre-Poulsen, P., Voigt, M., Aagaard, P. & Fallentin, N. (1997). Mechanisms contributing to different joint moments observed during human walking. *Scandinavian Journal of Medicine and Science in Sports* **7**, 1–13.

Simperingham, K., & Cronin, J. (2014). Changes in sprint kinematics and kinetics with upper body loading and lower body loading using exogen exoskeletons: a pilot study. *J Aust Strength Cond*, *22*(5), 69-72.

Simpson, K. M., Munro, B. J., & Steele, J. R. (2011a). Backpack load affects lower limb muscle activity patterns of female hikers during prolonged load carriage. *Journal of Electromyography and Kinesiology*, *21*(5), 782-788.

Simpson, K. M., Munro, B. J., & Steele, J. R. (2011b). Effect of load mass on posture, heart rate and subjective responses of recreational female hikers to prolonged load carriage. *Applied ergonomics*, *42*(3), 403-410.

Simpson, K. M., Munro, B. J., & Steele, J. R. (2012). Effects of prolonged load carriage on ground reaction forces, lower limb kinematics and spatio-temporal parameters in female recreational hikers. *Ergonomics*, *55*(3), 316-326.

Smith, B., Ashton, K. M., Bohl, D., Clark, R. C., Metheny, J. B., & Klassen, S. (2006). Influence of carrying a backpack on pelvic tilt, rotation, and obliquity in female college students. *Gait & posture*, *23*(3), 263-267.

Smith, M. R., Marcora, S. M., & Coutts, A. J. (2015). Mental fatigue impairs intermittent running performance. *Med Sci Sports Exerc*, *47*(8), 1682-90.

Soule, R. G., & Goldman, R. F. (1969). Energy cost of loads carried on the head, hands, or feet. *Journal of Applied Physiology*, *27*(5), 687-690.

Stastny, P., Lehnert, M., Zaatar, A., Svoboda, Z., Xaverova, Z., & Jelen, K. (2014). Knee joint muscles neuromuscular activity during load-carrying walking. *Neuroendocrinology Letters*, *35*(7), 633-639.

Stenger, M. B., Evans, J. M., Knapp, C. F., Lee, S. M., Phillips, T. R., Perez, S. A., Moore, A.D., Paloski, W.H., & Platts, S. H. (2012). Artificial gravity training reduces bed rest-induced cardiovascular deconditioning. *European journal of applied physiology*, *112*(2), 605-616.

Stephens, M. J., & Yang, J. F. (1999). Loading during the stance phase of walking in humans increases the extensor EMG amplitude but does not change the duration of the step cycle. *Experimental Brain Research*, *124*(3), 363-370.

Sylos-Labini, F., Ivanenko, Y. P., Cappellini, G., Portone, A., MacLellan, M. J., & Lacquaniti, F. (2013). Changes of gait kinematics in different simulators of reduced gravity. *Journal of motor behavior*, *45*(6), 495-505.

Sylos-Labini, F., Lacquaniti, F., & Ivanenko, Y. P. (2014). Human locomotion under reduced gravity conditions: biomechanical and neurophysiological considerations. *BioMed research international*.

Symons, T. B., Sheffield-Moore, M., Chinkes, D. L., Ferrando, A. A., & Paddon-Jones, D. (2009). Artificial gravity maintains skeletal muscle protein synthesis during 21 days of simulated microgravity. *Journal of applied physiology*, *107*(1), 34-38.

Taylor, N. A., Lewis, M. C., Notley, S. R., & Peoples, G. E. (2012). A fractionation of the physiological burden of the personal protective equipment worn by firefighters. *European journal of applied physiology*, *112*(8), 2913-2921.

biodesen, L. P., Grabowski, A., & Kram, R. (2007). Effects of independently altering body weight and body mass on the metabolic cost of running. *Journal of Experimental Biology*, *210*(24), 4418-4427.

Thomson, A., Einarsson, E., Witvrouw, E., & Whiteley, R. (2017). Running speed increases plantar load more than per cent body weight on an AlterG® treadmill. *Journal of sports sciences*, *35*(3), 277-282.

Thornton, W. E., & Rummel, J. A. (1977). Muscular deconditioning and its prevention in space flight.

Tikuisis, P., Mclellan, T. M., & Selkirk, G. (2002). Perceptual versus physiological heat strain during exercise-heat stress. *Medicine & Science in Sports & Exercise*, *34*(9), 1454-1461.

Tilbury-Davis, D. C., & Hooper, R. H. (1999). The kinetic and kinematic effects of increasing load carriage upon the lower limb. *Human Movement Science*, *18*(5), 693-700.

Tözeren, A. (1999). *Human body dynamics: classical mechanics and human movement*. Springer Science & Business Media.

Trappe, S., Costill, D., Gallagher, P., Creer, A., Peters, J. R., Evans, H., Riley, D.A., & Fitts, R. H. (2009). Exercise in space: human skeletal muscle after 6 months aboard the International Space Station. *Journal of Applied Physiology*, *106*(4), 1159-1168.

Vacheron JJ, Poumarat G, Chandezon R., & Vanneuville G: The effects of loads carried on the shoulders. Milit Med 1999; 164: 597–9.

Van Hedel, H. J. A., Tomatis, L., & Müller, R. (2006). Modulation of leg muscle activity and gait kinematics by walking speed and bodyweight unloading. *Gait & posture*, *24*(1), 35-45.

Victor, R. G. (2015). Carotid baroreflex activation therapy for resistant hypertension. *Nature Reviews Cardiology*, *12*(8), 451.

Virji-Babul, N., Cooke, J. D., & Brown, S. H. (1994). Effects of gravitational forces on single joint arm movements in humans. *Experimental brain research*, *99*(2), 338-346.

Wakeling, J. M., Blake, O. M., & Chan, H. K. (2010). Muscle coordination is key to the power output and mechanical efficiency of limb movements. *Journal of Experimental Biology*, *213*(3), 487-492.

Waldie, J. M. (2005). Mechanical counter pressure space suits: advantages, limitations and concepts for martian exploration. *The Mars Society*, 1-16.

Waldie, J. M., & Newman, D. J. (2011). A gravity loading countermeasure skinsuit. *Acta Astronautica*, *68*(7), 722-730.

Walker, R. E., Swain, D. P., Ringleb, S. I., & Colberg, S. R. (2015). Effect of added mass on treadmill performance and pulmonary function. *The Journal of Strength & Conditioning Research*, *29*(4), 882-888.

Wang, S., Van Dijk, W., & van der Kooij, H. (2011, June). Spring uses in exoskeleton actuation design. In *Rehabilitation Robotics (ICORR), 2011 IEEE International Conference on* (pp. 1-6). IEEE.

Watson, J. C., Payne, R. C., Chamberlain, A. T., Jones, R. K., & Sellers, W. I. (2008). The energetic costs of load-carrying and the evolution of bipedalism. *Journal of Human Evolution*, *54*(5), 675-683.

Weltman A, Katch V, Sady S, Freedson P (1978) Onset of metabolic acidosis (anaerobic threshold) as a criterion measure of submaximum fitness. Res Q Am Assoc Health Phys Educ 49 : 218-227

Whalen, R. (1993). Musculoskeletal adaptation to mechanical forces on Earth and in space.

Whelan, P. J. (1996). Control of locomotion in the decerebrate cat. *Progress in neurobiology*, *49*(5), 481-515.

Winter DA. & Yack HJ (1987) EMG profiles during normal human walking: stride-to-stride and inter-subject variability. Electroencephalogr Clin Neurophysiol 67:402–411

Winter, D. A. (1991). *Biomechanics and motor control of human gait: normal, elderly and pathological*.

Woerner, J. (2016). Moon Village: A vision for global cooperation and Space 4.0. *Jan Woerner's blog, ESA*.

Yamashita-Goto, K., Okuyama, R., Honda, M., Kawasaki, K., Fujita, K., Yamada, T., Nonaka, I., Ohira, Y., & Yoshioka, T. (2001). Maximal and submaximal forces of slow fibers in human soleus after bed rest. *Journal of Applied Physiology*, *91*(1), 417-424.

Yang, Y., Kaplan, A., Pierre, M., Adams, G., Cavanagh, P., Takahashi, C., Kreitenberg, A., Hicks, J Keyak, J., & Caozzo, V. (2007a). Space cycle: a human-powered centrifuge that can be used for hypergravity resistance training. *Aviation, space, and environmental medicine*, *78*(1), 2-9.

Yang, Y., Baker, M., Graf, S., Larson, J., & Caiozzo, V. J. (2007b). Hypergravity resistance exercise: the use of artificial gravity as potential countermeasure to microgravity. *Journal of applied physiology*, *103*(5), 1879-1887.

Zander, V., Anken, R., Pesquet, T., Brungs, S., & Latsch, J. (2013). Short radius centrifuges–A new approach for life science experiments under hyper-g conditions for applications in space and beyond. *Recent Patents on Space Technology*, *3*(1), 74-81.

Zhang, Y., & Zhao, R. (2008). Overall thermal sensation, acceptability and comfort. *Building and environment*, *43*(1), 44-50.

1. Appendices

List of publications arising from this PhD

Published conference abstracts (* = presented personally at a conference; § presented by alternative author)**:**

Attias, J., Mileva, K.N., Russomano, T & Green, D.A. Axial body loading induces changes in the neuro-mechanics of human running. *23rd Annual congress of the European College of Sport Science conference (pending; July 2018). **

Richter, C., Braunstein, B., Staeudle., Attias, J., Suess, A., Weber, T., Mileva, K., Rittweger, J., Green, D & Albracht, K. (2018). In vivo fascicle length of the gastrocnemius muscle during walking in simulated martian gravity using two different body weight support devices. *23rd Annual congress of the European College of Sport Science conference (pending; July 2018).* §

Green, D.A, Süss, A., Attias, J., & Mileva, K.N (2018). WALKING ON THE MOON: KNOWN UNKNOWNS. *Aerospace Medicine and Human Performance* (AMHP), *89th Annual Aerospace Medicine Association conference* (pending; May 2018).§

Attias, J., Suss, A., Russomano, T., Mileva, K.N & Green, D.A. (2017). The effect of moderate axial body load on neuromuscular activation during running in simulated lunar gravity. *2nd Annual human physiology workshop, German Aerospace Centre (DLR), Cologne, Germany.**

Attias, J., Mileva, K.N., Russomano, T & Green, D.A. (2017). Axial body loading induces changes in the neuro-mechanics of human running. *Joint ISGP-ELGRA symposium, Nice, France.**

Attias, J., Russomano, T., Mileva, K.N & Green, D.A. (2016). The cardiorespiratory effects of axial re-loading during unloaded treadmill exercise. *1st Annual human physiology workshop, German Aerospace Centre (DLR), Cologne, Germany. **

Attias, J., Scott, J., Mileva, K.N., Russomano, T & Green, D.A (2016). The effect of axial body loading on lower limb neuromuscular activity during static and dynamic exercise. *Joint Life Science Meeting "Life in Space for Life on Earth". **

Attias, J., Scott, J. P. R., Russomano, T. & Green, D. A. (2015). The effect of the MK VI Gravity-Loading Countermeasure Skinsuit (GLCS) upon maximal aerobic exercise ($\dot{V}O_2Max$). *International Congress of Aviation and Space Medicine (ICASM), Oxford, UK**

Attias, J., Carvil, P.A.T., Waldie, J., Evetts, S.N & Green, D.A. (2015). Effect of the Mk III Gravity-Loading Countermeasure Skin Suit (GLCS) upon aerobic exercise performance. *European Low Gravity Research Association 22nd Symposium, Corfu, Greece.**

Carvil, P. A. T., Kristjánsson , J. G., Attias, J., Russomano, T. & Green, D. A. (2015). Elongation induced by four hours hyper-buoyancy floatation. *European Low Gravity Research Association 22nd Symposium, Corfu, Greece.* §

Green, D. A., Attias, J., Carvil, P. A. T., Evetts, S. N. & Scott, J. P. R. (2015). The Gravity-Loading Countermeasure Skinsuit – A collaborative journey to the ISS. *The Gravity Loading Countermeasures Skin Suit - a collaborative journey to the ISS. International Scientific and Practical Conference "Manned Space Flights"; Star city, Russia.* §

Green, D., Attias, J., Carvil, P., Fréchette, A. & Waldie, J. (2014) .Gravity-Loading Countermeasure Skinsuit (GLCS) tolerability & performance in models of weightlessness. *Charite in Space: 6th International congress of Medicine in Space and extreme Environments (ICMS).* §

Attias, J., Waldie, J., Evetts, S & Green, D (2014). The effect of the Gravity-Loading Skinsuit (GLCS) upon maximal aerobic performance ($\dot{V}O_2Max$) and Oxygen Kinetics. *Aviation, Space and Environmental Medicine, **85(3),** 352.**

Attias, J., Carvil, P.A.T., Waldie, J., Evetts, S. N., & Green, D. A. (2013). The effect of the Gravity-Loading Skinsuit (GLCS) upon aerobic exercise performance. *Aviation, Space, and Environmental Medicine, **84(4).****

Planned/pending manuscripts

Weber, T., Attias, J., Sies, W., Frechette, A., Braunstein, B., Green, D.A & Rittweger, J. (2018). Hopping in hypogravity - a rationale for a plyometric exercise countermeasure in planetary exploration missions. *PLOS ONE*

Attias, J., Mileva, K.N., Russomano, T & Green, D.A. (2018). Axial body loading modulates the EMG muscle activity and coordination during cycling. *J Electromyography and Kinesiology*

Attias, J., Mileva, K.N., Russomano, T & Green, D.A (2018). Axial body loading reduces exercise tolerance whilst maintaining maximal aerobic capacity during cycling and running. *J Appl Phys*

Attias, J., Mileva, K.N., Russomano, T & Green, D.A. (2019). Axial body loading induces changes in the neuro-mechanics of human running. *J Electromyography and Kinesiology*

Attias, J., Rittweger, J. Weber, T., Mileva, K.N., Russomano, T., Green, D.A (2019). The influence of axial body reloading on neuromuscular function during running in simulated lunar gravity. *J Appl Phys*

2. Example consent form

CONSENT FORM FOR PARTICIPANTS IN RESEARCH STUDIES

Please complete this form after you have read the Information Sheet and/or listened to an explanation about the research.

Title of Study: _____

King's College Research Ethics Committee Ref:_____

Thank you for considering taking part in this research. The person organising the research must explain the project to you before you agree to take part. If you have any questions arising from the Information Sheet or explanation already given to you, please ask the researcher before you decide whether to join in. You will be given a copy of this Consent Form to keep and refer to at any time.

	Please tick or initial
I confirm that I understand that by ticking/initialling each box I am consenting to this element of the study. I understand that it will be assumed that unticked/initialled boxes mean that I DO NOT consent to that part of the study. I understand that by not giving consent for any one element I may be deemed ineligible for the study.	☐

	Please tick or initial
1. ***I confirm that I have read and understood the information sheet dated [INSERT DATE AND VERSION NUMBER] for the above study. I have had the opportunity to consider the information and asked questions which have been answered satisfactorily.**	☐
2. ***I understand that my participation is voluntary and that I am free to withdraw at any time without giving any reason. Furthermore, I understand that I will be able to withdraw my data up to 09/01/2017**	☐
3. ***I consent to the processing of my personal information for the purposes explained to me. I understand that such information will be handled in accordance with the terms of the UK Data Protection Act 1998.**	☐

4. ***I understand that my information may be subject to review by responsible individuals from the College for monitoring and audit purposes.** ☐

5. **I understand that confidentiality and anonymity will be maintained and it will not be possible to identify me in any publications** ☐
   OR

6. I agree to be contacted in the future by King's College London researchers who would like to invite me to participate in follow up studies to this project, or in future studies of a similar nature. ☐

7. I agree that the research team may use my data for future research and understand that any such use of identifiable data would be reviewed and approved by a research ethics committee. (In such cases, as with this project, data would/would not be identifiable in any report). ☐

8. I understand that the information I have submitted will be published as a report and I wish to receive a copy of it. ☐

9. I understand that I must not take part if I fall under the exclusion criteria as detailed in the information sheet and explained to me by the researcher. ☐

10. I have informed the researcher of any other research in which I am currently involved or have been involved in during the past 12 months ☐

_____	_____	_____
Name of Participant	**Date**	**Signature**

_____	_____	_____
Name of Researcher	**Date**	**Signature**

3. Example information sheet for participants

1/11/15 V1

INFORMATION SHEET FOR PARTICIPANTS

***REC Reference Number**:* LRS-15/16-1944

YOU WILL BE GIVEN A COPY OF THIS INFORMATION SHEET

Title of the Study: The effect of axial loading upon cardiorespiratory responses, neuromuscular activity and biomechanics during variable treadmill exercise

We would like to invite you to participate in this original research project. Before you decide whether you want to take part, it is important for you to understand why the research is being done and what your participation will involve. Please take time to read the following information carefully and discuss it with others if you wish. You should only agree to take part in the study if, having read the following information, you are happy that you understand it and wish to participate. Choosing not to take part will not disadvantage you in any way. Please ask us if there is anything that is not clear or if you would like more information or time to decide.

Background of the Study

ESA astronaut Andreas Mogensen's will be flying to the International Space Station in September 2015, during which time he will be wearing a specially-tailored suit that has been designed to help recreate the gravitational load that we experience on Earth, called the SkinSuit. An investigation of how the SkinSuit may influence his and future crewmembers treadmill exercise performance is necessary. Additionally, it is necessary to ensure that the SkinSuit does not negatively affect his biomechanics and increase his risk of injury during such exercise.

What do I have to do?

You must be a male between 18 and 50 years of age as the heart, circulation and musculoskeletal systems undergo many changes as we age. You must not be taking medication, have or have a history of visual, balance, neurological, musculoskeletal cardiorespiratory or psychological disorder.

You will initially be required to attend the laboratory for a total of 3 occasions, varying in duration, ranging from 1-2 hours each time. You will be required to perform the same protocol twice; once in gym clothes (GYM) and once in the SkinSuit, separated by at least 2 days. The trials will be carried out on a treadmill equipped with an body weight support device; a harness attachment which essentially lifts you off the treadmill in varying degrees which reduces the amount of pressure/gravity-load your lower body is exposed to. Each visit will require you to perform an incremental exercise test up to your maximal effort ($\dot{V}O_2$Max; 15-20 minutes in duration) without any bodyweight support. The intensity will start low and will increase in small increments every 3 minutes until a pre-determined intensity is reached and you have completed the 3 minutes there. You will be taken through a brief warm up prior to the protocol, and a stretch following the protocol. After sufficient rest, you will then be asked to run for 9 minutes at a submaximal intensity, which is set at a speed of 10kkm·h^{-1} at both 1Gz (normal bodyweight) and at 0.8Gz (20% of your bodyweight removed via the harness).

For each laboratory visit you will be asked to avoid caffeine (tea, coffee and cola) and nicotine for 12 hours prior to the study. We also ask that participants do not consume alcohol for 24 hours prior to testing. Water is allowed during lab visits, although ideally not whilst carrying out the protocol.

Adhesive electrodes will be placed on your skin on the upper and lower leg muscles to measure your muscle activity and on either side of your collar bone and under your left rib cage for ECG heart rate measurement. There will be skin preparation in the form of wiping the skin with an alcohol wipe and removal of hair over small regions (2 x 3cm) with a razor. Devices that measure joint angle will be attached to the skin on one side of the left knee and hip, with adhesive tape. You will be required to wear a mask over your mouth and nose for measurement of breathing. You will also be asked to wear a pair of sandals known as the ForceShoes, which will enable measurement of the gravity-load provided by the SkinSuit during the protocol.

What risks are there?

Donning the SkinSuit can sometimes results in soreness around the shoulders, due to its' tight fitting nature. You may have slight skin markings that quickly resolve.

All sections pose little risk to the user other than the potential to have slight muscle soreness, mainly in the thigh, in the 24-48 hours post-testing. This is a normal response to muscle contractions and should alleviate within a 2-3 days. If you have any injuries to any of the leg muscles, then please tell us, as you may not be suitable for this study.

You may find yourself somewhat sweaty and tired towards the end, depending upon your level of fitness, but you should not feel any discomfort. Please let us know if you have any heart arrhythmias that are brought on with exercise as you may not be suitable for this test. If at any point you wish to terminate the test, you will be able to do so.

Electromyography and Goniometry are both widely-used techniques for measuring muscle function, and have few risks. However, if you have a pacemaker or another implanted device, broken skin, or allergies please tell us, as you may not be suitable to take part in this study.

Wearing the ForceShoes is similar to wearing walking shoes and therefore poses no risk.

Exclusion criteria:

Females

Current medication

Current/History of visual, balance or neurological disorder

Current/History of musculoskeletal disorder (including lower back pain)

Injury prohibiting exercise

Current/History of cardiorespiratory disorder

Current/history of arrhythmias

Current/History of psychological disorder

Those with any significant history or current pain or injury will be excluded.

Will the information gathered be kept confidential?

All information collected in the study will be recorded and stored securely and anonymously using a study participant identification code on a password-protected computer at King's College London. You will be able to withdraw your data from the study at any point up until 2nd November 2016.

What will happen to the data obtained from the research study?

The data collected will be collected and analysed at King's College London. Data will be presented together for all of the participants, thus, there will be nothing that would identify an individual. You will not be identifiable in any part of the work. The report might also be written up as a research paper for publication.

It is up to you to decide whether to take part or not. If you decide to take part you are still free to withdraw from the study at any time and without giving a reason.

If this study has harmed you in any way or if you wish to make a complaint about the conduct of the study you can contact King's College London using the details below for further advice and information: The Chair, BDM Research Ethics Subcommittee (RESC), rec@kcl.ac.uk

If you have any questions or require more information about this study, please contact the researcher using the following contact details: Julia Attias, number: 0207 848 6679 email: Julia.attias@kcl.ac.uk. Postal Address: 3.11 Shepherd's House, Kings College London, *Guy's Campus*, London SE1 1UL

Alternatively you may contact the project supervisor: Dr David Green, email david.a.green@kcl.ac.uk, Tel 020 7848 8176 Postal Address: Shepherd's House room 4.4, Guy's Campus, King's College London, SE1 1UL

In the event of you suffering any adverse effects as a consequence of your participation in this study, you will be compensated through King's College London's No Fault Compensation Scheme'.

4. Power calculations for each study using G-power statistical software

Effect of ABL whilst cycling (study 1):

Cardiorespiratory: suggested sample size 10

Ref: Driller, M. W., & Halson, S. L. (2013). The effects of wearing lower body compression garments during a cycling performance test. *International journal of sports physiology and performance*, *8*(3), 300-306.

Neuromuscular: suggested sample size 10

Ref: Baum, B. S., & Li, L. (2003). Lower extremity muscle activities during cycling are influenced by load and frequency. *Journal of Electromyography and Kinesiology*, *13*(2), 181-190.

Effect of ABL running (study 2):

Cardiorespiratory (loaded): suggested sample size 3

Ref: Phillips, D. B., Ehnes, C. M., Stickland, M. K., & Petersen, S. R. (2016). The impact of thoracic load carriage up to 45 kg on the cardiopulmonary response to exercise. *European journal of applied physiology*, *116*(9), 1725-1734.

Cardioresp (unloaded): suggested sample size 6

Ref: McNeill, D. K., de Heer, H. D., Williams, C. P., & Coast, J. R. (2015). Metabolic accommodation to running on a body weight-supported treadmill. *European journal of applied physiology*, *115*(5), 905-910.

Neuromuscular: suggested sample size 3

Ref: Fenuta, A., & Hicks, A. L. (2014). Muscle activation during body weight-supported locomotion while using the ZeroG. *Journal of rehabilitation research and development*, *51*(1), 51-58.

Biomechanical responses whilst running in simulated partial gravity (study 3): suggested sample size: 5

Ref: Grabowski, A. M. (2010). Metabolic and biomechanical effects of velocity and weight support using a lower-body positive pressure device during walking. *Archives of physical medicine and rehabilitation*, *91*(6), 951-957.